

AWARD NUMBER:

**PR110507, W81XWH-12-1-0311**

TITLE:

**Early Intervention with Cdk9 Inhibitors to Prevent Post-Traumatic Osteoarthritis**

PRINCIPAL INVESTIGATOR:

**Dominik R. Haudenschild, Ph.D.**

CONTRACTING ORGANIZATION: University of California, Davis  
Davis, CA 95618-6134

REPORT DATE: October 2015

TYPE OF REPORT: Annual

PREPARED FOR: U.S. Army Medical Research and Materiel Command  
Fort Detrick, Maryland 21702-5012

DISTRIBUTION STATEMENT: Approved for Public Release;  
Distribution Unlimited

The views, opinions and/or findings contained in this report are those of the author(s) and should not be construed as an official Department of the Army position, policy or decision unless so designated by other documentation.

REPORT DOCUMENTATION PAGE				Form Approved OMB No. 0704-0188	
Public reporting burden for this collection of information is estimated to average 1 hour per response, including the time for reviewing instructions, searching existing data sources, gathering and maintaining the data needed, and completing and reviewing this collection of information. Send comments regarding this burden estimate or any other aspect of this collection of information, including suggestions for reducing this burden to Department of Defense, Washington Headquarters Services, Directorate for Information Operations and Reports (0704-0188), 1215 Jefferson Davis Highway, Suite 1204, Arlington, VA 22202-4302. Respondents should be aware that notwithstanding any other provision of law, no person shall be subject to any penalty for failing to comply with a collection of information if it does not display a currently valid OMB control number. PLEASE DO NOT RETURN YOUR FORM TO THE ABOVE ADDRESS.					
1. REPORT DATE October 2015		2. REPORT TYPE Annual		3. DATES COVERED 30Sep2014 - 29Sep2015	
4. TITLE AND SUBTITLE Early Intervention with Cdk9 Inhibitors to Prevent Post-Traumatic Osteoarthritis				5a. CONTRACT NUMBER W81XWH-12-1-0311	
				5b. GRANT NUMBER PR110507	
				5c. PROGRAM ELEMENT NUMBER	
6. AUTHOR(S)  Dominik R. Haudenschild, Ph.D.  E-Mail: DRHaudenschild@ucdavis.edu				5d. PROJECT NUMBER	
				5e. TASK NUMBER	
				5f. WORK UNIT NUMBER	
7. PERFORMING ORGANIZATION NAME(S) AND ADDRESS(ES)  Univ. of California Davis 1850 Research Park Drive #300 Davis, CA 95618-6134				8. PERFORMING ORGANIZATION REPORT NUMBER	
9. SPONSORING / MONITORING AGENCY NAME(S) AND ADDRESS(ES)  U.S. Army Medical Research and Materiel Command Fort Detrick, Maryland 21702-5012				10. SPONSOR/MONITOR'S ACRONYM(S)	
				11. SPONSOR/MONITOR'S REPORT NUMBER(S)	
12. DISTRIBUTION / AVAILABILITY STATEMENT  Approved for Public Release; Distribution Unlimited					
13. SUPPLEMENTARY NOTES					
14. ABSTRACT We proposed to test (in aim 1) whether inhibition of Cdk9 would reduce the early transcriptional response to joint injury, and (in aim 2) whether this would delay or prevent the subsequent development of post-traumatic osteoarthritis. In the first progress report, we made significant progress on Aim 1, essentially demonstrating that Cdk9 inhibitors reduce early transcriptional responses to joint injury using in-vitro and in-vivo models. In this progress report, we made substantial progress in Aim2, demonstrating that prevention of early transcriptional response to joint injury reduces many of the early signs of osteoarthritis initiation and progression. We show this both in-vitro using cartilage explants, and in-vivo in our mouse model of ACL-rupture PTOA. In-vitro, using explant cartilage subjected to impact injury, Cdk9 inhibitors prevent mechanical injury-induced inflammation, apoptosis and matrix degradation. In-vivo, Cdk9 inhibitors reduce inflammation, synovitis, fibrosis, loss of cartilage mechanical properties, loss of subchondral bone, and osteophyte formation.					
15. SUBJECT TERMS PTOA, acute injury response, inflammation, transcriptional elongation, Cdk9					
16. SECURITY CLASSIFICATION OF:			17. LIMITATION OF ABSTRACT  Unclassified	18. NUMBER OF PAGES  97	19a. NAME OF RESPONSIBLE PERSON USAMRMC
a. REPORT  Unclassified	b. ABSTRACT  Unclassified	c. THIS PAGE  Unclassified			19b. TELEPHONE NUMBER (include area code)

## TABLE OF CONTENTS

	<u>Page</u>
Introduction.....	5
Body.....	5
Key Research Accomplishments.....	6
Reportable Outcomes.....	11
Conclusion.....	14
References.....	14
Appendix 1.....	15
Appendix 2.....	25
Appendix 3.....	26
Appendix 4.....	36
Appendix 5.....	45
Appendix 6.....	51
Appendix 7.....	61
Appendix 8.....	67
Appendix 9 .....	79
Appendix 10 .....	89
Appendix 11 .....	95
Appendix 12 .....	96
Appendix 13 .....	97

**--- Page intentionally left blank ---**

## INTRODUCTION:

We propose that a fundamental flaw in current OA management is its focus on treating an irreversibly damaged joint during end-stage organ failure, rather than preventing the onset of cartilage and bone degeneration following traumatic joint injury. Our **GLOBAL HYPOTHESIS** is that OA is initiated at the molecular and cellular level shortly after an injury occurs, thus the optimal time frame for therapeutic intervention is also shortly after the injury. The **goal** of this research proposal is to develop an early therapeutic strategy, delivered just after a joint injury, which will prevent or delay the onset of joint degradation and OA.

Joint Injury induces an acute cellular response, which occurs on a time-scale of minutes to hours after injury. This acute cellular response is characterized by mRNA transcription of early response genes and release of inflammatory mediators, which initiate a destructive cascade of events leading to the degradation of joint matrix and osteoarthritis. The mRNA transcription of these early response genes is controlled by a central checkpoint, where Cdk9 kinase activity is the rate-limiting step. We hypothesized that inhibitors of Cdk9 would reduce mRNA transcription of the early response genes, and therefore prevent the destructive cascade of events leading to osteoarthritis.

In aim 1 of this proposal we test whether inhibition of Cdk9 reduces the early mRNA transcriptional response to joint injury. For aim 1 we examine early responses (1 hour to 1 week after joint injury), and we test short-term outcomes (mRNA expression, local protease activity, cytokine production). The goal of aim 1 is to determine a treatment window (time and dose) wherein we can reduce the acute response to injury by inhibition of Cdk9. In aim 2 we test whether this early intervention delays or prevents the subsequent development of post-traumatic osteoarthritis using long-term outcomes (joint degradation, arthritis grade, proteoglycan loss). These experiments are performed in our recently developed non-invasive mouse model of joint injury in mice.

## BODY:

### *Scientifically we made significant progress on Aim 1 and Aim 2.*

The first manuscript describing the in-vitro results on the chondro-protective effects of Cdk9 inhibitors is published in Arthritis & Rheumatology (A&R), which is the highest-impact journal dedicated to arthritis research and has stringent peer review (appendix 1). This publication received considerable attention, and a follow-up question and reply are also published in A&R (appendix 2). As a next step to this A&R manuscript (mainly in-vitro experiments), we published another manuscript describing the protective effects of Cdk9 inhibitors in an *ex-vivo* cartilage explant system. This study provides additional evidence of Cdk9 inhibition on preventing the detrimental effects of injury-induced damage to cartilage, which include apoptosis and cartilage matrix degradation. This second manuscript was submitted to the publisher as of the previous progress report. It has now been revised and published in European Cells and Materials, a high impact journal published by the AO foundation (appendix 3).

Towards the completion of Aim 2, we published the third and fourth manuscripts describing the in-vivo imaging of protease activities in the injured knee joint to monitor post-traumatic osteoarthritis progression are published in the peer-reviewed journal Osteoarthritis and Cartilage (OA&C) (appendix 4), and in the journal Biochemical and Biophysical Research Communications (BBRC) (appendix 5).

As proposed in Aim 1, we began testing whether inhibition of Cdk9 in mouse knees protects against the acute inflammatory response at early times post-injury. At first we tested the transcription of early response genes since that process is directly controlled by Cdk9. *These tests were very successful: a single intraperitoneal injection of Cdk9 inhibitor significantly reduced the acute response, and multiple injections reduced the acute response to baseline levels.* We have performed additional analyses on the tissue inflammatory responses and catabolic protease activities, and the remodeling of subchondral bone microstructure within the injured joints, and on the ability of Cdk9 inhibitors to prevent development of osteoarthritis in the long-

term as proposed in Aim 2. Detailed description of the observations and results is presented in bullet format in the next section.

## **KEY RESEARCH ACCOMPLISHMENTS**

### **SPECIFIC AIM 1 – SHORT TERM EXPERIMENTS TO REDUCE INJURY-RESPONSE**

#### **TASK 1 – GENE EXPRESSION ANALYSIS AT BASELINE AND AT 1-240 HOURS POST-INJURY**

- A. Injure Mice According to the Schedule, with n=6 for each data point.

Progress: We have completed most of this task.

- B. Sacrifice mice at given times and dissect out the injured and contralateral uninjured knee joints, and also harvest and store blood for Task 2.

Progress: We have completed most of this task.

- C. Isolate total RNA and perform PCR-Array quantitative gene expression analysis on 84 NFkB dependent primary response genes.

Progress: We have successfully isolated total RNA from all the harvested joints, and performed quantitative RT-PCR on select primary response genes to estimate the responsiveness of the genes.

- D. Perform statistical analysis of the results.

Progress: Complete for the data collected.

**Milestone:** We identified a peak response of gene expression at 4-6 hours post-injury. This peak response is rapidly induced by the injury, with some genes (such as IL-6) responding with approximately 80-fold induction in the injured leg compared to the uninjured contralateral knee. The peak is also rapidly resolved by 8 hours for most genes analyzed to date, with gene expression returning to 1-5 times that in the uninjured contralateral knee. Inhibition of Cdk9 with a single dose of inhibitor greatly reduces the injury-related increase of primary response gene expression. Two injections, 0 and 6 hours post-injury, effectively prevents the injury-related increase of the primary response genes assayed. Injections of Cdk9 inhibitor given during 3 hour window after injury appear to be most effective in reducing primary response gene expression.

#### **TASK 2 – ANALYSIS OF SERUM CYTOKINE LEVELS AT BASELINE AND AT 1-240 HOURS POST-INJURY**

- A. Blood/serum has been collected as part of Task 1A, with n=6 for each data point

Progress: Blood/serum has been collected and stored appropriately

- B. Multiplexed bead immunoassay analysis to quantify 32 pro-and anti-inflammatory cytokines

Progress: Analysis is underway, see notes below.

- C. Statistical analysis of the results

Progress: Initial results showed statistically insignificant changes of circulating cytokines in the plasma samples, with the exception of IL-6 that showed a mild increase. In light of this, we started a revised approach using micro-dissected knee joints to extract cytokines, with the hope that the cytokine abundance would be greater in the joints than in the serum. This data would provide insight into the local cytokine response, presumably with greater sensitivity because only local tissue is analyzed (not diluted into the systemic circulation). This approach was successful for certain primary response genes (for example Nox4). However, for the more commonly cited OA-related responses (IL-6, MMP-3 and MMP-13), this approach was also not successful as the amounts of cytokine were still below the detection limits of the

assays. We did not further pursue this line of investigation given the high cost of animals, and the success of other outcomes.

**Milestone:** We identified a mild increase in serum levels of IL-6, and joint levels of Nox4, but not other cytokines, in response to joint injury.

### **TASK 3 – IN-VIVO IMAGING OF JOINT PROTEASE ACTIVITY AT BASELINE AND AT 1-240 HOURS POST-INJURY**

- A. Mice will be injected with Imaging Reagents prior to imaging

Progress: Done for all time points.

- B. Mice will be injured according to the protocol

Progress: Done for all time points.

- C. Non-invasive functional imaging of Joint Protease activity will be performed on live mice.

Progress: Done for all time points. Published in 2014 OA&C (appendix 4), and in 2015 BBRC (appendix 5).

- D. Mice will be sacrificed for uCT analysis in Task 4.

**Milestone:** Protease activity within the joint is induced within 1 hour, peaks at 2-4 days post-injury, and remains elevated out to at least 8 weeks after injury. Inhibition of Cdk9 at the time of injury effectively prevents joint protease activity for the first 24 hours. Based on our experience (Task 2) with gene expression, we expect that multiple injections will be required to reduce injury-induced joint protease activity. Published in 2014 OA&C (appendix 4), and in 2015 BBRC (appendix 5).

### **TASK 4 – MICROCT ANALYSIS OF THE REMODELING IN SUBCHONDRAL BONE AT BASELINE AND AT 1-240 HOURS POST-INJURY**

- A. The same mice will be used for both imaging studies (tasks 3 and 4), n=5 for each data point.

Progress: Done for most time points.

- B. Mice will be scanned 1 day before injury to obtain a baseline measurement, and then again at the indicated times.

Progress: We have obtained scan data from sufficient animals to establish a baseline measurement. This baseline will be used as normal uninjured bone density for comparison to all other measurements.

Progress: A single dose of Cdk9 inhibitor significantly prevented bone loss after injury at day 3 post-injury. For later time points, we found that multiple doses of Cdk9 inhibitor are required, which is not unexpected given that flavopiridol has an in-vivo half life of under 6 hours. We have repeated the experiments with multiple doses of Cdk9 inhibitor and are analyzing the micro CT scans to measure the degree of bone loss and the amount of osteophyte formation due to the knee injury

**Milestone:** Inhibition of Cdk9 activity with a single injection of flavopiridol post-injury prevents or reduces bone loss at day 3 post-injury. Daily injections of flavopiridol (out to 3 days) are required to prevent OA-like changes at later time points (7 to 10 days post-injury).

## **SPECIFIC AIM 2 – LONG TERM EXPERIMENTS TO PREVENT OA**

### **TASK 1 – HISTOLOGICAL ASSESSMENT OF OA AT TIMES 2, 3, 4 MONTHS POST-INJURY**

- A. Injured mice will be sacrificed at the indicated times, joints processed for histology, and stained with Safranin-O with a Fast-Green Counter-stain.

Progress: We have encountered a difficulty in completing this aim. Specifically, because our injury model ruptures the ACL, and due to the bent position of the knee in mice, we substantially alter the biomechanics of the joint and in-effect establish a new articulation point. The result of the altered biomechanics is that all animals develop arthritis, even though the initial injury is relatively mild. We have taken two approaches to address this: The first approach is to use our existing model of ACL rupture, but examine earlier time points for intervention efficacy. We have chosen to assess OA progression at the 6-week time point, with the Cdk9 inhibitor administered 3-times per week for up to 3-week post-injury. The drugs were given at a reduced dosage to prevent long-term toxicity in this experiment. Using this approach we found that Cdk9 inhibition significantly reduced the early signs of OA. This includes synovitis, inflammation, gene expression, and loss of cartilage matrix mechanical properties. The second approach is to use an even milder non-invasive mechanical injury model that does not alter the biomechanics of the knee joint. For this we had to re-engineer the platens on our mechanical testing instrument to prevent the rupture of the ACL, while still allowing for high forces to be transmitted to the cartilage. We succeeded in re-engineering the mechanical setup, and can now apply twice the compressive force to the joint without causing ACL rupture. We are now in the process of characterizing the biological responses to this compression. This will go beyond the current scope of the grant as it is a new model of PTOA.

### **2. SUBSTANTIAL PROGRESS TOWARDS OVERALL GOAL:**

- We established a cartilage explant injury model, where we mechanically compress bovine cartilage explants to 30% strain at a rate of 100% strain/second. Using this model we observed increased expression of injury response genes within 2 hours, including IL-6, iNOS, and others. Treatment with flavopiridol prevented elevation of these genes by injury at 2, 6, and 24 hours after injury. (appendix 1 and 2)
- We show that mechanical injury in cartilage explant leads to chondrocyte apoptosis that is prevented by Cdk9 inhibitor treatment. These data for the first time connects mechanical injury to cartilage explant causes direct cellular damage to chondrocytes. This detrimental effect is prevented by Cdk9 inhibition (appendix 3).
- In the cartilage explant injury model, we observed that mechanical injury causes degradation of the cartilage matrix and results in a decrease in the mechanical properties of injured cartilage compared to uninjured control. Treatment with flavopiridol prevented this loss of mechanical properties by the simulated injury (appendix 3). In fact, even uninjured controls in the presence of flavopiridol had greater mechanical properties than in the absence of flavopiridol.
- Using our in-vivo mouse model of joint injury, we found a peak of inflammatory gene expression at about 2 hours post-injury. This timing was conserved between many genes, including iNOS, IL-6, MMP13, ADAMTS, TNFa, and others, suggesting a common regulatory mechanism (we presume Cdk9 is involved). Since many of these genes follow a similar pattern of induction after joint injury, we focused on the most highly induced genes, IL-6 and iNOS, for cost saving.
- In the mouse model of joint injury, a single injection of flavopiridol reduced and delayed the activation of inflammatory genes. However, a single injection of flavopiridol did not completely prevent the activation of inflammatory genes. This is not surprising given the half-life of flavopiridol is under 6 hours.

- In the mouse model of joint injury, a single injection of flavopiridol did not reduce the extent of remodeling in subchondral bone as measured by micro-CT within 1 week. We therefore switched to multiple post-injury injections of flavopiridol from here on.
- Multiple injections of flavopiridol completely prevented the activation of pro-inflammatory cytokines and catabolic proteases at the mRNA level after knee injury at all times measured.
- In-vivo imaging of MMP activity after injury showed elevated MMP activity in the injured joint became detectable perhaps as soon as 1 hour after injury. The 1 hour time point did not quite reach statistical significance with n=8 mice, but all other time points (2h, 3h, 4h, 6h, 8h, 12h, 1day, 2day, 4days, 7 days) showed significantly elevated in-vivo MMP activity in the injured joint.
- A single injection of flavopiridol after injury substantially reduced in-vivo MMP activity to near baseline levels during the first 24 hours, and MMP activity remained lower at all time points tested.
- Injury-induced inflammation and synovial hypertrophy are reduced if flavopiridol is administered after injury.
- Multiple injections of flavopiridol after injury prevents subchondral bone loss at 3 and 7 days post-injury.

In **summary**, the results from these experiments are very positive. The data conclusively demonstrates that Cdk9 inhibition strongly reduced or even completely prevented every one of the acute local responses to joint injury that we tested. Given these positive results during the acute phase, we are well-positioned to initiate the longer-term studies we proposed in aim 2, namely to ask whether reducing the acute response will slow or prevent the development of osteoarthritis.

*Given these very positive results in the context of joint injury, we are pursuing a similar Cdk9-inhibition strategy in additional injury situations, such as preventing systemic inflammation upon severe trauma, etc.*

## **2. NEGATIVE FINDINGS AND PROBLEMS IN ACCOMPLISHING TASKS:**

***Overall the progress has been substantial, in some respects faster and much better than anticipated. The results have been universally very positive, almost without exception. A few minor difficulties are below. Importantly, these are all technical problems in accomplishing tasks, rather than negative findings that disprove our hypothesis:***

**2.a: Deaths of mice:** We attribute the following negative events to our own mistakes, but we feel obligated to report them for the sake of transparency. Four mice died in the groups where mice received single or multiple injections of flavopiridol, while no deaths occurred in the vehicle-control or un-injected groups. The deaths occurred at 1 to 2 days after intraperitoneal injection of flavopiridol, and we believe it was because the needle accidentally punctured an internal organ rather than staying within the intraperitoneal space. This is from a total of 519 mice used so far in the study, of which between 1/3 and 1/2 of received flavopiridol injections. We also discovered that repeated administering of the Cdk9 inhibitors at the maximum dose is not tolerated by the mice and resulted in death due to severed peritoneal infection. We have used a lower dosage of the drug in the current experiment with multiple injections at a schedule that still effectively prevented the short-term adverse effects of the knee injury, and none of the animals show adverse effects from the drug. We realized that we purchased a bad batch of inhibitor from supplier (Santa-Cruz Biotech). We realized this when performing in-vitro tests using this batch of drug, observing significant cell death under otherwise well-tolerated concentrations. We believe that this was in fact the reason for the mouse deaths we observed. We have switched suppliers to a more reputable source, and now also routinely perform in-vitro (cell-based) toxicity screens with any new batch of drug, before using the drug in animals.

**2.b: Effort and budget underestimated:** I underestimated the amount of effort, and also the budget, required for the proposed studies.

With respect to the effort - in the first year, I was able to recruit unpaid manpower onto this project. Without the uncompensated help of these individuals, progress would not have been as fast. A student from Zhejiang University (a University with which UC Davis has a close connection) joined the project as his PhD

Thesis. He was appointed a Research Associate without Salary position here for 13 months ending in December 2013, and worked full-time (>50hrs/wk) on this project. In addition, two first-year medical students in the UC Davis School of Medicine were awarded research fellowships to complete aspects of this project, and four undergraduate interns put in many hours during the school year and even more hours during the summer to help complete aspects of this project. In addition, contributions from members of other labs were required. Many of these contributors are listed as co-authors in the ORS abstract.

With respect to the budget - prices of everything increased substantially since the original budget proposal, this includes salaries & benefit rates, reagents & supplies, animals, internal recharge rates for services such as in-vivo imaging and microCT, and external services such as histology. We also switched drug suppliers because of lot-to-lot inconsistencies and toxicity of certain lots with the previous supplier. The new supplier is higher quality, but also much higher price. Because of these changes, we limited the analyses that added little further insight into the effect of Cdk9 inhibition on PTOA development. For example, we monitor the most highly responsive mRNAs individually using low-cost RT-PCR assays, rather than purchase 84-cytokine low-density arrays to analyze multiple mRNAs.

In retrospect I attribute the effort/budget underestimation to my own inexperience. My original proposal was an honest (not over-inflated) estimate for doing the proposed work at the time of budget preparation.

Freezer Loss: We had a catastrophic failure of our -80 freezer, resulting in the loss of all archived RNA and serum samples. This was a serious setback, necessitating the repeat of several key experiments.

Long term mouse injury model: Our mouse PTOA model is ideally suited for studying short-term acute responses to injury. However, the injury inevitably leads to PTOA in 8-12 weeks due to altered biomechanics of the joint, making it less than ideal for long-term experiments to evaluate therapeutic efficacy. We have re-engineered our system to also include a new milder model, wherein the cartilage is severely compressed but no changes in biomechanics occur because the ACL stays intact. We will use this model for future long term (8-12 week studies) and use our original ACL rupture model for shorter time points (under 6 weeks). In addition, we have identified that long-term

***In summary, at the end of year 3 we are scientifically on track with excellent results and only very minor setbacks, but somewhat over budget and over-worked.***

## REPORTABLE OUTCOMES

### MANUSCRIPTS, ABSTRACTS, AND PRESENTATIONS

- 2014 Manuscript published in Arthritis & Rheumatology, title “Cyclin-Dependent Kinase 9 inhibition protects cartilage from the catabolic effects of pro-inflammatory cytokines”, PMID: 24470357. Included as Appendix 1. Much of the work for this manuscript was directly funded by this award.
- 2015 Letter to the Editor, and our reply, regarding the results published in Arthritis & Rheumatology. PMID- DOI 10.1002/art.38817. Included as Appendix 2.
- 2016 Manuscript published in European Cells & Materials, title “Inhibition of Cdk9 prevents mechanical injury-induced inflammation, apoptosis, and matrix degradation in cartilage explants”, PMID26859911. Included as Appendix 3. Much of the work for this manuscript was directly funded by this award.
- 2014 Manuscript published in Osteoarthritis and Cartilage, title “In Vivo Fluorescence Reflectance Imaging to Quantify Sex-Based Differences in Protease, MMP, and Cathepsin K Activity in a Mouse Model of Post-Traumatic Osteoarthritis”. Included as Appendix 4. No funds from this grant were used, but the work was greatly facilitated by the expertise we developed through this grant.
- 2015 Manuscript published in Biochem Biophys Res Commun, title “In-vitro and in-vivo imaging of MMP activity in cartilage and joint injury”. Included as Appendix 5. Some funds were used from this grant, and the work was greatly facilitated by the expertise we developed through this grant.
- 2014 Manuscript published in Journal of Orthopaedic Research, title “Comparison of Loading Rate-Dependent Injury Modes in a Murine Model of Post-Traumatic Osteoarthritis”, PMID: 24019199. Included as Appendix 6. No funds from this grant were used, but the work was greatly facilitated by the expertise we developed through this grant.
- 2014 Manuscript published in Biochem Biophys Res Commun, title “High abundant protein removal from rodent blood for biomarker discovery”. Included as Appendix 7. No funds from this grant were used, but the work was influenced by our inability to quantify low-abundance serum cytokine levels in our PTOA model.
- 2015 Manuscript published in Osteoarthritis & Cartilage, title “Non-Invasive mouse models of Post-Traumatic Osteoarthritis”. Included as Appendix 8. This is a review article, enabled by the expertise we developed in mouse PTOA with the funds from this current grant.
- 2015 Book Chapter “Closed-Joint ACL Disruption in Murine Models of Post-Traumatic Arthritis”. Chapter 7 in book “Post-Traumatic Arthritis: Pathogenesis, Diagnosis and Management” edited by Steve Olson and Farshid Guilak. Included as Appendix 9. This is a book chapter directly enabled by the expertise we developed in mouse PTOA with the funds from this current grant.
- 2015 Manuscript published in “Journal of Orthopaedic Trauma”, title “Articular Cartilage Injury and Potential Remedies”. Included as Appendix 10. This is a summary of a session at the annual meeting of the Orthopaedic Trauma Association, made possible by the expertise we developed in mouse PTOA with the funds from this current grant.
- Abstracts, either funded directly by this grant, or enabled by the expertise we developed with funds from this grant.
  - 2013 Poster presentation at World Congress of Osteoarthritis (OARSI), title “Early Transient Induction of IL-6 in a Mouse Joint Injury Model.”
  - 2013 Poster presentation at World Congress of Osteoarthritis (OARSI), title “Fluorescence Reflectance Imaging of Early Processes of Post-Traumatic Osteoarthritis in Male and Female Mice.”
  - 2014 Poster presentation at Orthopaedic Research Society’s 60<sup>th</sup> Annual Meeting in New Orleans. Title “CDK9 inhibition attenuates acute inflammatory response and reduces bone loss in a non-invasive post- traumatic osteoarthritis mouse model.” Appendix 11 pg 95.

- 2015 Poster presentation at Orthopaedic Research Society's 61th Annual Meeting in Las Vegas, March. Title "CDK9 inhibition attenuates inflammatory response and apoptosis in cartilage explants to preserve matrix integrity in a single impact mechanical injury model"
- 2015 Haudenschild DR, Zignego DL, Hu Z, Yik JHN, and June RK. Flavopiridol Restores Global Metabolome in Mouse Post-Traumatic Osteoarthritis. 61th Annual Meeting of the Orthopaedic Research Society (ORS)
- 2015 Yik JHN, Liu N, Shidara K, Cissell D, Athanasiou KA, and Haudenschild DR. Cdk9 Inhibitors Preserve the Mechanical Properties of Osteochondral Explants after Prolonged Storage. 61th Annual Meeting of the Orthopaedic Research Society (ORS) in 2015.
- 2015 Fukui T, Yik JHN, and Haudenschild DR. The Effect of Inhibitors of Brd4 and Cdk9 on Early Phase of Post-Traumatic Osteoarthritis. 61th Annual Meeting of the Orthopaedic Research Society (ORS)
- 2015 Fukui T, Tenborg E, Yik JHN, and Haudenschild DR. In-vitro and in-vivo Imaging of MMP Activity in Cartilage and Joint Injury. 61th Annual Meeting of the Orthopaedic Research Society (ORS)
- 2015 Fukui T, Castillo AB, Russel A, Yik JHN, and Haudenschild DR. Comprehensive Transcriptome Analysis of Aging-Related Changes in Early Phase of Post-Traumatic Osteoarthritis. 61th Annual Meeting of the Orthopaedic Research Society (ORS)
- 2015 Fukui T, Yik JHN, and Haudenschild DR. The In Vivo and In Vitro Effect of Inhibitors of Brd4 and CDK9 on Early Phase of Post Traumatic Osteoarthritis. Poster Presentation, Osteoarthritis Research Society International (OARSI), Seattle, WA
- 2015 Hamil A, Haudenschild DR, Dowdy SF, and June RK. Evidence of In Vivo Drug Delivery via the TAT Protein Transduction Domain. Poster Presentation, Osteoarthritis Research Society International (OARSI), Seattle, WA
- 2016 Wegner AM, Robbins MA, Campos NR, Haddad AF, Christiansen BA, Yik JHN, and Haudenschild DR. Acute Changes in Nox4 Activity in Early Post-Traumatic Osteoarthritis (Poster). Orthopaedic Research Society 2016 Annual Meeting. [Appendix 12 pg 96](#).
- 2016 Yik JHN, Doyran B, Haudenschild DR, and Han L. Early Cellular Responses Degrade Cartilage Mechanical Properties after Joint Injury. OARSI, Amsterdam. [Appendix 13 pg97](#)
- 2016 Adam M. Wegner, Nestor R. Campos, Michael A. Robbins, Andrew F. Haddad, Jasper H.N. Yik, Blaine A. Christiansen, Cathy S. Carlson, Dominik R. Haudenschild. Acute changes in NADPH Oxidase 4 in post-traumatic arthritis . Oxygen Club of California.  
\*\*Orthopaedic Resident Wegner received the "Young Investigator's Award" for this mentored research project
- 2016 Haudenschild DR. Joint Tissue Biomechanics: Joint Responses to Biomechanical Impact (Theories of Growth and Adaptation). OARSI 2016, S4.

- Presentations:

- 2012 November 20, ACL Damage as a Model for Early Osteoarthritis, UC Davis Medical Center Osteoarthritis Meeting, headed by Nancy Lane.
- 2013 January 23, Early Molecular Events in Joint Injury, Invited Seminar at the UC Davis Veterinary Orthopaedic Research Laboratory seminar series.
- 2013 January 28, CDK9 Inhibition Protects Cartilage from the Catabolic Effects of Pro-Inflammatory Cytokines, by Yik JHN (presenting), Kumari R, Christiansen BA, and Haudenschild DR., Session 42 - "MMP Regulation in Articular Chondrocytes" at the 2013 Meeting of the Orthopaedic Research Society in San Antonio, TX.
- 2013 June 5, Osteoarthritis: The need for Imaging Early Stages of Disease, Given at the "Frontiers in Biomedical Imaging" seminar series held by the Radiology Department of UC Davis.

- 2013 June 20, “Early Response to Joint Injury”, University of California Davis Department of Orthopaedic Surgery Research Symposium, Lawrence J. Ellison Musculoskeletal Research Center.
- 2013 October 15, “Early Response to Joint Injury and Osteoarthritis”, UC Davis Department of Orthopaedic Surgery Grand Rounds invited Seminar
- 2014 November 11, “Cdk9, a revolutionary molecular target for suppressing inflammation after knee trauma”, UC Davis Department of Biophysics invited Seminar
- 2015 Fukui T, Tenborg E, Yik JHN, and Haudenschild DR. In-vitro and In-vivo Imaging of MMP Activity with MMPsense in Cartilage and Joint Injury. International Cartilage Repair Society (ICRS) 2015 annual meeting, Oral Presentation by Dr. Fukui.
- 2015 Fukui T, Castillo AB, Yik HJN, and Haudenschild DR. Comprehensive transcriptome analysis of aging-related gene expression in early phase of post-traumatic osteoarthritis. Osteoarthritis Research Society International (OARSI), Oral Presentation by Dr. Fukui.
- 2015 Targeting Acute Joint Injury Responses to Prevent Osteoarthritis, Invited Presentation at University of California San Francisco, to the seminar series organized by Bernard Halloran Group. Yik and Haudenschild, presented by Haudenschild.
- 2015 Targeting Acute Joint Injury Responses to Prevent Osteoarthritis, UC Davis "LIMB" Leaders in Musculoskeletal Biology Seminar Series.
- Arresting Cartilage Degradation after Injury: Focus on Primary Response Genes, UC Davis Dean's Symposium, Translating Basic Science to Clinical Care.
- 2015 , Early Response Gene Activation in Mouse Post-Traumatic Osteoarthritis, Invited presentation at Rush University, Chicago.
- 2015 Early Response Genes in Osteoarthritis Pathogenesis, . Invited Presentation at Lawrence Livermore National Laboratories .
- 2015 Early Response Genes in Osteoarthritis Pathogenesis, UC Davis Presentation to Bruce Hammock Laboratory at UC Davis
- 2016 Fukui T, Yik JHN, Davis J, Adamopoulos IE, and Haudenschild DR. The Effect of Inhibitors of Brd4 and Cdk9 on Post Traumatic Osteoarthritis. (Presented by Tomoaki Fukui), Orthopaedic Research Society (ORS) 2016 Annual Meeting at DisneyWorld, Florida.
- 2016 Osteoarthritis and Mechanobiology, UC Davis New Horizons Translational Research Colloquium.
- 2016 Joint Tissue Biomechanics: Joint Responses to Biomechanical Impact (Theories of Growth and Adaptation), **Invited Plenary Talk** at 2016 Osteoarthritis Research Society International World Congress of Osteoarthritis Meeting, Amsterdam NL

#### **LICENSES APPLIED FOR AND/OR ISSUED**

- None during the last 12 months

#### **DEGREES OBTAINED THAT ARE SUPPORTED BY THIS AWARD**

- None during the last 12 months

#### **DEVELOPMENT OF CELL LINES, TISSUES, OR SERUM REPOSITORIES**

- None during the last 12 months

#### **INFORMATICS SUCH AS DATABASES AND ANIMAL MODELS**

- None during the last 12 months

## **FUNDING APPLIED FOR BASED ON WORK SUPPORTED BY THIS AWARD**

- We applied for an R21 grant to test whether we could reduce systemic inflammation after severe trauma, using similar inhibition of Cdk9 with flavopiridol as in this award. The grant was favorably reviewed (priority score 33) but not funded. We submitted a revision, which was not funded
- We applied for an NIH R01 grant to further study the mechanisms behind Cdk9 inhibition in PTOA. This was scored favorably (23<sup>rd</sup> percentile) but the revision was not discussed.
- We submitted a letter of intent for additional DOD funding (TTDA award through PRMRP), with the overall aims to create a suitable sustained-release formulation of Cdk9 inhibitors for use in larger animal models. The second aim would then test this formulation in a sheep model of PTOA by surgical destabilization of the stifle joint by ACL resection.

## **EMPLOYMENT OR RESEARCH OPPORTUNITIES APPLIED FOR AND/OR RECEIVED BASED ON EXPERIENCE/TRAINING SUPPORTED BY THIS AWARD**

- We obtained funding from the Orthopaedic Trauma Association to study whether we could reduce systemic inflammation after severe trauma, using similar inhibition of Cdk9 with flavopiridol as in this award. This is a \$50,000 award for 2 years ending December 31, 2016. This was used to train an Orthopaedic Resident (Nasser Heyrani) in the surgical procedures involved in creating a polytrauma mouse model.

## **CONCLUSION**

In **conclusion**, the results from these experiments are very positive. Our goal in Aim 1 was to inhibit the early response to joint injury. The data collected thus far conclusively demonstrates that Cdk9 inhibition strongly reduced or even completely prevented every one of the acute local responses to joint injury that we tested. These results are currently being finalized, and readied for submission as two back-to-back manuscripts to Arthritis & Rheumatism.

Given these positive results, both during and in the longer-term studies we proposed in aim 2, we are gearing up for larger animal pre-clinical studies in sheep, using local delivery of Cdk9 inhibitor formulated to provide sustained release of the compound.

## **REFERENCES**

None

## **APPENDICES**

1. Arthritis & Rheumatology Manuscript, Published
2. Arthritis & Rheumatology Letter to the Editor and Reply, Published
3. European Cells & Materials Manuscript, Published
4. Osteoarthritis & Cartilage Manuscript, Published
5. BBRC Manuscript (imaging), Published
6. Journal of Orthopaedic Research Manuscript, Published
7. BBRC Manuscript (biomarkers), Published
8. Osteoarthritis & Cartilage Manuscript, Published
9. Book Chapter, Published
10. Journal of Orthopaedic Trauma Summary, Published

## **SUPPORTING DATA**

All supporting data is contained in the appendices.

# Cyclin-Dependent Kinase 9 Inhibition Protects Cartilage From the Catabolic Effects of Proinflammatory Cytokines

Jasper H. N. Yik,<sup>1</sup> Zi'ang Hu,<sup>2</sup> Ratna Kumari,<sup>3</sup> Blaine A. Christiansen,<sup>1</sup> and Dominik R. Haudenschild<sup>1</sup>

**Objective.** Cyclin-dependent kinase 9 (CDK-9) controls the activation of primary inflammatory response genes. The purpose of this study was to determine whether CDK-9 inhibition protects cartilage from the catabolic effects of proinflammatory cytokines.

**Methods.** Human chondrocytes were challenged with different proinflammatory stimuli (interleukin-1 $\beta$  [IL-1 $\beta$ ], lipopolysaccharides, and tumor necrosis factor  $\alpha$ ) in the presence or absence of either the CDK-9 inhibitor flavopiridol or small interfering RNA (siRNA). The expression of messenger RNA (mRNA) for inflammatory mediator genes, catabolic genes, and anabolic genes were determined by real-time quantitative reverse transcription–polymerase chain reaction (qRT-PCR) analysis. Cartilage explants were incubated for 6 days with IL-1 $\beta$  in the presence or absence of flavopiridol. Cartilage matrix degradation was assessed by the re-

lease of glycosaminoglycan (GAG) and cleaved type II collagen (COL2A) peptides.

**Results.** CDK-9 inhibition by flavopiridol or knockdown by siRNA effectively suppressed the induction of mRNA for inducible nitric oxide synthase by all 3 proinflammatory stimuli. Results from NF- $\kappa$ B–targeted PCR array analysis showed that flavopiridol suppressed IL-1 $\beta$  induction of a broad range of inflammatory mediator genes (59 of 67 tested). CDK-9 inhibition also suppressed the induction of catabolic genes (matrix metalloproteinase 1 [MMP-1], MMP-3, MMP-9, MMP-13, ADAMTS-4, and ADAMTS-5), but did not affect the basal expression of anabolic genes (COL2A, aggrecan, and cartilage oligomeric matrix protein) and housekeeping genes. Flavopiridol had no apparent short-term cytotoxicity, as assessed by G6PDH activity. Finally, in IL-1 $\beta$ –treated cartilage explants, flavopiridol reduced the release of the matrix degradation product GAG and cleaved COL2A peptides, but did not affect long-term chondrocyte viability.

**Conclusion.** CDK-9 activity is required for the primary inflammatory response in chondrocytes. Flavopiridol suppresses the induction of inflammatory mediator genes and catabolic genes to protect cartilage from the deleterious effects of proinflammatory cytokines, without affecting cell viability and functions.

Osteoarthritis (OA) affects more than half of the US population over the age of 65 years. OA is a degenerative disease of the articular joints characterized by slow but progressive loss of cartilage. The main protein component of articular cartilage is a fibrillar network of type II collagen (COL2A), which provides tensile strength to the cartilage. The compressive stiffness of the cartilage is provided by the proteoglycan components, through their attraction of water molecules. Although the cause of OA remains incompletely understood, various inflammatory conditions that cause

Supported by the National Natural Science Fund of China (grants 81101378 and 81271971 to Dr. Hu), University of California Davis (Departmental Startup Funds to Drs. Christiansen and Haudenschild), the Arthritis Foundation (2012 IRG award to Dr. Haudenschild), the US Department of Defense (PRMRP IIRA award PR110507 to Dr. Haudenschild), and the NIH (National Institute of Arthritis and Musculoskeletal and Skin Diseases grant R21-AR-063348 to Dr. Haudenschild).

<sup>1</sup>Jasper H. N. Yik, PhD, Blaine A. Christiansen, PhD, Dominik R. Haudenschild, PhD: University of California Davis, Sacramento, California; <sup>2</sup>Zi'ang Hu, MD: Sir Run Run Shaw Hospital and Zhejiang University, Hangzhou, China, and University of California Davis, Sacramento, California; <sup>3</sup>Ratna Kumari, PhD: University of California Davis, Sacramento, California, and KIIT University, Bhubaneswar, India.

Drs. Yik, Christiansen, and Haudenschild have submitted a patent application for the use of a cyclin-dependent kinase 9 inhibitor in posttraumatic osteoarthritis.

Address correspondence to Dominik R. Haudenschild, PhD, University of California Davis, Department of Orthopaedic Surgery, Lawrence J. Ellison Musculoskeletal Research Center, Research Building 1, Suite 2000, 4635 Second Avenue, Sacramento, CA 95817. E-mail: Dominik.Haudenschild@ucdmc.ucdavis.edu.

Submitted for publication July 2, 2013; accepted in revised form January 21, 2014.

damage to the collagens and proteoglycans in cartilage are suspected of initiating OA.

Proinflammatory cytokines are induced by a variety of stress conditions in cartilage, including joint overloading and physical damage such as occurs in sports-related injuries. Proinflammatory cytokines, such as interleukin 1 $\beta$  (IL-1 $\beta$ ) and tumor necrosis factor  $\alpha$  (TNF $\alpha$ ), elicit a cascade of events that activate inflammatory mediator genes and apoptosis in chondrocytes (for review, see ref. 1). Proinflammatory cytokines can also induce the expression of proteinases that degrade cartilage matrix, including matrix metalloproteinases (MMPs), aggrecanases, and cathepsins (for review, see ref. 2). Therefore, a strategy for effectively suppressing the inflammatory response in cartilage may prevent or delay the onset of OA.

Acute tissue stress and inflammatory signaling activate primary response genes that do not require de novo protein synthesis. Recent advances demonstrate that despite their initiation by diverse signaling pathways, the transcriptional activation of most, if not all, primary response genes is similarly controlled by a general transcription factor (3,4), namely, cyclin-dependent kinase 9 (CDK-9). It was believed for many years that the rate-limiting step in the transcriptional activation of primary response genes is the recruitment of transcription factors and RNA polymerase II (Pol II) complex to the promoters. However, recent studies have shown that in order for these primary response genes to be rapidly activated, the Pol II complex is already preassembled and producing short messenger RNA (mRNA) transcripts in their basal, unstimulated states (3,4). In the absence of inflammatory signals, Pol II remains paused  $\sim$ 40 bp downstream of the transcription start site. Upon inflammatory stimulus, CDK-9 is recruited to the transcription complex by bromodomain-containing protein 4 (BRD-4) through its association with acetylated histones (3,4). Once recruited, CDK-9 phosphorylates Pol II to induce a conformational change that allows Pol II to enter possessive elongation to efficiently transcribe full-length mRNAs (for review, see ref. 5). Thus, CDK-9 regulation represents a central mechanism for activating primary response gene transcription and has a broad impact on many aspects of biologic functions.

Given that CDK-9 controls a common mechanism of all primary response gene activation, it is an attractive target for antiinflammatory therapy (for review, see ref. 6). The objective of this study was to determine whether CDK-9 inhibition effectively suppresses the inflammatory response in chondrocytes and

protects cartilage from the catabolic effects of proinflammatory cytokines in vitro.

## MATERIALS AND METHODS

**Articular chondrocytes and cartilage explants.** Human primary chondrocytes and cartilage explants were isolated from cartilage tissues obtained (with Institutional Review Board approval) at the time of total knee arthroplasty from 15 donors with end-stage OA (ages 44–80 years). Samples were cultured in Dulbecco's modified Eagle's medium (DMEM) with 10% fetal bovine serum (FBS) as described elsewhere (7). The chondrocytes were used in experiments within 3–5 days, without passaging (to avoid dedifferentiation). Samples from 5 of the 15 OA cartilage explant donors were used for the matrix degradation studies. All other experiments were performed with chondrocytes from at least 3 of the 15 OA donors.

Full-thickness bovine cartilage explants from the stifle joints of young veal calves were obtained by 6-mm punch biopsy. Samples were maintained in DMEM with 10% FBS.

**Treatment of chondrocytes with inflammatory stimuli and small-molecule inhibitors.** Primary chondrocytes were seeded in 12-well plates at a density of  $2 \times 10^4$  cells/cm<sup>2</sup> and allowed to reach  $\sim$ 80% confluence ( $\sim 4 \times 10^4$  cells/cm<sup>2</sup>). The cells were treated with 10 ng/ml of lipopolysaccharide (LPS; Sigma), 10 ng/ml of IL-1 $\beta$  (R&D Systems), or 10 ng/ml of TNF $\alpha$  (R&D Systems) for various times, with or without pharmacologic inhibitors. The inhibitors used in this study included flavopiridol (Sigma), JQ-1 (a kind gift from Dr. James Bradner, Harvard University, Boston, MA [8]), BS-181 HCl (Selleckchem), and SNS-032 (Selleckchem). After treatment, the cells were washed 3 times with phosphate buffered saline and harvested for gene and protein expression analyses.

**Lentiviral small interfering RNA (siRNA) constructs.** The CDK-9–targeting siRNA used in this study (AGGGA-CATGAAGGCTGCTAAT) was inserted into the Age I and Eco RI sites of the lentiviral vector pLKO.1 (plasmid no. 8453; Addgene). An siRNA targeting green fluorescent protein (GFP) was used as control. Lentiviral particles were generated and titered as described previously (9). Human chondrocytes were seeded at  $1 \times 10^4$  cells/cm<sup>2</sup> in 12-well plates. Lentiviral particles harboring CDK-9– or GFP–targeting siRNA were then added at a multiplicity of infection of 10, in the presence of 1  $\mu$ g/ml of Polybrene (American Bioanalytical). The medium was replaced after 16 hours, and the cells were used for experiments after 5 days. Knockdown of CDK-9 was confirmed by Western blotting.

**Real-time quantitative reverse transcription–polymerase chain reaction (qRT-PCR).** For the determination of individual mRNA expression, cytokine/inhibitor-treated chondrocytes in 12-well plates were harvested by scraping, transferred to Eppendorf tubes, and subjected to cell lysis and reverse transcription to generate complementary DNA (cDNA) using a Cells-to-C<sub>T</sub> kit (Ambion) according to the manufacturer's instructions. A total of 2  $\mu$ l of cDNA was used for qRT-PCR (in a final volume of 10  $\mu$ l), which was performed in triplicate using a 7900HT RT-PCR system with gene-specific TaqMan probes (Applied Biosystems) according to the manufacturer's instructions. Results were normalized to 18S ribosomal RNA (rRNA) and calculated as the fold change

in mRNA expression relative to untreated controls, using the  $2^{-\Delta\Delta C_t}$  method. The probes used are as follows: for inducible nitric oxide synthase (iNOS), Hs01060345\_m1; for MMP-1, Hs00899658\_m1; for MMP-3, Hs00968305\_m1; for MMP-9, Hs03234579\_m1; for MMP-13, Hs0023992\_m1; for ADAMTS-4, Hs00192708\_m1; for ADAMTS-5, Hs00199841\_m1; for aggrecan, Hs00202971\_m1; for cartilage oligomeric matrix protein (COMP), Hs00154339\_m1; for COL2A, Hs01060345\_m1; and for 18S rRNA, 4319413E.

For PCR array analysis, IL-1 $\beta$ /flavopiridol-treated chondrocytes grown in 10-cm plates were harvested, and total RNA was isolated using an RNeasy Mini kit (Qiagen). RNA quality and quantity were assessed with a NanoDrop 2000 spectrophotometer (Thermo Scientific), and ~500 ng of total RNA was reverse transcribed using a SuperScript First-Strand kit (Invitrogen). RT-PCR was performed using a 7900HT RT-PCR system and PCR Arrays for Human NF- $\kappa$ B Signaling Targets (catalog no. 330231; Qiagen) according to the manufacturer's protocol. PCR array data were analyzed by the accompanying online analysis software provided by Qiagen (available online at [www.qiagen.com](http://www.qiagen.com)).

**Cytotoxicity/viability assays.** To determine the short-term cytotoxic effects of flavopiridol, chondrocytes were seeded in 96-well plates at 1, 5, or 10  $\times 10^3$  cells/well and treated for 5 hours with 300 nM flavopiridol. Cytotoxicity was assessed using a Vybrant cytotoxicity assay kit (catalog no. V23111; Invitrogen) according to the manufacturer's protocol, measuring soluble and total G6PD activity with resazurin as substrate. Fluorescence was detected using a Synergy HT plate reader (BioTek Instruments) with excitation and emission filters set at 528 nm and 635 nm, respectively.

To determine the long-term effects of flavopiridol on the viability of chondrocytes in cartilage, bovine cartilage explants (6-mm disk) in 6-well plates were cultured for 6 days in DMEM and 10% FBS, in the presence or absence of 300 nM flavopiridol, with medium changes every other day. The live and dead cells were stained using a Live/Dead Viability/Cytotoxicity kit (catalog no. L3224; Invitrogen) according to the manufacturer's protocol. The percentages of live and dead cells were determined by counting the cell numbers in 3 random fields of the cross-sectional images of explants captured using a fluorescence microscope. A total of 3 different donors were used.

**Western blot analysis.** Chondrocytes grown in 12-well plates were harvested and lysed with sample loading buffer (50 mM Tris HCl, pH 6.8, 100 mM dithiothreitol, 4% 2-mercaptoethanol, 2% sodium dodecyl sulfate [SDS], and 10% glycerol). Lysates were resolved by 4–12% SDS-polyacrylamide gels and transferred onto nitrocellulose membranes (Bio-Rad). The membranes were blocked with 3% skim milk in TBST (25 mM Tris HCl, pH 7.5; 125 mM NaCl; 0.1% Tween 20), followed by overnight incubation at 4°C with rabbit anti-CDK-9 (0.6  $\mu$ g/ml) (10), mouse anti-MMP-13 (1:500 dilution) (catalog no. IM78; Calbiochem), or mouse anti-GAPDH (1:5,000 dilution) (catalog no. AM4300; Ambion). Blots were then probed with horseradish peroxidase-conjugated secondary antibody (Santa Cruz Biotechnology), and reactive protein bands were visualized with Western Lightning Plus-ECL (PerkinElmer) on radiographic films.

**Assessment of cartilage degradation.** Human cartilage explants (~3-mm cubes) were treated for 6 days with 1 ng/ml

of IL-1 $\beta$ , in the presence or absence of 6 nM or 300 nM flavopiridol (with medium change on day 3). The amount of glycosaminoglycan (GAG) released into the medium from day 3 to day 6 was determined by colorimetric assay using dimethylmethylene blue dye, with chondroitin sulfate as standard (11). The release of COL2A degradation products into the medium was determined by measuring the amount of cleaved COL2A peptides (12) with the use of a C2C enzyme-linked immunosorbent assay kit (Ibex Pharmaceuticals) according to the manufacturer's protocol.

**Statistical analysis.** Values of all measurements were expressed as the mean  $\pm$  SD. Changes in gene expression were analyzed by one-way analysis of variance (ANOVA) using SPSS version 16.0 software. The fold change in mRNA was used as variables to compare samples between different treatment groups. The least significant difference post hoc analysis was conducted using a significance level of  $P < 0.05$ .

## RESULTS

**Role of CDK-9 in the induction of the primary response gene iNOS.** Although the rate-limiting step for transcriptional activation of primary inflammatory response genes in lymphocytes is controlled by CDK-9 (3,4), whether CDK-9 plays a similar role in articular chondrocytes has not been investigated. Therefore, we took advantage of a widely used and well-characterized pharmacologic CDK-9 inhibitor, flavopiridol, to determine the role of CDK-9 in the activation of primary response genes in chondrocytes. To activate primary response genes, chondrocytes in culture were treated with IL-1 $\beta$  in the presence or absence of 300 nM flavopiridol (the effective plasma concentration determined in clinical trials [13]). The induction of the stress response gene iNOS (14) was determined at various time points. The results showed that the level of mRNA for iNOS was unchanged after 1 hour of IL-1 $\beta$  treatment but was induced to significant levels after 3 and 5 hours (Figure 1A). However, cotreatment with flavopiridol completely suppressed the induction of iNOS by IL-1 $\beta$  (Figure 1A). These results indicate a time-dependent induction of iNOS by IL-1 $\beta$  that is sensitive to flavopiridol treatment.

The above findings demonstrated the effects of flavopiridol administered concurrently with the inflammatory cytokines. We next tested whether a delay in the addition of flavopiridol could still suppress iNOS induction by IL-1 $\beta$ . Chondrocytes were treated with IL-1 $\beta$  for a total of 5 hours, with either no delay or a 1- or 3-hour delay in the addition of flavopiridol. The data showed that when compared to no flavopiridol treatment (~235-fold iNOS induction), the addition of flavopiridol markedly repressed iNOS induction if administered without

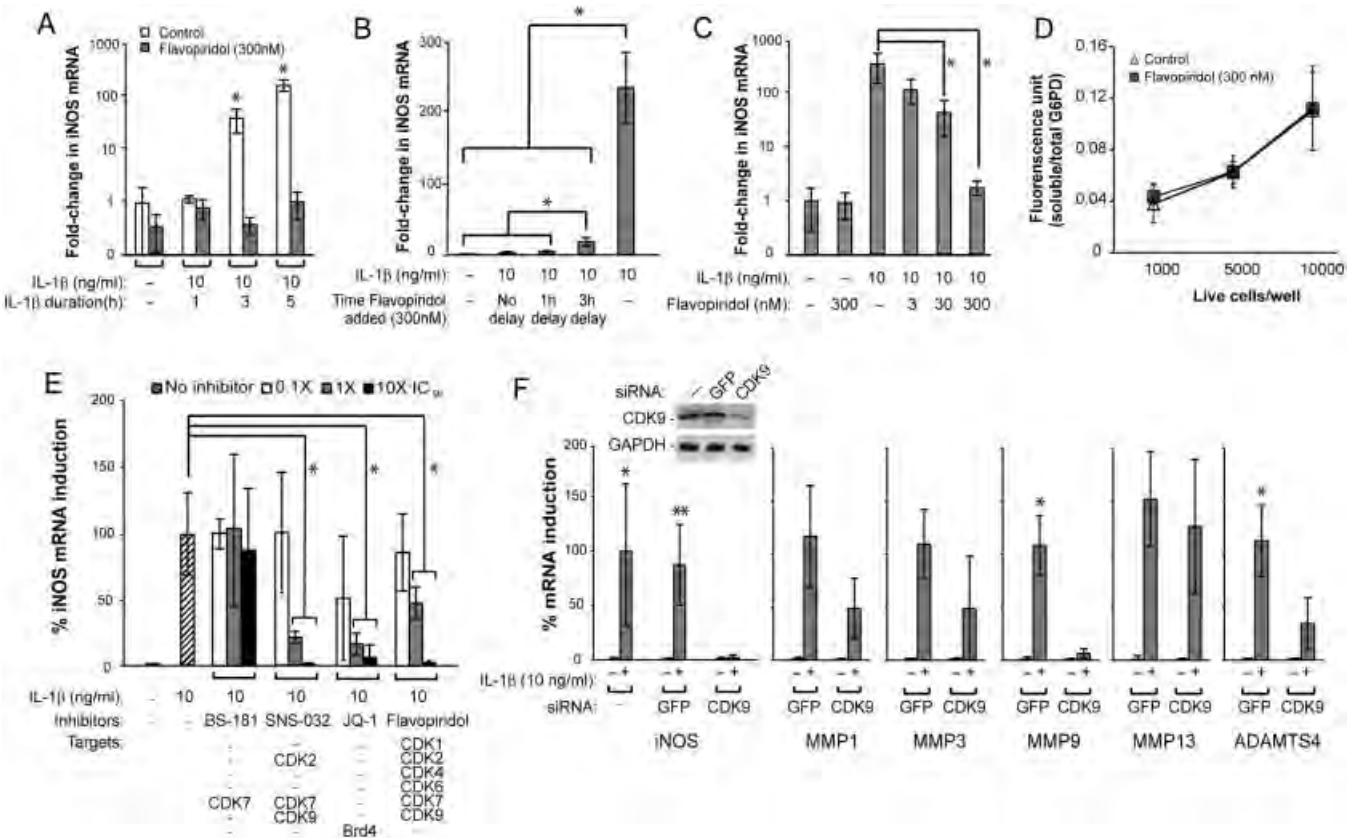


**Figure 1.** Characterization of the effects of flavopiridol-induced cyclin-dependent kinase 9 (CDK-9) inhibition on the induction of inducible nitric oxide synthase (iNOS). **A**, Kinetics of interleukin-1 $\beta$  (IL-1 $\beta$ )-induced iNOS expression. Human chondrocytes were treated with 10 ng/ml of IL-1 $\beta$  in the presence or absence of 300 nM flavopiridol for the indicated times. The fold induction of mRNA for iNOS relative to the untreated control was determined by quantitative reverse transcription-polymerase chain reaction (qRT-PCR) analysis. **B**, Time window of flavopiridol administration for iNOS suppression. Chondrocytes were treated for 5 hours with IL-1 $\beta$  and flavopiridol was added at the indicated time points to determine the window of opportunity for effective suppression of iNOS induction. **C**, Dose-dependent suppression of iNOS induction by flavopiridol. Chondrocytes were treated for 5 hours with IL-1 $\beta$  and flavopiridol was added at the indicated concentrations to determine the dose-response for suppressing iNOS induction. **D**, Cytotoxicity assays. Chondrocytes were seeded in 96-well plates at the indicated cell density, treated for 5 hours with 300 nM flavopiridol, and then soluble/total G6PD activity was measured to determine the cytotoxic effects of flavopiridol. **E**, Suppression of iNOS induction by different inhibitors. Chondrocytes were treated for 5 hours with IL-1 $\beta$  in the presence or absence of the indicated concentrations of various small-molecule inhibitors, and IL-1 $\beta$  induction of mRNA for iNOS was determined (maximum induction in the absence of inhibitor was set at 100%). The selected 50% inhibition concentrations (IC<sub>50</sub>) of various drugs based on their kinase inhibition are as follows: for BS-181, 21 nM for CDK-7; for SNS-032, 60 nM for CDK-7 (used in this experiment) and 4 nM for CDK-9; and for flavopiridol, 30 nM for CDK-9. JQ-1 is not a kinase inhibitor but prevents CDK-9 recruitment to primary response gene promoters through suppression of the binding of bromodomain-containing protein 4 (BRD-4) to acetylated histones at an IC<sub>50</sub> of 300 nM. **F**, Impairment of iNOS and catabolic gene induction by small interfering RNA (siRNA)-mediated depletion of CDK-9. Chondrocytes were transduced with lentiviral particles harboring siRNA against CDK-9 or green fluorescent protein (GFP; control). After 5 days, cells were treated for 5 hours with IL-1 $\beta$  and harvested for Western blotting for protein levels and qRT-PCR for mRNA expression. While IL-1 $\beta$  induction of iNOS was not significantly different between the control (\*) and GFP siRNA (\*\*) groups, iNOS induction was markedly suppressed by CDK-9 knockdown. IL-1 $\beta$ -induced expression of mRNA for matrix metalloproteinases (MMPs) 1, 3, 9, and 13 as well as ADAMTS-4 in cells with GFP siRNA was similar to that of the control (data not shown), but their induction was reduced by CDK-9 siRNA. Values are the mean  $\pm$  SD of 3 different donors. \* =  $P$  < 0.05 versus all other conditions and for the indicated comparisons.

delay (~2.7-fold induction) or with a 1-hour delay (~4-fold induction) (Figure 1B). Although less effective, a 3-hour delay still allowed significant repression of iNOS induction (~18-fold) (Figure 1B). These results indicate that there is at least a 3-hour window of opportunity for administering flavopiridol in order to

suppress iNOS induction after initial treatment with IL-1 $\beta$ .

We next demonstrated that flavopiridol suppressed iNOS induction by IL-1 $\beta$  in a dose-dependent manner, with the most effective dose being 300 nM (Figure 1C). Importantly, there was no apparent cytotoxicity

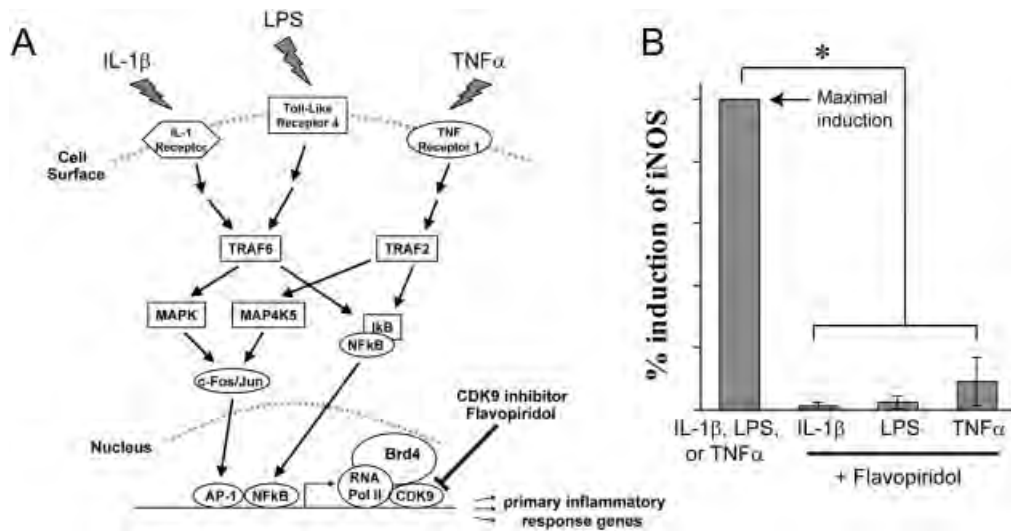


**Figure 2.** Effectiveness of the cyclin-dependent kinase 9 (CDK-9) inhibitor flavopiridol against different inflammatory stimuli. **A**, Activation of inflammatory genes by diverse signals. Multiple proinflammatory stimuli, such as interleukin-1 $\beta$  (IL-1 $\beta$ ), lipopolysaccharide (LPS), and tumor necrosis factor  $\alpha$  (TNF $\alpha$ ), activate their respective cell surface receptors. These signals are then transmitted through different intracellular mediators/pathways, which ultimately converge on CDK-9-dependent transcription of inflammatory genes. Bromodomain-containing protein 4 (BRD-4) recruits CDK-9 to the activated promoters. TRAF6 = TNF receptor-associated factor 6; AP-1 = activator protein 1; RNA Pol II = RNA polymerase II. **B**, Effectiveness of flavopiridol against multiple inflammatory stimuli. Human chondrocytes in monolayer culture were treated for 5 hours with 10 ng/ml of the indicated inflammatory stimuli in the presence or absence of 300 nM flavopiridol. Expression of mRNA for iNOS was determined by real-time quantitative reverse transcription-polymerase chain reaction analysis as a measure of the inflammatory response. The induction of iNOS by each stimulus alone was arbitrarily set at 100% (left bar) and was compared to the value obtained in the samples cotreated with the respective inflammatory stimulus plus flavopiridol. Values are the mean  $\pm$  SD of 3 different donors. \* =  $P < 0.05$  for the indicated comparisons.

icity of flavopiridol when administered at the highest dose on cultured chondrocytes in terms of G6PD activity within the 5-hour period tested (Figure 1D).

Besides CDK-9, flavopiridol has off-target effects that include other CDKs (see Figure 1E). While these CDKs do not affect primary response gene activation directly, we nevertheless used additional CDK inhibitors to rule out their involvement in the suppression of iNOS induction. To this end, we tested the ability of the following 3 small-molecule inhibitors to suppress iNOS induction: BS-181 HCl (specific for CDK-7) (15), SNS-032 (targets CDKs 2, 7, and 9) (16), and JQ-1 (specific for BRD-4, which is required for the function of CDK-9 [8]). The data showed that only SNS-032, JQ-1, and flavopiridol, but not BS-181, suppressed iNOS induction in a dose-dependent manner (Figure 1E), thus effectively ruling out the involvement of CDK-7 in IL-1 $\beta$ -induced iNOS transcription. It is important to note that unlike the other CDK inhibitors we tested, JQ-1 does not directly inhibit the kinase activity of CDK, but rather, it prevents the association of acetylated histones with BRD-4 (8), which specifically recruits CDK-9 to the promoters for activation of the transcription of primary response genes (4,5). Therefore, the above results

strongly suggest that CDK-9 is involved in iNOS induction.

To definitively prove this, we used siRNA to specifically knockdown CDK-9 expression in chondrocytes and then determined the effects on iNOS induction. The results showed that in CDK-9-depleted cells (confirmed by Western blotting [Figure 1F, inset]), IL-1 $\beta$  failed to induce iNOS. Similar results were obtained when other catabolic genes, such as MMPs 1, 3, 9, and 13 as well as ADAMTS-4, were examined (Figure 1F), thus demonstrating the requirement of CDK-9 in catabolic gene induction. Taken together, our results clearly show the specific involvement of CDK-9, but not other CDKs, in the induction of iNOS by IL-1 $\beta$ .

Since flavopiridol is the first small-molecule CDK inhibitor in clinical trials with well-characterized pharmacokinetics, it has the highest potential for translation into clinical studies. Therefore, we used flavopiridol exclusively in the remainder of this study.

**CDK-9 control of the activation of the inflammatory response from diverse signals.** Primary response genes are activated by diverse inflammatory signals. Regardless of the sources, however, most inflammatory signals converge on the rate-limiting step of transcrip-

tional elongation of primary response genes, which is controlled by CDK-9. In order to illustrate this, 3 different inflammatory signaling pathways were selected, namely, IL-1 $\beta$ , lipopolysaccharide, and TNF $\alpha$ . The cellular response to IL-1 $\beta$ , LPS, or TNF $\alpha$  is mediated by 3 distinct pathways: activation of the IL-1 receptor, Toll-Like receptor 4, or TNF receptor type I, respectively (Figure 2A).

Chondrocytes were treated independently with 3 inflammatory stimuli, in the presence or absence of the CDK-9 inhibitor flavopiridol. The expression of mRNA for iNOS, a common effector gene for all 3 pathways (14), was then determined. The results showed that flavopiridol greatly suppressed the activation of iNOS expression by all 3 pathways (Figure 2B), demonstrating the effectiveness and broad range of flavopiridol in preventing the inflammatory response from diverse signals. Thus, our data confirmed previous findings in other cellular systems (4,5) and established CDK-9 as a central regulatory point for the primary inflammatory response in chondrocytes.

**Prevention of the activation of a broad spectrum of inflammatory response genes by inhibition of CDK-9.** To further investigate the effects of CDK-9 inhibition on the activation of other mediators of inflammation, the gene expression profiles of chondrocytes treated for 5 hours with IL-1 $\beta$  were determined by real-time PCR arrays. The PCR array contained 84 key genes responsive to NF- $\kappa$ B signal transduction (Qiagen), which is central to the regulation of multiple cellular processes, such as the inflammatory response, the immune response, and the stress response. The gene expression profiles from 3 chondrocyte donors were averaged and are presented as heat maps, in which low and high relative expression values are represented by green and red colors, respectively (Figure 3). (The array data are available in numerical format upon request from the corresponding author.)

The results showed that IL-1 $\beta$  strongly activated the majority of the 84 NF- $\kappa$ B target genes tested (Figure 3), while CDK-9 inhibition by flavopiridol almost completely abolished the effects of IL-1 $\beta$ . On average, across the 3 chondrocyte donors, CDK-9 inhibition repressed IL-1 $\beta$  activity by more than 86% and suppressed 59 of 67 NF- $\kappa$ B target genes that were activated at least 1.5-fold by IL-1 $\beta$ . Importantly, housekeeping genes, as well as genes not induced by IL-1 $\beta$ , were not affected by flavopiridol. These data demonstrated that CDK-9 can be targeted to effectively suppress only the activation of a cascade of downstream inflammatory response genes, without affecting the basal expression of nonresponsive genes.

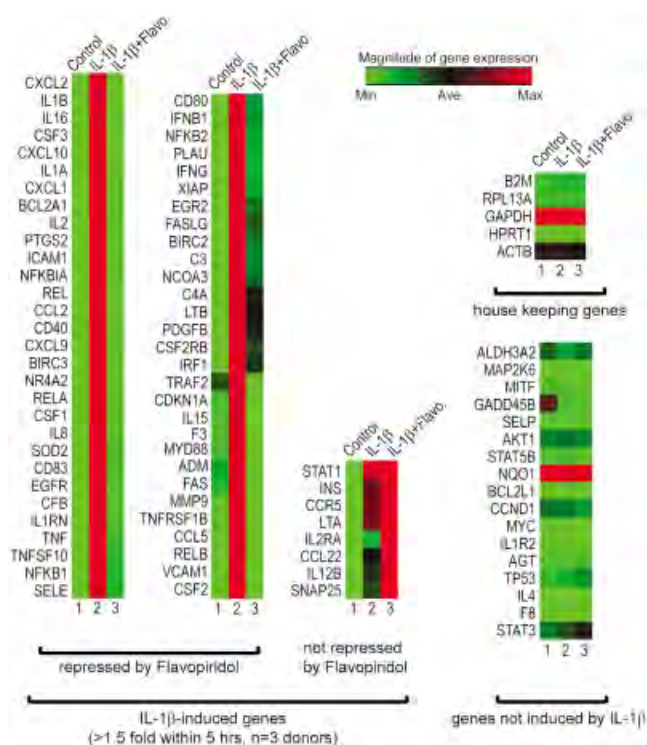


**Figure 3.** Effectiveness of flavopiridol (flavo.) in suppressing the induction of a broad range of inflammatory mediators. Primary human chondrocytes ( $n = 3$  different donors) in monolayer culture were treated for 5 hours with 10 ng/ml of interleukin-1 $\beta$  (IL-1 $\beta$ ) in the presence or absence of 300 nM flavopiridol. Gene expression was analyzed using real-time polymerase chain reaction arrays for NF- $\kappa$ B targets, and the results are shown as heat maps, where green indicates minimum expression and red indicates maximum expression. Of the 84 NF- $\kappa$ B target genes tested, 67 were induced >1.5-fold by IL-1 $\beta$  (compare lane 1 with lane 2). Flavopiridol almost completely abolished the effects of IL-1 $\beta$  in 59 of these 67 genes (lane 3). Importantly, housekeeping genes and noninducible genes were unaffected by either IL-1 $\beta$  or flavopiridol.

**Prevention of catabolic gene activation, but no effect on basal expression of anabolic genes, by inhibition of CDK-9 in chondrocytes.** Besides activating the acute-phase inflammatory response genes, proinflammatory cytokines, such as IL-1 $\beta$  and TNF $\alpha$ , can also stimulate the expression of catabolic genes in chondrocytes (2,17). These catabolic genes include the various matrix MMPs and ADAMTS genes that degrade the cartilage matrix. Given the role of CDK-9 in the activation of inflammatory genes, we next examined the effects of CDK-9 inhibition on the induction of MMPs and ADAMTS in chondrocytes treated independently with IL-1 $\beta$ , LPS, and TNF $\alpha$  for 5 hours. The results showed that the IL-1 $\beta$ -mediated up-regulation of mRNA for MMPs 1, 3, 9, and 13 as well as ADAMTS-4 was markedly suppressed by cotreatment with flavopiri-

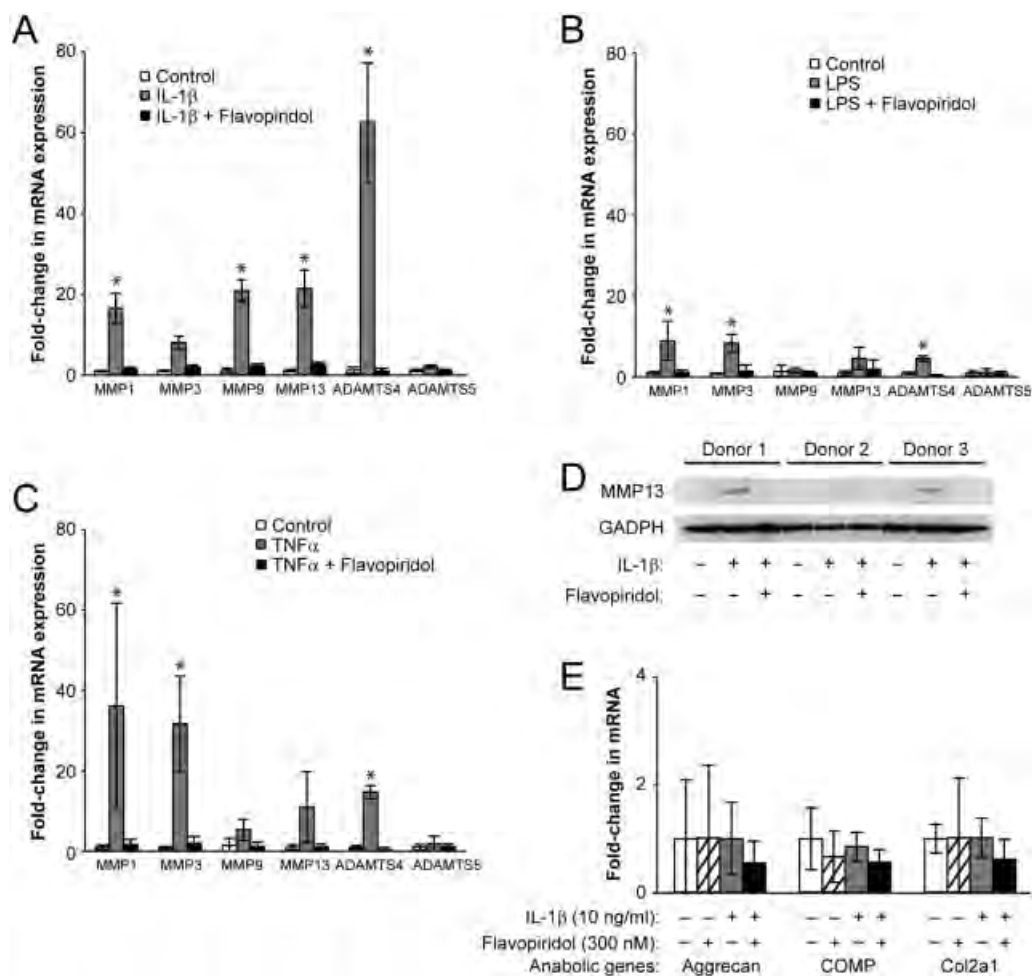


**Figure 4.** Cyclin-dependent kinase 9 inhibition and prevention of the induction of matrix metalloproteinase (MMP) and ADAMTS expression by various inflammatory stimuli. **A–C**, Primary chondrocytes were treated for 5 hours with 10 ng/ml of interleukin-1 $\beta$  (IL-1 $\beta$ ) (**A**), lipopolysaccharide (LPS) (**B**), or tumor necrosis factor  $\alpha$  (TNF $\alpha$ ) (**C**) in the presence or absence of 300 nM flavopiridol, and the relative expression of mRNA for the cartilage-degrading enzymes MMPs 1, 3, 9, and 13 as well as ADAMTS-4 and ADAMTS-5 was determined by real-time quantitative reverse transcription–polymerase chain reaction (qRT-PCR) analysis. **D**, Human chondrocytes from 3 different donors were grown in 6-well plates and treated for 2 days with 10 ng/ml of IL-1 $\beta$  in the presence or absence of 300 nM flavopiridol. Expression of cell-associated active MMP-13 protein (~48 kD) was suppressed by flavopiridol, as determined by Western blotting. GAPDH was included as a loading control. **E**, Chondrocytes were treated for 5 hours with IL-1 $\beta$  and/or flavopiridol, and the expression of mRNA for the cartilage matrix genes aggrecan, cartilage oligomeric matrix protein (COMP), and type II collagen (COL2A) was determined by qRT-PCR analysis. Basal expression of these anabolic genes was not affected by treatment with flavopiridol. Values are the mean  $\pm$  SD of 3 different donors. \* =  $P < 0.05$  versus the other experimental conditions and for the indicated comparisons.

dol (Figure 4A). Similar trends were observed in LPS- or TNF $\alpha$ -treated samples (Figures 4B and C). These data indicated that CDK-9 inhibition prevented the transcriptional activation of catabolic genes in chondrocytes.

Next, we sought to confirm the up-regulation of MMP-13 at the protein level, which is implicated in collagen degradation and osteoarthritis (18). Chondrocytes were treated for 2 days with IL-1 $\beta$ , with or without flavopiridol. Cell-associated active MMP-13 protein (~48 kD) was then detected by Western blotting. The

data showed that MMP-13 protein expression was elevated in all 3 donors treated with IL-1 $\beta$ , but remained at basal levels with IL-1 $\beta$  plus flavopiridol treatment (Figure 4D). Thus, the results of the protein expression analysis corroborated the mRNA expression profiles of MMP-13. In contrast, the mRNA expression of selected anabolic genes (aggrecan, COMP, and COL2a) in chondrocytes was not significantly affected by IL-1 $\beta$  or flavopiridol within the same 5-hour time frame (Figure 4E). Taken together, these results demonstrate that

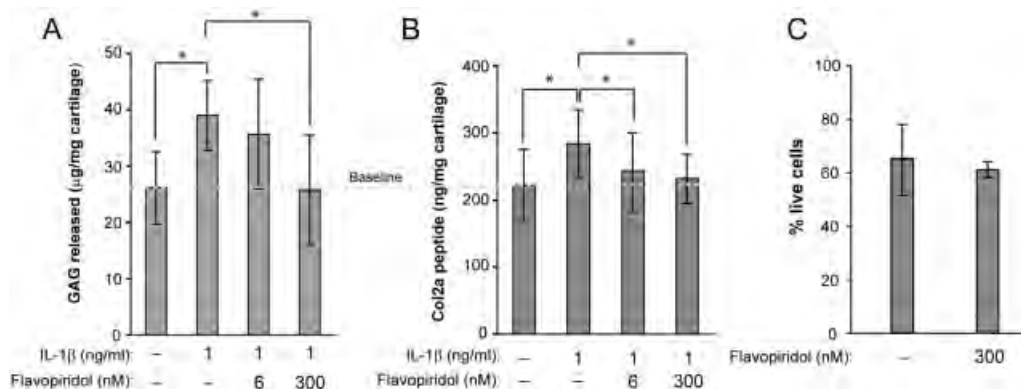


**Figure 5.** Protection of cartilage from the catabolic effects of interleukin-1 $\beta$  (IL-1 $\beta$ ) by inhibition of cyclin-dependent kinase 9. **A**, Breakdown of glycosaminoglycans (GAGs) in cartilage explants. Explants of human arthritic cartilage samples (3-mm cubes) were treated for 6 days with 1 ng/ml of IL-1 $\beta$  and the indicated concentrations of flavopiridol (medium change on day 3). The amount of GAG released into the medium was measured by dimethylmethylene blue dye binding assay. Results were normalized to the wet weight of the explants. Treatment with IL-1 $\beta$  alone caused cartilage degradation, as indicated by increased GAG release. In the presence of 300 nM flavopiridol, levels of GAG release returned to baseline. **B**, Degradation of type II collagen (COL2A) in human cartilage explants. Samples from 5 donors were treated for 6 days with 1 ng/ml of IL-1 $\beta$  with the indicated concentrations of flavopiridol (medium change on day 3). The amount of cleaved COL2A peptides released into the medium was measured by enzyme-linked immunosorbent assay for a serum biomarker of type II collagen degradation (C2C). Results were normalized to the wet weight of the explants. Treatment with IL-1 $\beta$  alone caused cartilage degradation, as indicated by increased levels of COL2A peptides. In the presence of flavopiridol, the levels returned to baseline. Values in **A** and **B** are the mean  $\pm$  SD of 5 different donors. \* =  $P < 0.05$  for the indicated comparisons. **C**, No reduction in chondrocyte viability following long-term treatment of bovine cartilage explants with flavopiridol. Bovine cartilage explants (6-mm full-thickness disks;  $n = 3$  donors) were treated for 6 days in the presence or absence of 300 nM flavopiridol. The explants were sliced in half and stained with Live/Dead stain as described in Materials and Methods. The numbers of live and dead cells in 3 random fields were counted, and the percentages of live cells were calculated. Values are the mean  $\pm$  SD.

flavopiridol selectively suppresses only the induction of catabolic genes by proinflammatory stimuli while having negligible effects on the basal expression of anabolic genes.

**Protection of cartilage from the catabolic effects of IL-1 $\beta$  by inhibition of CDK-9.** Since CDK-9 inhibition suppresses the activation of inflammatory genes and catabolic enzymes in chondrocytes, we next determined whether flavopiridol could protect cartilage from the deleterious effects of proinflammatory cytokines. Explants of human arthritic cartilage samples were isolated and cultured for 6 days in medium containing 1 ng/ml of IL-1 $\beta$  in the presence or absence of flavopiridol. Note that the concentration of IL-1 $\beta$  was reduced from the 10 ng/ml used in the short-term monolayer cultures, to a level similar to those detected in the synovial fluid samples from inflamed joints (19–21). Degradation of cartilage matrix was then assessed by measuring the release of GAG and COL2A cleavage peptides into the culturing medium.

As expected, IL-1 $\beta$  treatment increased the amount of both GAG (Figure 5A) and COL2A peptides (Figure 5B) released by human cartilage samples into the medium. However, the concentrations of both GAG and COL2A peptides were reduced by treatment with 6 nM flavopiridol and returned to baseline levels by treat-

ment with 300 nM flavopiridol (Figures 5A and B). Thus, our data provide evidence that CDK-9 inhibition prevents the catabolic destruction of cartilage by IL-1 $\beta$ .

Importantly, the percentages of live/dead cells in bovine cartilage explants were similar in both untreated and flavopiridol-treated samples (Figure 5C). This result indicates that prolonged treatment of cartilage with flavopiridol did not have an adverse effect on the viability of chondrocytes in cartilage explants. Taken together, our data indicate that CDK-9 inhibition protects cartilage explants from the catabolic effects of IL-1 $\beta$ .

## DISCUSSION

The cause of primary OA remains incompletely understood, and involvement of the inflammatory response is a subject of some controversy. However, it is well established that damage to the collagen network originates around chondrocytes at the cartilage matrix surface (22). Since the inflammatory response induces chondrocyte apoptosis and cartilage matrix breakdown (2), there are several anti-OA strategies that target either specific branches of the inflammatory signaling cascade (e.g., IL-1, IL-6, TNF $\alpha$ , and NF- $\kappa$ B inhibitors) (17,23,24) or downstream events (e.g., apoptosis with

caspase inhibitors) (1). However, because inflammation can be induced by a variety of stimuli, the above individual approaches would have limited effectiveness in handling the diverse simultaneous challenges in a biologic system, as well as limited abilities in efficiently suppressing a broad range of inflammatory mediator expression. A novel approach to addressing these limitations is to directly target CDK-9, which activates transcription of primary inflammatory response genes. Using the pharmacologic CDK-9 inhibitor flavopiridol, we showed that cartilage can be protected from the harmful effects of proinflammatory cytokines.

Our study is the first to demonstrate in chondrocytes that flavopiridol effectively suppresses the acute response to multiple inflammatory stimuli (Figure 2) and prevents the induction of a broad range of inflammatory mediators (Figure 3), as well as catabolic genes that contribute to the degradation of the cartilage matrix (Figure 4). In most cases, flavopiridol almost completely abolished the activation of inflammatory mediator expression. For example, with the PCR array data (Figure 3 and data available in numerical format upon request from the corresponding author), IL-1 $\beta$  induced the expression of IL-6 by 492-fold, but by only 4.2-fold in the presence of flavopiridol, representing a 99.2% repression of IL-1 $\beta$ -dependent transcription.

Importantly, our data demonstrate the selectivity of flavopiridol-mediated inhibition, in which only the IL-1 $\beta$ -inducible genes are suppressed, but not the basal expression of noninducible genes, housekeeping genes (Figure 3), and the anabolic genes (COL2A, COMP, and aggrecan) in chondrocytes (Figure 4E). The gene expression profiles are further supported by the experiments demonstrating flavopiridol can effectively prevent cartilage degradation induced by IL-1 $\beta$  (Figures 5A and B). The reduction in matrix degradation products was not due to changes in cell viability in cartilage treated with flavopiridol, since staining for live/dead cells revealed similar chondrocyte viabilities in control and flavopiridol-treated bovine cartilage explants (Figure 5C). Bovine cartilage was used instead of human cartilage because normal, healthy human cartilage is not routinely available and because the ratio of live to dead cells in arthritic human cartilage obtained at the time of knee surgery was erratic even when adjacent areas were examined.

Flavopiridol is an ATP analog that preferentially inhibits CDK-9 kinase activity ( $K_i = 30$  nM) by a high-affinity interaction with its ATP-binding pocket (25). Although flavopiridol can potentially inhibit other CDKs, numerous studies using a combination of specific

inhibitors and siRNA have demonstrated that only CDK-9 inhibition is responsible for the antiinflammatory action of flavopiridol (26,27). We have also shown that both JQ-1-mediated inhibition of BRD-4, which does not directly interact with other CDKs (10), and siRNA-mediated inhibition of CDK-9 lead to the loss of IL-1 $\beta$ -mediated induction of iNOS in chondrocytes (Figures 1E and F). In addition, we did not document a pronounced effect of other CDKs involved in cell cycle regulation on the transcriptional activation of a broad range of primary response genes within the 5-hour time frame used in this study. Therefore, our results provide strong evidence that only CDK-9 is responsible for the activation of primary response genes in chondrocytes.

Flavopiridol was originally known for its antiproliferation properties by suppressing cell-cycle progression in rapidly dividing cells (e.g., cancers) or in cells with a short lifespan (e.g., neutrophils). Its pharmacologic activity has been well-documented over the last 2 decades because of its use in clinical trials as an antiproliferation/anticancer agent (for review, see ref. 28). Sekine et al (29) demonstrated that systemic administration of flavopiridol reduced synovial hyperplasia without inducing apoptosis, and as a result, it prevented the development of rheumatoid arthritis in a collagen-induced mouse model. However, it is not known whether the antiarthritic activity of flavopiridol is due to the systematic suppression of the leukocyte-mediated immune response to the injected collagen or to the localized suppression of the inflammatory response of chondrocytes in cartilage.

Our group of investigators has developed a non-invasive knee injury mouse model for posttraumatic OA (30). Preliminary data indicate that systemic administration of flavopiridol effectively suppresses the production of proinflammatory cytokines locally at the injured knee, thus confirming our in vitro findings detailed in the present study. Future experiments are needed to determine whether flavopiridol treatment will prevent or delay the development of posttraumatic OA in our mouse model or in other existing models of posttraumatic OA (31,32).

In summary, our data for the first time demonstrate the absolute requirement of CDK-9 activity in the activation of primary response genes in human chondrocytes. In addition, our data strongly indicate that flavopiridol is an effective agent to prevent the activation of acute inflammatory response and catabolic pathways in cartilage. Our results thus may provide a new strategy to prevent or delay the onset of OA.

## AUTHOR CONTRIBUTIONS

All authors were involved in drafting the article or revising it critically for important intellectual content, and all authors approved the final version to be published. Dr. Haudenschild had full access to all of the data in the study and takes responsibility for the integrity of the data and the accuracy of the data analysis.

**Study conception and design.** Yik, Hu, Kumari, Christiansen, Haudenschild.

**Acquisition of data.** Yik, Hu, Kumari, Haudenschild.

**Analysis and interpretation of data.** Yik, Hu, Kumari, Haudenschild.

## REFERENCES

- Lotz MK, Kraus VB. New developments in osteoarthritis: post-traumatic osteoarthritis: pathogenesis and pharmacological treatment options [review] [published erratum appears in *Arthritis Res Ther* 2010;12:408]. *Arthritis Res Ther* 2010;12:211.
- Goldring MB, Otero M, Tsuchimochi K, Ijiri K, Li Y. Defining the roles of inflammatory and anabolic cytokines in cartilage metabolism. *Ann Rheum Dis* 2008;67 Suppl 3:iii75–82.
- Hargreaves DC, Horng T, Medzhitov R. Control of inducible gene expression by signal-dependent transcriptional elongation. *Cell* 2009;138:129–45.
- Zippo A, Serafini R, Rocchigiani M, Pennacchini S, Krepelova A, Oliviero S. Histone crosstalk between H3S10ph and H4K16ac generates a histone code that mediates transcription elongation. *Cell* 2009;138:1122–36.
- Zhou Q, Yik JH. The Yin and Yang of P-TEFb regulation: implications for human immunodeficiency virus gene expression and global control of cell growth and differentiation. *Microbiol Mol Biol Rev* 2006;70:646–59.
- Krystof V, Baumli S, Furst R. Perspective of cyclin-dependent kinase 9 (CDK9) as a drug target. *Curr Pharm Des* 2012;18:2883–90.
- Li H, Haudenschild DR, Posey KL, Hecht JT, Di Cesare PE, Yik JH. Comparative analysis with collagen type II distinguishes cartilage oligomeric matrix protein as a primary TGF $\beta$ -responsive gene. *Osteoarthritis Cartilage* 2011;19:1246–53.
- Filippakopoulos P, Qi J, Picaud S, Shen Y, Smith WB, Fedorov O, et al. Selective inhibition of BET bromodomains. *Nature* 2010;468:1067–73.
- Dull T, Zufferey R, Kelly M, Mandel RJ, Nguyen M, Trono D, et al. A third-generation lentivirus vector with a conditional packaging system. *J Virol* 1998;72:8463–71.
- Yang Z, Yik JH, Chen R, He N, Jang MK, Ozato K, et al. Recruitment of P-TEFb for stimulation of transcriptional elongation by the bromodomain protein Brd4. *Mol Cell* 2005;19:535–45.
- Farndale RW, Buttle DJ, Barrett AJ. Improved quantitation and discrimination of sulphated glycosaminoglycans by use of dimethylmethylene blue. *Biochim Biophys Acta* 1986;883:173–7.
- Poole AR, Ionescu M, Fitzcharles MA, Billingham RC. The assessment of cartilage degradation in vivo: development of an immunoassay for the measurement in body fluids of type II collagen cleaved by collagenases. *J Immunol Methods* 2004;294:145–53.
- Fornier MN, Rathkopf D, Shah M, Patil S, O'Reilly E, Tse AN, et al. Phase I dose-finding study of weekly docetaxel followed by flavopiridol for patients with advanced solid tumors. *Clin Cancer Res* 2007;13:5841–6.
- Maier R, Bilbe G, Rediske J, Lotz M. Inducible nitric oxide synthase from human articular chondrocytes: cDNA cloning and analysis of mRNA expression. *Biochim Biophys Acta* 1994;1208:145–50.
- Ali S, Heathcote DA, Kroll SH, Jogalekar AS, Scheiper B, Patel H, et al. The development of a selective cyclin-dependent kinase inhibitor that shows antitumor activity. *Cancer Res* 2009;69:6208–15.
- Heath EI, Bible K, Martell RE, Adelman DC, Lorusso PM. A phase 1 study of SNS-032 (formerly BMS-387032), a potent inhibitor of cyclin-dependent kinases 2, 7 and 9 administered as a single oral dose and weekly infusion in patients with metastatic refractory solid tumors. *Invest New Drugs* 2008;26:59–65.
- Kobayashi M, Squires GR, Mousa A, Tanzer M, Zukor DJ, Antoniou J, et al. Role of interleukin-1 and tumor necrosis factor  $\alpha$  in matrix degradation of human osteoarthritic cartilage. *Arthritis Rheum* 2005;52:128–35.
- Wang M, Sampson ER, Jin H, Li J, Ke QH, Im HJ, et al. MMP13 is a critical target gene during the progression of osteoarthritis. *Arthritis Res Ther* 2013;15:R5.
- Fiocco U, Sfriso P, Oliviero F, Roux-Lombard P, Scagliori E, Cozzi L, et al. Synovial effusion and synovial fluid biomarkers in psoriatic arthritis to assess intraarticular tumor necrosis factor- $\alpha$  blockade in the knee joint. *Arthritis Res Ther* 2010;12:R148.
- McNiff PA, Stewart C, Sullivan J, Showell HJ, Gabel CA. Synovial fluid from rheumatoid arthritis patients contains sufficient levels of IL-1 $\beta$  and IL-6 to promote production of serum amyloid A by Hep3B cells. *Cytokine* 1995;7:209–19.
- Deirmengian C, Hallab N, Tarabishy A, Della Valle C, Jacobs JJ, Lonner J, et al. Synovial fluid biomarkers for periprosthetic infection. *Clin Orthop Relat Res* 2010;468:2017–23.
- Hollander AP, Pidoux I, Reiner A, Rorabeck C, Bourne R, Poole AR. Damage to type II collagen in aging and osteoarthritis starts at the articular surface, originates around chondrocytes, and extends into the cartilage with progressive degeneration. *J Clin Invest* 1995;96:2859–69.
- Attur M, Millman JS, Dave MN, Al-Mussawir HE, Patel J, Palmer G, et al. Glatiramer acetate (GA), the immunomodulatory drug, inhibits inflammatory mediators and collagen degradation in osteoarthritis (OA) cartilage. *Osteoarthritis Cartilage* 2011;19:1158–64.
- Attur MG, Dave M, Cipolletta C, Kang P, Goldring MB, Patel IR, et al. Reversal of autocrine and paracrine effects of interleukin 1 (IL-1) in human arthritis by type II IL-1 decoy receptor: potential for pharmacological intervention. *J Biol Chem* 2000;275:40307–15.
- Ni W, Ji J, Dai Z, Papp A, Johnson AJ, Ahn S, et al. Flavopiridol pharmacogenetics: clinical and functional evidence for the role of SLCO1B1/OATP1B1 in flavopiridol disposition. *PLoS One* 2010;5:e13792.
- Wang K, Hampson P, Hazeldine J, Krystof V, Strnad M, Pechan P, et al. Cyclin-dependent kinase 9 activity regulates neutrophil spontaneous apoptosis. *PLoS One* 2012;7:e30128.
- Schmerwitz UK, Sass G, Khandoga AG, Joore J, Mayer BA, Berberich N, et al. Flavopiridol protects against inflammation by attenuating leukocyte-endothelial interaction via inhibition of cyclin-dependent kinase 9. *Arterioscler Thromb Vasc Biol* 2011;31:280–8.
- Wang LM, Ren DM. Flavopiridol, the first cyclin-dependent kinase inhibitor: recent advances in combination chemotherapy. *Mini Rev Med Chem* 2010;10:1058–70.
- Sekine C, Sugihara T, Miyake S, Hirai H, Yoshida M, Miyasaka N, et al. Successful treatment of animal models of rheumatoid arthritis with small-molecule cyclin-dependent kinase inhibitors. *J Immunol* 2008;180:1954–61.
- Christiansen BA, Anderson MJ, Lee CA, Williams JC, Yik JH, Haudenschild DR. Musculoskeletal changes following non-invasive knee injury using a novel mouse model of post-traumatic osteoarthritis. *Osteoarthritis Cartilage* 2012;20:773–82.
- Glasson SS, Blanchet TJ, Morris EA. The surgical destabilization of the medial meniscus (DMM) model of osteoarthritis in the 129/SvEv mouse. *Osteoarthritis Cartilage* 2007;15:1061–9.
- Furman BD, Strand J, Hembree WC, Ward BD, Guilak F, Olson SA. Joint degeneration following closed intraarticular fracture in the mouse knee: a model of posttraumatic arthritis. *J Orthop Res* 2007;25:578–92.

2. Stylianou E, Saklatvala J. Interleukin-1. *Int J Biochem Cell Biol* 1998;30:1075–9.
3. Tang C, Sula MJ, Bohnet S, Rehman A, Taishi P, Krueger JM. Interleukin-1 $\beta$  induces CREB-binding protein (CBP) mRNA in brain and the sequencing of rat CBP. *Brain Res Mol Brain Res* 2005;137:213–22.
4. Sambol EB, Ambrosini G, Geha RC, Kennealey PT, DeCarolis P, O'Connor R, et al. Flavopiridol targets c-KIT transcription and induces apoptosis in gastrointestinal stromal tumor cells. *Cancer Res* 2006;66:5858–66.

DOI 10.1002/art.38817

**Reply***To the Editor:*

We are appreciative that Chung took the time to carefully read our article and bring up interesting and salient points for discussion. We agree that some genes do not seem to “fit” with the conclusion that flavopiridol inhibits the induction of inflammatory mediator genes. However, we believe that we accurately represented the data by stating that most genes were not induced by IL-1 $\beta$  in the presence of flavopiridol, and that we were transparent by also showing genes that were exceptions and by including the raw data as supplemental information.

In our study, the response of some genes was not expected, especially the responses of *CCR5* and *STAT1*, both of which are implicated in inflammatory arthritis and osteoarthritis (1–3). For example, CDK-9 inhibition in the presence of interferon- $\gamma$  inhibited *STAT1* activation and downstream effects in other cell types (4). It would be reasonable to expect a similar response to IL-1 $\beta$ . Although messenger RNA levels (e.g., of *STAT1* and *CCR5*) may not always correspond to protein levels or biologic activity, protein levels or biologic activities were not examined, because that was beyond the scope of the current study. We agree that further analysis of these genes would better explain the exact relationship of IL-1 and CDK-9/flavopiridol with these particular inflammatory mediators, especially in the context of cartilage and chondrocytes.

There are several additional points to consider when evaluating these unexpected findings. First, in our experiments we used a 5-hour time point for the PCR array analysis. This time point was chosen because it yielded high-magnitude responses to the IL-1 $\beta$  treatment, but it does not necessarily preclude the possibility of secondary responses that are not regulated in the same CDK-9-dependent manner. Second, primary human cell strains and human cartilage explants remain largely untested with respect to CDK-9/flavopiridol and the regulation of primary response gene transcriptional elongation. These cells and tissues may not respond exactly as the other cell lines or tissues in the studies referenced by Chung. Finally, there is considerable variation in the response of human cartilage and isolated chondrocytes to IL-1 $\beta$ . In our study, we repeated all experiments on samples from least 3 different human donors, indicating that the results shown are somewhat reproducible for both the expected responses and the unexpected responses of genes such as *CCR5* and *STAT1*.

In summary, most of the inflammatory genes in the PCR array panel responded similarly, although there were a few outliers that had unexpected responses. Given the important roles of some of these outliers in arthritis, their relationship with the CDK-9–flavopiridol axis is fertile ground for further investigations.

Dominik R. Haudenschild, PhD  
Jasper H. N. Yik, PhD  
*University of California, Davis  
Sacramento, CA*

1. Kasperkovitz PV, Verbeet NL, Smeets TJ, van Rietschoten JG, Kraan MC, Kraan T, et al. Activation of the STAT1 pathway in rheumatoid arthritis. *Ann Rheum Dis* 2004;63:233–9.
2. Lee YH, Bae SC, Song GG. Association between the chemokine receptor 5  $\Delta 32$  polymorphism and rheumatoid arthritis: a meta-analysis. *Mod Rheumatol* 2013;23:304–10.
3. Qin SX, Rottman JB, Myers P, Kassam N, Weinblatt M, Loetscher M, et al. The chemokine receptors CXCR3 and CCR5 mark subsets of T cells associated with certain inflammatory reactions. *J Clin Invest* 1998;101:746–54.
4. Terashima T, Hague A, Kajita Y, Takeuchi A, Nakagawa T, Yokochi T. Flavopiridol inhibits interferon- $\gamma$ -induced nitric oxide production in mouse vascular endothelial cells. *Immunol Lett* 2012;148:91–6.

DOI 10.1002/art.38812

**Fibromyalgia syndrome and small-fiber neuropathy:  
comment on the article by Caro and Winter**

*To the Editor:*

I read with interest the recent article by Caro and Winter (1), in which they reported decreased epidermal nerve fiber density (ENFD) in a series of 41 patients with fibromyalgia (FM), in accordance with other recent studies suggesting the involvement of small nerve fibers in FM as shown by reduced ENFD (2–4) and abnormal function of silent C-fiber nociceptors (5). These findings strengthen the concept that pain in FM syndrome is actually of the neuropathic type and point to the role of peripheral components, apparently opposite to the current opinion of FM as a condition characterized by central pain amplification (6).

Unfortunately, Caro and Winter reported only that the overall mean ENFD was lower in patients compared with controls, without detailing the findings in individual cases. This is a crucial point, because the involvement of small nerve fibers seems to be limited to a subset of patients with FM. In previous studies by Oaklander et al (3) and Giannoccaro et al (4), only a minority of patients had reduced intraepidermal ENFD in skin biopsy specimens. Üçeyler et al (2) reported abnormalities in the function and morphology of small fibers in all 25 FM patients they studied. However, direct evidence of damage to small fibers was provided by reduced intraepidermal ENFD in only 16 patients, whereas the remaining patients had abnormal results on other tests (quantitative sensory testing and pain-related evoked potentials) that are not strictly specific for small fibers but rather investigate the whole length of the somatosensory system. In contrast, Serra et al (5) demon-

## INHIBITION OF CDK9 PREVENTS MECHANICAL INJURY-INDUCED INFLAMMATION, APOPTOSIS AND MATRIX DEGRADATION IN CARTILAGE EXPLANTS

Z. Hu<sup>1,2,#</sup>, J.H.N. Yik<sup>2,#</sup>, D.D. Cissell<sup>3</sup>, P.V. Michelier<sup>2</sup>, K.A. Athanasiou<sup>3,1</sup> and D.R. Haudenschild<sup>2,\*</sup>

<sup>1</sup>Department of Orthopaedic Surgery, Sir Run Run Shaw Hospital, School of Medicine, Zhejiang University, Hangzhou, 310016 PR China.

<sup>2</sup>University of California Davis, Department of Orthopaedic Surgery, Lawrence J. Ellison Musculoskeletal Research Center, Research Building 1 Suite 2000, 4635 Second Avenue, Sacramento, CA 95817, USA.

<sup>3</sup>Department of Biomedical Engineering, College of Engineering, University of California, Davis, California 95618, USA.

<sup>#</sup>These two authors contributed equally

### Abstract

Joint injury often leads to post-traumatic osteoarthritis (PTOA). Acute injury responses to trauma induce production of pro-inflammatory cytokines and catabolic enzymes, which promote chondrocyte apoptosis and degrade cartilage to potentiate PTOA development. Recent studies show that the rate-limiting step for transcriptional activation of injury response genes is controlled by cyclin-dependent kinase 9 (CDK9), and thus it is an attractive target for limiting the injury response. Here, we determined the effects of CDK9 inhibition in suppressing the injury response in mechanically-injured cartilage explants. Bovine cartilage explants were injured by a single compressive load of 30 % strain at 100 %/s, and then treated with the CDK9 inhibitor Flavopiridol. To assess acute injury responses, we measured the mRNA expression of pro-inflammatory cytokines, catabolic enzymes, and apoptotic genes by RT-PCR, and chondrocyte viability and apoptosis by TUNEL staining. For long-term outcome, cartilage matrix degradation was assessed by soluble glycosaminoglycan release, and by determining the mechanical properties with instantaneous and relaxation moduli. Our data showed CDK9 inhibitor markedly reduced injury-induced inflammatory cytokine and catabolic gene expression. CDK9 inhibitor also attenuated chondrocyte apoptosis and reduced cartilage matrix degradation. Lastly, the mechanical properties of the injured explants were preserved by CDK9 inhibitor. Our results provide a temporal profile connecting the chain of events from mechanical impact, acute injury responses, to the subsequent induction of chondrocyte apoptosis and cartilage matrix deterioration. Thus, CDK9 is a potential disease-modifying agent for injury response after knee trauma to prevent or delay PTOA development.

**Keywords:** CDK9, Flavopiridol, inflammatory cytokines, chondrocytes, cartilage.

\*Address for correspondence:

Dominik R. Haudenschild

University of California Davis, Department of Orthopaedic Surgery,

Lawrence J. Ellison Musculoskeletal Research Center, Research Building 1 Suite 2000, 4635 Second Avenue, Sacramento, CA 95817, USA

Tel: +1 916-734-5015

Fax: +1 916-734-5750

E-mail: drhaudenschild@ucdavis.edu

### Introduction

Osteoarthritis (OA) is a disease characterised by progressive articular cartilage degradation and loss of mechanical properties, joint pain and dysfunction (Blumberg *et al.*, 2008; Guilak *et al.*, 2004). Although most OA cases are idiopathic, a major risk factor is traumatic joint injury such as an Anterior Cruciate Ligament (ACL) or meniscus tear. Roughly, half of the people with these types of knee injury will develop post-traumatic osteoarthritis (PTOA) in 5-20 years (Lohmander *et al.*, 2007). Shortly after an injury, an acute injury and inflammatory response is triggered at the cellular level to prevent infection and to initiate healing. However, excessive inflammation can lead to adverse secondary effects, such as cartilage and subchondral bone erosion that is not detected at the time of injury, but becomes apparent a few days later in our mouse model of ACL rupture (Christiansen *et al.*, 2012; Lockwood *et al.*, 2014). Activation of the inflammatory cascade can disrupt joint tissue homeostasis through augmentation of the catabolic response, causing overexpression of extracellular enzymes (Lee *et al.*, 2005), such as the various matrix metalloproteinases and aggrecanases that degrade the cartilage matrix (Imgenberg *et al.*, 2013). In addition, the inflammatory response can also trigger chondrocytes apoptosis (D'Lima *et al.*, 2001; Rosenzweig *et al.*, 2012) that further accelerates cartilage erosion. Therefore, a strategy to prevent excessive inflammation-induced

secondary damage after knee injury may prevent or delay the onset of PTOA.

Inflammation is initiated at the cellular level, by the activation of the primary response genes involved in the inflammatory process. Recent advances demonstrate that the rate-limiting step in primary response gene activation is controlled by the general transcription factor cyclin-dependent kinase 9 (CDK9). A unique feature of primary response genes is their instant activation upon stimulation without *de novo* protein synthesis. In order to achieve instant activation, the basal transcription of primary response genes is already pre-initiated by Ribonucleic Acid (RNA) Polymerase II (Pol II), even in the absence of inflammatory signals. However, only truncated mRNA transcripts are produced, because Pol II is paused shortly after the transcription start site (reviewed in (Zhou and Yik, 2006)). This promoter proximal pausing of Pol II at a basal resting state is currently recognised as a hallmark for all primary response genes (Fowler *et al.*, 2011). Upon inflammatory signal activation, the transcription factor CDK9 is rapidly recruited to the transcription complex, where it phosphorylates Pol II to induce a conformational change that allows Pol II to overcome promoter pausing and continue to produce full-length mRNA transcripts (Zhou and Yik, 2006). Hence, the kinase activity of CDK9 is the rate-limiting step, and a common requirement for the activation of all primary response genes. Thus, CDK9 represents a novel attractive target efficiently and effectively to inhibit the acute inflammatory response, regardless of the source of inflammation.

In a previous report, we highlighted the effectiveness of CDK9 inhibitors in protecting chondrocytes and cartilage explants from the catabolic effects of pro-inflammatory cytokines (Yik *et al.*, 2014). In the presence of exogenously added inflammatory cytokines, we found that the small molecule CDK9 inhibitor Flavopiridol (Wang and Ren, 2010) significantly suppressed the transcriptional activation of inflammatory response genes as well as catabolic genes, resulting in reduced cartilage matrix degradation (Yik *et al.*, 2014). While this study demonstrates the feasibility of targeting CDK9 as a viable strategy for protecting cartilage from exogenously added pro-inflammatory cytokines, the experimental conditions may not accurately represent the physical damage and inflammatory stimulation that the cartilaginous tissues may experience in the event of an actual traumatic knee injury. Various *ex vivo* impact injury models have been used for studying the effects of mechanical loading on cartilage explants (Borrelli *et al.*, 2003; D'Lima *et al.*, 2001; Imgenberg *et al.*, 2013; Ko *et al.*, 2013; Lee *et al.*, 2005; Nishimuta and Levenston, 2012; Rosenzweig *et al.*, 2012). Mechanical over-loading in cartilage explants can lead to chondrocyte cell death by both necrosis and apoptosis, and cause an inflammatory/catabolic response that damages the cartilage matrix and alters its physical properties (Hembree *et al.*, 2007; Murray *et al.*, 2004). These *ex vivo* impact injury models are invaluable tools to study the injury response in cartilage, since they recapitulate the physical injury and the subsequent biological response in the cartilage during traumatic knee injury.

In this study, we examined the therapeutic potential of the CDK9 inhibitor Flavopiridol in a single impact injury model with bovine cartilage explants. The ability of Flavopiridol to prevent the activation of the injury-induced inflammatory and catabolic responses, chondrocyte apoptosis, and cartilage matrix degradation was determined.

## Materials and Methods

### Cartilage explants

Bovine calf (~ 2 months old,  $n = 40$  joints, sex unknown) stifle joints were obtained from a local slaughterhouse (Petaluma, CA) within 1 d of slaughtering. 6-8 cylindrical cartilage explants were harvested from each femoral condyle with a 6 mm biopsy punch inserted perpendicular to the weight bearing area of the articular surface. The explants were then trimmed into ~ 3 mm thickness (with the articular surface intact and the deep layer cut flat) using a custom jig. The explants were washed with phosphate buffered saline and cultured for 24 h in high-glucose Dulbecco's Modified Eagle's Medium (DMEM) supplemented with 10 % foetal bovine serum (Invitrogen), penicillin ( $1 \times 10^4$  units/mL) and streptomycin ( $1 \times 10^4$  µg/mL) at 37 °C, 5 % CO<sub>2</sub>, and 95 % relative humidity.

### Single impact *ex vivo* injury model

After a 24 h recovery and equilibration period, the cartilage explants were subjected to a single impact mechanical injury. The precise thickness of each individual explant was measured by a calliper before it was placed onto a custom-built unconfined loading chamber, with the articular surface facing upward. A 20 mm diameter stainless steel platen was lowered onto the explant surface to a pre-load of 0.5 N (~ 17.7 kPa) on a hydraulic material testing instrument (Instron 8511.20). All explants including the uninjured controls were subjected to this 0.5 N pre-loading step. To avoid potential variation due to the positional differences from where the explants were harvested on the condyles, two adjacent explants were purposefully matched as a control and injured pair for later comparison. After pre-loading, the Instron was programmed to deliver a single compression of 30 % strain at 100 %/s, followed by immediate release. After the single impact loading, the explant was sliced in half and weighed. One half of the explant was placed in 3 mL medium and the other half placed in medium containing 300 nM Flavopiridol (Sigma) and cultured for various times (see Fig. 1A). The medium was changed every other day, with fresh Flavopiridol added. The explants and the culturing medium were then subjected to further processing and analysis as described below.

### Quantitative real-time PCR

At 2, 6 and 24 h post-injury, the explants were frozen in liquid nitrogen and pulverised with a pestle and mortar while frozen. Total RNA was isolated with the miRNeasy Mini Kit (Qiagen) according to the manufacturer's instruction, with the exception that the RNA was extracted

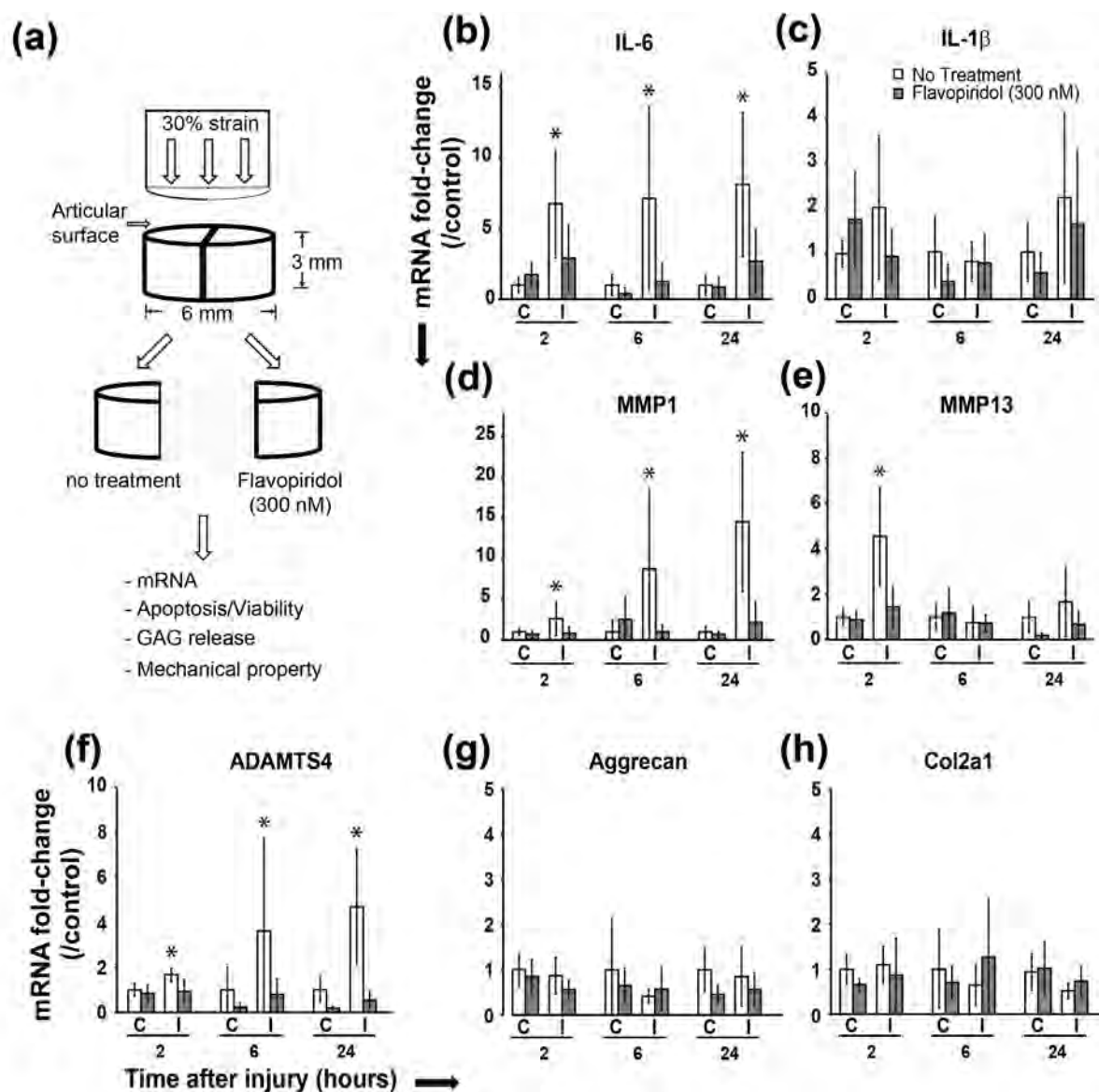


**Fig. 1:** CDK9 inhibition prevents injury-induced upregulation of pro-inflammatory cytokine and catabolic genes. **A)** Schematic representation of the cartilage explant injury and drug treatment, and the subsequent tests. **B-F)** Suppression of pro-inflammatory cytokine and catabolic enzyme genes by Flavopiridol in cartilage explants (C = control uninjured, I = injured) within 24 h post-injury, **G-H)** Flavopiridol does not affect the expression of the anabolic genes aggrecan and collagen 2A. All values were the mean  $\pm$  standard deviation obtained from  $n = 6$  individual donors (\*  $p < 0.05$ ).

twice with the Qiazol reagents to adequately remove the cartilage matrix constituents. The quantity and quality of the total RNA were determined by a Nanodrop-2000 spectrophotometer. 2.5  $\mu$ g of total RNA from each sample was used for reverse transcription with the SuperScript First-Strand RT kit (Invitrogen). Individual mRNA expression was determined with quantitative real-time PCR performed in triplicates in a 7900HT system (Applied Biosystems). Results were normalised to the 18s rRNA (catalogue no. 4319413E, Applied Biosystems) and calculated as fold-change in mRNA expression relative to control, using the  $2^{-\Delta\Delta CT}$  method. Probes used for individual bovine genes were custom made by Integrated DNA Technologies.

#### Chondrocyte viability

The live and dead cells in the explants 5 d after mechanical injury were stained using a Live/Dead Viability/Cytotoxicity kit (catalogue no. L3224, Invitrogen), according to the manufacturer's protocol. The percentages of live and dead cells were determined by counting the cell numbers in 3 random fields of the cross-sectional images of the explants ( $n = 6$  for each sample group) captured using a Nikon TE2000 inverted fluorescence microscope and a 20 $\times$  objective.

#### Staining for apoptotic cells

After 1, 3 and 5 d after injury, the explants were fixed with 4 % paraformaldehyde for 24 h and transferred to 75 % ethanol, followed by sectioning for histological

analysis. *In situ* detection of apoptosis was performed on 5 µm-thick whole explant cross-section using the DeadEnd Fluorometric TUNEL system kit (Promega). This kit measures the fragmented DNA of apoptotic cells by catalytically incorporating fluorescein-12-dUTP at 3'-OH DNA ends using the Terminal Deoxynucleotidyl Transferase recombinant enzyme (rTdT). Nuclei were counter-stained with DAPI. The sections were mounted and examined under a fluorescence microscope. The percentage of apoptotic cells ( $n = 3$  different donors) was determined by counting the number of TUNEL positive cells (green) and calculated as a percentage of the total cells (DAPI). Sections incubated with DNase I were used as positive control while those incubated with buffer only were used as negative control.

### GAG release

At 5 d post-injury, the culturing medium was collected and the amount of glycosylaminoglycan (GAG) was determined by the dimethyl-methylene blue (DMMB) colorimetric assay with chondroitin sulphate as the standard. Total GAG released into the medium was calculated and normalised to the wet weight of the explant (determined at the day of injury).

### Cartilage mechanical properties

To test if CDK9 inhibition preserves the mechanical properties of cartilage explants after injury, injured and control explants were cultured for 4 weeks in media with or without Flavopiridol. Cartilage sample compressive properties were assessed by stress-relaxation testing in unconfined compression using a mechanical testing system (Instron 5565, Norwood, MA). Prior to testing, a 3 mm diameter, 2 mm thick compression sample was prepared using a dermal biopsy punch, then placed in phosphate buffered saline and centred beneath a 16 mm stainless steel platen. The platen was slowly lowered until a preload of 0.2 N was observed, indicating contact between the platen and the cartilage sample. The sample was then preconditioned by fifteen cycles of 5 % strain. All strains, including the preconditioning, were applied at a strain rate of 10 % *per* second. Immediately following preconditioning, the sample was subject to 10 % compressive strain; the 10 % strain was held constant and the load recorded for 380 s. At the end of the 10 % strain application, the compressive strain was increased to 20 % and held constant while the load was recorded for an additional 530 s. The compressive properties: instantaneous modulus, relaxation modulus, and coefficient of viscosity, were calculated from the individual stress-relaxation curves using data analysis software (MATLAB R2013a, Natick, MA), according to a standard linear solid model of viscoelasticity as previously described (Allen and Athanasiou, 2006). This mechanical test and model were chosen for their simplicity and accuracy in approximating the viscoelastic behaviour of cartilage. The compressive properties of freshly isolated (day 0) bovine cartilage explants from 6 donors were determined as baseline values for comparison to 4 week post-injury samples.

### Statistical analysis

Values of all measurements were expressed as the mean  $\pm$  standard deviation. Changes in gene expression were analysed by one-way Analysis of Variance (ANOVA) with SPSS 16.0 software. The fold-change in mRNA was used as variables to compare samples between different treatment groups. The least significant difference *post-hoc* analysis was conducted with a significance level of  $p < 0.05$ .

Changes in compressive properties were analysed by one-way ANOVA with Tukey's *post hoc* test using JMP Pro software (version 11.2.0) with a significance level of  $p < 0.05$ .

## Results

### CDK9 inhibition suppresses injury-induced pro-inflammatory and catabolic genes

CDK9 controls the rate-limiting step of inflammatory gene activation (Hargreaves *et al.*, 2009; Zippo *et al.*, 2009) and we have previously shown that *in vitro* CDK9 inhibition protects chondrocytes and cartilage from the catabolic effects of exogenously added pro-inflammatory cytokines (Yik *et al.*, 2014). However, the effects of CDK9 inhibition on cartilage that receives a direct impact injury, similar to what may happen in a knee injury have not been examined. We hypothesise that CDK9 inhibition in mechanically injured cartilage will prevent an inflammatory response, which in turn will reduce the subsequent deleterious effects on chondrocytes and the cartilage matrix. To test our hypothesis, bovine cartilage explants were mechanically injured by subjecting them to an impact loading at a 30 % strain rate (Fig. 1A). This magnitude of loading induces chondrocyte apoptosis and cartilage matrix degradation (Borrelli *et al.*, 2003; D'Lima *et al.*, 2001; Hembree *et al.*, 2007; Loening *et al.*, 2000; Morel and Quinn, 2004; Rosenzweig *et al.*, 2012; Waters *et al.*, 2014). The injured explants were cultured in the presence or absence of the CDK9 inhibitor Flavopiridol, for various times. The mRNA expression of inflammatory cytokines and catabolic genes induced in the injured explants were determined and compared to uninjured controls. The addition of Flavopiridol reduced the induction of cytokine mRNA by injury (Fig. 1B&C, grey bars). This effect was most pronounced in the expression of IL-6 mRNA, which was significantly induced by injury at all time points tested (Fig. 1B, open bars), and the IL-6 induction was markedly suppressed by Flavopiridol (Fig. 1B, grey bars). Similar trends were observed for IL-1 $\beta$  (Fig. 1C), although this did not reach statistical significance. These data indicate that, as expected, CDK9 inhibition in cartilage explants suppresses inflammatory cytokine induction in response to mechanical injury.

We next examined the injured-induced changes in mRNA expression of the catabolic genes MMP-1 and MMP-13, and ADAMTS4, which are induced by inflammatory cytokines and degrade the cartilage matrix. The results showed that injury induced MMP-1 and ADAMTS4 expression significantly at all time points

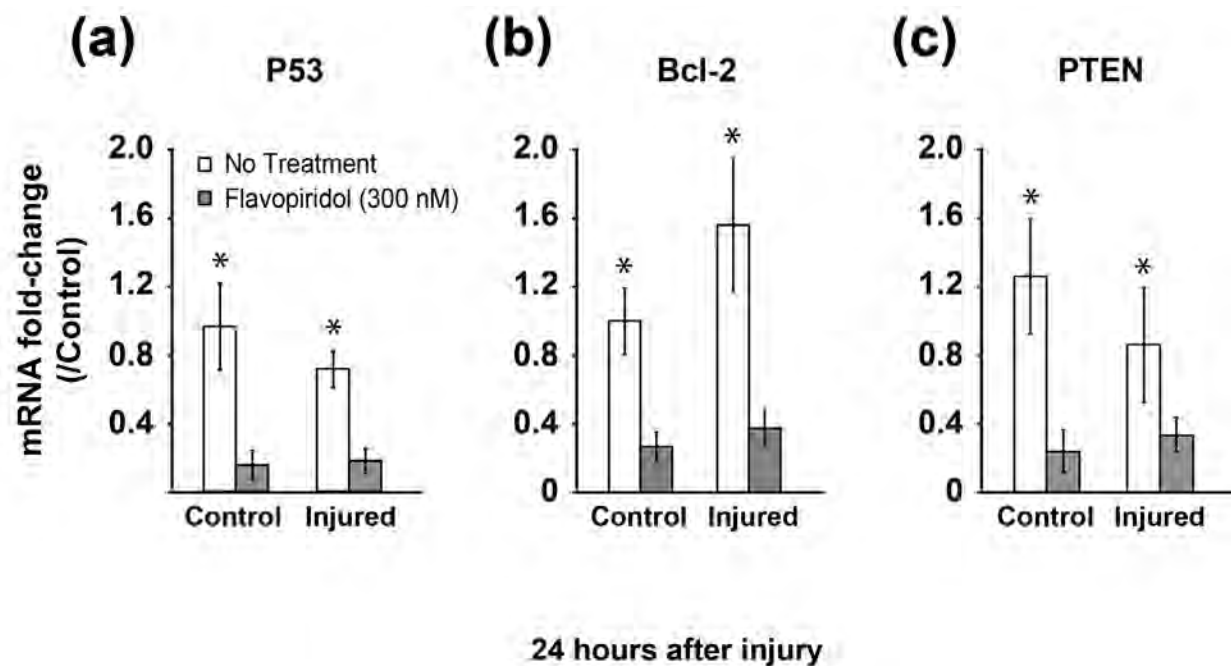


**Fig. 2:** CDK9 inhibition reduces mRNA expression of apoptotic mediators. Flavopiridol suppresses mRNA expression of the pro-apoptotic genes p53, Bcl-2, and PTEN. All values were the mean  $\pm$  standard deviation obtained from  $n = 6$  individual donors (\*  $p < 0.05$ ).

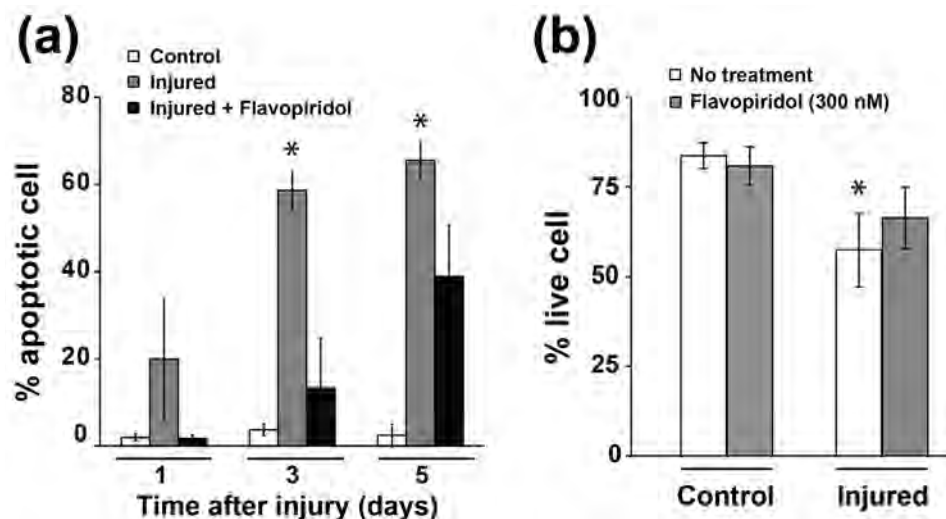


**Fig. 3:** CDK9 inhibition rescues chondrocyte from injury-induced apoptosis. **A)** Flavopiridol treatment prevents chondrocyte apoptosis. At the indicated times, cartilage explants were processed for histological examination and TUNEL staining. Injury increased apoptosis in cartilage explants but Flavopiridol reduced the apoptotic cell population. Results were the mean  $\pm$  standard deviation obtained from  $n = 3$  individual donors (\*  $p < 0.05$ ). **B)** Flavopiridol enhances chondrocyte survival. At 5-days post-injury, cartilage explants were stained with LIVE/DEAD viability stain. Injury decreased cell viability but the cells were rescued by Flavopiridol. Results were the mean  $\pm$  standard deviation obtained from  $n = 6$  individual donors (\*  $p < 0.05$ ).

and MMP-13 at the 2 h time-point (Fig. 1D-F, open bars). Inhibition of CDK9 effectively prevented the induction of these genes in the injured samples at all time points tested (Fig. 1D-F, grey bars). In contrast, the mRNA expression of the anabolic genes Aggrecan and Col2a1 were not affected by injury, whether or not Flavopiridol is present (Fig. 1G-H). Taken together, these results indicate that CDK9 inhibition suppressed injury-induced catabolic mediators of cartilage matrix degradation, while the basal

levels of anabolic genes are not affected by injury or CDK9 inhibition at the time points tested.

#### CDK9 inhibition reduces injury-induced chondrocyte apoptosis

Besides inducing an inflammatory response, mechanical injury also causes chondrocyte apoptosis in cartilage explants (Borrelli *et al.*, 2003; D'Lima *et al.*, 2001; Hembree *et al.*, 2007; Rosenzweig *et al.*, 2012). We

**Fig. 4:** Protection of cartilage from injury-induced matrix degradation. Mechanically injured cartilage explants were treated for 5 d with Flavopiridol. The amount of GAG released into the medium was measured by dimethylmethylene blue dye binding assay. Results were normalised to the wet weight of the explants. Injury caused cartilage degradation, as indicated by increased GAG release. In the presence of 300 nM Flavopiridol, levels of GAG release returned to baseline. Results were the mean  $\pm$  standard deviation obtained from  $n = 6$  individual donors ( $*p < 0.05$ ).

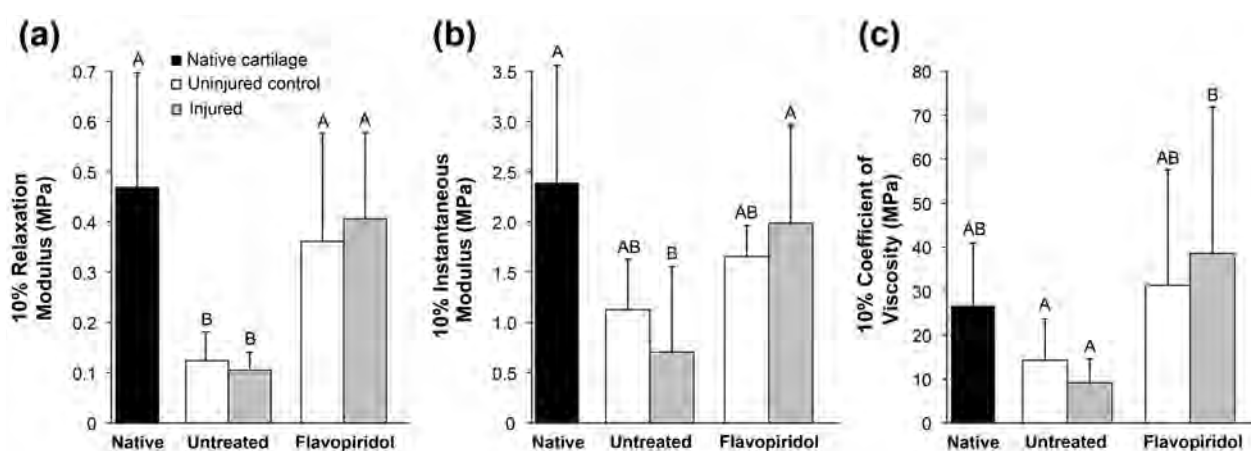
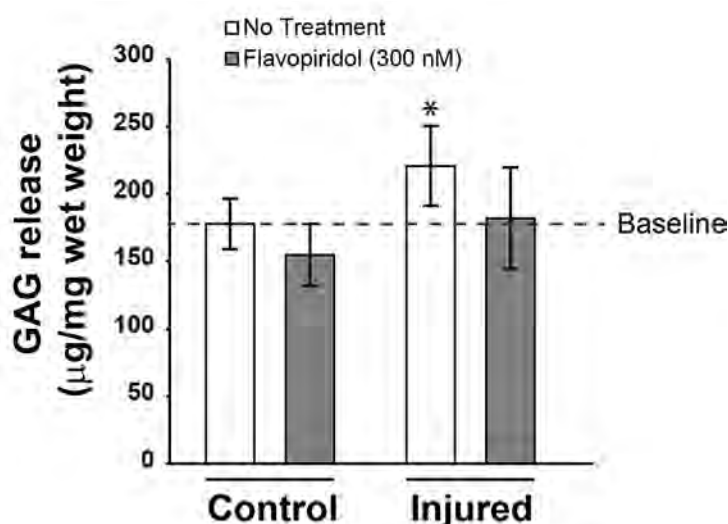


**Fig. 5:** CDK9 inhibition preserves the mechanical properties of injured cartilage. Cartilage explants were cultured for 4 weeks post-injury. The cartilage compressive properties were assessed by stress-relaxation testing in unconfined compression. The 10 % relaxation and instantaneous moduli, and coefficient of viscosity are shown. Flavopiridol treatment enhanced the compressive properties of both the injured and uninjured explants. Results were the mean  $\pm$  standard deviation obtained from  $n = 6$  individual donors. Within each chart, means that do not share a letter are significantly different from each other ( $p < 0.05$ ).

therefore investigated the effects of CDK9 inhibition on apoptosis, using our explant injury model. The mRNA expression of three selected genes (P53, Bcl-2 and PTEN) that are central to the apoptotic process were examined in the cartilage explants 24 h post-injury. P53 initiates apoptosis when DNA damage is irreparable (Amaral *et al.*, 2010). Bcl-2 is the founding member of anti-apoptotic factors (Czabotar *et al.*, 2014) and PTEN is a crucial regulator of apoptosis (Zheng *et al.*, 2010). Although mechanical injury itself did not significantly change the mRNA expression of P53, Bcl-2, and PTEN (Fig. 2, open bars), Flavopiridol significantly decreased the expression of these apoptotic mediators in both the injured and uninjured groups (Fig. 2, grey bars).

The reduced basal level of apoptotic mediators has prompted us to determine directly the number of apoptotic chondrocytes in the injured cartilage explants. Cartilage explants from three different donors collected at 1-, 3-, and 5-day post-injury were examined by TUNEL stain and the

percentage of apoptotic cells relative to the total number of nuclei in each sample was determined. The results showed that injury increased the percentage of apoptotic chondrocytes to ~ 20 % at 1 d post-injury, and to ~ 60 % 3 d after injury (Fig. 3A). In contrast, CDK9 inhibition significantly reduced the percentage of apoptotic cells in the injured explants in all time points tested (Fig. 3A). These results were further corroborated by the data on live/dead staining of cartilage explants collected 5 d post-injury (Fig. 3B). The live/dead stain showed that injury significantly reduced the number of live chondrocytes from ~ 80 % to ~ 55 % (Fig. 3B, open bars). Flavopiridol treatment enhanced cell survival in the injured explants and did not significantly affect cell survival in uninjured explants (Fig. 3B, grey bars). Taken together, the above results indicate that CDK9 inhibition decreases injury-induced apoptosis in cartilage explants and enhance chondrocyte survival after impact injury.

### CDK9 inhibition prevents injury-induced cartilage matrix degradation

Since injury-induced catabolic response leads to upregulation of matrix degrading enzymes, we next investigated if CDK9 inhibition could prevent cartilage matrix degradation after injury. The cartilage explants were continuously cultured for 5 d in the presence or absence of 300 nM Flavopiridol after injury, the culturing media was collected and the GAG content released into the media was determined as a measure of matrix degradation. GAG release was significantly increased upon injury (Fig. 4, open bars); however, in samples treated with Flavopiridol, GAG release by injured cartilage was not increased above the uninjured control baseline. This result indicates that the CDK9 inhibition attenuates mechanical injury-induced cartilage matrix degradation and proteoglycan release.

### CDK9 inhibition preserves the mechanical properties of cartilage explants after injury

The compressive properties of freshly isolated cartilage were determined from 6 individual donors and their mean values were indicated by the dotted lines in Fig. 5. The compressive properties of the cartilage explants following four weeks of culture demonstrate increased 10 % relaxation modulus, 10 % instantaneous modulus, and 10 % coefficient of viscosity in samples treated with Flavopiridol, when compared to injured, untreated samples (Fig. 5). Similar results were observed for the moduli and coefficients of viscosity calculated from the 20 % strain stress-relaxation curves (not shown). The positive effect of Flavopiridol on compressive properties was observed in both injured and uninjured cartilage samples; no significant difference was observed for any compressive property between injured and uninjured cartilage samples when treated with Flavopiridol. Although injured, untreated cartilage samples exhibited the lowest compressive properties among all groups, there was no significant difference between injured and uninjured cartilage samples in the absence of Flavopiridol. Interestingly, cartilage samples treated with Flavopiridol exhibited greater relaxation moduli than untreated, uninjured controls. Furthermore, injured cartilage samples treated with Flavopiridol also have greater instantaneous moduli and coefficients of viscosity than untreated, uninjured controls. These results indicate that Flavopiridol has a beneficial effect on the compressive properties of cartilage samples cultured *in vitro*.

## Discussion

This study examined the effects of CDK9 inhibition on the biological and mechanical properties of cartilage explants after injury by compressive loading. This injury model caused a significant induction of pro-inflammatory cytokines and catabolic enzymes (Fig. 1) within the first 24 h. Although apoptotic genes were unchanged within this period (Fig. 2), apoptotic chondrocytes could be detected in the explants at 1 d following injury and peaked after 5 d (Fig. 3). Injury also accelerated cartilage matrix degradation, as measured by GAG release (Fig. 4).

However, CDK9 inhibition by Flavopiridol suppressed all those changes and preserved the mechanical properties similar to those of native cartilage (Fig. 5), thus effectively protecting the chondrocytes and the cartilage from the harmful effects of physical injury and the inflammatory response that follows.

A high incidence of OA is associated with traumatic knee injury and hence the term post-traumatic OA (PTOA). Although the pathology of the development of PTOA from injury remains unclear, several lines of evidence point to the involvement of the inflammatory response in this process. Elevated levels of the inflammatory cytokines IL-1 $\beta$  and IL-6 are detected in the human joints within 24 h after an ACL injury (Irie *et al.*, 2003). (Ko *et al.*, 2013) demonstrate that inflammation and the accompanying dysregulated cytokines activities likely contribute to the disruption of the balance between anabolism and catabolism in OA (Goldring and Berenbaum, 2004). *In vitro* and *in vivo* studies have implicated pro-inflammatory cytokines, particularly IL-1 $\beta$ , in the destruction of articular cartilage in OA (Goldring and Berenbaum, 2004; Kobayashi *et al.*, 2005). In cartilage, chondrocytes are the main target of pro-inflammatory cytokines, which dysregulate the expression of catabolic and anabolic genes. Cytokine-stimulated chondrocytes produce a variety of matrix-degrading enzymes, like MMP-1, -3, -13 and the aggrecanase ADAMTS-4, -5 (Lee *et al.*, 2005; Nishimuta and Levenston, 2012). All these data implicate the involvement of the inflammatory response in cartilage matrix degradation. Our results in this study strongly indicate that CDK9 inhibition prevents induction of inflammatory and catabolic response genes and thus is a novel target for preventing injury-induced damage.

The influences of mechanical injury on chondrocyte anabolic gene expression are still controversial. It has been reported that IL-1 $\beta$  suppresses the expression of Col2a1 in chondrocytes *in vitro* (Okazaki *et al.*, 2002). However, other OA studies show that in osteoarthritic cartilage, there is enhanced aggrecan and Col2a1 gene expression and biosynthesis, when compared to normal cartilage (Bau *et al.*, 2002; Hermansson *et al.*, 2004). Our results showed no significant change of anabolic gene expression in injured cartilage in the first 24 hours. This is supported by large-scale expression profiling studies use full-thickness cartilage, which demonstrated that many anabolic genes, including Col2a1, are only enhanced in late-stage OA (Aigner *et al.*, 2006; Ijiri *et al.*, 2008). More importantly, our result demonstrates that Flavopiridol has no adverse side effects on anabolic gene expression in the first 24 h after mechanical injury.

Mechanical injury to cartilage leads to chondrocyte apoptosis. D'Lima *et al.* (2001) applied a 30 % strain to injure cartilage explants and found 34 % apoptotic chondrocytes in 96 h, compared to only 4 % apoptosis in the control group. Similarly, our explant injury model also leads to chondrocyte apoptosis; we detected ~ 20 % apoptotic chondrocytes in 24 h and more than 60 % apoptotic cells after 72 h (Fig. 3A). Given that injury to cartilage and chondrocyte apoptosis lead to cartilage degradation, the development of drugs designed to block this could be beneficial in preventing PTOA development (Borrelli *et al.*, 2003; D'Lima *et al.*, 2001). For example,

when mechanically injured cartilage explants were treated with caspase inhibitors, a 50 % reduction of apoptosis was seen (D'Lima *et al.*, 2001). However, few studies have focused on the correlation between the acute injury response within hours, such as induction of inflammatory cytokine and catabolic genes, and the subsequent apoptosis that followed, usually at several days post-injury. Pro-inflammatory cytokines like IL-1 $\beta$  and IL-6 have the capacity to activate a diverse array of intracellular signalling pathways, such as c-Jun N-terminal Kinase (JNK), p38 Mitogen-activated Protein Kinase (MAPK) and NF- $\kappa$ B (Goldring *et al.*, 2011), and further induce the expression of various pro-apoptotic genes like p53 (Amaral *et al.*, 2010), BCL-2 (Czabotar *et al.*, 2014) and PTEN (Zheng *et al.*, 2010). In chondrocytes, JNK and p38 signalling pathways are thought to be pro-apoptotic in an injury response (Rosenzweig *et al.*, 2012). Results from this study provide a temporal profile connecting the chain of events that happen after mechanical injury to cartilage, from the induction of inflammatory cytokines and catabolic genes, to the subsequent induction of chondrocyte apoptosis. Importantly, Flavopiridol treatment effectively blocks the initial phase of the injury response, and thus prevents subsequent damage to the cartilage.

In contrast to the anti-apoptotic property in this study, Flavopiridol has been reported to induce apoptosis in many cancer cells. Notably, Flavopiridol was originally known for its anti-proliferation properties by suppressing cell-cycle progression in rapidly dividing cells (*e.g.* cancers) (Wang and Ren, 2010). This is due to the off-target suppressive effect of Flavopiridol on other CDKs that directly regulate the cell cycle. We believe that mature chondrocytes, which do not normally divide (Kobayashi *et al.*, 2005), are therefore less sensitive to the anti-proliferative effect of Flavopiridol.

Flavopiridol has a beneficial effect on the compressive, viscoelastic properties of injured cartilage explants after four weeks of culture. Specifically, both injured and uninjured cartilage samples treated with Flavopiridol have increased stiffness upon initial compression (instantaneous modulus) and upon reaching equilibrium during prolonged static compression (relaxation modulus) compared to injured-untreated samples. The increased instantaneous and relaxation moduli are likely associated with preservation of glycosaminoglycans (GAG) in the cartilage extracellular matrix (ECM) and of the elastic stiffness of the ECM, respectively. Furthermore, injured samples treated with Flavopiridol exhibit a slower rate of relaxation toward equilibrium following compression compared to injured-untreated samples as evidenced by a greater coefficient of viscosity in the treated samples. An increased coefficient of viscosity is likely associated with retention of GAG in the ECM, which resists movement of water out of cartilage during compression. Overall, treatment with Flavopiridol helps maintain the viscoelastic, compressive properties of cultured cartilage samples close to values observed for uncultured native cartilage samples (Fig. 5). Flavopiridol may preserve cartilage mechanical properties *in vivo* following injury as well as *in vitro* during culture.

The lack of difference in the mechanical properties between injured cartilage explants and uninjured control

explants was an unexpected finding of this study. Although the injured explants cultured without Flavopiridol had the lowest instantaneous modulus and coefficient of viscosity among all treatment groups, the difference between injured and uninjured samples was not statistically significant ( $p > 0.05$ ). Cartilage degradation and loss of GAG, known to occur during prolonged culture of immature cartilage (Bian *et al.*, 2010), may have caused the loss of cartilage compressive properties observed in the untreated-uninjured cartilage explants. We suspect that testing samples after shorter culture duration may demonstrate a greater difference between the injured and uninjured cartilage.

In summary, our data demonstrated, for the first time, the effectiveness of CDK9 inhibition in the suppression of pro-inflammatory cytokine induced by mechanical injury and prevention of chondrocyte apoptosis in cartilage explants. In addition, our data strongly indicate that Flavopiridol is an effective agent to prevent cartilage matrix degradation and to preserve its mechanical properties after injury. Thus, CDK9 inhibition by Flavopiridol may provide a new strategy to prevent or delay PTOA after knee joint trauma.

## Conclusion

Our data indicate that CDK9 inhibition by Flavopiridol prevents inflammation-induced apoptosis and protects cartilage from the deleterious effects of mechanical injuries. The immediate mechanical damage during an injury event can weaken cartilage and predispose the joint to future OA. Here, we show that CDK9-dependent cell-mediated secondary events initiated by the mechanical impact also contribute to OA-like degradative changes. This, perhaps, suggests that joint injuries should be treated during the acute injury response phase to suppress the secondary cell-mediated damage and alter the trajectory of OA progression. Our results suggest that CDK9 is a viable target to suppress the injury response effectively.

## Competing interest

The authors declare that they have no competing interest.

## Acknowledgements

This study was supported by an Arthritis Foundation 2012 IRG award to DRH, a DOD PRMRP IIRA award #PR110507 to DRH, R21-AR063348 from NIAMS/NIH to DRH, Departmental Funds to DRH, and the National Natural Science Fund of China (81271971) to ZH and T32 OD 011147 to DDC.

No author received any financial support or other benefits from commercial sources for the work reported on in this manuscript, and no author has any other financial interest that could create a potential conflict of interest or the appearance of a conflict of interest with regard to the work.

## References

- Aigner T, Fundel K, Saas J, Gebhard PM, Haag J, Weiss T, Zien A, Obermayr F, Zimmer R, Bartnik E (2006) Large-scale gene expression profiling reveals major pathogenetic pathways of cartilage degeneration in osteoarthritis. *Arthritis Rheum* **54**: 3533-3544.
- Allen KD, Athanasiou KA (2006) Viscoelastic characterization of the porcine temporomandibular joint disc under unconfined compression. *J Biomech* **39**: 312-322.
- Amaral JD, Xavier JM, Steer CJ, Rodrigues CM (2010) The role of p53 in apoptosis. *Discov Med* **9**: 145-152.
- Bau B, Haag J, Schmid E, Kaiser M, Gebhard PM, Aigner T (2002) Bone morphogenetic protein-mediating receptor-associated Smads as well as common Smad are expressed in human articular chondrocytes but not up-regulated or down-regulated in osteoarthritic cartilage. *J Bone Miner Res* **17**: 2141-2150.
- Bian L, Stoker AM, Marberry KM, Ateshian GA, Cook JL, Hung CT (2010) Effects of dexamethasone on the functional properties of cartilage explants during long-term culture. *Am J Sports Med* **38**: 78-85.
- Blumberg TJ, Natoli RM, Athanasiou KA (2008) Effects of doxycycline on articular cartilage GAG release and mechanical properties following impact. *Biotechnol Bioeng* **100**: 506-515.
- Borrelli J Jr, Tinsley K, Ricci WM, Burns M, Karl IE, Hotchkiss R (2003) Induction of chondrocyte apoptosis following impact load. *J Orthop Trauma* **17**: 635-641.
- Christiansen BA, Anderson MJ, Lee CA, Williams JC, Yik JH, Haudenschild DR (2012) Musculoskeletal changes following non-invasive knee injury using a novel mouse model of post-traumatic osteoarthritis. *Osteoarthritis Cartilage* **20**: 773-782.
- Czabotar PE, Lessene G, Strasser A, Adams JM (2014) Control of apoptosis by the BCL-2 protein family: implications for physiology and therapy. *Nat Rev Mol Cell Biol* **15**: 49-63.
- D'Lima DD, Hashimoto S, Chen PC, Colwell CW Jr, Lotz MK (2001) Human chondrocyte apoptosis in response to mechanical injury. *Osteoarthritis Cartilage* **9**: 712-719.
- Fowler T, Sen R, Roy AL (2011) Regulation of primary response genes. *Mol Cell* **44**: 348-360.
- Goldring MB, Berenbaum F (2004) The regulation of chondrocyte function by proinflammatory mediators: prostaglandins and nitric oxide. *Clin Orthop Relat Res*: S37-46.
- Goldring MB, Otero M, Plumb DA, Dragomir C, Favero M, El Hachem K, Hashimoto K, Roach HI, Olivetto E, Borzi RM, Marcu KB (2011) Roles of inflammatory and anabolic cytokines in cartilage metabolism: signals and multiple effectors converge upon MMP-13 regulation in osteoarthritis. *Eur Cell Mater* **21**: 202-220.
- Guilak F, Fermor B, Keefe FJ, Kraus VB, Olson SA, Pisetsky DS, Setton LA, Weinberg JB (2004) The role of biomechanics and inflammation in cartilage injury and repair. *Clin Orthop Relat Res*: 17-26.
- Hargreaves DC, Horng T, Medzhitov R (2009) Control of inducible gene expression by signal-dependent transcriptional elongation. *Cell* **138**: 129-145.
- Hembree WC, Ward BD, Furman BD, Zura RD, Nichols LA, Guilak F, Olson SA (2007) Viability and apoptosis of human chondrocytes in osteochondral fragments following joint trauma. *J Bone Joint Surg Br* **89**: 1388-1395.
- Hermansson M, Sawaji Y, Bolton M, Alexander S, Wallace A, Begum S, Wait R, Saklatvala J (2004) Proteomic analysis of articular cartilage shows increased type II collagen synthesis in osteoarthritis and expression of inhibin betaA (activin A), a regulatory molecule for chondrocytes. *J Biol Chem* **279**: 43514-43521.
- Ijiri K, Zerbini LF, Peng H, Otu HH, Tsuchimochi K, Otero M, Dragomir C, Walsh N, Bierbaum BE, Mattingly D, van Flandern G, Komiya S, Aigner T, Libermann TA, Goldring MB (2008) Differential expression of GADD45beta in normal and osteoarthritic cartilage: potential role in homeostasis of articular chondrocytes. *Arthritis Rheum* **58**: 2075-2087.
- Imgenberg J, Rolaufts B, Grodzinsky AJ, Schunke M, Kurz B (2013) Estrogen reduces mechanical injury-related cell death and proteoglycan degradation in mature articular cartilage independent of the presence of the superficial zone tissue. *Osteoarthritis Cartilage* **21**: 1738-1745.
- Irie K, Uchiyama E, Iwaso H (2003) Intraarticular inflammatory cytokines in acute anterior cruciate ligament injured knee. *Knee* **10**: 93-96.
- Ko FC, Dragomir C, Plumb DA, Goldring SR, Wright TM, Goldring MB, van der Meulen MC (2013) *In vivo* cyclic compression causes cartilage degeneration and subchondral bone changes in mouse tibiae. *Arthritis Rheum* **65**: 1569-1578.
- Kobayashi M, Squires GR, Mousa A, Tanzer M, Zukor DJ, Antoniou J, Feige U, Poole AR (2005) Role of interleukin-1 and tumor necrosis factor alpha in matrix degradation of human osteoarthritic cartilage. *Arthritis Rheum* **52**: 128-135.
- Lee JH, Fitzgerald JB, Dimicco MA, Grodzinsky AJ (2005) Mechanical injury of cartilage explants causes specific time-dependent changes in chondrocyte gene expression. *Arthritis Rheum* **52**: 2386-2395.
- Lockwood KA, Chu BT, Anderson MJ, Haudenschild DR, Christiansen BA (2014) Comparison of loading rate-dependent injury modes in a murine model of post-traumatic osteoarthritis. *J Orthop Res* **32**: 79-88.
- Loening AM, James IE, Levenston ME, Badger AM, Frank EH, Kurz B, Nuttall ME, Hung HH, Blake SM, Grodzinsky AJ, Lark MW (2000) Injurious mechanical compression of bovine articular cartilage induces chondrocyte apoptosis. *Arch Biochem Biophys* **381**: 205-212.
- Lohmander LS, Englund PM, Dahl LL, Roos EM (2007) The long-term consequence of anterior cruciate ligament and meniscus injuries: osteoarthritis. *Am J Sports Med* **35**: 1756-1769.
- Morel V, Quinn TM (2004) Cartilage injury by ramp compression near the gel diffusion rate. *J Orthop Res* **22**: 145-151.
- Murray MM, Zurakowski D, Vrahas MS (2004) The death of articular chondrocytes after intra-articular fracture in humans. *J Trauma* **56**: 128-131.
- Nishimuta JF, Levenston ME (2012) Response of cartilage and meniscus tissue explants to *in vitro*

compressive overload. *Osteoarthritis Cartilage* **20**: 422-429.

Okazaki K, Li J, Yu H, Fukui N, Sandell LJ (2002) CCAAT/enhancer-binding proteins beta and delta mediate the repression of gene transcription of cartilage-derived retinoic acid-sensitive protein induced by interleukin-1 beta. *J Biol Chem* **277**: 31526-31533.

Rosenzweig DH, Djab MJ, Ou SJ, Quinn TM (2012) Mechanical injury of bovine cartilage explants induces depth-dependent, transient changes in MAP kinase activity associated with apoptosis. *Osteoarthritis Cartilage* **20**: 1591-1602.

Wang LM, Ren DM (2010) Flavopiridol, the first cyclin-dependent kinase inhibitor: recent advances in combination chemotherapy. *Mini Rev Med Chem* **10**: 1058-1070.

Waters NP, Stoker AM, Carson WL, Pfeiffer FM, Cook JL (2014) Biomarkers affected by impact velocity and maximum strain of cartilage during injury. *J Biomech* **47**: 3185-3195.

Yik JH, Hu Z, Kumari R, Christiansen BA, Haudenschild DR (2014) Cyclin-dependent kinase 9 inhibition protects cartilage from the catabolic effects of proinflammatory cytokines. *Arthritis Rheumatol* **66**: 1537-1546.

Zheng T, Meng X, Wang J, Chen X, Yin D, Liang Y, Song X, Pan S, Jiang H, Liu L (2010) PTEN- and p53-mediated apoptosis and cell cycle arrest by FTY720 in gastric cancer cells and nude mice. *J Cell Biochem* **111**: 218-228.

Zhou Q, Yik JH (2006) The Yin and Yang of P-TEFb regulation: implications for human immunodeficiency virus gene expression and global control of cell growth and differentiation. *Microbiol Mol Biol Rev* **70**: 646-659.

Zippo A, Serafini R, Rocchigiani M, Pennacchini S, Krepelova A, Oliviero S (2009) Histone crosstalk between H3S10ph and H4K16ac generates a histone code that mediates transcription elongation. *Cell* **138**: 1122-1136.

## Discussion with Reviewers

**Farshid Guilak:** Have the authors considered the effect of using immature cartilage in these experiments and whether there would be more of a difference if less hydrated mature cartilage was used instead?

**Authors:** That's really a good suggestion. In this present study, we used well hydrated healthy young cartilage. These samples are readily available and have a consistent baseline values for the assays we used. Our intent is to model a young athletic patient that suffers a joint injury. In a future study, it will be interesting to look at the effect of Cdk9 inhibition on injured cartilage that is less hydrated, aged, and/or diseased.

**Editor's Note:** Scientific Editor in charge of the paper: Mauro Alini.

## *In vivo* fluorescence reflectance imaging of protease activity in a mouse model of post-traumatic osteoarthritis



P.B. Satkunananthan <sup>†‡</sup>, M.J. Anderson <sup>†</sup>, N.M. De Jesus <sup>‡§</sup>, D.R. Haudenschild <sup>†‡</sup>,  
 C.M. Ripplinger <sup>‡§</sup>, B.A. Christiansen <sup>†‡\*</sup>

<sup>†</sup> Department of Orthopaedic Surgery, University of California-Davis Medical Center, USA

<sup>‡</sup> Biomedical Engineering Graduate Group, University of California-Davis, USA

<sup>§</sup> Department of Pharmacology, University of California-Davis Medical Center, USA

### ARTICLE INFO

#### Article history:

Received 21 May 2014

Accepted 10 July 2014

#### Keywords:

Fluorescence reflectance imaging

Post-traumatic osteoarthritis

Inflammation

Bone resorption

Protease

Cathepsin

### SUMMARY

**Objective:** Joint injuries initiate a surge of inflammatory cytokines and proteases that contribute to cartilage and subchondral bone degeneration. Detecting these early processes in animal models of post-traumatic osteoarthritis (PTOA) typically involves *ex vivo* analysis of blood serum or synovial fluid biomarkers, or histological analysis of the joint. In this study, we used *in vivo* fluorescence reflectance imaging (FRI) to quantify protease, matrix metalloproteinase (MMP), and Cathepsin K activity in mice following anterior cruciate ligament (ACL) rupture. We hypothesized that these processes would be elevated at early time points following joint injury, but would return to control levels at later time points. **Design:** Mice were injured via tibial compression overload, and FRI was performed at time points from 1 to 56 days after injury using commercially available activatable fluorescent tracers to quantify protease, MMP, and cathepsin K activity in injured vs uninjured knees. PTOA was assessed at 56 days post-injury using micro-computed tomography and whole-joint histology.

**Results:** Protease activity, MMP activity, and cathepsin K activity were all significantly increased in injured knees relative to uninjured knees at all time points, peaking at 1–7 days post-injury, then decreasing at later time points while still remaining elevated relative to controls.

**Conclusions:** This study establishes FRI as a reliable method for *in vivo* quantification of early biological processes in a translatable mouse model of PTOA, and provides crucial information about the time course of inflammation and biological activity following joint injury. These data may inform future studies aimed at targeting these early processes to inhibit PTOA development.

© 2014 Osteoarthritis Research Society International. Published by Elsevier Ltd. All rights reserved.

### Introduction

Osteoarthritis (OA) is a primary musculoskeletal health concern, affecting approximately 27 million Americans<sup>1</sup>. Post-traumatic osteoarthritis (PTOA) is commonly observed within 10–20 years following anterior cruciate ligament (ACL) rupture<sup>2–4</sup>. Traumatic joint injuries initiate a surge of inflammatory cytokines, matrix metalloproteinases (MMPs), cathepsin proteases, and other degradative enzymes that contribute to cartilage and subchondral bone degeneration<sup>2,5–11</sup>. Detecting these early biological processes

in animal models of OA typically involves analysis of blood serum or synovial fluid biomarkers, or destructive histological analysis of the joint. The ability to quantify these processes non-invasively *in vivo* has the distinct advantages of rapid measurement time, relatively low cost, and the capability to perform repeated longitudinal measurements in the same animals at multiple time points or following therapy. Additionally, non-invasive *in vivo* analyses preclude the possibility of exacerbated inflammation or damage to the joint as a direct result of the sampling procedure.

Near-infrared protease activatable probes combined with fluorescence reflectance imaging (FRI) have become widely used for *in vivo* imaging to visualize and quantify cellular activity. These optical tracers are fluorescently quenched until a linker domain is cleaved by a specific protease of interest, which then produces a robust fluorescent signal. These techniques have been extensively validated and used in studies of cancer<sup>12–15</sup> and atherosclerosis<sup>16–19</sup>, but are also potentially useful for studies of the

\* Address correspondence and reprint requests to: B.A. Christiansen, UC Davis Medical Center, Department of Orthopaedic Surgery, 4635 2nd Ave, Suite 2000, Sacramento, CA 95817, USA. Tel: 1-916-734-3974; Fax: 1-916-734-5750.

E-mail addresses: psatkun@ucdavis.edu (P.B. Satkunananthan), mranderson@ucdavis.edu (M.J. Anderson), ndejesus@ucdavis.edu (N.M. De Jesus), drhaudenschild@ucdavis.edu (D.R. Haudenschild), criplinger@ucdavis.edu (C.M. Ripplinger), bchristiansen@ucdavis.edu (B.A. Christiansen).

musculoskeletal system to measure markers of inflammation and matrix degradation (cathepsin proteases and MMPs) and bone turnover (cathepsin K), which have vital roles in OA progression. Commercially available fluorescent activatable probes have been validated for use in musculoskeletal applications<sup>20–23</sup>. However, no studies have utilized these methods in an animal model of PTOA to determine the dynamic protease profile following joint injury or to quantify disease severity or progression.

In this study, we used FRI to quantify the time course of biological processes associated with PTOA progression following non-invasive joint injury in mice. We hypothesized that inflammatory biomarkers and degradative processes would be elevated at early time points following traumatic joint injury (1–14 days), but would return to control levels at later time points (4–8 weeks). These results of this study reveal, for the first time, the dynamic time course of protease activity in joints following injury, and establish FRI imaging as a feasible method for *in vivo* quantification of these biological processes in a mouse model of PTOA.

## Methods

### Animals

A total of 54 C57BL/6 mice (27 male, 27 female; 10 weeks old at the time of injury) were obtained from Harlan Sprague Dawley, Inc. (Indianapolis, IN, USA). Forty-eight mice (24 male, 24 female) were injured using tibial compression overload, while 6 mice (3 male, 3 female) were sham injured. Animals were housed in a compliant facility at UCDMC for a 2-week acclimation period prior to injury. All animals were maintained and used in accordance with National Institutes of Health guidelines on the care and use of laboratory animals, and the study was approved by our institutional Animal Studies Committee.

### Tibial compression-induced knee injury

Mice were subjected to non-invasive ACL rupture induced by a single overload cycle of tibial compression as previously described<sup>24</sup>. Briefly, mice were anesthetized and placed in a prone position in a materials testing system (Bose ElectroForce 3200, Eden Prairie, MN, USA) with tibial compression loading platens (Fig. 1). A single dynamic axial compressive load was applied at 1 mm/s to the right lower leg to a target compressive force of 12 N to produce ACL rupture. This loading protocol produces failure of the ACL with avulsion fracture from the distal femur<sup>24,25</sup>. Contralateral limbs remained uninjured, and served as internal controls. Sham injury was performed by anesthetizing mice and loading them into the tibial compression system, then applying a 1–2 N compressive load for ~5 s.

### Fluorescent reflectance imaging (FRI)

All mice were imaged on days 1, 3, 7, 14, 28, and 56 after injury using *in vivo* FRI to quantify levels of fluorescence from activated probes in injured knees vs contralateral knees. Three probes were

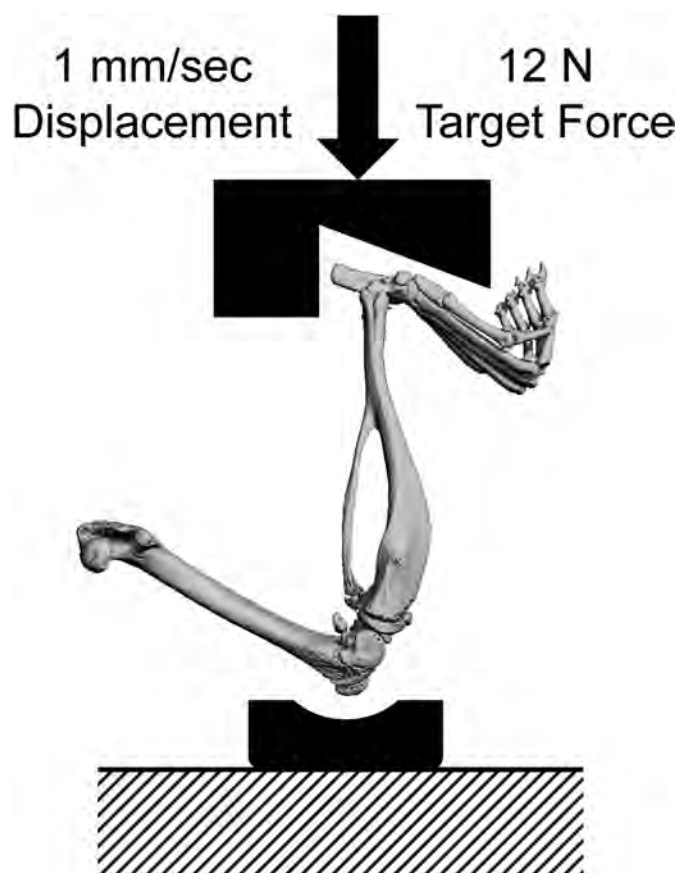


**Fig. 1.** Tibial compression setup for non-invasive knee injury. A single dynamic axial compressive load was applied at 1 mm/s to the right lower leg to a target compressive force of 12 N to produce ACL rupture. For uninjured mice, sham injury was performed by applying a 1–2 N compressive load.

used in this study: ProSense 680, MMPsense 680, and CatK 680 FAST (Table 1; PerkinElmer, Waltham, MA). Sixteen injured mice (8 male, 8 female) were analyzed with each of the fluorescent activatable probes; 6 uninjured (sham) mice (3 male, 3 female) were analyzed with ProSense 680 in order to confirm that there were no right/left differences in uninjured mice, and to quantify possible systemic inflammation that may be measurable in contralateral limbs of injured mice. In previous studies, both MMPsense<sup>26,27</sup> and ProSense<sup>13,16</sup> have been shown to localize to sites of inflammation, while CatK has been demonstrated to localize to sites of increased bone resorption and osteoclast activity<sup>28</sup>.

Before each imaging time point (24 h prior for ProSense 680 and MMPsense 680, and 6 h prior for CatK 680 FAST), mice were anesthetized via isoflurane inhalation, and 10  $\mu$ L (~0.1 mg/kg, IV) of probe was administered to each mouse. Hair was removed with a depilatory from the ventral aspect of both legs, and mice were imaged three at a time (22.5 cm field of view) in the imaging system (IVIS Spectrum, PerkinElmer, Waltham, MA). Each mouse was

**Table 1**  
Fluorescent tracers used to quantify early processes of PTOA

Imaging agent	Action	Indication
MMPsense 680	Activated by MMPs including MMP-2, -3, -9, -13	Localizes to inflammatory infiltrates involved in the degradation of collagens
ProSense 680	Activated by proteases such as Cathepsin B, L, S and Plasmin	Activated by family of lysosomal cathepsin proteases, allows detection of activated macrophages, neutrophils, eosinophils in the inflammatory response
CatK 680 FAST	Activated by Cathepsin K proteinase (Cat K)	Specific indicator of bone resorption

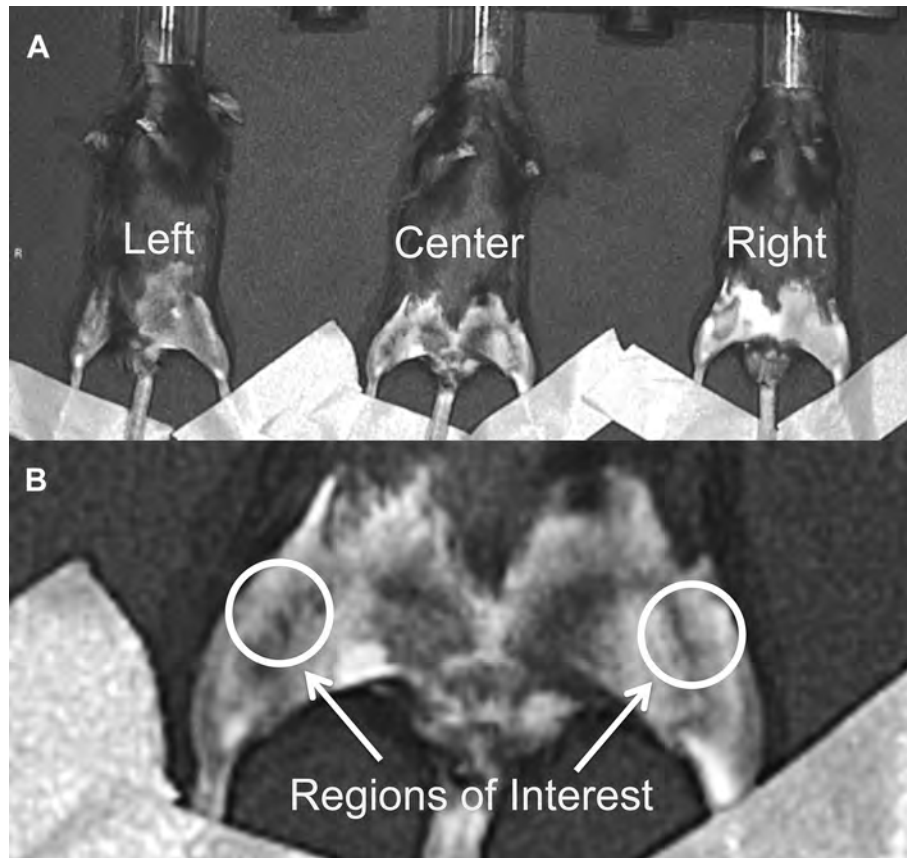


**Fig. 2.** (A) Imaging positions for mice in the IVIS Spectrum system. Each mouse was imaged twice at each time point in two different positions, and results from the two images were averaged for each mouse/time point. (B) Regions of interest for quantifying fluorescent signals in each knee. The ROI was a uniform circle of 12.3 mm<sup>2</sup> that was anatomically selected around the knee on a grayscale photograph of the mice, such that the selection criteria were unbiased by the fluorescent signals.

imaged twice at each time point in two different positions (left, right, or center; Fig. 2A), and results from the two images were averaged for each mouse/time point. Mouse legs were positioned such that the anterior-medial aspect of the knees was horizontal to allow for even epi-illumination. The legs were taped down across the ankle, and image processing and quantification was performed via IVIS Living Image software.

The excitation and emission filters for all probes were  $675 \pm 35$  nm and  $700 \pm 35$  nm, respectively, and were chosen based on the peak excitation and emission spectra of the probes (680/700 nm ex/em for ProSense 680 and MMPsense 680; 675/693 nm ex/em for CatK 680 FAST). The exposure time for each probe was 0.75 s for ProSense 680, 0.75 s for MMPsense 680, and 1.0 s for CatK 680 FAST. Spatial binning of pixels was set at the Medium option and the F/Stop was set to 2. Quantification of fluorescence intensity was performed by evaluating the total radiant efficiency ([photons/sec]/[ $\mu\text{W}/\text{cm}^2$ ]) of the signal within a region of interest (ROI). The ROI was a uniform circle of 12.3 mm<sup>2</sup> that was anatomically selected around the knee on a grayscale photograph of the mice [Fig. 2(B)], such that the ROI selections encapsulated the entire knee and were unbiased by the fluorescent signals. Subsequently, the total radiant efficiency of the injured knee was normalized to the contralateral uninjured knee of each mouse, to account for mouse-to-mouse variation in delivery of the fluorescent probe.

#### Micro-computed tomography analysis of epiphyseal trabecular bone and osteophyte formation

Injured and uninjured knees from 8 male and 8 female mice were analyzed with micro-computed tomography ( $\mu\text{CT}$  35,

SCANCO, Brüttisellen, Switzerland) to quantify trabecular bone structure of the distal femoral epiphysis and osteophyte formation around the joint. All mice were sacrificed 56 days post-injury following the last time point for FRI imaging. Dissected limbs were fixed in 4% paraformaldehyde for 48 h, then preserved in 70% ethanol. Knees were scanned according to the guidelines for  $\mu\text{CT}$  analysis of rodent bone structure<sup>29</sup> (energy = 55 kVp, intensity = 114 mA, 10  $\mu\text{m}$  nominal voxel size, integration time = 900 ms). Analysis of trabecular bone in the distal femoral epiphysis was performed by manually drawing contours on 2D transverse slices; the distal femoral epiphysis was delineated as the region of trabecular bone enclosed by the growth plate and sub-chondral cortical bone plate (Fig. 3). Using the manufacturer's analysis software, we quantified trabecular bone volume per total volume (BV/TV), trabecular thickness (Tb.Th), trabecular separation (Tb.Sp), trabecular number (Tb.N), bone tissue mineral density (Tissue BMD; mg HA/cm<sup>3</sup> BV), and apparent mineral density (Apparent BMD; mg HA/cm<sup>3</sup> TV). Osteophyte volume was calculated for each knee. For this analysis, manual contours were drawn to quantify all non-native mineralized tissue in and around the joint space, excluding naturally ossified structures (patella, fabella, anterior and posterior horns of the menisci; Fig. 3).

#### Whole-joint histology of articular cartilage

Following  $\mu\text{CT}$  imaging, knees from the same 8 male mice and 8 female mice were analyzed with whole-joint histology to quantify cartilage and joint deterioration. Knee joints were decalcified for 4 days in 10% buffered formic acid, and processed for standard paraffin embedding. From each joint, four sagittal slices of 6  $\mu\text{m}$

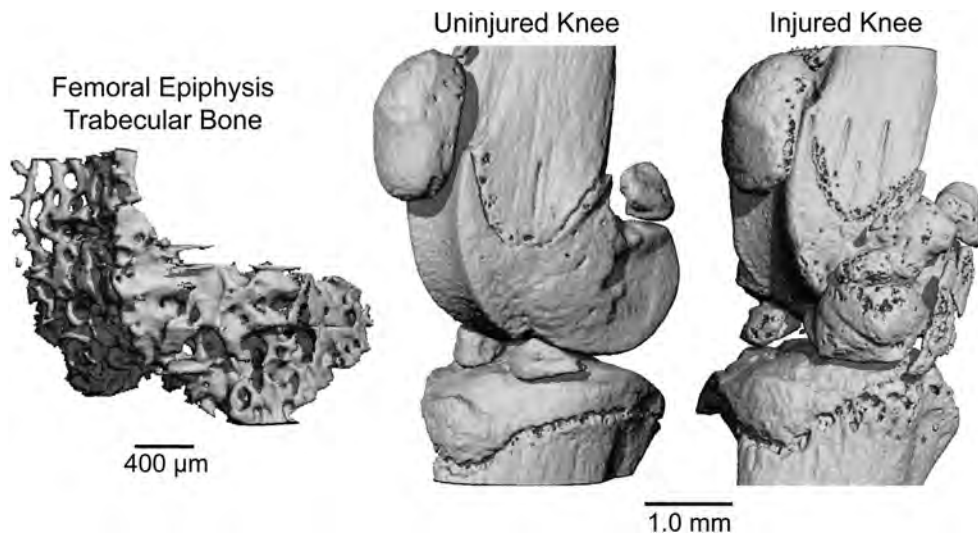


**Fig. 3.** (Left) Trabecular bone volume of interest from the femoral epiphysis. (Right) Uninjured and injured mouse knees at 56 days post-injury. Considerable osteophyte formation and joint degeneration are apparent on the injured knee.

thickness were sectioned from the medial joint, separated by 250 µm. The medial joint was analyzed since this is the primary site of joint degeneration in our previous studies, and in studies by other investigators using similar models<sup>24,30</sup>. Slides were stained with Safranin-O and Fast Green in order to assess proteoglycan content, articular cartilage degeneration, and overall joint integrity. Slides were blinded and graded by three independent readers using the semi-quantitative OARSI scale<sup>31</sup>. Grades were assigned to the medial tibial plateau and medial femoral condyle. Grades from the three readers were averaged for each section, and all gradable sections were averaged for each knee.

#### Statistical analysis

For all analyses, paired Student's *t*-tests were used within each experimental group in order to determine differences in injured vs uninjured knees. Differences in FRI readings between time points were analyzed with repeated measures ANOVA. FRI, µCT, and histology data were compared between male and female mice at each time point using unpaired *t*-test. Differences were considered statistically significant at  $P < 0.05$  for all tests. All data is presented as mean  $\pm$  95% confidence interval. We also performed a statistical analysis to assess the effect of mouse position within the imaging chamber (left, right, center). We performed repeated-measures ANOVA on radiant efficiencies of mice imaged in the three positions, by delineating both the position on the stage and the position of a mouse leg with respect to the center as additional ordinal variables.

## Results

#### FRI quantification of protease, MMP, and cathepsin K activity

Protease activity (ProSense 680), MMP activity (MMPsense 680), and cathepsin K activity (CatK 680 FAST) were all significantly increased in the injured knee compared to the contralateral (uninjured) knee at all time points (Figs. 4 and 5;  $P < 0.05$ ). No significant differences were observed between male and female mice for any of the probes at any of the time points examined. Uninjured mice did not exhibit significant differences between the right and left knees at any time points. No differences in protease activity

(ProSense 680) were observed between uninjured mice and contralateral knees at any time points except at 14 days post-injury, at which point protease activity of uninjured mice was significantly lower than contralateral knees, and significantly lower than all other time points for uninjured mice.

Normalization of fluorescence data (injured/contralateral for each mouse) indicated that MMPsense and ProSense were elevated 33–77% from days 1–14 post-injury, then decreased at

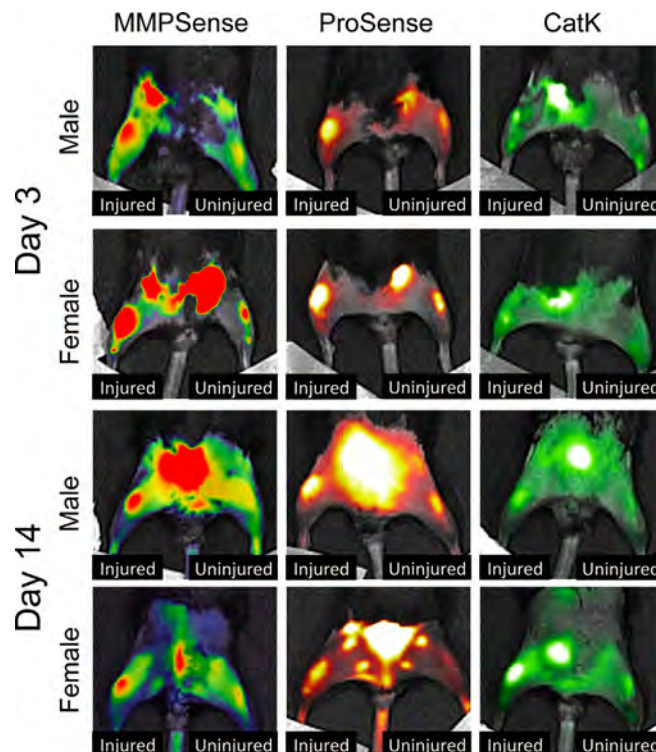


**Fig. 4.** Representative pseudo-colored images of male and female mice imaged with each of the fluorescent tracers at 3 and 14 days post-injury. Protease activity (ProSense 680), MMP activity (MMPsense 680), and cathepsin K activity (CatK 680 FAST) were all significantly increased in the injured knee compared to the contralateral knee at all time points.

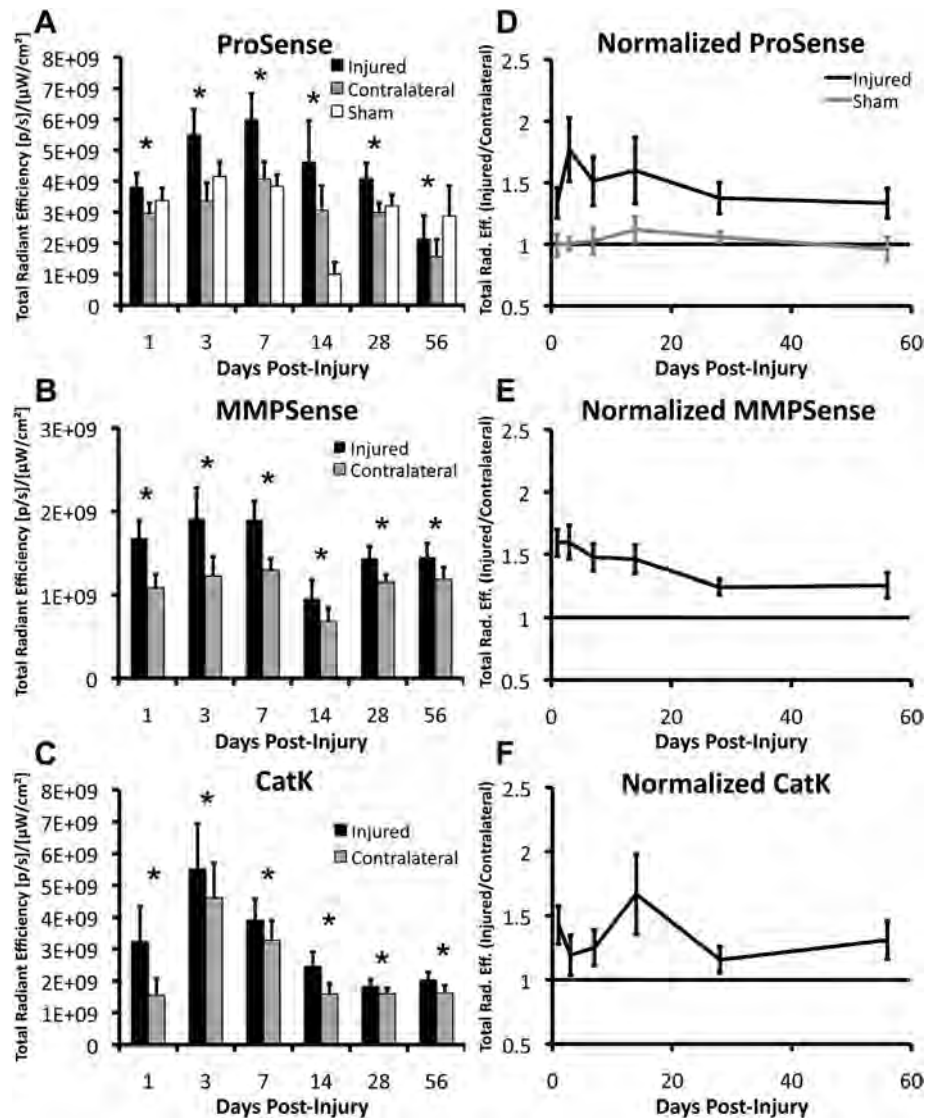


**Fig. 5.** (A–C) Total radiant efficiency values from each fluorescent activatable probe at each time point of interest ( $n = 16$  mice/time point for Injured and Contralateral data,  $n = 6$  for Sham data). (D–F) Normalized time course of total radiant efficiency (fluorescence intensity: injured knee/contralateral knee) for the three probes. Normalized fluorescence levels of MMPSense and ProSense were elevated from days 1 through 14, and decreased slightly at later time points while still remaining significantly elevated compared to uninjured limbs (above 1.0). CatK 680 FAST signals were increased in both the injured and contralateral knees at days 3–7, suggesting a systemic bone loss at these time points. All data presented as mean  $\pm$  95% confidence interval. \*Injured > Contralateral ( $P < 0.05$ ).

later time points while still remaining 24–37% greater than contralateral limbs until at least 56 days post-injury. Normalized data from the CatK probe exhibited a less consistent time course, with noticeable peaks in Cathepsin K activity at days 1 and 14. The raw (non-normalized) CatK 680 signal exhibited significant increases in both the injured and contralateral knees (Fig. 5), particularly at days 3 and 7 relative to other time points. Fluorescence intensity for ProSense and MMPSense of the contralateral knees also varied throughout the time course of the study, but did not exhibit the nearly 3-fold increase observed for the CatK probe at day 3.

Analysis of imaging positions within the IVIS Spectrum confirmed that there were significant differences in total radiant efficiency quantified between each of the respective positions ( $P < 0.001$ ) due to slight differences in illumination intensity. To account for this, mouse position was included as a factor in all statistical analyses. Future studies will utilize only one imaging position (center) in order to eliminate this confounding factor.

#### Micro-computed tomography of femoral epiphysis

MicroCT analysis of injured and uninjured joints at Day 56 revealed a ~27% loss of trabecular bone volume and notable osteophyte formation in injured joints relative to uninjured joints, consistent with our previous findings<sup>24,25</sup> (Fig. 6). We observed no significant difference between males and females in osteophyte formation or trabecular bone adaptation, as injured-contralateral differences in trabecular bone volume fraction (BV/TV), connectivity density (Conn.Dens), structural model index (SMI), trabecular number (Tb.N), trabecular thickness (Tb.Th), and trabecular separation (Tb.Sp) were all similar for both sexes. We did, however, observe significant differences in the absolute values of some trabecular bone parameters between male and female mice (not considering adaptation to injury). For example, males exhibited significantly higher connectivity density ( $P < 0.001$ ) and trabecular number ( $P < 0.001$ ) than females, while females exhibited significantly higher trabecular thickness ( $P < 0.001$ ) and trabecular

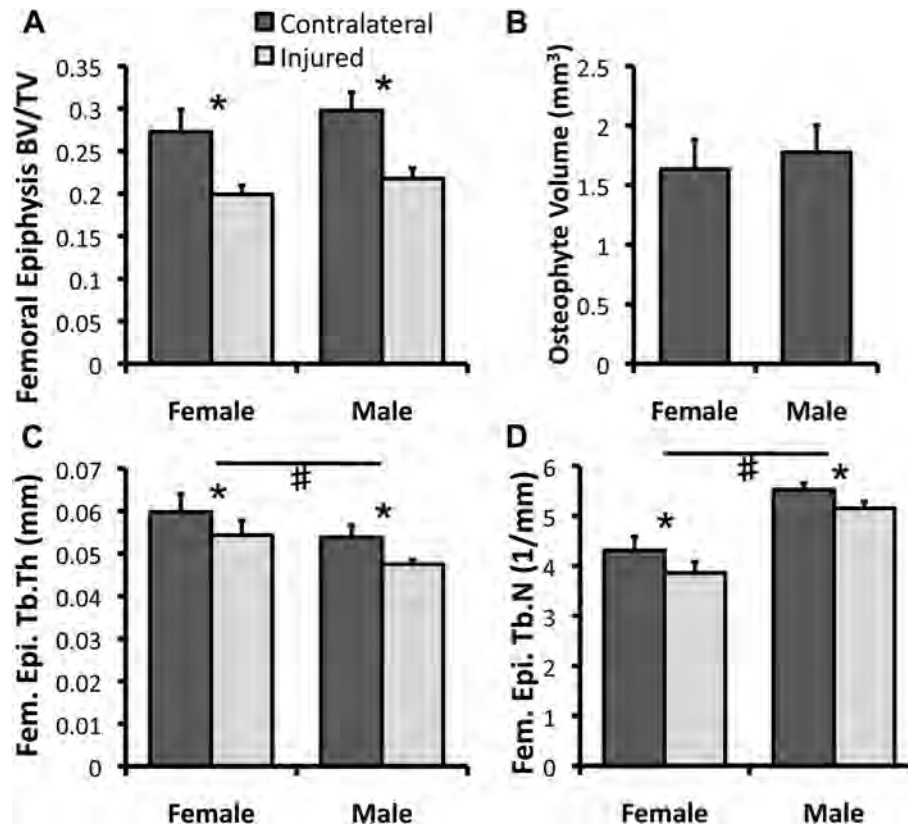


**Fig. 6.** (A, C, D) MicroCT analysis of femoral epiphysis trabecular bone structural parameters from injured and contralateral joints and (B) osteophyte volume of injured joints at 56 days post-injury ( $n = 8$  mice/sex). No significant differences were observed for any parameters between males and females in adaptation to injury. All data presented as mean  $\pm$  95% confidence interval. \*Injured vs Contralateral ( $P < 0.05$ ), # Male vs Female ( $P < 0.05$ ).

separation ( $P < 0.001$ ) than male mice. This is consistent with previously published findings in mice<sup>32</sup>.

#### Histological analysis of articular cartilage of the medial joint

Whole-joint histology of injured and uninjured knees revealed severe deterioration of articular cartilage and subchondral bone in injured knees, often including full loss of thickness and erosion of subchondral bone, representative of severe OA (Fig. 7). Degradation of cartilage often extended into the subchondral bone causing bone-to-bone contact. Osteophyte formation was also observed on the tibia and femur, along with growth of new mineralized cartilage from menisci. The anterior portion of the tibial plateau was not noticeably damaged, while the posterior tibial plateau exhibited erosion extending to the growth plate. This pattern of degeneration is similar to what we have observed at 12 and 16 weeks post injury<sup>25</sup>. Histological grading revealed significant differences between injured joints and uninjured control joints for both the tibial plateau ( $P < 0.001$ ) and femoral condyle ( $P < 0.001$ ). No significant differences were observed between male and female mice.

#### Discussion

In this study, we used FRI to visualize and quantify the time course of the biological response to traumatic joint injury in mice *in vivo* using near-infrared fluorescent activatable probes that report on protease activity, MMP activity, and cathepsin K activity. We confirmed that these processes are significantly increased in injured joints relative to uninjured joints, particularly at early time points (1–14 days post-injury), but contrary to our initial

hypothesis, these processes did not return to control values at later time points. Rather, the increased protease activity observed in injured joints remained for the duration of the study (8 weeks).

This study used FRI to quantify and characterize the dynamic protease profile longitudinally in the same animals during the development of injury-induced PTOA. We were able to demonstrate that injured joints exhibited increased levels of protease activity, MMP activity, and cathepsin K activity compared to uninjured knees. ProSense 680 specifically reports on cysteine proteases such as Cathepsins B, L, and S, while CatK 680 reports specifically on Cathepsin K activity, and MMPsense reports on a family of MMPs involved in inflammation. A role for cathepsins (excluding Cathepsin K) is well-established in osteoarthritic progression, though they may not be the prime mediators of articular cartilage deterioration or bone turnover<sup>33–36</sup>. Cathepsin K plays a major role in bone resorption and aggrecan degradation; it has been recognized as one of the most abundant and primary proteases in osteoclastic activity. Additionally, Cathepsin K has shown the ability to degrade type II collagen, therefore it may also be directly involved in the degradation of articular cartilage in addition to its role in osteoclast function<sup>37</sup>. MMPs are the primary collagenolytic enzymes of osteoarthritic cartilage; MMP-13 is extremely active and MMP-3 is thought to be a collagenase activator<sup>33</sup>, and MMP-9 is highly responsible for initiating osteoclastic resorption by removing the collagenous layer from the bone surface before demineralization begins<sup>38</sup>.

In this study we observed increased Cathepsin K activity at days 3 and 7 post-injury relative to other time points in both injured and contralateral knees following injury. This is consistent with our previous study<sup>24</sup>, in which we observed a decrease in trabecular

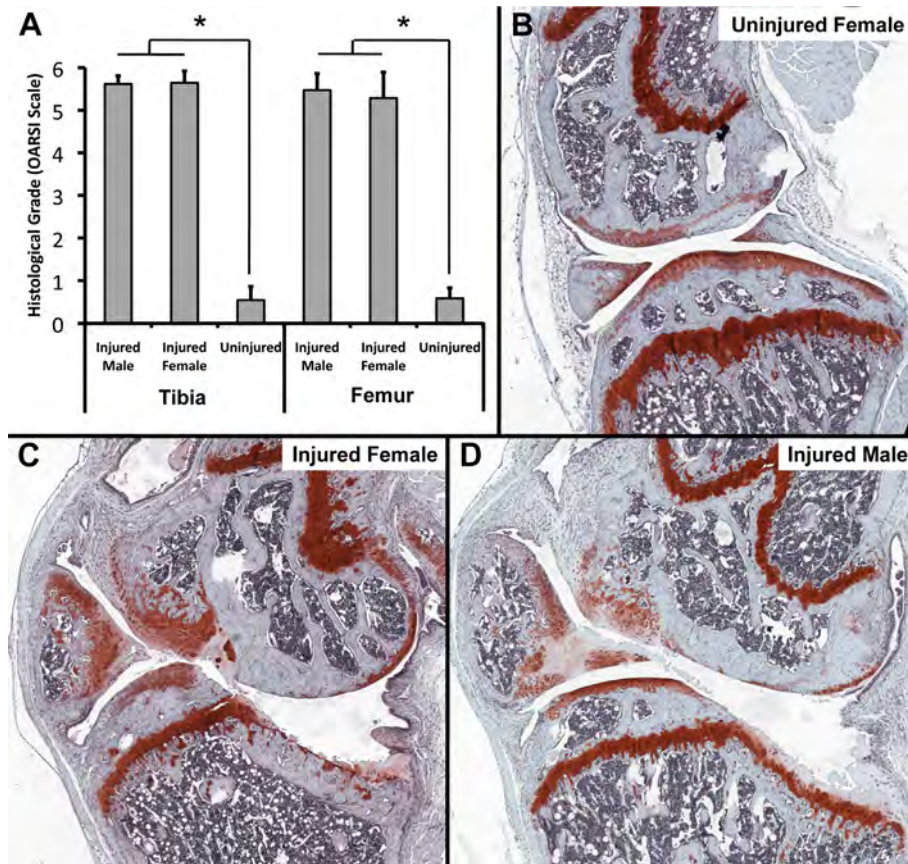


**Fig. 7.** Whole-joint histology of the medial aspect of injured and contralateral joints at 56 days post-injury ( $n = 8$  mice/sex for Injured data,  $n = 6$  mice for Uninjured data). Injured joints exhibited considerable deterioration of articular cartilage and subchondral bone, often including full loss of thickness and erosion of subchondral bone, representative of severe progressive OA (B–D). The anterior portion of the tibial plateau was not noticeably damaged, while the posterior tibial plateau exhibited erosion extended down to the growth plate. Articular cartilage grading revealed severe OA on both the tibial plateau and femoral condyle (A). No significant differences were observed between male and female mice. All data presented as mean  $\pm$  95% confidence interval. \*Injured vs Contralateral ( $P < 0.05$ ).

bone volume from the femoral epiphysis of both injured and contralateral knees by 7 days post-injury. Similarly, a study of injured and contralateral knees in human subjects following traumatic joint injury showed an increase in concentrations of aggrecan and cartilage oligomeric matrix protein (COMP) fragments and stromelysin-I in contralateral knees<sup>39</sup>. In the current study we did not observe significant increases in early protease activity or MMP activity in the contralateral knee relative to uninjured mice or later time points. However, this contralateral effect should be carefully considered for studies of OA using FRI, and future studies should more extensively utilize uninjured (sham) mice. It is common practice to use an internal control for normalizing fluorescent signals with FRI measurements, as this accounts for possible mouse-to-mouse differences in probe delivery. Systemic variations in fluorescent signal strength may be due to probe delivery, exact placement on the imaging stage, or illumination intensity. Normalizing by an internal control for each mouse can theoretically account for these systemic variations in difference in signal strength. However, taking into account the possible contralateral increases in these biological processes following an acute injury, this may not be a suitable analysis method for future studies of OA.

We did not detect any differences in PTOA development between male and female mice using any of the analysis methods in this study. It is well known that female athletes are 4–6 times more likely than male athletes to sustain an ACL rupture during exercise or sports<sup>40–43</sup>, however studies of both humans and animal models suggest that males may have a greater tendency to develop PTOA

following traumatic joint injury<sup>44–46</sup>. However, the specific mechanisms contributing to this sex-related disparity are unknown. In the current study we did not observe any sex-based differences in the protease profile at any of the time points. Furthermore, we did not observe any sex-based differences in articular cartilage or subchondral bone degeneration at 56 days post-injury. This may be due to examining a single time point when severe OA has already developed. An intermediate time point may be useful for detecting sex-based differences in OA progression, similar to those observed previously<sup>45,46</sup>.

*In vivo* FRI was able to detect significant differences in fluorescent signal in injured vs contralateral knees using three different probes, however the high variability of this *in vivo* imaging technique may limit the capability to observe relatively small differences in fluorescence levels. For example, quantification of fluorescent signals using the IVIS Spectrum system exhibited large variance and a strong dependence on position of mice within the system. The IVIS Spectrum system produces a circular beam of light from the epi-illumination excitation light source above the stage. Because we imaged three mice at a time, the centrally located mouse received the most uniform illumination; whereas the mice on the left and right sides had more non-uniformity. An analysis of mouse position within the imaging system helped elucidate this issue, and by performing a repeated-measures ANOVA on radiant efficiencies on mice imaged in different positions, we confirmed that there was a significant difference in brightness between each respective position on the stage, as well as the position of each leg,

with respect to the center line. In addition, typical issues of auto-fluorescence and attenuation by tissue are continually a concern for *in vivo* imaging studies. In this respect, variations from mouse to mouse can make it difficult to quantify fluorescence with accuracy and reliability, as the depth of penetration of irradiated light can be considerably different. Future studies will minimize measurement variability by using only the center imaging position, however the precision of this imaging technique for detecting small differences in fluorescent signals remains unclear. However, despite these limitations, we were able to successfully track the time course of protease, MMP, and cathepsin K activity following knee injury in mice. This imaging method is non-invasive, time and cost effective, and provides longitudinal data from individual mice at multiple time points. In this way, FRI is a meaningful step forward for quantification of early biological processes in mouse models of PTOA.

This study is also somewhat limited because we did not validate our *in vivo* fluorescent signals with a histological “gold standard” such as immunohistochemistry or *in situ* hybridization. Therefore, we are unable to attribute the observed fluorescent signals to specific tissues associated with PTOA development. However, each of these fluorescent activatable probes has been extensively validated and compared to histological standards<sup>12–19</sup>, and in particular have been validated for studies of musculoskeletal tissues<sup>20–23</sup>, therefore we are confident that the fluorescent signals are indicative of cellular processes at the level of the whole joint. Our future studies will utilize histological techniques to further characterize the specific tissues in which these fluorescent signals originate following traumatic joint injury using this animal model.

Using commercially available fluorescent agents we were able to quantify the time course of protease activity, MMP activity, and cathepsin K activity following traumatic injury to the ACL, with noticeable peaks at early time points (1–7 days post-injury). This early response may point to a “window of opportunity” in which treatments may be administered to most efficiently stall the progression of OA. Cathepsin and MMP inhibitors have both been utilized experimentally, both in the molecular and transcriptional pathways, as potential therapies for hindering OA progression<sup>33</sup>. Future studies could investigate effective time periods for treatment in the murine model, which can then be extrapolated into larger animal models and human subjects.

## Conclusions

Using *in vivo* FRI, we observed substantial increases in protease activity, MMP activity, and cathepsin K activity in injured joints compared to uninjured joints in mice following traumatic knee injury. We successfully described the dynamic protease profile following joint injury, and established FRI as a useful analysis method contributing to the quantification of OA progression in mice. This study provides crucial information about the time course of inflammation and cellular activity in a translatable mouse model of knee injury, and may inform future studies aimed at targeting early inflammation to reduce the development of PTOA.

## Author contributions

All authors were fully involved in this study and in preparation of the manuscript.

## Role of funding sources

Research reported in this publication was supported by the National Institute of Arthritis and Musculoskeletal and Skin Diseases, part of the National Institutes of Health, under Award Number AR062603 (BAC) and AR063348 (DRH). The content is solely the

responsibility of the authors and does not necessarily represent the official views of the National Institutes of Health.

## Competing interest statement

The authors have no potential conflicts of interest to disclose.

## Acknowledgments

We would like to acknowledge Susan Stover and David Fyhrie for their meaningful contributions to this study.

## References

- Lawrence RC, Felson DT, Helmick CG, Arnold LM, Choi H, Deyo RA, et al. Estimates of the prevalence of arthritis and other rheumatic conditions in the United States. Part II. *Arthritis Rheum* 2008;58:26–35.
- Lohmander LS, Englund PM, Dahl LL, Roos EM. The long-term consequence of anterior cruciate ligament and meniscus injuries: osteoarthritis. *Am J Sports Med* 2007;35:1756–69.
- Gillquist J, Messner K. Anterior cruciate ligament reconstruction and the long-term incidence of gonarthrosis. *Sports Med* 1999;27:143–56.
- Myklebust G, Bahr R. Return to play guidelines after anterior cruciate ligament surgery. *Br J Sports Med* 2005;39:127–31.
- Madry H, Luyten FP, Facchini A. Biological aspects of early osteoarthritis. *Knee Surg Sports Traumatol Arthrosc* 2012;20:407–22.
- Goldring MB, Goldring SR. Osteoarthritis. *J Cell Physiol* 2007;213:626–34.
- Anderson DD, Chubinskaya S, Guilak F, Martin JA, Oegema TR, Olson SA, et al. Post-traumatic osteoarthritis: Improved understanding and opportunities for early intervention. *J Orthop Res* 2011;29:802–9.
- Kurz B, Lemke AK, Fay J, Pufe T, Grodzinsky AJ, Schunke M. Pathomechanisms of cartilage destruction by mechanical injury. *Ann Anat* 2005;187:473–85.
- Fitzgerald JB, Jin M, Dean D, Wood DJ, Zheng MH, Grodzinsky AJ. Mechanical compression of cartilage explants induces multiple time-dependent gene expression patterns and involves intracellular calcium and cyclic AMP. *J Biol Chem* 2004;279:19502–11.
- Brophy RH, Rai MF, Zhang Z, Torgomyan A, Sandell LJ. Molecular analysis of age and sex-related gene expression in meniscal tears with and without a concomitant anterior cruciate ligament tear. *J Bone Joint Surg Am* 2012;94:385–93.
- Irie K, Uchiyama E, Iwasa H. Intraarticular inflammatory cytokines in acute anterior cruciate ligament injured knee. *Knee* 2003;10:93–6.
- Zhang H, Morgan D, Cecil G, Burkholder A, Ramocki N, Scull B, et al. Biochromoendoscopy: molecular imaging with capsule endoscopy for detection of adenomas of the GI tract. *Gastrointest Endosc* 2008;68:520–7.
- Gounaris E, Tung CH, Restaino C, Maehr R, Kohler R, Joyce JA, et al. Live imaging of cysteine-cathepsin activity reveals dynamics of focal inflammation, angiogenesis, and polyp growth. *PLoS One* 2008;3:e2916.
- Sheth RA, Mahmood U. Optical molecular imaging and its emerging role in colorectal cancer. *Am J Physiol Gastrointest Liver Physiol* 2010;299:G807–20.
- Clapper ML, Hensley HH, Chang WC, Devarajan K, Nguyen MT, Cooper HS. Detection of colorectal adenomas using a bio-activatable probe specific for matrix metalloproteinase activity. *Neoplasia* 2011;13:685–91.

16. Nahrendorf M, Sosnovik DE, Waterman P, Swirski FK, Pande AN, Aikawa E, *et al.* Dual channel optical tomographic imaging of leukocyte recruitment and protease activity in the healing myocardial infarct. *Circ Res* 2007;100:1218–25.
17. Jaffer FA, Kim DE, Quinti L, Tung CH, Aikawa E, Pande AN, *et al.* Optical visualization of cathepsin K activity in atherosclerosis with a novel, protease-activatable fluorescence sensor. *Circulation* 2007;115:2292–8.
18. Jaffer FA, Libby P, Weissleder R. Optical and multimodality molecular imaging: insights into atherosclerosis. *Arterioscler Thromb Vasc Biol* 2009;29:1017–24.
19. Razansky D, Harlaar NJ, Hillebrands JL, Taruttis A, Herzog E, Zeebregts CJ, *et al.* Multispectral optoacoustic tomography of matrix metalloproteinase activity in vulnerable human carotid plaques. *Mol Imaging Biol* 2012;14:277–85.
20. Kozloff KM, Quinti L, Patntirapong S, Hauschka PV, Tung CH, Weissleder R, *et al.* Non-invasive optical detection of cathepsin K-mediated fluorescence reveals osteoclast activity in vitro and in vivo. *Bone* 2009;44:190–8.
21. Kozloff KM, Quinti L, Tung C, Weissleder R, Mahmood U. Non-invasive imaging of osteoclast activity via near-infrared cathepsin-K activatable optical probe. *J Musculoskelet Neuronal Interact* 2006;6:353.
22. Kozloff KM, Volakis LI, Marini JC, Caird MS. Near-infrared fluorescent probe traces bisphosphonate delivery and retention in vivo. *J Bone Miner Res* 2010;25:1748–58.
23. Kozloff KM, Weissleder R, Mahmood U. Noninvasive optical detection of bone mineral. *J Bone Miner Res* 2007;22:1208–16.
24. Christiansen BA, Anderson MJ, Lee CA, Williams JC, Yik JH, Haudenschild DR. Musculoskeletal changes following non-invasive knee injury using a novel mouse model of post-traumatic osteoarthritis. *Osteoarthritis Cartilage* 2012;20:773–82.
25. Lockwood KA, Chu BT, Anderson MJ, Haudenschild DR, Christiansen BA. Comparison of loading rate-dependent injury modes in a murine model of post-traumatic osteoarthritis. *J Orthop Res* 2013;32:79–88.
26. Barber PA, Rushforth D, Agrawal S, Tuor UI. Infrared optical imaging of matrix metalloproteinases (MMPs) up regulation following ischemia reperfusion is ameliorated by hypothermia. *BMC Neurosci* 2012;13:76.
27. Liu N, Shang J, Tian F, Nishi H, Abe K. In vivo optical imaging for evaluating the efficacy of edaravone after transient cerebral ischemia in mice. *Brain Res* 2011;1397:66–75.
28. Hoff BA, Chughtai K, Jeon YH, Kozloff K, Galban S, Rehemtulla A, *et al.* Multimodality imaging of tumor and bone response in a mouse model of bony metastasis. *Transl Oncol* 2012;5:415–21.
29. Bouxsein ML, Boyd SK, Christiansen BA, Guldberg RE, Jepsen KJ, Muller R. Guidelines for assessment of bone microstructure in rodents using micro-computed tomography. *J Bone Miner Res* 2010;25:1468–86.
30. Glasson SS, Blanchet TJ, Morris EA. The surgical destabilization of the medial meniscus (DMM) model of osteoarthritis in the 129/SvEv mouse. *Osteoarthritis Cartilage* 2007;15:1061–9.
31. Glasson SS, Chambers MG, Van Den Berg WB, Little CB. The OARSI histopathology initiative – recommendations for histological assessments of osteoarthritis in the mouse. *Osteoarthritis Cartilage* 2010;18(Suppl 3):S17–23.
32. Glatt V, Canalis E, Stadmeier L, Bouxsein ML. Age-related changes in trabecular architecture differ in female and male C57BL/6J mice. *J Bone Miner Res* 2007;22:1197–207.
33. Troeberg L, Nagase H. Proteases involved in cartilage matrix degradation in osteoarthritis. *Biochim Biophys Acta* 1824;2012:133–45.
34. Woessner Jr JF. Purification of cathepsin D from cartilage and uterus and its action on the protein-polysaccharide complex of cartilage. *J Biol Chem* 1973;248:1634–42.
35. Fosang AJ, Neame PJ, Last K, Hardingham TE, Murphy G, Hamilton JA. The interglobular domain of cartilage aggrecan is cleaved by PUMP, gelatinases, and cathepsin B. *J Biol Chem* 1992;267:19470–4.
36. Hembry RM, Knight CG, Dingle JT, Barrett AJ. Evidence that extracellular cathepsin D is not responsible for the resorption of cartilage matrix in culture. *Biochim Biophys Acta* 1982;714:307–12.
37. Dejica VM, Mort JS, Lavery S, Antoniou J, Zukor DJ, Tanzer M, *et al.* Increased type II collagen cleavage by cathepsin K and collagenase activities with aging and osteoarthritis in human articular cartilage. *Arthritis Res Ther* 2012;14:R113.
38. Logar DB, Komadina R, Prezelj J, Ostanek B, Trost Z, Marc J. Expression of bone resorption genes in osteoarthritis and in osteoporosis. *J Bone Miner Metab* 2007;25:219–25.
39. Dahlberg L, Roos H, Saxne T, Heinegard D, Lark MW, Hoerrner LA, *et al.* Cartilage metabolism in the injured and uninjured knee of the same patient. *Ann Rheum Dis* 1994;53:823–7.
40. Arendt E, Dick R. Knee injury patterns among men and women in collegiate basketball and soccer – Ncaa data and review of literature. *Am J Sports Med* 1995;23:694–701.
41. Powell JW, Barber-Foss KD. Sex-related injury patterns among selected high school sports. *Am J Sports Med* 2000;28:385–91.
42. Hewett TE, Myer GD, Ford KR, Heidt Jr RS, Colosimo AJ, McLean SG, *et al.* Biomechanical measures of neuromuscular control and valgus loading of the knee predict anterior cruciate ligament injury risk in female athletes: a prospective study. *Am J Sports Med* 2005;33:492–501.
43. Zelisko JA, Noble HB, Porter M. A comparison of men's and women's professional basketball injuries. *Am J Sports Med* 1982;10:297–9.
44. Li RT, Lorenz S, Xu Y, Harner CD, Fu FH, Irrgang JJ. Predictors of radiographic knee osteoarthritis after anterior cruciate ligament reconstruction. *Am J Sports Med* 2011;39:2595–603.
45. van Osch GJ, van der Kraan PM, Vitters EL, Blankevoort L, van den Berg WB. Induction of osteoarthritis by intra-articular injection of collagenase in mice. Strain and sex related differences. *Osteoarthritis Cartilage* 1993;1:171–7.
46. Ma HL, Blanchet TJ, Peluso D, Hopkins B, Morris EA, Glasson SS. Osteoarthritis severity is sex dependent in a surgical mouse model. *Osteoarthritis Cartilage* 2007;15:695–700.



# *In-vitro* and *in-vivo* imaging of MMP activity in cartilage and joint injury



Tomoaki Fukui, Elizabeth Tenborg, Jasper H.N. Yik, Dominik R. Haudenschild\*

Lawrence J. Ellison Musculoskeletal Research Center, Department of Orthopaedic Surgery, University of California Davis Medical Center, 4635 Second Avenue Suite 2000, Sacramento CA 95817, USA

## ARTICLE INFO

### Article history:

Received 7 March 2015

Available online 26 March 2015

### Keywords:

Cartilage

*In-vivo* imaging

MMP activity

MMPsense750

Osteoarthritis

## ABSTRACT

Non-destructive detection of cartilage-degrading activities represents an advance in osteoarthritis (OA) research, with implications in studies of OA pathogenesis, progression, and intervention strategies. Matrix metalloproteinases (MMPs) are principal cartilage degrading enzymes that contribute to OA pathogenesis. MMPsense750 is an *in-vivo* fluorimetric imaging probe with the potential to continuously and non-invasively trace real-time MMP activities, but its use in OA-related research has not been reported. Our objective is to detect and characterize the early degradation activities shortly after cartilage or joint injury with MMPsense750. We determined the appropriate concentration, assay time, and linear range using various concentrations of recombinant MMPs as standards. We then quantified MMP activity from cartilage explants subjected to either mechanical injury or inflammatory cytokine treatment *in-vitro*. Finally, we performed *in-vivo* MMP imaging of a mouse model of post-traumatic OA. Our *in-vitro* results showed that the optimal assay time was highly dependent on the MMP enzyme. In cartilage explant culture media, mechanical impact or cytokine treatment increased MMP activity. Injured knees of mice showed significantly higher fluorescent signal than uninjured knees. We conclude that MMPsense750 detects human MMP activities and can be used for *in-vitro* study with cartilage, as well as *in-vivo* studies of knee injury, and can offering real-time insight into the degradative processes that occurring within the joint before structural changes become evident radiographically.

© 2015 Elsevier Inc. All rights reserved.

## 1. Introduction

Osteoarthritis (OA) is a degenerative disease of the whole joint organ characterized by cartilage degradation [1], and the number of OA patients continues to increase, estimated at nearly 27 million in the United States [2] and there is no effective treatment to prevent OA or restore joints after the onset of OA. At this time, the gold standard for clinical OA diagnosis and evaluation are morphologic assessments, such as radiography [3–5], computed tomography (CT) [5,6], and magnetic resonance imaging (MRI) [3,5,6]. These imaging technologies primarily reveal the morphological changes that become evident at the later stages of OA, but do not offer insight into the process of cartilage degradation. As the field of OA research moves toward OA prevention it is becoming important to also measure the biological processes responsible for joint

degradation, processes that precede the morphological and structural changes.

It is generally accepted that enzymatic activities contribute to cartilage degradation and loss in OA, and that elevated enzymatic activity precedes morphological joint space narrowing [7,8]. The ability to non-destructively image and quantify enzymatic activity would be an important tool to assess OA initiation and progression, and the efficacy of intervention strategies. While primary OA is considered idiopathic, in post-traumatic OA (PTOA) the time point of OA initiation (trauma) can be easily identified, and this is therefore an appropriate model to study the enzymatic activities during the early phases of OA.

Matrix metalloproteinases (MMPs) are a family of zinc-dependent degradative proteinases with roles in the enzymatic cartilage degradation and OA progression. MMP-mediated degradation of type II collagen fibrils is considered one of the first irreversible steps in OA pathogenesis (reviewed in Ref. [9]), and the presence of MMPs correlates with OA symptoms, including joint effusion and pain [10,11]. Although serum level of MMP-3 is used as a biomarker for rheumatoid arthritis (RA), there is no clinically

\* Corresponding author. Fax: +1 916 734 5750.

E-mail address: [DRHaudenschild@ucdavis.edu](mailto:DRHaudenschild@ucdavis.edu) (D.R. Haudenschild).

established MMP biomarker for OA [12]. Most studies investigating MMP activity in OA rely on assays such as ELISA [13,14] or Western Blotting [14,15], and RT-PCR [14,16] to estimate protein levels and mRNA expression, respectively. However, these assays are not suitable for *in-vivo* use, and can only measure the amount of MMP protein but do not directly assay MMP activity. Direct measurements of MMP activity include zymography [14,16,17] and more recently fluorimetric MMP assays [14,16], but again these assays are generally not suited for *in-vivo* imaging. The development of a method to visualize MMP activities *in-vivo* hence may offer new insight into OA initiation and treatment efficacy.

An *in-vivo* fluorimetric probe was recently developed that allows non-destructive imaging of activity from a broad spectrum of MMPs (MMPsense™ 750 FAST PerkinElmer, Inc., Boston, MA). This near-infrared fluorescent probe is a peptide substrate that enables the detection of MMP activities by exhibiting fluorescent signal when cleaved by MMPs [13,15,18]. *In-vivo* imaging with this reagent has the potential to continuously measure real-time MMP activities non-invasively. This probe has been successfully used to detect tumor progression [13,18] or ischemia reperfusion in brain [15] with *in-vivo* mouse model, but to our best knowledge there is no previous report investigating MMPsense750 for the assessment of MMP activity in cartilage or joint injury. Moreover, although this probe is expected to be utilized for human patients in clinical setting in future, no paper has studied the kinetics of this substrate using human MMPs. The objective of the present study is to investigate the potential of MMPsense750 for detection of human MMPs and to use in an assay with cartilage explants, as well as an *in-vivo* mouse model of knee injury leading to PTOA.

## 2. Methods

### 2.1. Assessment of optimal MMPsense750 concentration

We first wanted to determine the appropriate MMPsense750 concentration for *in-vitro* studies using purified recombinant human MMPs. Human MMP-3, -9, and -13 were chosen based on their established importance in OA [11,19,20]. To achieve comparable results between the different enzymes, the amount of active enzyme in each assay was normalized using the specific activity (Units of enzyme activity per weight) provided by the manufacturer (Supplementary information 1). MMPsense750 was added to media containing the active proteases, the reactions were incubated at 37 °C, and the resulting fluorescent signal was measured at different time points as described in detail below.

Recombinant human MMP-3 (Enzo Life Sciences, Farmingdale, USA) was reconstituted to various concentrations in assay buffer consisting of 50 mM sodium acetate, 10 mM CaCl<sub>2</sub>, 150 mM NaCl and 0.05% Brij-35 at pH 6.0 [9]. Recombinant human MMP-9 and MMP-13 (Enzo Life Sciences) were reconstituted in the assay buffer consisting of 50 mM HEPES, 10 mM CaCl<sub>2</sub> and 0.05% Brij-35 at pH 7.5 [21].

MMPsense750 (24 nmol per vial) was reconstituted in 1200 µl sterile phosphate-buffered saline (Invitrogen) as recommended by the manufacturer, then added into the MMP solutions at 0.2, 0.7 and 2.0 µM final concentration. Imaging was performed on an IVIS-Spectrum imaging system at multiple time points for up to 72 h after adding MMPsense750.

### 2.2. Cartilage explants

Cartilage explants were harvested from the weight-bearing area of the femoral articular surfaces of bovine stifle knee joints purchased from a local slaughterhouse (Petaluma, CA). A 6 mm dermal biopsy punch was used to isolate cartilage cylinders, which

were then cut to 2 mm height from the articular surface using a custom jig. Explants were cultured for 3 days in DMEM with 10% FBS and 1% penicillin-streptomycin (all from Invitrogen, Carlsbad, CA) at 37 °C and 5% CO<sub>2</sub>. Six joints were used, and 1 or 2 explants from each joint was randomly assigned to one of three treatment groups; IL-1β, mechanical injury, or control. There was no significant difference among the cartilage weights of each group. The IL-1β group was treated with 10 ng/ml IL-1β (R&D Systems, Minneapolis, MN). The explants in the mechanical injury group were mechanically compressed with an Instron 8511.20 digital servo-hydraulic mechanical testing device using displacement control. A compressive preload of ~0.5 N was applied, and then the explant was loaded to 30% strain at a strain rate of 100%/s, held at 30% strain for 100 ms, then unloaded. Following compression, all loaded explants were transferred to fresh culture medium and returned to an incubator at 37 °C and 5% CO<sub>2</sub> until the termination of the experiment. In the control group, the explants were given a preload of ~0.5 N and then returned to the culture media. The culture media were replenished at day 3. The media were collected at 3 and 6 days after IL-1β stimulation or mechanical injuries. MMPsense750 was added to a final concentration of 0.7 µM, and the fluorescence measured at 60 min and 24 h after adding MMPsense.

### 2.3. Animal model of joint injury

Eight adult male BALB/cByJ mice (9-week-old at time of injury) were obtained from Jackson Laboratory (Bar Harbor, Maine). All animals were maintained and used in accordance with National Institutes of Health guidelines on the care and use of laboratory animals. This study was approved by our Institutional Animal Care and Use Committee (IACUC). The right knees of the mice were injured with a single mechanical compression as previously described in our PTOA model [22]. Briefly, the tibial compression system consists of two custom-built loading platens; the bottom platen that holds the knee flexed, and the top platen that holds the heel. The platens were aligned vertically and positioned within an electromagnetic materials testing machine (Bose ElectroForce 3200) (Eden Prairie, MN). Mice were anesthetized using isoflurane inhalation, then the right leg of each mouse was subjected to a single dynamic axial compression (1 mm/s loading rate) to a target load of 12 N. This causes a transient anterior subluxation of the tibia, which injures the anterior cruciate ligament and leads to PTOA within 8 weeks. The contralateral uninjured knees served controls, and were used to normalize the data within each animal.

All mice received an injection of 2 nmol of MMPsense750 via the orbital sinus at 24-h post-injury, and IVIS imaging was performed 24 h after the injection (48-h post-injury). Mice were euthanized immediately after the imaging and both knees were dissected for isolation of total RNA and analysis of mRNA expression.

### 2.4. Quantitative real-time RT-PCR

Total RNA was extracted from injured and uninjured knees using the miRNeasy Mini Kit (Qiagen Valencia, CA) and reverse transcribed by the QuantiTect Reverse Transcription Kit (Qiagen). 2 µl of cDNA was used for quantitative RT-PCR (in a final volume of 10 µl) performed in triplicate in a 7900HT RT-PCR system with gene-specific probes according to the manufacturer's conditions. Results were normalized to the 18s rRNA and calculated as fold-change in mRNA expression relative to the untreated control, using the  $2^{-\Delta\Delta CT}$  method. The probes used are shown in Supplementary information 2.

## 2.5. IVIS imaging

An IVIS Spectrum imaging system (Perkin Elmer) was utilized to monitor fluorescent signal of MMPsense750. For imaging of media cultured with cartilage explants, the samples were placed in black plates. For *in-vivo* imaging of mice, the hairs from the lower trunk and both legs were removed, and then imaging was performed under general anesthesia by isoflurane inhalation. The excitation and emission wavelengths were set to 745 and 800 nm, respectively. The fluorescence intensities were analyzed by Living Image software 4.2 (Perkin Elmer). Grid type and circle type of regions of interest (ROI) were set for plates and mice, respectively. Average radiant efficiency [ $\text{p/s/cm}^2/\text{sr}/[\mu\text{W/cm}^2]$ ] in the ROI was measured as an index of intensity of fluorescent signal. For the experiment with MMP enzymes, normalized average radiant efficiency was calculated by subtracting the value of average radiant efficiency with 0(m)U of MMPs from that with each concentration of MMPs and used for the assessment. For the purpose of clarity, we use the term “fluorescence intensity” to indicate normalized average radiant efficiency in the ROI.

## 2.6. Statistical analysis

The results were statistically analyzed using a software package (GraphPad Prism; MDF Software, Inc.). Values of all measurements were expressed as the mean with error bars representing the 95% confidence interval. Correlation between MMP concentration and MMPsense signal was evaluated with Pearson correlation coefficient. Differences of MMPsense signal with MMP enzymes and *in-vivo* study were analyzed by paired *t* tests. Comparison of MMPsense signal between different concentrations of MMPs and of MMPsense signal with cartilage explants were analyzed by unpaired *t* test. Comparison of mRNA expression was analyzed by Wilcoxon signed rank test.

## 3. Results

### 3.1. Determination of the optimal MMPsense750 concentration for *in-vitro* experiments

To examine how well the normalized fluorescent signal correlated to the MMP activity at each time point, Pearson's correlation coefficients (*R*) were calculated for each combination of MMPsense and time (Fig. 1). For all MMPs, the best correlation between MMP activity and fluorescent signal occurred at the higher concentrations of MMPsense probe, 0.7 or 2.0  $\mu\text{M}$ . Perhaps more surprisingly the best time to measure fluorescence intensity was highly dependent on the types of MMP enzyme. For MMP-13, high correlations were observed as early as 15 min, while MMP-3 started to become significant after 60 min, and MMP-9 not until after 24 h. At the later time points the MMP activity and fluorescent signal were highly correlated for all three MMP enzymes.

To estimate the detection limit of the assay at each concentration of MMPsense750 over time, we statistically analyzed the differences between fluorescent intensity for each concentration increase of MMP (Supplementary Fig. 1). The intermediate concentrations of MMP generated significantly different fluorescence signal in all conditions, but there were variations in the lower and upper detection limits. With respect to the upper detection limit, we examined the fluorescent signal over time for each enzyme and the higher MMPsense probe concentrations (Fig. 2). While higher concentrations of MMPsense yielded greater absolute fluorescence signals, the statistical analysis showed no benefit of the 2  $\mu\text{M}$  compared to 0.7  $\mu\text{M}$  MMPsense probe.

Taken together, these results indicate that 0.7  $\mu\text{M}$  of MMPsense750 at a 24 h time point would yield the best assay to measure the activities of the three MMPs over the greatest range of concentrations.

### 3.2. MMP activity in IL-1 $\beta$ -treated cartilage explants

Three days of IL-1 $\beta$  treatment caused a significant increase in fluorescence intensity of culture media, indicating elevated MMP activity in cartilage explants (Fig. 3A). Specifically, the fluorescence signal of the IL-1 $\beta$  group at day 3 was significantly greater than that of the control group both at 60 min and 24 h after adding MMPsense750. At day 6, fluorescence intensity in the IL-1 $\beta$ -treated group was significantly greater than that of the control group at 24 h (but not 60 min) after adding MMPsense750.

### 3.3. MMP activity in mechanically injured cartilage explants

As observed with the IL-1 $\beta$  treatment, the fluorescence of the mechanical injury group at day 3 was significantly greater than that of the control group at both 60 min and 24 h after adding MMPsense750. At day 6, the trends are similar to the IL-1 $\beta$  treatment, with greater fluorescence at the 24 h, although this did not reach statistical significance (Fig. 3B).

### 3.4. MMP activity *in-vivo* after knee injury

The non-surgical joint injury caused a substantial increase in the fluorescence intensity in the injured right knee relative to the uninjured left knee of the same animal, indicating that injury increased the local MMP activity (Fig. 4A). The real-time RT-PCR results showed elevated mRNA expression of MMP-3 in the injured knee at this time point (48 h after injury), while the expression of MMP-9 and -13 were not statistically different in the injured and contralateral limb at this time point (Fig. 4B).

## 4. Discussion

Imaging technologies used in OA primarily measure structural morphology rather than the biological processes that contribute to joint degradation. The results in the present study demonstrate that the MMPsense750 is useful with human MMPs, providing insight into the parameters to consider when interpreting the data, and show a good response of the assay in *in-vitro* studies of cartilage explants and in a mouse model of joint injury. Although there are a few previous reports using MMPsense680, precedent product of MMPsense, to investigate MMP activity in OA or RA with human cartilage or mouse model [23–25], this article is the first studying OA-related assay with cartilage and joint injury using MMPsense750. This is an important contribution because MMPsense680 and MMPsense750 have different substrate specificities and different *in-vivo* kinetics, and MMPsense750 has the advantage that it enables a shorter time between injection and imaging (6 h versus 24 h for MMPsense680). Although human MMPs, bovine cartilage and mice were used in the current study, MMPs share a high degree of orthology among most vertebrates [26,27] and we do not expect significant species-related differences in the substrate–enzyme interactions.

With all MMPs tested, the fluorescent signal increased as the MMP activity increased. Interestingly, the reaction kinetics of the enzymes were different for the three MMPs. Namely, recombinant human MMP-13 caused a rapid increase in fluorescence within 15 min even at low enzyme concentrations, and longer incubations past 24 h decreased the assay linearity. In contrast, human MMP-9 required at least 24 h to show a dose-dependent increase in

R<sup>2</sup>(R: Pearson Correlation Coefficient)

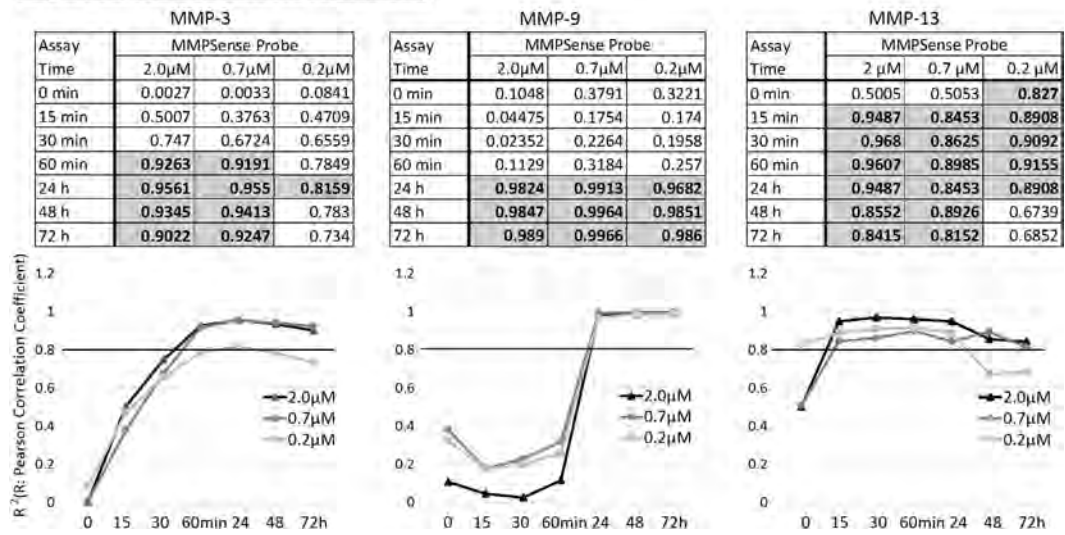


Fig. 1. Correlation between MMP Activity and MMPsense750 Signal. R<sup>2</sup> (R: Pearson correlation coefficient) as indices of correlation of the relationship between MMPs concentration and fluorescent signals at each time point were shown in tables and figures. R<sup>2</sup> greater than 0.8 were shown in the table with bold letters and shaded background.

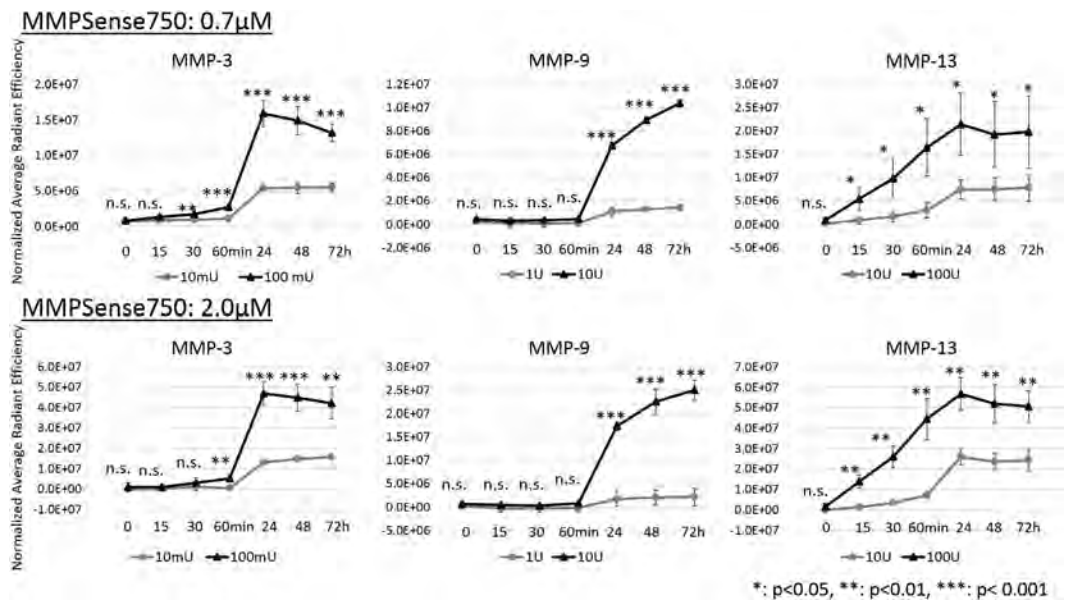
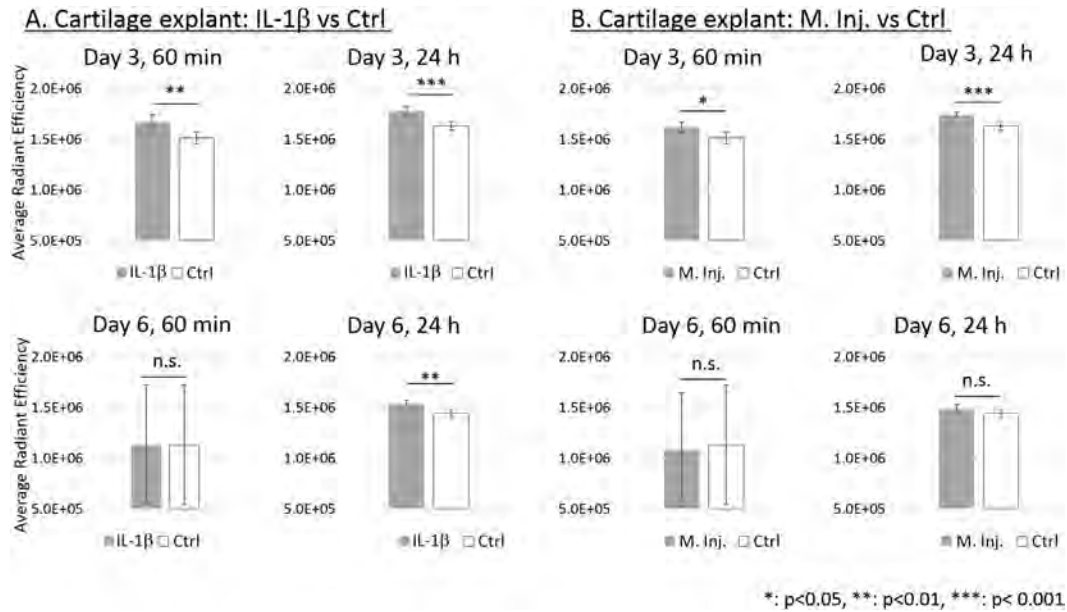


Fig. 2. Substrate Activation over Time. The normalized average radiant efficiency of the greatest and the second greatest concentration of each MMP with 0.7 or 2.0 μM of MMPsense750. p-values vs. the second greatest concentrations at the same time points. (n = 3).

substrate activation, and longer incubations out to 3 days improved the assay linearity. Human MMP-3 was intermediate, showing linear response after 1 h out to 2 days, but decreasing at 3 days. The experiments were all performed within the reported tissue half-life of 72 h for the MMPsense750 reagent. MMPsense produces fluorescent signal upon MMP-mediated hydrolysis, and the discrepancy of the detection time between MMPs may suggest the kinetics of cleavage differs between MMPs. We examined MMP-3, -9 and -13 in the current study, but according to the manufacturer MMPsense750 can also detect the activities of MMP-2, -7, and -12. In summary, it is important to recognize that a fluorescent signal indicates activities from multiple MMPs with differing sensitivities and reaction kinetics.

The result from cartilage explants assay provides a novel non-destructive method to quantify the MMP activity. At day 6, significantly higher fluorescence was detected in the IL-1β group when compared with the control group, while there was no significant difference between the mechanical injury group and the control group at both 60 min and 24 h after adding MMPsense. A possible reason for this difference could be the continuous presence of IL-1β during the 6 days, compared to a single mechanical injury at day 0. In the *in-vivo* mouse model, injured knees showed significantly higher signals of MMPsense750 than the contralateral uninjured knees, indicating that MMP activity was elevated 48 h after injury. This provides a novel real-time non-destructive imaging method to quantify knee injury response and the progression of cartilage



**Fig. 3.** Increased MMP Activity in Models of Cartilage Explant Injury. The average radiant efficiency in culture media at day 3 of the IL- $\beta$  group (A) and the mechanical injury group (B) measured at 60 min and 24 h after adding MMPsense was significantly greater than that of the control group. As for the media collected at day 6, the average radiant efficiency of the IL- $\beta$  group measured at 24 h was significantly greater than the other, while there was no significant difference in the radiant efficiency measured at 60 min of the IL- $\beta$  group and at 60 min and 24 h of the mechanical injury group compared to the control group. M. Inj.: mechanical injury group, Ctrl: control group. ( $n = 10$ ).

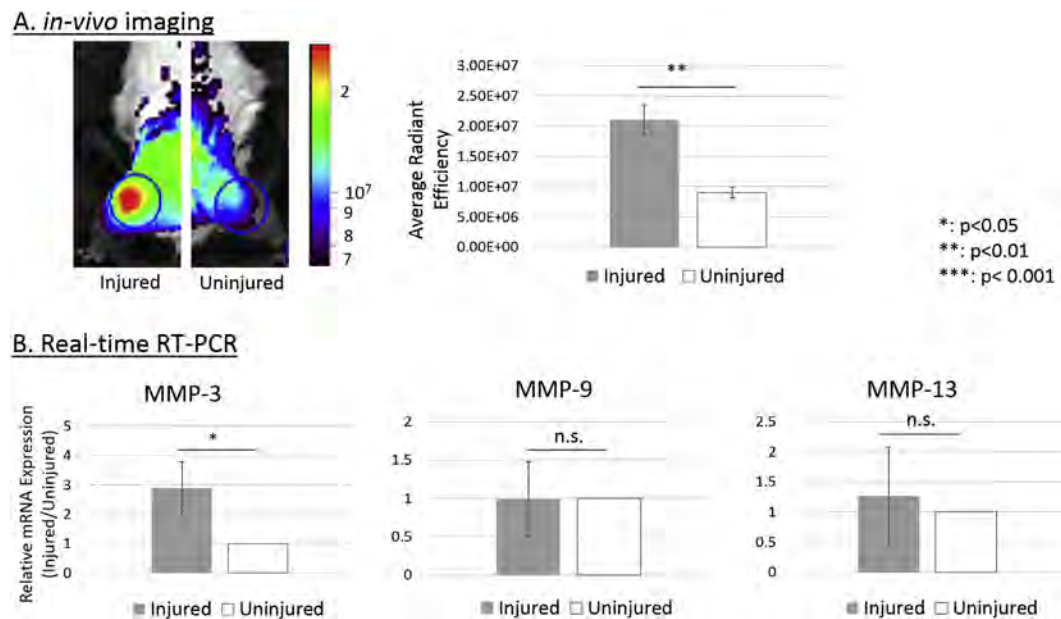


**Fig. 4.** Increased MMP Activity and mRNA in a Mouse Model of Joint Injury. A. Representative IVIS imaging of knees after MMPsense750 injection are shown. The image is a merged picture of fluorescent signal in color and a grayscale picture of the mouse. Blue circles on both knees are ROI with same shape and size as each other. The graph shows that average radiant efficiency in injured knees was significantly higher than the controls. ( $n = 8$ ). B. mRNA expression of MMP-3 in injured knees were significantly greater than in uninjured knees. No significant difference in MMP-9 and MMP-13 mRNA expression was detected between the knees at this time point. ( $n = 8$ ). (For interpretation of the references to color in this figure legend, the reader is referred to the web version of this article.)

degradation and OA based on MMP activity. Interestingly, when we examined MMP mRNA expression at 48 h after injury, we found that only MMP-3 was still elevated. In a separate study, we found that mRNA up-regulation of MMP expression after injury peaked at 4 h after injury and returned to baseline after 24 h using the same animal model (data not shown). MMPs are secreted as inactive pro-enzymes that are later activated in the extracellular matrix, which may explain the apparent discrepancy between the mRNA

expression and the protease activity and highlight the importance of quantifying the enzymatic activity.

A limitation of the imaging technology is that we did not have sufficient resolution to determine the exact tissue source of MMP activity. It is likely that MMPs are active in multiple tissues, including cartilage, bone, and synovium. In our explant experiments we were able to detect activity of MMP secreted by cartilage, but not within the cartilage itself. Based on these observations we

speculate that the *in-vivo* source of fluorescent signal might be joint tissues other than cartilage, although this does not preclude the MMP activity in the cartilage. In future experiments we would like to localize the source of MMP activity more precisely.

In conclusion, we established experimental parameters to use the MMPsense750 imaging reagent to quantify MMP activity *in-vitro* in cartilage explants, and *in-vivo* in a mouse joint injury model. The advantages of MMPsense750 over other techniques to evaluate MMP activity include its non-destructive nature, enabling repeated measurements on the same samples. This provides an imaging opportunity to monitor the destructive enzymatic processes that contribute to OA progression, and complements traditional imaging technologies that quantify the resulting structural changes.

## Acknowledgments

This work was funded by NIH/NIAMS grant AR063348 to Dominik R. Haudenschild.

The authors declare that they have no competing interests.

Imaging work was performed at the Center for Molecular and Genomic Imaging (CMGI), University of California, Davis. We would like to acknowledge Douglas Rowland and Jennifer Fung for help with the *in-vivo* and *in-vitro* imaging on the IVIS-Spectrum instrument.

## Appendix A. Supplementary data

Supplementary data related to this article can be found at <http://dx.doi.org/10.1016/j.bbrc.2015.03.100>.

## Conflict of interest

None.

## Transparency document

Transparency document related to this article can be found online at <http://dx.doi.org/10.1016/j.bbrc.2015.03.100>.

## References

- [1] R.F. Loeser, S.R. Goldring, C.R. Scanzello, M.B. Goldring, Osteoarthritis: a disease of the joint as an organ, *Arthritis Rheum.* 64 (2012) 1697–1707.
- [2] E. Losina, A.M. Weinstein, W.M. Reichmann, S.A. Burbine, D.H. Solomon, M.E. Daigle, B.N. Rome, S.P. Chen, D.J. Hunter, L.G. Suter, J.M. Jordan, J.N. Katz, Lifetime risk and age at diagnosis of symptomatic knee osteoarthritis in the US, *Arthritis Care Res. Hob.* 65 (2013) 703–711.
- [3] T.P. Lozito, R.S. Tuan, Endothelial cell microparticles act as centers of matrix metalloproteinase-2 (MMP-2) activation and vascular matrix remodeling, *J. Cell. Physiol.* 227 (2012) 534–549.
- [4] K. Yoshida, R.J. Barr, S. Galea-Soler, R.M. Aspden, D.M. Reid, J.S. Gregory, Reproducibility and diagnostic accuracy of Kellgren-Lawrence grading for osteoarthritis using radiographs and dual-energy X-ray absorptiometry imQ2 ages, *J. Clin. Densitom.* (2014) [Epub ahead of print].
- [5] A. Guermazi, F. Eckstein, M.P. Hellio Le Graverand-Gastineau, P.G. Conaghan, D. Burstein, H. Keen, F.W. Roemer, Osteoarthritis: current role of imaging, *Med. Clin. North Am.* 93 (2009), 101–126, xi.
- [6] A. Williams, J.R. Smith, D. Allaway, P. Harris, S. Liddell, A. Mobasheri, Carprofen inhibits the release of matrix metalloproteinases 1, 3, and 13 in the secretome of an explant model of articular cartilage stimulated with interleukin 1beta, *Arthritis Res. Ther.* 15 (2013) R223.
- [7] L. Troeberg, H. Nagase, Proteases involved in cartilage matrix degradation in osteoarthritis, *Biochim. Biophys. Acta* 1824 (2012) 133–145.
- [8] P. Verma, K. Dalal, ADAMTS-4 and ADAMTS-5: key enzymes in osteoarthritis, *J. Cell. Biochem.* 112 (2011) 3507–3514.
- [9] P.E. Di Cesare, D.R. Haudenschild, J. Samuels, S.B. Abramson, Pathogenesis of osteoarthritis, in: G.S. Firestein, W.N. Kelley (Eds.), *Kelley's Textbook of Rheumatology*, 2013, pp. 1617–1635.
- [10] N.M. Cattano, J.B. Driban, E. Balasubramanian, M.F. Barbe, M. Amin, M.R. Sittler, Biochemical comparison of osteoarthritic knees with and without effusion, *BMC Musculoskelet. Disord.* 12 (2011) 273.
- [11] P.I. Mapp, D.A. Walsh, J. Bowyer, R.A. Maciewicz, Effects of a metalloproteinase inhibitor on osteochondral angiogenesis, chondropathy and pain behavior in a rat model of osteoarthritis, *Osteoarthr. Cartil.* 18 (2010) 593–600.
- [12] H. Yamanaka, Y. Matsuda, M. Tanaka, W. Sendo, H. Nakajima, A. Taniguchi, N. Kamatani, Serum matrix metalloproteinase 3 as a predictor of the degree of joint destruction during the six months after measurement, in patients with early rheumatoid arthritis, *Arthritis Rheum.* 43 (2000) 852–858.
- [13] C.P. Hollis, H.L. Weiss, B.M. Evers, R.A. Gemeinhart, T. Li, In vivo investigation of hybrid paclitaxel nanocrystals with dual fluorescent probes for cancer theranostics, *Pharm. Res.* 31 (2014) 1450–1459.
- [14] M. Hufeland, M. Schunke, A.J. Grodzinsky, J. Imgenberg, B. Kurz, Response of mature meniscal tissue to a single injurious compression and interleukin-1 *in vitro*, *Osteoarthr. Cartil.* 21 (2013) 209–216.
- [15] P.A. Barber, D. Rushforth, S. Agrawal, U.I. Tuor, Infrared optical imaging of matrix metalloproteinases (MMPs) up regulation following ischemia reperfusion is ameliorated by hypothermia, *BMC Neurosci.* 13 (2012) 76.
- [16] M.H. Moon, J.K. Jeong, Y.J. Lee, J.W. Seol, C.J. Jackson, S.Y. Park, SIRT1, a class III histone deacetylase, regulates TNF-alpha-induced inflammation in human chondrocytes, *Osteoarthr. Cartil.* 21 (2013) 470–480.
- [17] R. Schure, K.D. Costa, R. Rezaei, W. Lee, C. Laschinger, H.C. Tenenbaum, C.A. McCulloch, Impact of matrix metalloproteinases on inhibition of mineralization by fetuin, *J. Periodontol. Res.* 48 (2013) 357–366.
- [18] B. Waschku, A. Faust, M. Schafers, C. Bremer, Performance of a new fluorescence-labeled MMP inhibitor to image tumor MMP activity *in vivo* in comparison to an MMP-activatable probe, *Contrast Media Mol. Imaging* 8 (2013) 1–11.
- [19] U. Vaatainen, L.S. Lohmander, E. Thonar, T. Hongisto, U. Agren, S. Ronkko, H. Jaroma, V.M. Kosma, M. Tammi, I. Kiviranta, Markers of cartilage and synovial metabolism in joint fluid and serum of patients with chondromalacia of the patella, *Osteoarthr. Cartil.* 6 (1998) 115–124.
- [20] T.P. Misko, M.R. Radabaugh, M. Highkin, M. Abrams, O. Friese, R. Gallavan, C. Bramson, M.P. Hellio Le Graverand, L.S. Lohmander, D. Roman, Characterization of nitrotyrosine as a biomarker for arthritis and joint injury, *Osteoarthr. Cartil.* 21 (2013) 151–156.
- [21] Y.C. Lu, C.H. Evans, A.J. Grodzinsky, Effects of short-term glucocorticoid treatment on changes in cartilage matrix degradation and chondrocyte gene expression induced by mechanical injury and inflammatory cytokines, *Arthritis Res. Ther.* 13 (2011) R142.
- [22] B.A. Christiansen, M.J. Anderson, C.A. Lee, J.C. Williams, J.H. Yik, D.R. Haudenschild, Musculoskeletal changes following non-invasive knee injury using a novel mouse model of post-traumatic osteoarthritis, *Osteoarthr. Cartil.* 20 (2012) 773–782.
- [23] E.F. Jones, J. Schooler, D.C. Miller, C.R. Drake, H. Wahnishe, S. Siddiqui, X. Li, S. Majumdar, Characterization of human osteoarthritic cartilage using optical and magnetic resonance imaging, *Mol. Imaging Biol.* 14 (2012) 32–39.
- [24] J. Zhou, Q. Chen, B. Lanske, B.C. Fleming, R. Terek, X. Wei, G. Zhang, S. Wang, K. Li, L. Wei, Disrupting the Indian hedgehog signaling pathway *in vivo* attenuates surgically induced osteoarthritis progression in Col2a1-CreERT2; *lhhfl/fl* mice, *Arthritis Res. Ther.* 16 (2014) R11.
- [25] C.L. Galligan, E.N. Fish, Circulating fibrocytes contribute to the pathogenesis of collagen antibody-induced arthritis, *Arthritis Rheum.* 64 (2012) 3583–3593.
- [26] B.C. Jackson, D.W. Nebert, V. Vasilou, Update of human and mouse matrix metalloproteinase families, *Hum. Genomics* 4 (2010) 194–201.
- [27] I. Massova, L.P. Kotra, R. Fridman, S. Mobashery, Matrix metalloproteinases: structures, evolution, and diversification, *FASEB J.* 12 (1998) 1075–1095.

# Comparison of Loading Rate-Dependent Injury Modes in a Murine Model of Post-Traumatic Osteoarthritis

Kevin A. Lockwood, Bryce T. Chu, Matthew J. Anderson, Dominik R. Haudenschild, Blaine A. Christiansen

Department of Orthopaedic Surgery, University of California-Davis Medical Center, 4635 2nd Ave, Suite 2000, Sacramento, California 95817

Received 19 April 2013; accepted 14 August 2013

Published online in Wiley Online Library (wileyonlinelibrary.com). DOI 10.1002/jor.22480

**ABSTRACT:** Post-traumatic osteoarthritis (PTOA) is a common long-term consequence of joint injuries such as anterior cruciate ligament (ACL) rupture. In this study we used a tibial compression overload mouse model to compare knee injury induced at low speed (1 mm/s), which creates an avulsion fracture, to injury induced at high speed (500 mm/s), which induces midsubstance tear of the ACL. Mice were sacrificed at 0 days, 10 days, 12 weeks, or 16 weeks post-injury, and joints were analyzed with micro-computed tomography, whole joint histology, and biomechanical laxity testing. Knee injury with both injury modes caused considerable trabecular bone loss by 10 days post-injury, with the Low Speed Injury group (avulsion) exhibiting a greater amount of bone loss than the High Speed Injury group (midsubstance tear). Immediately after injury, both injury modes resulted in greater than twofold increases in total AP joint laxity relative to control knees. By 12 and 16 weeks post-injury, total AP laxity was restored to uninjured control values, possibly due to knee stabilization via osteophyte formation. This model presents an opportunity to explore fundamental questions regarding the role of bone turnover in PTOA, and the findings of this study support a biomechanical mechanism of osteophyte formation following injury. © 2013 Orthopaedic Research Society. Published by Wiley Periodicals, Inc. *J Orthop Res* XX:XXX–XXX, 2013.

**Keywords:** mouse model; post-traumatic osteoarthritis; ACL injury; joint stability; osteophyte

Osteoarthritis (OA) is the most common joint disease, and the knee is the most commonly affected joint.<sup>1</sup> OA causes pain and stiffness in the joint, and severely limits mobility for those people who are affected. Current evidence indicates that after non-contact anterior cruciate ligament (ACL) injury, patients have an increased chance of developing post-traumatic osteoarthritis (PTOA) within 10–20 years after injury.<sup>2,3</sup>

Animal models are useful tools for studying PTOA, since the disease process can be studied in a more controlled environment on a dramatically condensed time line. There have been a number of mouse models developed for studying PTOA,<sup>4–7</sup> but many of these still have significant drawback such as invasive surgery or multiple bouts of mechanical loading. Our lab has developed a non-invasive mouse model that induces ACL rupture in mice *in vivo* by a single tibial compression overload.<sup>8</sup> This model closely mimics traumatic ACL rupture in humans without the costs and complications of surgery.

Our previous study using this mouse model had limitations, including ACL damage primarily by avulsion fractures rather than midsubstance tears, induction of only mild osteoarthritis by the end of the study (8 weeks post-injury), and little quantification of joint biomechanics.<sup>8</sup> Avulsion fracture is not a common injury mode in adults,<sup>9</sup> therefore a more clinically relevant mouse model would induce a midsubstance tear of the ACL rather than failure by an avulsion fracture. Based on the results from Crowninshield et al.<sup>10</sup> and Noyes et al.,<sup>11</sup> we hypothesized that

increasing the loading rate during knee injury would cause midsubstance ACL tears and decrease the likelihood of an avulsion fracture.

In this study we used our non-invasive mouse injury model to compare biomechanical and structural changes in the joint following ACL injury either with avulsion fracture or with midsubstance tear. We examined short term (10 days) and long term (12–16 weeks) structural changes in subchondral bone and epiphyseal trabecular bone, osteophyte formation, articular cartilage degeneration, and biomechanical stability of injured vs. uninjured knees. We hypothesized that injury mode (avulsion vs. midsubstance tear) would not significantly affect structural bone changes, osteoarthritis development, or biomechanical stability.

## METHODS

### Animals

A total of 80 male C57BL/6N mice (10 weeks old at time of injury) were obtained from Harlan Sprague Dawley, Inc. (Indianapolis, IN). Mice underwent a 1-week acclimation period in a housing facility before injury. Mice were caged individually and were maintained and used in accordance with National Institutes of Health guidelines on the care and use of laboratory animals. All procedures were approved by our Institutional Animal Care and Use Committee.

### Non-Invasive Knee Injury

ACL injury was induced as previously described.<sup>8</sup> Briefly, mice were anesthetized using isoflurane inhalation, then the right lower leg was positioned between two loading platens: an upper platen that held the flexed ankle at approximately 30 degrees of dorsiflexion and a lower platen that held the flexed knee. The platens were aligned vertically in an electromagnetic materials testing machine (Bose Electro-Force 3200, Eden Prairie, MN). A preload of 1 N was applied to the knee before a single dynamic axial compressive load was applied to a target displacement of –1.7 mm at a loading rate of either 1 or 500 mm/s. A target displacement was chosen rather than a target compressive load (as in our

Grant sponsor: National Institute of Arthritis and Musculoskeletal and Skin Diseases; Grant sponsor: National Institutes of Health; Grant numbers: AR062603, AR063348.

Correspondence to: Blaine A. Christiansen (T: 1-916-734-3974, F: 1-916-734-5750; E-mail: bchristiansen@ucdavis.edu)

© 2013 Orthopaedic Research Society. Published by Wiley Periodicals, Inc.

previous study) to minimize overshoot at high loading rates. Compressive loads at ACL rupture were comparable for both 1 and 500 mm/s loading rates, and were similar to those observed in our previous study (8–12 N). After injury, mice were given a subcutaneous injection of buprenorphine (0.5 mg/kg body weight) for analgesia. Mice were allowed normal cage activity until sacrifice.

### Characterization of Joint Injury

To determine the effect of tibial compression loading rate on injury mode (avulsion fracture vs. midsubstance tear), both knees of six mice were injured at loading rates of 1 or 500 mm/s ( $n=6$  knees per group). Immediately following injury, mice were sacrificed and injured knees were imaged with micro-computed tomography ( $\mu$ CT) as described below to detect the presence of bone fragments in the joint space indicative of avulsion fracture. To further characterize the injuries induced by High Speed or Low Speed tibial compression loading rate, both knees of 10 mice were injured using 1 mm/s ( $n=7$  knees) or 500 mm/s ( $n=7$  knees) loading rates, or left intact ( $n=6$  knees). Mice were sacrificed immediately after injury. Contrast enhanced  $\mu$ CT was performed on six knees ( $n=2$  per group). Knees were stained with phosphotungstic acid (PTA; 0.3% in 70% ethanol) for 1 week before being scanned with  $\mu$ CT (2  $\mu$ m nominal voxel size, Micro Photonics, Inc., Allentown, PA). The remaining 14 knees ( $n=4$ –5 per group) were decalcified, sectioned in the sagittal plane, and stained with hematoxylin and eosin (H&E) to assess joint structure.

### Comparison of High Speed and Low Speed Injury Models

**Study Design:** A total of 64 mice were used for this study (Table 1). Half of the injured mice were injured with the 1 mm/s load rate (Low Speed injury;  $n=26$ ); the other half were injured with the 500 mm/s load rate (High Speed injury;  $n=26$ ). An additional 12 mice underwent sham injury (anesthetized and loaded with the 1 N preload only). Following injury, mice were immediately sacrificed ( $n=12$ ) or returned to normal cage activity for 10 days ( $n=22$ ), 12 weeks ( $n=15$ ), or 16 weeks ( $n=15$ ), at which point they were euthanized by CO<sub>2</sub> asphyxiation and both hind limbs were excised for analysis. The left limb served as an internal control for each mouse.

### Micro-Computed Tomography of Distal Femoral Epiphysis, Tibial Subchondral Bone, and Osteophytosis

Injured and uninjured knees were imaged with micro-computed tomography (SCANCO  $\mu$ CT 35, Bassersdorf, Switzerland) to quantify trabecular bone structure in the distal femoral epiphysis, subchondral bone structure at the proximal tibia, and osteophyte formation around the joint. Dissected limbs were fixed in 4% paraformaldehyde for 24–

48 h, then transferred to 70% ethanol. Knees were scanned according to the guidelines for micro-computed tomography ( $\mu$ CT) analysis of rodent bone structure<sup>12</sup> (energy = 55 kVp, intensity = 114 mA, 10  $\mu$ m nominal voxel size, integration time = 900 ms). Trabecular bone in the distal femoral epiphysis was analyzed by manually drawing contours on 2D transverse slices. The distal femoral epiphysis was designated as the region of trabecular bone enclosed by the growth plate and subchondral cortical bone plate. We quantified trabecular bone volume per total volume (BV/TV), trabecular thickness (Tb.Th), trabecular number (Tb.N), and apparent bone mineral density (Apparent BMD; mg HA/cm<sup>3</sup> TV) using the manufacturer's analysis tools. In our previous study<sup>8</sup> we observed comparable trabecular bone changes at the femoral epiphysis, tibial epiphysis, and tibial metaphysis following knee injury. The current study investigated only the femoral epiphysis, since it has the largest volume for analysis and therefore will yield the most consistent trabecular bone parameters. Subchondral bone of the proximal tibial plateau was analyzed for 12- and 16-week knees. The subchondral bone was segmented for 500  $\mu$ m (50 slices) distal to the most proximal point of the tibia, excluding the trabecular bone compartment and any osteophytes growing from the tibia. We quantified cortical thickness (Ct.Th) and bone mineral density (BMD; mg HA/cm<sup>3</sup> BV) of the subchondral bone using the manufacturer's analysis tools. We investigated only the tibial subchondral bone because analysis of the subchondral bone of the femoral condyles is technically challenging, as is highly dependent on the orientation of the femur in the  $\mu$ CT scan. Osteophyte volume was calculated for 12- and 16-week knees, and included all mineralized tissue in and around the joint space, excluding naturally ossified structures (patella, fabella, and anterior and posterior horns of the menisci).

### Anterior–Posterior Joint Laxity

We quantified joint laxity of injured and uninjured mouse knees using a laxity tester based on previous designs.<sup>13,14</sup> This tester was designed to interface with a materials testing machine (Bose ElectroForce 3200). The protocol was similar to that described by Blankevoort et al.<sup>14</sup> for anterior–posterior (AP) laxity. Briefly, after fixation in brass tubes with polymethyl methacrylate (PMMA), the right and left knees of mice at day 0 ( $n=12$ ), week 12 ( $n=15$ ), and week 16 ( $n=15$ ) after injury were tested at 30°, 60°, and 90° of flexion. For each joint angle, knees underwent five loading cycles to a target force of  $\pm 1.5$  N at a rate of 0.5 mm/s (Fig. 6). The force was applied normal to the longitudinal axis of the tibia. The femur was fixed during testing, but the tibia was allowed to translate and rotate about its longitudinal axis, giving the system three degrees of freedom of motion. Similar to Blankevoort et al., total AP joint laxity was computed based on the difference between displacement at +0.8 N and –0.8 N.

To assess whether fixation in 4% paraformaldehyde and 70% ethanol had an effect on joint laxity, day 0 limbs were tested fresh-frozen, and then retested after being fixed in 4% paraformaldehyde and preserved in 70% ethanol for 4 weeks. Fixed limbs were allowed to rehydrate in a bath of phosphate buffered saline (PBS) for 3 min before potting and testing. During testing, the limbs were continuously hydrated with PBS.

### Long Term Whole Joint Histology

Knees were analyzed with whole joint histology to determine the extent of articular cartilage degeneration. Intact joints

**Table 1.** Animal Numbers and Experimental Groups for “Comparison of High Speed and Low Speed Injury Models”

Time Point	Low Speed	High Speed	Sham
Day 0	6	6	
Day 10	8	8	6
Week 12	6	6	3
Week 16	6	6	3

were decalcified for 4 days in 10% buffered formic acid and then processed for standard paraffin embedding. For each limb, 6–7 sagittal sections (6  $\mu\text{m}$  thickness) were cut across the entire joint separated by 250  $\mu\text{m}$ . Slides were stained with Safranin-O and Fast Green to assess articular cartilage and other joint structures (meniscus, subchondral bone, osteophytes, etc.). Slides were blinded and graded by four independent readers using the semi-quantitative OARSI scale described by Glasson et al.<sup>15</sup> Grades were assigned to the medial and lateral tibial plateau, and medial and lateral femoral condyles.

#### Statistical Analysis

Trabecular bone  $\mu\text{CT}$  results for High Speed and Low Speed injury modes were compared at each time point by calculating the difference between injured and uninjured knees for each mouse (injured–uninjured) and using analysis of variance (ANOVA) to compare between groups. Joint laxity of uninjured control (UIC), 1, and 500 mm/s injury rate joints were compared at each time point using one-way ANOVA. Differences in joint laxity as a function of knee flexion angle were compared using repeated measures ANOVA. Histology OARSI scores of UIC, 1, and 500 mm/s injured knees were averaged between readers for each slide, then for all slides for each mouse, and were then compared using one-way ANOVA for each joint region (medial femur, medial tibia, lateral femur, lateral tibia). Significance was defined as  $p < 0.05$  for all tests. Mean  $\pm$  standard deviation is presented for all data.

## RESULTS

### Characterization of Joint Injury

Non-invasive injury of mice using tibial compression overload with increasing loading rates yielded observable differences in injury mode at the high speed loading rate (500 mm/s) compared to the low speed

loading rate (1 mm/s). Using  $\mu\text{CT}$  imaging of injured mouse knees, we were able to observe bone fragments indicative of avulsion fracture for all mice injured at 1 mm/s, but we observed no bone fragments at a loading rate of 500 mm/s. We concluded that “High Speed injury” at 500 mm/s caused midsubstance disruption of the ligament, while “Low Speed injury” at 1 mm/s caused a combination injury involving ligament disruption with avulsion fracture. Contrast-enhanced  $\mu\text{CT}$  and whole joint histology showed disruption of the ACL for both 1 and 500 mm/s injury rates, with no obvious damage to the posterior collateral ligament, menisci, or other structures of the joint (Fig. 1). Consistent with our hypothesis, Low Speed injury (1 mm/s) caused disruption of the ACL with an avulsion fracture from the posterior femur. High Speed injury (500 mm/s) resulted in disruption of the ACL only, with no evidence of avulsion fracture.

### Comparison of High Speed and Low Speed Injury Models

#### Micro-Computed Tomography of Distal Femoral Epiphysis, Tibial Subchondral Bone, and Osteophytosis

Both injury modes initiated a rapid loss of epiphyseal trabecular bone in the distal femur by 10 days post-injury, and long-term joint degeneration and osteophytosis by 12 and 16 weeks post-injury. At all time points, knees injured with either the High Speed or Low Speed loading rates had significantly reduced trabecular BV/TV at the femoral epiphysis compared to uninjured contralateral knees and UIC mice (Fig. 2). At 10 days post-injury, knees injured using the Low Speed loading rate had significantly greater

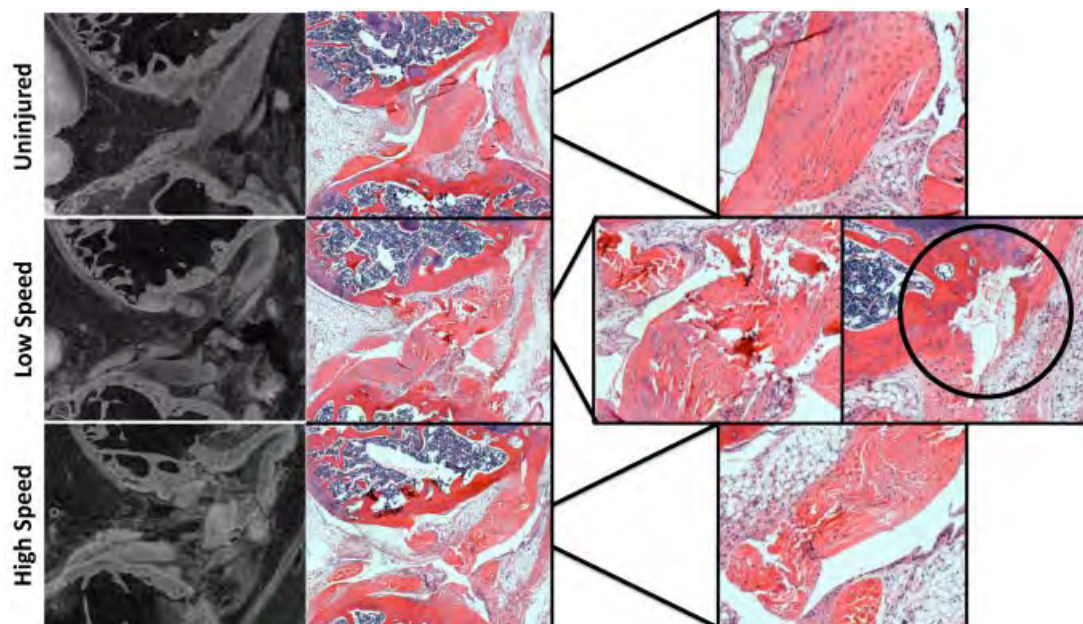


**Figure 1.** Imaging of injured and uninjured knee joints. Contrast-enhanced  $\mu\text{CT}$  images (left column) show disruption of the ACL in both High Speed and Low Speed injuries. Hemotoxylin and Eosin sections of intact, High Speed, and Low Speed injury modes (middle and right columns) show disruption of the ACL with both injury modes compared to uninjured ligament. Low Speed injury (1 mm/s) caused avulsion of the ACL from the posterior femur (circle). No avulsion was detected in the High Speed (500 mm/s) injury group.

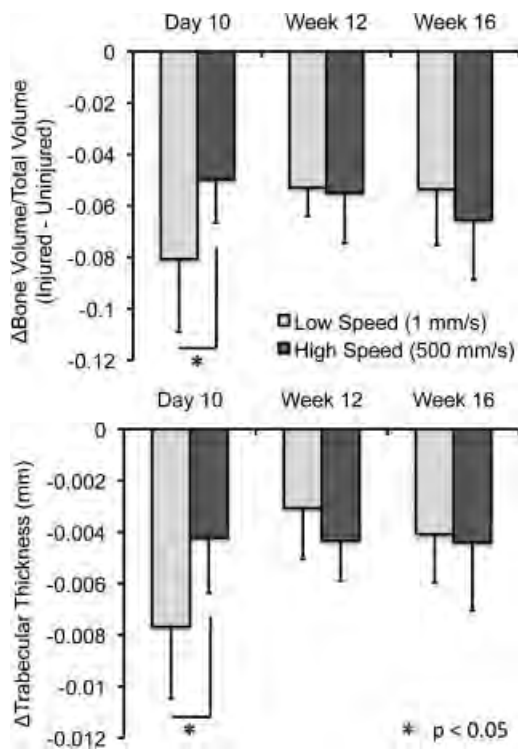


**Figure 2.** Difference in bone volume fraction (BV/TV) and trabecular thickness (Tb.Th) of the distal femoral epiphyses for Low Speed (1 mm/s) and High Speed (500 mm/s) injury groups. Values are the average difference between injured and contralateral control legs for each mouse. Injured versus uninjured values were significantly different for all groups and all time points ( $p < 0.05$ ). Mice injured at Low Speed, which induced avulsion from the distal femur, exhibited greater trabecular bone loss at 10 days post-injury. After 12–16 weeks, injured knees still had significantly reduced bone volume and trabecular thickness compared to uninjured knees, although there were no differences between High Speed and Low Speed injuries in trabecular structure at these time points.

loss of trabecular BV/TV compared to those injured with the High Speed loading rate (–31% vs. –20%, respectively). By 12 and 16 weeks post-injury, there were no differences in trabecular BV/TV between the High Speed and Low Speed injury modes, although BV/TV of injured knees remained significantly lower than contralateral knees ( $p < 0.05$ ). At 12 weeks post-injury, BV/TV of High Speed and Low Speed injured knees was 20.9% and 19.6% lower than contralateral knees, respectively, while at 16 weeks, BV/TV of injured knees was 22.9% and 21.5% lower, respectively. Trabecular thickness (Tb.Th) and apparent BMD of the femoral epiphysis followed a similar pattern, with the Low Speed injury rate exhibiting a significantly lower thickness and apparent BMD than the High Speed injury rate at 10 days. At 12 and 16 weeks there were no significant differences between injury modes, but injured limbs had reduced Tb.Th and BMD compared to uninjured contralateral limbs.

Analysis of subchondral bone at the proximal tibia revealed significant thickening of the subchondral bone plate in injured knees by 12 and 16 weeks post-injury (Fig. 3). Cortical thickness was 20–26% larger

for injured knees compared to contralateral knees for both injury modes and both time points ( $p < 0.05$ ). However, we observed no significant differences in cortical thickness increase between time points or between injury modes. BMD of the subchondral bone plate was significantly higher for Low Speed injured knees compared to contralateral knees at week 12 only (908.7 vs. 891.7 mg HA/cm<sup>3</sup>;  $p = 0.001$ ). No significant differences in subchondral bone BMD were observed for High Speed injured knees or for any knees at 16 weeks post-injury.

Injured knees exhibited significant osteophytosis using both the High Speed and Low Speed injury modes by 12 and 16 weeks post-injury (Figs. 4–6). The pattern of osteophyte formation was consistent for all mice at 12 and 16 weeks, regardless of injury mode. Specifically, there was considerable osteophyte formation on the anterior-medial aspect of the distal femur, the menisci (particularly the medial meniscus) exhibited hypertrophy and osteophyte formation, primarily extending in an anteromedial direction from the joint (Fig. 5). The posterior medial tibial plateau exhibited bone formation in the posterior direction, and extreme erosion of the tibial plateau was observable with  $\mu$ CT, exposing the underlying subchondral bone.

Both injury models exhibited increased osteophyte volume from 12 to 16 weeks, although this increase was only significant for the Low Speed injury group (Fig. 6). The High Speed injury group exhibited higher osteophyte volume compared to the low speed injury group at both time points; this difference was statistically significant at 12 weeks ( $p = 0.04$ ). We were able to observe preliminary signs of osteophyte formation on transverse  $\mu$ CT images of injured joints as early as 10 days post-injury, particularly on the anteromedial aspect of the distal femur (Fig. 5).

#### Anterior–Posterior Joint Laxity

We observed a greater than twofold increases in AP joint laxity immediately following joint injury with both injury modes (Fig. 7). We observed no significant difference in joint laxity between flexion angles for any group at any time point. By 12 and 16 weeks post-injury, AP joint laxity for both injured groups was reduced to control values. During AP laxity testing of week 16 legs, one control leg was broken during potting. Additionally, injured knees of week 16 mice had severely diminished range of motion and were difficult to extend to 30°. As a result, three of the 1 mm/s and two of the 500 mm/s week 16 knees were also fractured. Thirty-degree extension was tested last to ensure that data was collected for 60° and 90° joint angles.

No change in joint laxity was observed for day 0 uninjured joints after fixation in 4% paraformaldehyde and preservation in 70% ethanol for 4 weeks (compared to fresh-frozen joints), but injured joints exhibited significantly increased joint laxity after fixation (+18% AP joint laxity). Subsequently, joint laxity

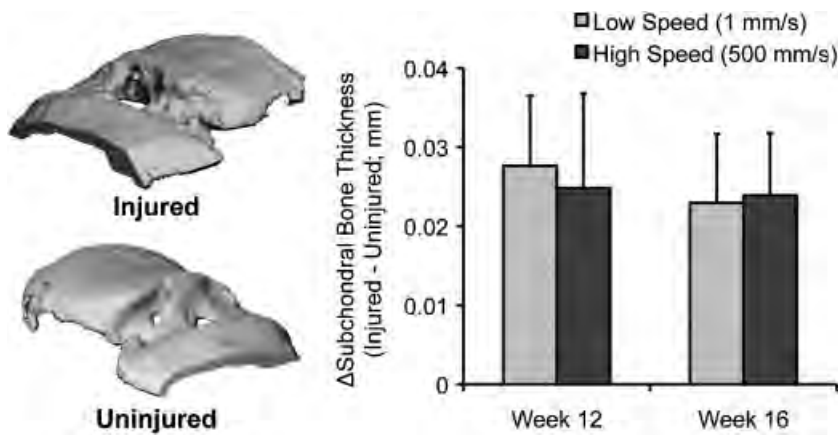


**Figure 3.** Left: Micro-computed tomography reconstructions of the subchondral bone plate of the tibial plateau of injured and uninjured knees, with a medial cut for visualization of subchondral bone thickness. Right: Difference in subchondral bone thickness of the proximal tibial plateau for Low Speed (1 mm/s) and High Speed (500 mm/s) injury groups. Values are the average difference between injured and contralateral control legs for each mouse. Injured versus uninjured values were significantly different for all groups and all time points ( $p < 0.05$ ). No significant differences were observed between injury modes or time points.

values of day 0 preserved knees were used for all comparisons between day 0, week 12, and week 16 data.

#### Long Term Whole Joint Histology

Whole joint histology showed extreme degeneration and OA for both injury modes at 12 and 16 weeks post-injury (Fig. 8). OARSI scores were significantly higher than UIC joints at 12 and 16 weeks for both injury modes, however there were no significant differences between High Speed and Low Speed injured joints (Fig. 9). Injured joints exhibited extreme erosion of cartilage on both the medial and lateral aspects of

the tibia and femur. Many injured joints had bone-bone contact and even erosion of subchondral bone, sometimes extending as far as the growth plate. There was extreme fibrosis within the joint space and osteophytes present on the tibia and femur. The menisci on both sides were hypertrophied and degenerated. Inspection of individual sections showed the most severe degeneration on the posterior aspect of the tibial plateau of injured joints, while the anterior aspect appeared comparable to UICs. At 16 weeks the UIC joints were given an average OARSI score of approximately 2, indicating mild OA occurring naturally in the mice by 26 weeks of age.

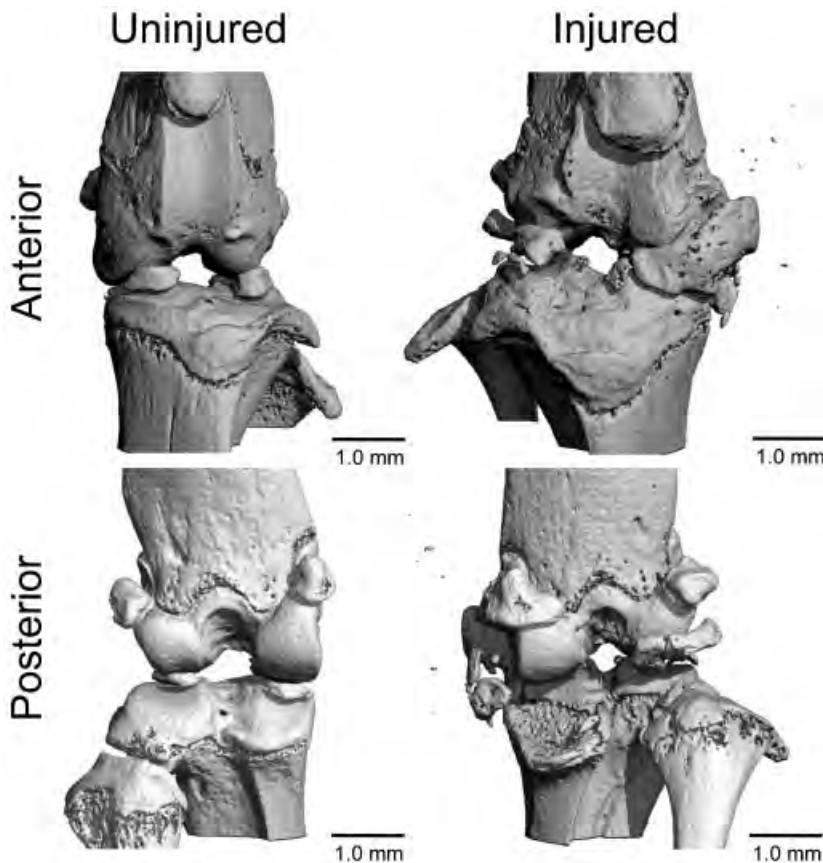


**Figure 4.**  $\mu$ CT images of injured and uninjured mouse knees at 12 weeks post-injury (Low Speed injury). Substantial osteophytosis and joint degeneration were observed in all injured knees. In particular, osteophytes were observed on the anteriomedial aspect of the distal femur, the posteromedial aspect of the proximal tibia, and the medial meniscus.

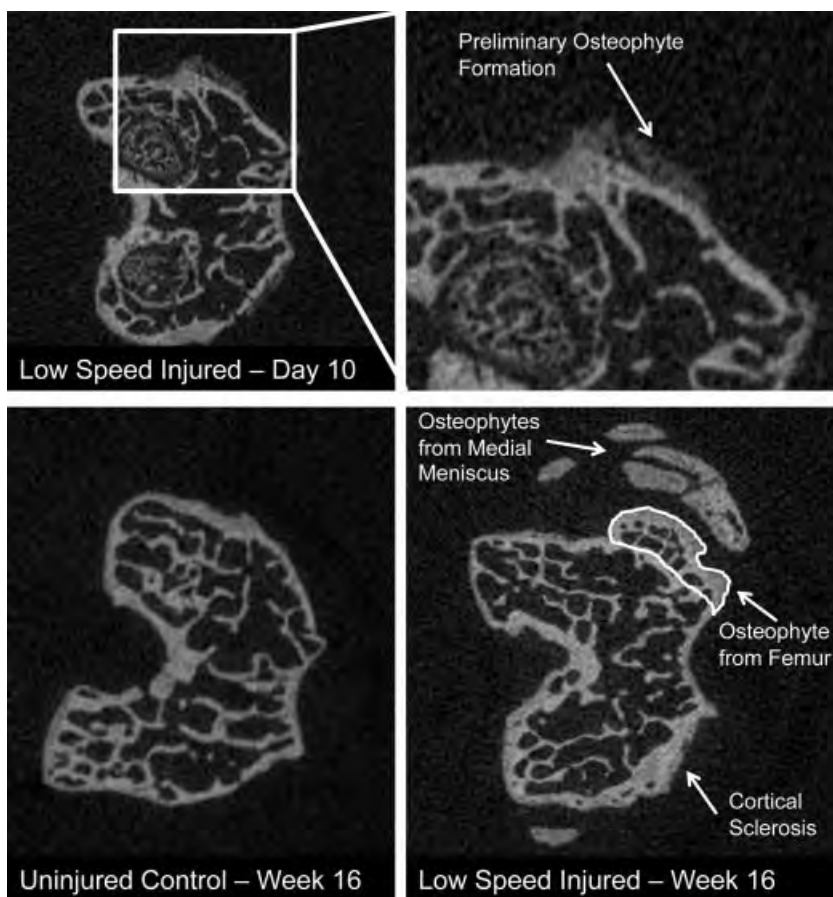


**Figure 5.** Transverse  $\mu$ CT slices of the distal femur. Top: Femoral epiphysis of an injured joint 10 days postinjury, with expanded image showing early osteophytosis from the anteromedial femur. Bottom: Uninjured (left) and injured (right) femoral epiphysis at 16 weeks showing considerable osteophyte formation from the anteromedial femur and medial meniscus, as well as sclerosis of cortical plate on the lateral condyle.

## DISCUSSION

In this study we used a non-invasive injury model in mice to compare two similar but distinctly different injury modes, and assess potential differences in PTOA development. Using different tibial compression loading rates, we were able to produce two unique injury modes in the knees of mice: ACL rupture with avulsion fracture (“Low Speed injury”, 1 mm/s loading rate) or midsubstance ACL rupture (“High Speed injury”, 500 mm/s loading rate). Consistent with our hypothesis, we found that the two injury modes were not significantly different from each other with respect to long-term changes in bone structure, joint laxity, and cartilage degeneration. However, we observed a greater loss of trabecular bone in the distal femoral epiphysis at 10 days post-injury in the Low Speed injury model compared to High Speed injury. This difference is likely due to direct bone damage caused by avulsion of the ACL in the Low Speed injury group. We also observed significant differences in osteophyte formation, with High Speed injured knees developing greater osteophyte volume. Altogether, these results suggest that ACL injury mode in mice is a minor contributing factor to the subsequent joint degeneration that follows traumatic joint injury after 12–16 weeks.

The role of subchondral bone in progression of OA has been an active topic of discussion,<sup>16–18</sup> with

authors hypothesizing that cartilage health is influenced by the structure of the underlying subchondral bone. However, early changes in subchondral bone and epiphyseal trabecular bone are not well defined in human subjects, but rather established (severe) OA is

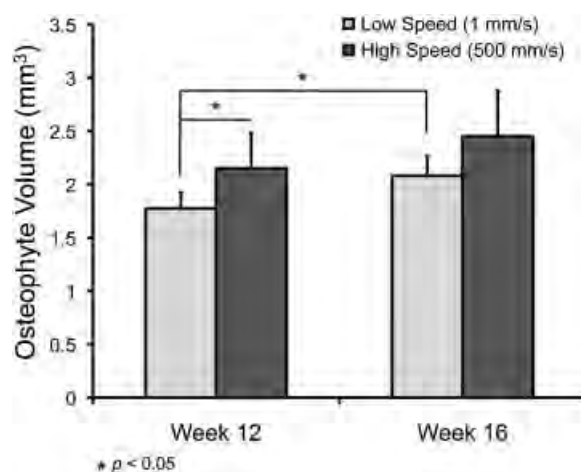


**Figure 6.** Osteophyte volume of injured joints. Non-native bone formation was quantified for Low Speed (1 mm/s) and High Speed (500 mm/s) injured joints at 12 and 16 weeks post-injury. High Speed injured joints exhibited greater osteophyte volume than Low Speed injured joints at 12 weeks postinjury. Osteophyte volume increased from 12 to 16 weeks for both groups, but this increase was only significant for Low Speed injured mice ( $p < 0.05$ ).

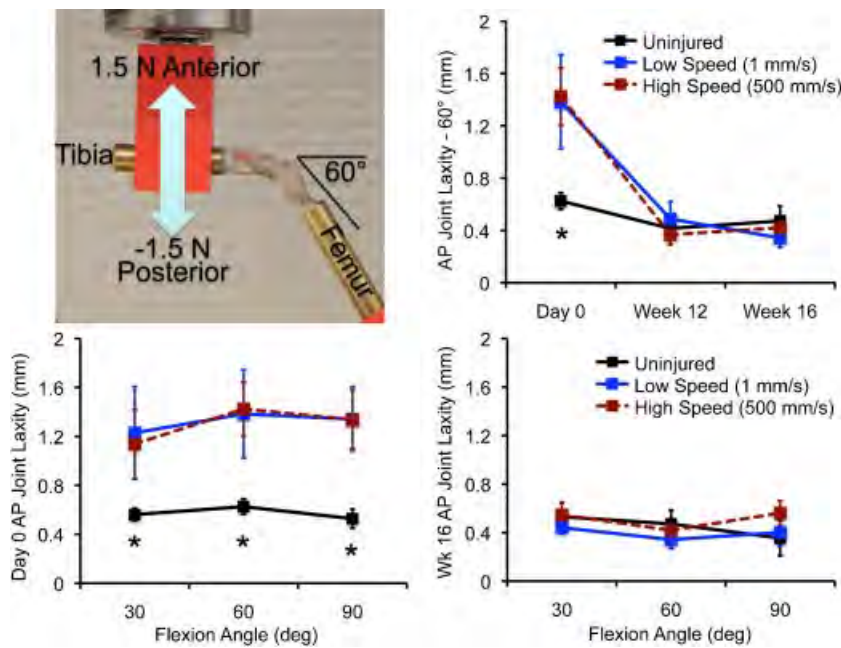


**Figure 7.** Top left: Joint laxity test setup for 60° of flexion. Top right: Total anterior-posterior joint laxity at 60° for day 0, week 12, and week 16 knees. \* $p < 0.05$  between injured and uninjured values. Injured joints had a greater than twofold increase in joint laxity at day 0, but joint stability was returned to control values by 12 and 16 weeks post-injury. Bottom: Total anterior-posterior joint laxity at day 0 (left) and week 16 (right) at 30°, 60°, and 90° of knee flexion. \* $p < 0.05$  between injured and uninjured values. There were no significant differences between joint angles, or between injury modes (High Speed vs. Low Speed injury).

typically studied.<sup>19</sup> A few recent studies have investigated epiphyseal trabecular bone changes in the knees of osteoarthritic subjects using MRI imaging,<sup>20,21</sup> and have observed decreased trabecular bone parameters (loss of trabecular bone) in osteoarthritic knees, particularly in the lateral compartment. This is consistent with the current study and our previous study<sup>8</sup> that showed trabecular bone loss from both the medial and lateral compartments in mice, although our previous study found similar magnitudes of trabecular bone loss from the medial and lateral compartments. Subchondral bone sclerosis and osteophyte formation are also common findings in humans with OA.<sup>22</sup> This is consistent with the current study, in which we observed thickening of the tibial subchondral bone plate, and considerable osteophyte formation around the joint by 12 and 16 weeks post-injury. The relative-

ly large scale of osteophytes observed in this study is not typical for OA in humans, although this may be due to the fact that bone features do not scale linearly with body size between mice and humans. For example, body mass in humans is approximately 2,000–4,000 times greater than that of mice, while trabecular thickness in humans is approximately 4–7 times greater (100–350  $\mu\text{m}$  in humans vs. 25–50  $\mu\text{m}$  in mice). Altogether, the subchondral and trabecular bone changes observed in this mouse model of PTOA are generally consistent with the bone changes observed in human OA.

By both 12 and 16 weeks post-injury we observed severe OA in injured knees. This is in contrast to our previous study, in which joints exhibited only mild OA by 8 weeks post-injury, with loss of Safranin-O staining, minor fissuring, and cell death in the superficial

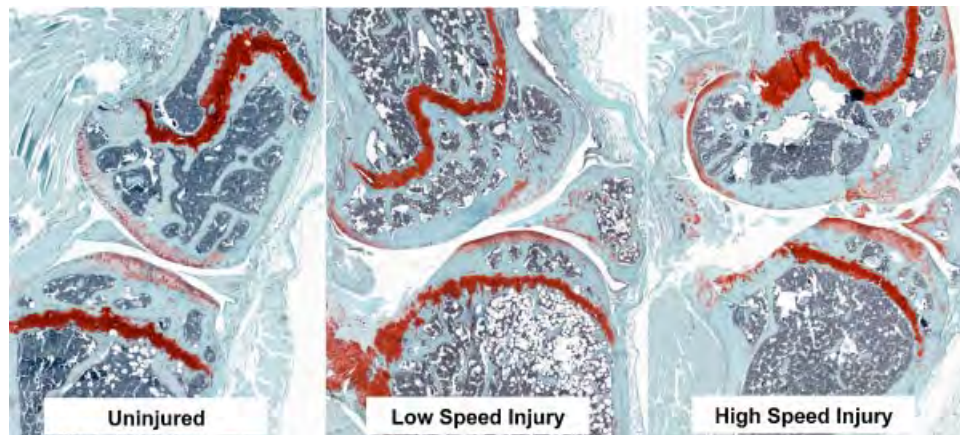


**Figure 8.** Whole joint histology at 12 weeks. Sagittal sections of the medial condyle stained with Safranin-O and Fast Green. By 12 weeks post-injury we observed significant degeneration of both the tibia and femur. In particular, the posterior aspect of the medial tibia has severe degeneration of cartilage and bone erosion, often extending as far as the growth plate.

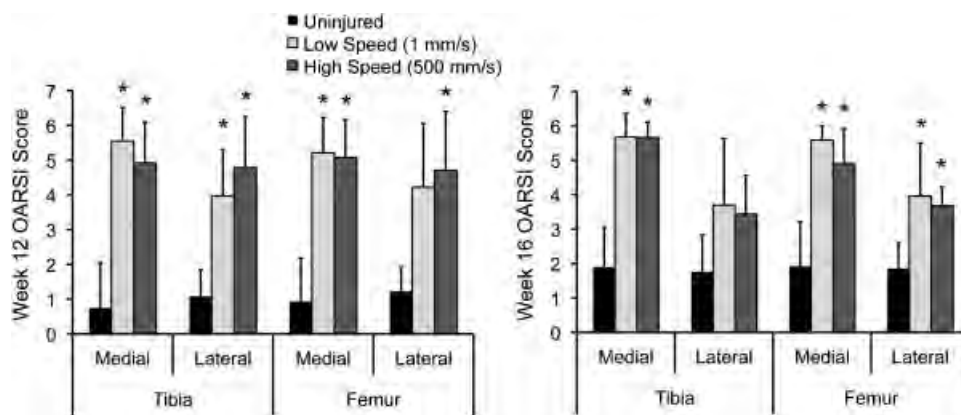


**Figure 9.** OARSI scores for whole joint histology at 12 and 16 weeks. We observed severe osteoarthritis of both the tibia and femur at both time points, often with degeneration of articular cartilage extending to the subchondral bone (\* indicates significant difference from uninjured control. No statistically significant differences were observed in the OARSI score of knees injured with the High Speed versus Low Speed injury mode).

zone.<sup>8</sup> In the current study we found that by only 4 weeks later (12 weeks post injury), injured joints exhibited severe OA with total loss of cartilage tissue. In many joints there was bone on bone contact, extreme fibrosis, and severe meniscal degeneration visible by 12 weeks post-injury, often to a degree that is unnecessary for studies of arthritis development. The severe posterior bone erosion we observed on the tibial plateau, particularly on medial side, is not typical of ACL injury-induced PTOA in other animal species or in humans, although similar erosion has been described with surgical transection of the ACL in mice.<sup>4</sup> This posterior degeneration may therefore be specific to mouse models of ACL-induced PTOA irrespective of how the ACL is ruptured (with or without surgery). In this way, ACL injury in mice may be limited for translation to human injuries. For future studies with this model, we anticipate that an 8–10 weeks end point should be sufficient to show moderate to severe OA, and would be sufficient to detect any improvement in OA development due to treatment. In contrast, the DMM and ACLT models utilized by Glasson et al.<sup>4</sup> were able to induce moderate-to-severe OA by 4 weeks post-injury.

Changes in AP joint laxity of injured knees in this study were similar to values obtained from previous studies using C57BL/6 mice with healthy knees. At  $\pm 0.8$  N in healthy ACL intact joints, Blankevoort et al.<sup>14</sup> measured  $0.43 \pm 0.16$  mm and Wang et al.<sup>13</sup> measured  $0.50 \pm 0.09$  mm, compared to  $0.57 \pm 0.08$  mm in our study. The increased joint laxity measured in this study is likely due to the additional degree of freedom in our test fixture, which allowed rotation of the tibia about its longitudinal axis. The previous studies only allowed two degrees of freedom of motion.

In this study we observed consistent and repeatable patterns of osteophytosis around the joint capsule by 12 and 16 weeks post injury for both injury modes. In particular, we observed osteophytes forming from the anteriomedial femur, the posteromedial tibia, and the

medial meniscus. It is possible that osteophyte formation around the joint may have contributed to the reduction in joint laxity from day 0 values. The stabilizing effect of osteophytes in osteoarthritic joints was previously studied by Pottenger et al.<sup>23</sup> in humans undergoing total knee arthroplasty (TKA) by measuring varus-valgus (VV) laxity before and after removal of osteophytes. They observed an increase in VV joint laxity from  $11.0^\circ$  to  $14.7^\circ$  after osteophyte removal, showing that osteophytes helped stabilize the joint. These results support the hypothesis that osteophytes form as a response to joint instability. The drawback to restoring joint stability by osteophyte formation is severe reduction in joint range of motion, which was observed in the current study. Twelve- and sixteen-week knees were extremely stiff and resisted extension to  $30^\circ$ . This was supported by a study in humans undergoing TKA, in which residual posterior femoral condyle osteophytes were associated with reduced knee flexion after surgery. Removal of the osteophytes avoided impingement with the implant and allowed more flexion to occur.<sup>24</sup> Unfortunately, our study did not investigate AP joint laxity at intermediate time points between 0 and 12 weeks post-injury. Future analyses could investigate the time course of “re-stabilization” of the joint after ACL rupture, and could confirm the proposed correlation with osteophyte formation.

Future studies using this model should include additional biomechanical analyses to further characterize relationships between joint injury and OA progression. Gait analysis of injured mice could address questions concerning voluntary mechanical loading after injury and whether mice change limb-loading patterns. If the mice are unweighting the injured limb, then loss of bone volume may be partly explained due to disuse. Additionally, future studies could investigate the activity level of mice following joint injury. It is possible that voluntary cage activity is reduced, which would result in further mechanical loading-

related bone atrophy. The opposite is also likely true; increased cage activity or exercise (including fighting) could exacerbate PTOA progression following injury.

This study advances our previous study by analyzing multiple injury modes, quantifying biomechanical changes in the joint, and analyzing time points at which severe OA is present. However, there are still limitations that must be acknowledged. In particular, while anatomical structures between human and mice are similar, the bipedal gait of humans is very different from that of mice, and may result in divergent laxity changes, loading patterns, and locations of degeneration. Additionally, the severe osteophyte formation that we observe with this model is not typical for human joints, although it is comparable to other widely used mouse models,<sup>25</sup> and may be largely explained by the dramatic size difference between mouse and human joints. Finally, these studies used 10-week-old mice with open growth plates (the growth plates in mouse long bones typically remain open throughout the lifetime of the animal). This is a ubiquitous limitation of using mice for studies of bone, and may have contributed to the skeletal adaptation observed in this study. While this model may not be able to overcome all of these limitations, it still has several advantages over other existing mouse models of PTOA, and may be uniquely useful for investigating OA progression in humans.

In conclusion, in this study we found that ACL injury mode does not affect the long term bone changes or OA severity in mice, although it does affect short term trabecular bone turnover, with injury involving direct bone damage (avulsion) exhibiting greater short term trabecular bone loss. We also found that ACL injury dramatically increased AP joint laxity in mice immediately following injury, but joint stability is restored by 12 weeks post-injury, possibly due to extensive osteophyte formation around the joint. These studies further characterize the non-invasive knee injury mouse model developed in our lab, and begin to describe mechanical loading changes initiated by joint injury. The model presented provides an opportunity to explore fundamental questions regarding the role of bone turnover in PTOA progression, and findings from this model may point to bone turnover as a potential target for therapies aimed at slowing or preventing PTOA.

## ACKNOWLEDGEMENTS

Research reported in this publication was supported by the National Institute of Arthritis and Musculoskeletal and Skin Diseases, part of the National Institutes of Health, under Award Number AR062603 (B.A.C.) and AR063348 (D.R.H.). The content is solely the responsibility of the authors and does not necessarily represent the official views of the National Institutes of Health.

## REFERENCES

1. Felson DT. 1988. Epidemiology of hip and knee osteoarthritis. *Epidemiol Rev* 10:1–28.
2. Lohmander LS, Englund PM, Dahl LL, et al. 2007. The long-term consequence of anterior cruciate ligament and meniscus injuries: osteoarthritis. *Am J Sports Med* 35:1756–1769.
3. Oiestad BE, Engebretsen L, Storheim K, et al. 2009. Knee osteoarthritis after anterior cruciate ligament injury: a systematic review. *Am J Sports Med* 37:1434–1443.
4. Glasson SS, Blanchet TJ, Morris EA. 2007. The surgical destabilization of the medial meniscus (DMM) model of osteoarthritis in the 129/SvEv mouse. *Osteoarthritis Cartilage* 15:1061–1069.
5. Furman BD, Strand J, Hembree WC, et al. 2007. Joint degeneration following closed intraarticular fracture in the mouse knee: a model of posttraumatic arthritis. *J Orthop Res* 25:578–592.
6. van Beuningen HM, Glansbeek HL, van der Kraan PM, et al. 2000. Osteoarthritis-like changes in the murine knee joint resulting from intra-articular transforming growth factor-beta injections. *Osteoarthritis Cartilage* 8:25–33.
7. Poulet B, Hamilton RW, Shefelbine S, et al. 2011. Characterising a novel and adjustable non-invasive murine knee joint loading model. *Arthritis Rheum* 63:137–147.
8. Christiansen BA, Anderson MJ, Lee CA, et al. 2012. Musculoskeletal changes following non-invasive knee injury using a novel mouse model of post-traumatic osteoarthritis. *Osteoarthritis Cartilage* 20:773–782.
9. Gottsegen CJ, Eyer BA, White EA, et al. 2008. Avulsion fractures of the knee: imaging findings and clinical significance. *Radiographics* 28:1755–1770.
10. Crowninshield RD, Pope MH. 1976. The strength and failure characteristics of rat medial collateral ligaments. *J Trauma* 16:99–105.
11. Noyes FR, DeLucas JL, Torvik PJ. 1976. Biomechanics of anterior cruciate ligament failure: an analysis of strain-rate sensitivity and mechanisms of failure in primates. *J Bone Joint Surg Am* 56:236–253.
12. Bouxsein ML, Boyd SK, Christiansen BA, et al. 2010. Guidelines for assessment of bone microstructure in rodents using micro-computed tomography. *J Bone Miner Res Off J Am Soc Bone Miner Res* 25:1468–1486.
13. Wang VM, Banack TM, Tsai CW, et al. 2006. Variability in tendon and knee joint biomechanics among inbred mouse strains. *J Orthop Res Off Publ Orthop Res Soc* 24:1200–1207.
14. Blankevoort L, van Osch JVM, Janssen B, et al. 1996. In vitro laxity-testers for knee joints of mice. *J Biomechanics* 29:799–806.
15. Glasson SS, Chambers MG, Van Den Berg WB, et al. 2010. The OARSI histopathology initiative—Recommendations for histological assessments of osteoarthritis in the mouse. *Osteoarthritis Cartilage* 18:S17–S23.
16. Mansell JP, Tarlton JF, Bailey AJ. 1997. Biochemical evidence for altered subchondral bone collagen metabolism in osteoarthritis of the hip. *Br J Rheumatol* 36:16–19.
17. Hayami T, Pickarski M, Zhuo Y, et al. 2006. Characterization of articular cartilage and subchondral bone changes in the rat anterior cruciate ligament transection and meniscectomized models of osteoarthritis. *Bone* 38:234–243.
18. Radin EL, Rose RM. 1986. Role of subchondral bone in the initiation and progression of cartilage damage. *Clin Orthop Relat Res* 213:34–40.
19. Mastbergen SC, Lafeyber FP. 2011. Changes in subchondral bone early in the development of osteoarthritis. *Arthritis Rheum* 63:2561–2563.
20. Chiba K, Uetani M, Kido Y, et al. 2011. Osteoporotic changes of subchondral trabecular bone in osteoarthritis of the knee: a 3-T MRI study. *Osteoporos Int* 23:589–597.
21. Bolbos RI, Zuo J, Banerjee S, et al. 2008. Relationship between trabecular bone structure and articular cartilage

- morphology and relaxation times in early OA of the knee joint using parallel MRI at 3 T. *Osteoarthritis Cartilage* 16:1150–1159.
22. Jacobson JA, Girish G, Jiang Y, et al. 2008. Radiographic evaluation of arthritis: degenerative joint disease and variations. *Radiology* 248:737–747.
  23. Pottenger LA, Phillips FM, Draganich LF. 1990. The effect of marginal osteophytes on reduction of varus–valgus instability in osteoarthritic knees. *Arthritis Rheum* 33:853–858.
  24. Yau WP, Chiu KY, Tang WM, et al. 2005. Residual posterior femoral condyle osteophyte affects the flexion range after total knee replacement. *Int Orthop* 29:375–379.
  25. Moodie JP, Stok KS, Muller R, et al. 2011. Multimodal imaging demonstrates concomitant changes in bone and cartilage after destabilisation of the medial meniscus and increased joint laxity. *Osteoarthritis Cartilage* 19: 163–170.



# High abundant protein removal from rodent blood for biomarker discovery



Dominik R. Haudenschild<sup>a</sup>, Angela Eldridge<sup>b</sup>, Pamela J. Lein<sup>c</sup>, Brett A. Chromy<sup>b,\*</sup>

<sup>a</sup> Department of Orthopaedic Surgery, School of Medicine, University of California, Davis, United States

<sup>b</sup> Department of Pathology and Laboratory Medicine, School of Medicine, University of California, Davis, United States

<sup>c</sup> Department of Molecular Biosciences, School of Veterinary Medicine, University of California, Davis, United States

## ARTICLE INFO

### Article history:

Received 9 September 2014

Available online 24 October 2014

### Keywords:

Proteomics

Plasma

Affinity chromatography

MARS

2-D DIGE

Albumin

## ABSTRACT

In order to realize the goal of stratified and/or personalized medicine in the clinic, significant advances in the field of biomarker discovery are necessary. Adding to the abundance of nucleic acid biomarkers being characterized, additional protein biomarkers will be needed to satisfy diverse clinical needs. An appropriate source for finding these biomarkers is within blood, as it contains tissue leakage factors as well as additional proteins that reside in blood that can be linked to the presence of disease. Unfortunately, high abundant proteins and complexity of the blood proteome present significant challenges for the discovery of protein biomarkers from blood. Animal models often enable the discovery of biomarkers that can later be translated to humans. Therefore, determining appropriate sample preparation of proteomic samples in rodent models is an important research goal. Here, we examined both mouse and rat blood samples (including both serum and plasma), for appropriate high abundant protein removal techniques for subsequent gel-based proteomic experiments. We assessed four methods of albumin removal: antibody-based affinity chromatography (MARS), Cibacron® Blue-based affinity depletion (SwellGel® Blue Albumin Removal Kit), protein-based affinity depletion (ProteaPrep Albumin Depletion Kit) and TCA/acetone precipitation. Albumin removal was quantified for each method and SDS–PAGE and 2-DE gels were used to quantify the number of protein spots obtained following albumin removal. Our results suggest that while all four approaches can effectively remove high abundant proteins, antibody-based affinity chromatography is superior to the other three methods.

© 2014 Elsevier Inc. All rights reserved.

## 1. Introduction

Difficulties in sample preparation currently limit the discovery of protein biomarkers from biofluids, in particular blood plasma and serum. One of the biggest challenges in the study of blood plasma involves the broad concentration range of its protein constituents. In humans, there is approximately a 10<sup>9</sup> order of magnitude from most to least abundant proteins [1]. In addition, few high abundant proteins dominate the plasma, making biomarker discovery of lower abundance proteins even more difficult. For example, twenty-two proteins comprise over 90% of the total protein mass in human serum and albumin alone accounts for over

Abbreviations: TCA, trichloroacetic acid; SDS–PAGE, sodium dodecyl sulfate polyacrylamide gel electrophoresis; 2-DE, two dimensional electrophoresis; 2-D DIGE, two-dimensional difference gel electrophoresis; MARS, Multiple Affinity Removal system; PBS, phosphate buffered saline.

\* Corresponding author.

E-mail address: [bachromy@ucdavis.edu](mailto:bachromy@ucdavis.edu) (B.A. Chromy).

<http://dx.doi.org/10.1016/j.bbrc.2014.09.137>

0006-291X/© 2014 Elsevier Inc. All rights reserved.

50%. These dominant species prevent the detection of lower-abundance proteins that may be of greater interest as putative biomarkers [2]. Therefore, a successful system of proteomic sample preparation to remove these high abundant proteins is needed to examine lower abundant proteins of interest and to reduce the complexity for improved biomarker discovery. Researchers have developed successful ways to remove these proteins, but these methods vary in the efficiency and mechanism for removing targeted highly abundant proteins [3–7].

Putative protein biomarkers discovered after the removal of high abundant proteins may serve to detect diseases earlier with higher accuracy, but may prove to be challenging for subsequent validation in humans. Therefore, animal models are necessary to validate these biomarkers and for the discovery of additional biomarkers. Initial 2-DE proteome maps of mouse and rat produced species specific patterns and showed serum proteins can vary substantially [8–11]. However, these samples have a similar wide dynamic range in protein concentrations as seen in human

samples and therefore face some of the same technological challenges. Since the same high abundant proteins are found in blood of animals, their removal from these models is also necessary. There are many ways to accomplish high abundant protein removal for rodent blood including hydrophobic interactions [12], ammonium sulfate precipitation [13], ion exchange [10], antibody-based affinity chromatography [14,15], and TCA/acetone precipitation [16], and these approaches have been used to enable discovery of putative biomarkers [15,17–20]. In one of these studies, plasma protein biomarkers found in a mouse model of pancreatic cancer were used to translate to human protein orthologs, providing putative early detection markers applicable to human cancer [15]. These studies have focused on a single technique and have not directly compared removal methods to each other using the same samples. Moreover, each study has not compared these techniques for both serum and plasma obtained from both mice and rats.

In this study, four different methods for high abundant protein removal were compared using rat serum/plasma and mouse serum/plasma. SDS–PAGE was used to compare the extent of albumin removal between these methods. Further characterization using 2-D DIGE was done to assess the improvement in total protein spots after removal of high abundant proteins by each of the four different methods.

## 2. Materials and methods

### 2.1. Sample collection

Rodent blood was collected under IACUC protocols for (DH) and (PL). For mice, whole blood was collected by ocular bleed. For rats, blood was collected from the saphenous vein on the inside of the thigh using a 21 gauge needle. Serum was allowed to clot at room temperature for 2–5 h followed by centrifugation at 5000×g for 10 min. The supernatant was collected and stored at –80 °C in fresh tube. For plasma, blood was collected into BD 0.5 ml microtainer tubes containing Potassium EDTA (Becton Dickinson, Franklin Lakes, NJ). Blood was centrifuged at 15,000×g for 10 min to separate the plasma from the red blood cells. Plasma was collected, aliquoted and stored at –80 °C until analysis.

### 2.2. High abundant protein removal

Depletion of high abundant proteins was carried out according to the manufacturer's instructions with minor modifications as detailed below. TCA/acetone was carried out similarly as previously published [16]. TCA was dissolved in water to make a 20% solution and this solution was diluted 1:1 with the protein sample on ice for 30 min. Following incubation the proteins were centrifuged and the protein pellet was washed 2× with ice-cold acetone. The ProteaPrep procedure was carried out as described in the manufacturer's protocol (Protea). Protein samples were diluted in sample buffer 1:4 and then loaded into pre-packed columns containing a proprietary dry powder that facilitated non-antibody, affinity-based serum albumin removal. The capture ligand is a recombinant protein that claims to be more specific than an antibody-based system with stronger binding constants. For SwellGel® Blue Albumin (Pierce), 40 µl samples of plasma or serum were diluted into 160 µl of bind/wash buffer. Albumin binding incubations were done for 2 min (twice). Incubations were washed 3 times with 200 µl. The flow through and washes were pooled as the albumin removed sample. For antibody-affinity chromatography using the MARS MS-3 (Agilent Technologies), rodent plasma or serum was diluted five times in Buffer A (40 µl sample and 160 µl of buffer, 200 µl total volume) and centrifuged through a

0.22 micron spin filter tube (Millipore) at 16,000×g for 5 min to remove particulates. Then, plasma or serum was processed using 4.6 × 50 mm Multiple Affinity Removal Column Mouse-3 (Agilent Technologies), which specifically removes albumin, IgG, and transferrin. A low abundant protein fraction was collected for each sample. Fractions were concentrated by precipitating with an equal volume of 20% TCA solution and incubated at 4 °C for 30 min. Precipitate was spun down and washed twice with cold 100% acetone, allowed to air dry and then resuspended in DIGE labeling buffer (7 M urea, 2 M thiourea, 4% CHAPS, 30 mM Tris, pH 8.5). Protein quantification was performed using Precision Red Advanced Protein Assay Reagent (Cytoskeleton).

### 2.3. SDS–PAGE

Crude and high abundant protein depleted plasma or serum samples (5 µg) were mixed with 5× sample loading buffer (0.2 M Tris pH 6.8, 20% glycerol, 10% SDS, 5% BME), boiled for 10 min at 100 °C and resolved on a 4–20% Tris–Glycine gel (Invitrogen). Gels were stained for total protein using Sypro Ruby Protein Gel Stain (Invitrogen, S-12000) and visualized using the BioChem system (UVP BioImaging Systems).

### 2.4. 2-D DIGE

Crude and high abundant protein depleted plasma and serum samples were separated in two dimensions using the GE Life Sciences Ettan DIGE system protocol. Briefly, each sample (50 µg) was minimally labeled with 1 µl of 200 pM Cy2, Cy3 or Cy5 for 30 min. Labeling reactions were stopped by the addition of 1 µl of 1 mM lysine. The samples were pooled together and added to rehydration buffer (7 M urea, 2 M thiourea, 4% CHAPS, 1.2% DeStreak, 1% pharmalytes). A final volume of 450 µl sample was loaded onto 24 cm pH 3–10NL Immobiline DryStrips (GE Life Sciences) and focused by active overnight rehydration, followed by isoelectric focusing for a total of 62,500 Vhrs. Strips were equilibrated in SDS equilibration buffer (6 M urea, 30% glycerol, 2% SDS) for 15 min with 10 mg/ml DTT, then 15 min in fresh buffer with 25 mg/ml 15 min with IAA, then applied to DIGE gels (GE Life Sciences) for 2nd dimension separation. The resulting CyDye labeled protein gels were scanned using 100 micron resolution on Typhoon 9410 (GE Life Sciences).

### 2.5. Image analysis

Data analysis was carried out using DeCyder 2-D 7.0 software (GE Life Sciences). Spot detection and abundance quantification was performed using the differential in-gel analysis (DIA) module of DeCyder. Densitometry, using ImageJ processing program (available free online at [rsb.info.nih.gov/ij/](http://rsb.info.nih.gov/ij/)), was performed on selected albumin bands to determine the percent removed.

## 3. Results

Four different methods were tested for their ability to remove albumin from both rodent blood samples. Both rat and mouse samples of plasma and serum were used. SDS–PAGE and 2-DE were used to evaluate the overall improvements in proteomic sample preparation following high abundant protein removal. Table 1 shows the recovery of the total protein following these different methods. Most of the protein remains in the high abundant fraction, but this table shows that the total protein obtained from these different methods does not vary substantially. Therefore, none of these methods reduce total protein recovery more than another.

**Table 1**  
Protein recovered after high abundant protein removal is similar among four different methods. For all methods used for high abundant protein removal, most of the protein was removed (about 90%). The remaining lower abundant protein samples were similar in total amount of protein obtained, ranging from 109 to 177 µg. Some differences between samples were found but further experimentation needs to be done to ensure these differences are statistically valid.

Sample	Start total (µg)	Method			
		SG	Protea	TCA/Ac	MARS
Mouse serum	1960	174	160	152	150
Mouse plasma	1943	172	168	153	109
Rat serum	2082	171	148	177	174
Rat plasma	1942	151	174	137	155

After determining that the total amount of protein does not differ substantially due to sample preparation, we then examined the protein pattern using SDS–PAGE. We compared samples following each technique to each other and to raw serum and plasma. Fig. 1

shows SDS–PAGE images for both serum and plasma from mice. All methods were able to reduce the amount of albumin and increase the overall number of protein bands that could be detected. Albumin depletion strategies for rat serum and plasma showed similar results with decreased albumin and increased total protein spots (Fig. 2). The albumin removal results suggest that all methods chosen for study here can improve the proteomic spot pattern. However, important differences between techniques were found. For example, the method that removed the most albumin for mouse plasma was the antibody-based affinity chromatography, as it removed about twice as much albumin in some cases (Table 2).

Another issue for improved biomarker discovery using proteomics involves the concentration of the protein sample and the use of buffer exchange to ensure proper buffer conditions for subsequent proteomic analysis following high abundant protein removal. Specifically, after high abundant protein removal using

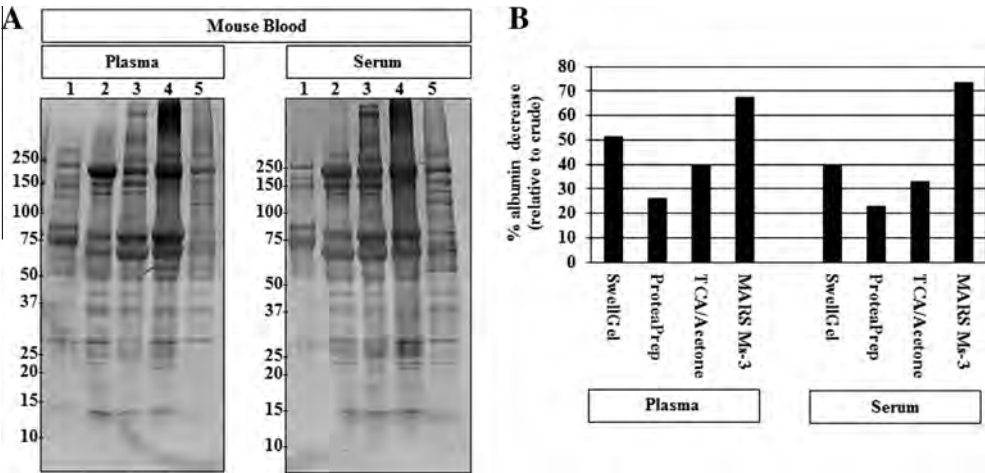


**Fig. 1.** Mouse blood SDS–PAGE. (A) Mouse plasma and serum, post-albumin removal by each method, was evaluated by SDS–PAGE. Lane 1 crude plasma (left); serum (right). 2. SwellGel® Blue Albumin 3. ProteaPrep Lane 4: TCA/acetone Lane 5: MARS Ms-3. Crude samples show a few protein bands and the presence of a dark band at roughly 70 kDa representing the main albumin band. All lanes show increased numbers of protein bands and a lower main albumin band following albumin removal. (B) Densitometry analysis of percent albumin decrease showed different depletion levels among the four tested methods. The antibody-based affinity chromatography method removed the most albumin for both plasma and serum samples. Percent albumin decrease was calculated using the main albumin band density, relative to each lane, divided by the percent albumin found in each crude sample.

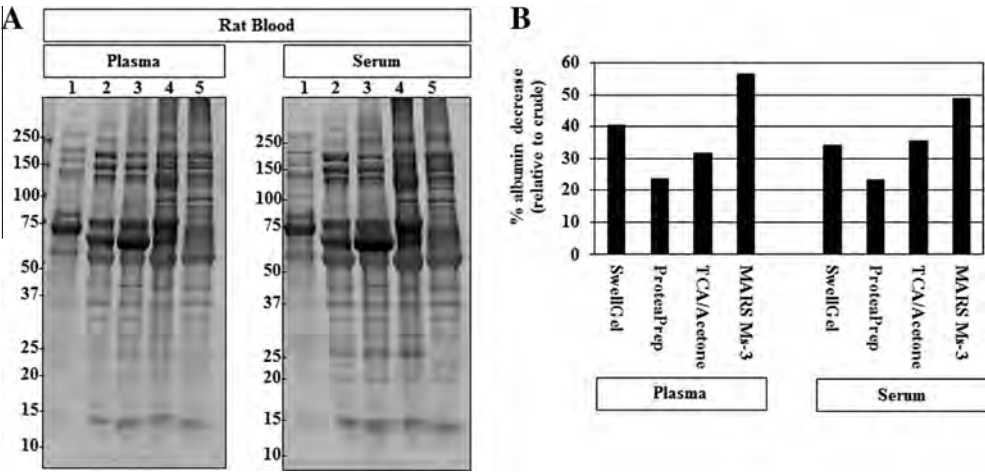


**Fig. 2.** Rat blood SDS–PAGE. (A) Rat plasma and serum, post-albumin removal by each method, was evaluated by SDS–PAGE. Lane 1 crude plasma (left); serum (right). 2. SwellGel® Blue Albumin 3. ProteaPrep Lane 4: TCA/acetone Lane 5: MARS Ms-3. Crude samples show a few protein bands and the presence of a dark band at roughly 70 kDa representing the main albumin band. All lanes show increased numbers of protein bands and a lower main albumin band following albumin removal. (B) Densitometry analysis of percent albumin decrease showed different depletion levels among the four tested methods. The antibody-based affinity chromatography method removed the most albumin for both plasma and serum samples. Percent albumin decrease was calculated using the main albumin band density, relative to each lane, divided by the percent albumin found in each crude sample.

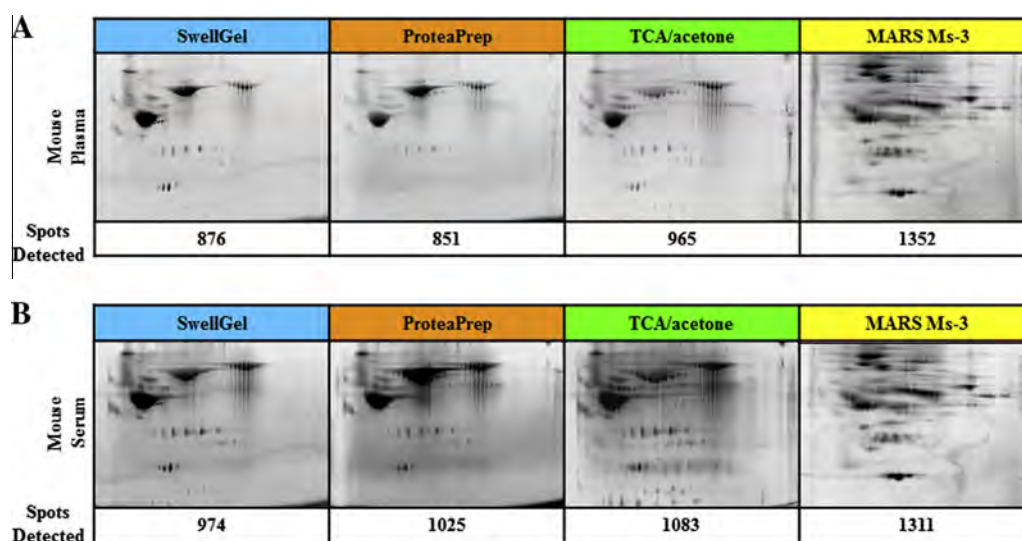
**Table 2**

Different sample preparation techniques yield significant albumin removal with different total protein spots. For all four sample types, antibody-based affinity chromatography proved to be the best technique for albumin removal and increased protein spots found in a 2D gel. For (A) mouse plasma/serum and (B) rat serum, TCA/acetone method provides the second most albumin removal and yields the second most 2-D gel spots.

<b>A</b>	Species	Mouse							
	Sample Type	Plasma				Serum			
	Albumin Removal Method	SwellGel	Protea Prep	TCA/acetone	MARS Ms-3	SwellGel	Protea Prep	TCA/acetone	MARS Ms-3
	Albumin Removed (SDS-PAGE)	51%	26%	39%	68%	39%	23%	33%	73%
	Total 2-D Spots Detected	876	851	965	1352	974	1025	1083	1311

<b>B</b>	Species	Rat							
	Sample Type	Plasma				Serum			
	Albumin Removal Method	SwellGel	Protea Prep	TCA/acetone	MARS Ms-3	SwellGel	Protea Prep	TCA/acetone	MARS Ms-3
	Albumin Removed (SDS-PAGE)	40%	24%	32%	56%	34%	23%	36%	49%
	Total 2-D Spots Detected	1008	943	1157	1285	1069	1069	1155	1263



**Fig. 3.** Mouse blood 2-D DIGE. (A) Albumin depleted mouse plasma and (B) serum. 2-D DIGE gel images are shown with corresponding number of detected protein spots. The antibody-based affinity chromatography method removed the most albumin for both plasma and serum samples.

SwellGel® Blue Albumin, ProteaPrep, and MARS, we examined differences between TCA precipitation and molecular weight cutoff in this subsequent concentration and buffer exchange step. SDS-PAGE was used to compare the two procedures (Supplemental Fig. 1). SDS-PAGE showed very similar banding patterns for both procedures, following the 3 different types of high abundant removal protocols. Since TCA/acetone and molecular weight cutoff removal were found to be similar, TCA/acetone was chosen for subsequent proteomic analysis.

To determine if a more sensitive proteomic technique could differentiate among these high abundant protein removal procedures, we used 2-D DIGE. Fig. 3 shows 2-D DIGE images of

the mouse serum and plasma samples following high abundant protein removal. Successful high abundant protein removal is demonstrated by the increased number of total spots and diverse spot pattern as compared to crude serum and plasma. The antibody-based affinity chromatography method showed significantly better albumin removal and more total protein spots for both mouse sample types. The three other methods removed substantial albumin and had similar numbers of total protein spots, but each had roughly half of the albumin removal and 200–300 fewer protein spots than the affinity chromatography.

Fig. 4 shows similar results of improved proteomic separation for rat plasma. Again, antibody-based affinity chromatography

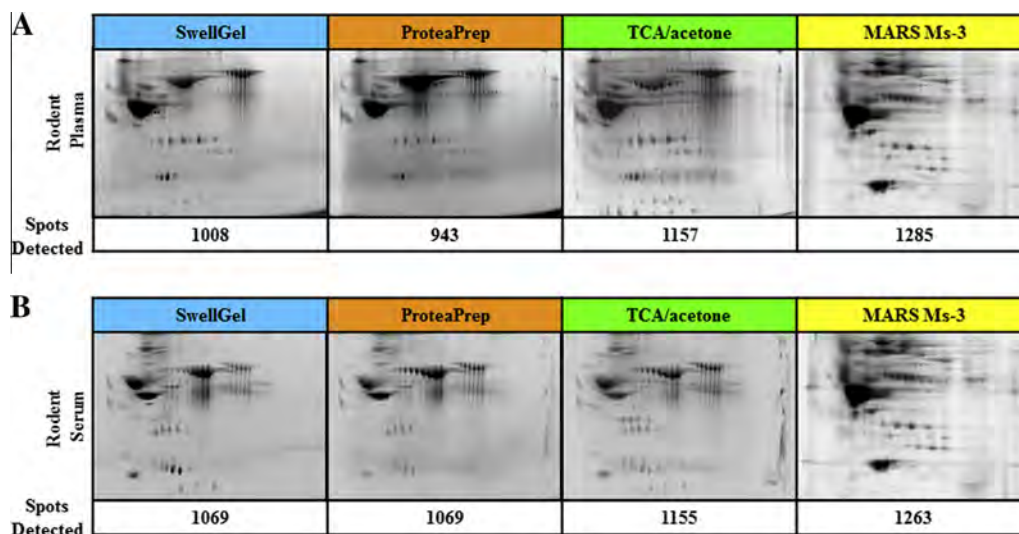


**Fig. 4.** Rat blood 2-D DIGE. (A) Albumin depleted rat plasma and (B) serum. 2-D DIGE gel images are shown with corresponding number of detected protein spots. Similar to the mouse blood data, antibody-based affinity chromatography shows the highest number of protein spots, specifically in the lower half of the gel.

removed significantly more albumin than the other three techniques, which were similar with respect to the amount of albumin removed. Total protein spots were also highest for the affinity chromatography by at least 100 spots. Over 1200 protein spots were found following the removal of the top three serum/plasma proteins using affinity chromatography. Even though this antibody column was optimized for mouse, the results shown here clearly demonstrate that the column can be useful for removal of high abundant rat serum/plasma proteins.

Table 2 shows the results of the albumin removal and the total protein spots found for all four sample types for all four albumin depletion methods, showing percent albumin decrease for each technique used. To validate which techniques removed substantial albumin, the amount of albumin that was removed was quantified using densitometry of the SDS-PAGE. These data show that antibody-based affinity chromatography removes the most albumin and shows the greatest number of total protein spots by a significant amount.

#### 4. Discussion

Successful proteomic sample preparation from blood often requires high abundant protein removal. High abundant proteins have been shown to be responsible for concealing putative markers. For example, albumin was found to obscure sex differences in blood plasma of rats and humans [2]. A failure to effectively remove high abundant proteins can also result in failed or incomplete biomarker studies. To determine the optimal protocol for subsequent biomarker discovery, we completed four methods of high abundant protein removal for both rat and mouse serum and plasma. Our results clearly show that antibody-based affinity chromatography is the superior method for this approach, similar to results we previously showed for human serum [3].

Several reports in the literature have addressed the issue of serum complexity and proteomic analyses. Pieper and co-workers used immunoaffinity subtraction chromatography to remove 10 proteins from human blood plasma. Following protein depletion, Coomassie blue stained 2-dimensional electrophoresis (2-DE) gels revealed approximately 650 protein spots compared with only 220 spots visible in a sample of crude serum. Silver staining of the protein-depleted sample revealed an even larger number, 950 spots [9]. Chan and coworkers used an affinity spin tube filter method

to remove albumin and IgG to enrich for low-abundant cancer biomarkers in serum. Over 250 potential biomarkers for breast cancer were identified in this study. TCA-acetone has been used to remove albumin from serum [5]. Finally, Steel and co-workers also used an immunoaffinity resin to remove albumin and IgG from human serum samples in order to simplify the serum proteome [21]. Our data demonstrate that antibody-based affinity chromatography removes the greatest percentage of albumin and results in the highest total number of lower abundant protein spots relative to any published work to date. We used 2-D DIGE [3], which can detect protein spots as low as 150–500 pg of a single protein, with a linear response in protein concentration over five orders of magnitude [22]. This method allowed us to detect over 1200 protein spots in each of these four rodent samples, by far the most protein spots detected for these sample types.

Antibody-based affinity chromatography often is the best choice for high abundant protein removal as we showed here for rodent samples. Importantly, since this column was designed using mouse antibodies, it was not clearly evident that it would work well with rat samples. However, our work shows that both rat serum and plasma can be improved for biomarker discovery using this approach. The specificity and efficiency of the microbead, IgY-based anti-rat immunoaffinity LC column has been previously examined and has improved protein detection using several different techniques including SELDI-TOF MS, 2-dimensional SDS-PAGE, and 2-dimensional liquid chromatography [14]. Although results here show more protein spots, we do not know if this is because of the relative improvement of the column used here or the highly sensitive visualization technique of 2-D DIGE, which is also highlighted as integral for improved protein biomarker identification [14]. Future work should be done to see if species specific antibodies improve upon the results found here. Species-specific differences may also explain why the ProteaPrep depletion kit was not better than antibody-affinity despite claims to that the recombinant protein capture ligand is more efficient than antibody-based methods. The ProteaPrep capture ligand is claimed to be more specific than antibodies and has a stronger binding constant to human serum albumin. The results here do not support this, which might be due to species-specific differences. Further investigation into human albumin removal is necessary to compare these removal methods.

In addition, we showed that TCA precipitation enables the complete removal of buffer for both concentration and exchange

purposes for these sample types. TCA precipitation has been widely used to concentrate protein samples and exchange existing buffers in proteomic sample preparation [23]. However, protein is denatured following TCA precipitation, so protein activity cannot be assessed. In addition, proteins cannot be resuspended easily in any non-denaturing buffer (such as PBS). Molecular weight cutoff membranes have also been widely used for concentration and buffer exchange. Molecular weight membranes enable the removal of buffer by centrifugation through filtration, while retaining proteins of at least 3 kDa. This procedure offers a single step sample concentration in a single tube for minimal sample handling and reduced sample loss. When comparing a single TCA/acetone step with molecular weight cutoff membranes following other types of high abundant protein removal, we did not notice substantial differences (Supplementary Fig. 1).

## Acknowledgments

The authors would like to thank Sasha Silvestrini for technical assistance. Part of this work is based upon work supported by the S.D. Bechtel, Jr. Foundation and by the National Science Foundation under Grant Nos. 0952013 and 0733758. Any opinions, findings, and conclusions or recommendations expressed in this material are those of the authors and do not necessarily reflect the views of the S.D. Bechtel, Jr. Foundation. The authors would like to acknowledge funding from NIH R21-AR063348 to D.R.H., NIH R01-ES016308 to P.J.L. and Dept. Pathology proteomics initiative funds to B.A.C.

## Appendix A. Supplementary data

Supplementary data associated with this article can be found, in the online version, at <http://dx.doi.org/10.1016/j.bbrc.2014.09.137>.

## References

- [1] N.L. Anderson, N.G. Anderson, The human plasma proteome: history, character, and diagnostic prospects, *Mol. Cell. Proteomics* 1 (2002) 845–867.
- [2] D.M. Gersten, B.S. Khirabadi, P. Kurian, R.S. Ledley, T. Mahany, E.R. Ramey, P.W. Ramwell, Albumin obscures sex differences in blood protein patterns of rats and humans, *Biochem. J.* 191 (1980) 869–872.
- [3] B.A. Chromy, A.D. Gonzales, J. Perkins, M.W. Choi, M.H. Corzett, B.C. Chang, C.H. Corzett, S.L. McCutchen-Maloney, Proteomic analysis of human serum by two-dimensional differential gel electrophoresis after depletion of high-abundant proteins, *J. Proteome Res.* 3 (2004) 1120–1127.
- [4] J.N. Adkins, S.M. Varnum, K.J. Auberry, R.J. Moore, N.H. Angell, R.D. Smith, D.L. Springer, J.G. Pounds, Toward a human blood serum proteome: analysis by multidimensional separation coupled with mass spectrometry, *Mol. Cell. Proteomics* 1 (2002) 947–955.
- [5] R. Pieper, C.L. Gatlin, A.J. Makusky, P.S. Russo, C.R. Schatz, S.S. Miller, Q. Su, A.M. McGrath, M.A. Estock, P.P. Parmar, M. Zhao, S.T. Huang, J. Zhou, F. Wang, R. Esquer-Blasco, N.L. Anderson, J. Taylor, S. Steiner, The human serum proteome: display of nearly 3700 chromatographically separated protein spots on two-dimensional electrophoresis gels and identification of 325 distinct proteins, *Proteomics* 3 (2003) 1345–1364.
- [6] V. Polaskova, A. Kapur, A. Khan, M.P. Molloy, M.S. Baker, High-abundance protein depletion: comparison of methods for human plasma biomarker discovery, *Electrophoresis* 31 (2010) 471–482.
- [7] Y. Amhad, N. Sharma, An effective method for the analysis of human plasma proteome using two-dimensional gel electrophoresis, *J. Proteomics Bioinform.* 2 (2009) 495–499.
- [8] P. Haynes, I. Miller, R. Aebersold, M. Gemeiner, I. Eberini, M.R. Lovati, C. Manzoni, M. Vignati, E. Gianazza, Proteins of rat serum: I. Establishing a reference two-dimensional electrophoresis map by immunodetection and microbore high performance liquid chromatography–electrospray mass spectrometry, *Electrophoresis* 19 (1998) 1484–1492.
- [9] X. Duan, D.M. Yarmush, F. Berthiaume, A. Jayaraman, M.L. Yarmush, A mouse serum two-dimensional gel map: application to profiling burn injury and infection, *Electrophoresis* 25 (2004) 3055–3065.
- [10] B.L. Hood, M. Zhou, K.C. Chan, D.A. Lucas, G.J. Kim, H.J. Issaq, T.D. Veenstra, T.P. Conrads, Investigation of the mouse serum proteome, *J. Proteome Res.* 4 (2005) 1561–1568.
- [11] M.S. Ritorto, J. Borlak, A simple and reliable protocol for mouse serum proteome profiling studies by use of two-dimensional electrophoresis and MALDI TOF/TOF mass spectrometry, *Proteome Sci.* 6 (2008) 25.
- [12] A. Mahn, A. Reyes, M. Zamorano, W. Cifuentes, M. Ismail, Depletion of highly abundant proteins in blood plasma by hydrophobic interaction chromatography for proteomic analysis, *J. Chromatogr. B Anal. Technol. Biomed. Life Sci.* 878 (2010) 1038–1044.
- [13] A. Mahn, M. Ismail, Depletion of highly abundant proteins in blood plasma by ammonium sulfate precipitation for 2D-PAGE analysis, *J. Chromatogr. B Anal. Technol. Biomed. Life Sci.* 879 (2011) 3645–3648.
- [14] T. Linke, S. Doraiswamy, E.H. Harrison, Rat plasma proteomics: effects of abundant protein depletion on proteomic analysis, *J. Chromatogr. B Anal. Technol. Biomed. Life Sci.* 849 (2007) 273–281.
- [15] V.M. Faca, K.S. Song, H. Wang, Q. Zhang, A.L. Krasnoselsky, L.F. Newcomb, R.R. Plentz, S. Gurumurthy, M.S. Redston, S.J. Pitteri, S.R. Pereira-Faca, R.C. Ireton, H. Katayama, V. Glukhova, D. Phanstiel, D.E. Brenner, M.A. Anderson, D. Misek, N. Scholler, N.D. Urban, M.J. Barnett, C. Edelstein, G.E. Goodman, M.D. Thorngquist, M.W. McIntosh, R.A. DePinho, N. Bardeesy, S.M. Hanash, A mouse to human search for plasma proteome changes associated with pancreatic tumor development, *PLoS Med.* 5 (2008) e123.
- [16] Y.Y. Chen, S.Y. Lin, Y.Y. Yeh, H.H. Hsiao, C.Y. Wu, S.T. Chen, A.H. Wang, A modified protein precipitation procedure for efficient removal of albumin from serum, *Electrophoresis* 26 (2005) 2117–2127.
- [17] D.E. Amacher, R. Adler, A. Herath, R.R. Townsend, Use of proteomic methods to identify serum biomarkers associated with rat liver toxicity or hypertrophy, *Clin. Chem.* 51 (2005) 1796–1803.
- [18] A.J. Kruger, C. Yang, S.W. Tam, D. Hinerfeld, J.E. Evans, K.M. Green, J. Leszyk, K. Yang, D.L. Guberski, J.P. Mordes, D.L. Greiner, A.A. Rossini, R. Bortell, Haptoglobin as an early serum biomarker of virus-induced autoimmune type 1 diabetes in biobreeding diabetes resistant and LEW1.WR1 rats, *Exp. Biol. Med.* (Maywood) 235 (2010) 1328–1337.
- [19] D. Karthik, S. Ilavenil, B. Kaleeswaran, S. Sunil, S. Ravikumar, Proteomic analysis of plasma proteins in diabetic rats by 2D electrophoresis and MALDI-TOF-MS, *Appl. Biochem. Biotechnol.* 166 (2012) 1507–1519.
- [20] M.M. Ivancic, E.L. Huttlin, X. Chen, J.K. Pleiman, A.A. Irving, A.D. Hegeman, W.F. Dove, M.R. Sussman, Candidate serum biomarkers for early intestinal cancer using 15N metabolic labeling and quantitative proteomics in the ApcMin/+ mouse, *J. Proteome Res.* 12 (2013) 4152–4166.
- [21] L.F. Steel, M.G. Trotter, P.B. Nakajima, T.S. Mattu, G. Gonye, T. Block, Efficient and specific removal of albumin from human serum samples, *Mol. Cell. Proteomics* 2 (2003) 262–270.
- [22] K.S. Lilley, D.B. Friedman, All about DIGE: quantification technology for differential-display 2D-gel proteomics, *Expert Rev. Proteomics* 1 (2004) 401–409.
- [23] L. Koontz, TCA precipitation, *Methods Enzymol.* 541 (2014) 3–10.

# Osteoarthritis and Cartilage



## Review

## Non-invasive mouse models of post-traumatic osteoarthritis



B.A. Christiansen <sup>†</sup>\*, F. Guilak <sup>‡</sup>, K.A. Lockwood <sup>†</sup>, S.A. Olson <sup>‡</sup>, A.A. Pitsillides <sup>§</sup>,  
L.J. Sandell <sup>||</sup>, M.J. Silva <sup>||</sup>, M.C.H. van der Meulen <sup>¶</sup>, D.R. Haudenschild <sup>†</sup>\*\*

<sup>†</sup> Department of Orthopaedic Surgery, University of California-Davis Medical Center, USA

<sup>‡</sup> Department of Orthopaedic Surgery, Duke University Medical Center, USA

<sup>§</sup> Department of Comparative Biomedical Sciences, The Royal Veterinary College London, UK

<sup>||</sup> Department of Orthopaedic Surgery, Washington University in St. Louis, USA

<sup>¶</sup> Department of Biomedical Engineering and Sibley School of Mechanical & Aerospace Engineering, Cornell University, USA

### ARTICLE INFO

#### Article history:

Received 13 February 2015

Accepted 10 May 2015

#### Keywords:

Post-traumatic osteoarthritis (PTOA)

Mouse model

Articular cartilage

Knee injury

### SUMMARY

Animal models of osteoarthritis (OA) are essential tools for investigating the development of the disease on a more rapid timeline than human OA. Mice are particularly useful due to the plethora of genetically modified or inbred mouse strains available. The majority of available mouse models of OA use a joint injury or other acute insult to initiate joint degeneration, representing post-traumatic osteoarthritis (PTOA). However, no consensus exists on which injury methods are most translatable to human OA. Currently, surgical injury methods are most commonly used for studies of OA in mice; however, these methods may have confounding effects due to the surgical/invasive injury procedure itself, rather than the targeted joint injury. Non-invasive injury methods avoid this complication by mechanically inducing a joint injury externally, without breaking the skin or disrupting the joint. In this regard, non-invasive injury models may be crucial for investigating early adaptive processes initiated at the time of injury, and may be more representative of human OA in which injury is induced mechanically. A small number of non-invasive mouse models of PTOA have been described within the last few years, including intra-articular fracture of tibial subchondral bone, cyclic tibial compression loading of articular cartilage, and anterior cruciate ligament (ACL) rupture via tibial compression overload. This review describes the methods used to induce joint injury in each of these non-invasive models, and presents the findings of studies utilizing these models. Altogether, these non-invasive mouse models represent a unique and important spectrum of animal models for studying different aspects of PTOA.

© 2015 Osteoarthritis Research Society International. Published by Elsevier Ltd. All rights reserved.

### Introduction

Osteoarthritis (OA) currently affects approximately 27 million people in the United States<sup>1</sup>, and 630 million people worldwide, and the knee is by far the most commonly affected joint<sup>2</sup>. OA can be

classified either as “primary” (or idiopathic), arising from unknown causes and affecting primarily older subjects, or “secondary” (or post-traumatic), arising as a consequence of a joint injury and often affecting much younger subjects. For example, after anterior cruciate ligament (ACL) or meniscus injury, patients are at a much higher risk of developing post-traumatic osteoarthritis (PTOA) within 10–20 years after injury<sup>3,4</sup>. This risk is even greater following high-energy impact joint injuries involving intra-articular bone fracture<sup>5,6</sup>. Altogether, approximately 10–12% of symptomatic OA cases can be considered post-traumatic<sup>7</sup>.

Animal models of OA are essential tools for investigating the development and mechanisms of the disease on a more rapid timeline than human OA. Spontaneous animal models of OA<sup>8–11</sup>, in which OA will develop in animals without any “injury” to the joint, are believed to be representative of primary (idiopathic) OA. However, the majority of animal models use a joint injury or other acute insult to initiate joint degeneration, making them more

\* Address correspondence and reprint requests to: B.A. Christiansen, Department of Orthopaedic Surgery, University of California-Davis Medical Center, 4635 2nd Ave, Suite 2000, Sacramento, CA 95817, USA. Tel: 1-916-734-3974.

\*\* Address correspondence and reprint requests to: D.R. Haudenschild, Department of Orthopaedic Surgery, University of California-Davis Medical Center, 4635 2nd Ave, Suite 2000, Sacramento, CA 95817, USA. Tel: 1-916-734-5015.

E-mail addresses: [bchristiansen@ucdavis.edu](mailto:bchristiansen@ucdavis.edu) (B.A. Christiansen), [guilak@duke.edu](mailto:guilak@duke.edu) (F. Guilak), [lockwoodemail@gmail.com](mailto:lockwoodemail@gmail.com) (K.A. Lockwood), [steven.olson@duke.edu](mailto:steven.olson@duke.edu) (S.A. Olson), [apitsillides@rvc.ac.uk](mailto:apitsillides@rvc.ac.uk) (A.A. Pitsillides), [sandell@wudosis.wustl.edu](mailto:sandell@wudosis.wustl.edu) (L.J. Sandell), [silvam@wudosis.wustl.edu](mailto:silvam@wudosis.wustl.edu) (M.J. Silva), [mcv3@cornell.edu](mailto:mcv3@cornell.edu) (M.C.H. van der Meulen), [drhaudenschild@ucdavis.edu](mailto:drhaudenschild@ucdavis.edu) (D.R. Haudenschild).

representative of PTOA. Little *et al.* identified five properties of the “ideal” animal model of OA<sup>12</sup>:

- 1) The model should induce consistent reproducible disease that occurs in a suitable time frame to allow reasonably high throughput studies.
- 2) The induced disease should be universally progressive in the time frame of the study to allow investigation of early, mid and late pathophysiology and treatment effects.
- 3) The animal should be a mammalian species that is tractable, inexpensive, easy to house and manage, large enough to allow multiple analyses/outcome measures, allows genome wide micro-array analysis and proteomic analysis, sequencing *etc.*
- 4) The disease process in the animal recapitulates the human pathology in all tissues of the articulating joint.
- 5) The model should be predictive of therapeutic disease modification in humans.

Numerous animal models of PTOA have been described, however it is not yet known if any of these models fully exhibit these “ideal” properties.

Mice are particularly useful model organisms and are commonly used to study OA and other musculoskeletal conditions, so extensive normative data on mouse musculoskeletal growth and metabolism are available. The abundance of available genetically modified or inbred mouse strains provide the unique ability to study molecular mechanisms contributing to OA development<sup>13–19</sup>. However, the use of mice for studies of OA also has important limitations<sup>20</sup> including the small size of the joint and the extreme thinness of the articular cartilage, which is only a few cell layers thick. Therapeutic strategies that are shown to be successful on this small scale may not prove as effective in the larger human joint. Additionally, the small joint size and thin cartilage make surgical repair or treatment of joint injuries unfeasible or impractical.

While numerous mouse models of PTOA have been described, no consensus exists on the injury methods used to initiate the development of OA. This limitation is crucially important, since the observed pattern of joint degeneration likely depends on the injury method used. For this reason, injury methods should be utilized in mice that recapitulate the human injury conditions as closely as possible. However, most mouse models use invasive (i.e., surgical) or non-physiologic methods to initiate joint degeneration.

### Surgical and injection mouse models of PTOA

Surgical injury methods initiate joint degeneration by disrupting joint structures such as ligaments and menisci that can alter the stability and biomechanics of the joint. Development of mouse models of PTOA based on this concept follows previous studies in larger animals. One of the first surgically-induced animal models of OA was ACL transection (ACLT), or Pond-Nuki model, in dogs in 1973<sup>21</sup>. The authors noted a histological progression of arthritis similar to naturally occurring arthritis, with gross fibrillation extending deep into the articular cartilage at long time points. This study laid the groundwork for further ACLT studies in dogs<sup>22–26</sup>, rats<sup>27–29</sup>, rabbits<sup>30–32</sup>, cats<sup>33,34</sup>, guinea pigs<sup>35,36</sup>, sheep<sup>37</sup>, and mice<sup>38,39</sup>.

Another common method of inducing OA in animal models involves partial or total removal of the medial meniscus<sup>40–44</sup>. Studies have combined meniscectomy and ACLT to model the combination injury seen clinically<sup>39,45,46</sup>. Destabilization of the medial meniscus (DMM) also initiates OA progression in mice<sup>19,38,47–50</sup>; this method has been the most commonly reported for studying OA in mice. DMM produces relatively predictable development of OA, although disease progression may be variable, particularly when the

procedure is performed by surgeons with disparate skill or experience. These factors may represent potential drawbacks to the DMM model or any other surgical method. These procedures can be technically difficult to perform, and require specialized equipment and personnel to effectively perform the procedure. Surgical techniques also require opening the joint capsule, which can disrupt the natural environment of the joint, and may therefore come with unintended adaptive and healing processes that are due to the surgery itself, rather than the intended “injury”. This consideration is particularly important when studying early time points following an injurious event, and thus require the use of “sham” surgeries and increased numbers of experimental animals.

Degenerative changes in the knee joint can also be achieved by intra-articular injection of degradative agents into the joint space, including proteolytic enzymes such as papain<sup>51–53</sup> and collagenase<sup>53–56</sup>, cytokines such as tumor necrosis factor alpha (TNF- $\alpha$ )<sup>57,58</sup>, transforming growth factor  $\beta$  (TGF- $\beta$ )<sup>59,60</sup>, and interleukin-1 (IL-1)<sup>55,61</sup>, or chemicals such as monosodium iodoacetate (MIA)<sup>53,62–64</sup> and colchicine<sup>65</sup>. Different agents will create pathological changes in the joint by different mechanisms, making these approaches appropriate for studies of particular biological mechanisms. However, these methods do not mimic human injury conditions, suggesting that the translatability of information garnered from these models may not be relevant to PTOA.

### Non-invasive mouse models of PTOA

Non-invasive models can initiate PTOA using externally applied mechanical loads, but do not break the skin or disrupt the joint capsule. Non-invasive injury models are therefore completely aseptic, and avoid potential confounding effects caused by the trauma of the surgical/invasive injury procedure.

A particular opportunity afforded by non-invasive injury models is investigating early adaptive processes that are initiated at the time of injury, with time scales of hours or days following injury (Fig. 1). This is a key advantage, as the window of opportunity for treatments aimed at slowing or inhibiting PTOA may be only a few days following injury. Non-invasive models more accurately recapitulate the mechanically-induced mechanisms involved in injuries leading to OA in humans, initiating joint degeneration through direct damage to cartilage, bone, or soft tissue structures of the joint. Additionally, non-invasive models may be simpler, quicker experimental procedures that are straightforward to implement and do not require technically difficult surgical or injury techniques.

Several non-invasive mouse models of PTOA have been described within the last few years. Each model initiates joint degeneration using different methods, and is therefore representative of specific conditions leading to the human disease. However, these non-invasive models represent a unique and important spectrum of animal models for studying different aspects of PTOA.

#### Intra-articular fracture of the tibial plateau

The first non-invasive mouse model of PTOA was described by Furman *et al.*, in 2007<sup>66</sup>. This model initiates symptoms using intra-articular fracture (IAF) of the proximal tibia, and includes blunt impaction of articular cartilage, fracture of the articular cartilage/subchondral bone layer, fragmentation of the articular surface, residual displacement of the articular surfaces, and exposure of blood and marrow products to the articular surface and synovium. This injury model is representative of higher-energy impact injuries that may be sustained by humans in events such as frontal automobile collisions.

To induce an articular fracture of the tibial plateau, C57BL/6 mice were positioned in a custom cradle with the lower limb at approximately 90° flexion, in a materials testing system (ELF 3200, Bose, Eden Prairie, MN), and a 10 N compressive preload was applied to the proximal tibia using a wedge-shaped indenter mounted to the testing system (Fig. 2) to a target compressive force of 55 N at a rate of 20 N/s. Fractures were characterized by anterior/posterior (A/P) and lateral radiographs. No fixation or surgical intervention was employed so that the natural history and healing of a closed articular fracture could be elucidated. Animals were allowed immediate full weight bearing with unlimited range of motion.

The IAF protocol was successful in 87% of the mice (27 of 31). Subsequent studies using this model have reported over 95% success in fracture creation<sup>62–64</sup>. The injuries induced by the protocol varied, with both simple and complex fractures of the tibia. Fractures were commonly located on the lateral side of the plateau and closely resembled those seen clinically (Fig. 2). Micro-computed tomography ( $\mu$ CT) results indicated that trabecular bone volume fraction (BV/TV) in the femoral condyles was significantly reduced in injured limbs at all time points compared to contralateral control limbs. Bone density was significantly lower in injured limbs in the femoral condyles, tibial plateau, and tibial metaphysis. The lateral femoral condyle and tibial plateau exhibited subchondral bone thickening in injured limbs compared to control limbs. Histology showed a progressive loss of Safranin-O staining over the first 8 weeks from the meniscus, and femoral and tibial articular cartilage, indicating a loss of proteoglycan. By 50 weeks, severe loss of articular cartilage and exposure of subchondral bone was present on both the tibia and femur, indicative of terminal OA.

The IAF model provides a fast and fairly reproducible non-invasive injury to the knee joints of mice using a single mechanical load, consistent with human injuries, and the resulting changes in bone and articular cartilage are representative of joint degeneration observed in human OA. This model is representative of articular fracture injuries, therefore this model may not be ideal for studying lower energy non-contact injuries that commonly lead to PTOA (e.g., ACL rupture or meniscus tear). The authors evaluated energy of injury using a liberated surface area analysis and found

good correlation between applied energy of fracture and liberated surface area, allowing investigators to create high and low energy articular fracture injuries<sup>62</sup> (Fig. 3). The variability in severity of fracture creates varying degrees of joint inflammation or abnormal loading of cartilage after injury, which affects the rate of joint degeneration on a mouse-to-mouse basis, therefore fracture severity needs to be quantified and included as a co-factor when comparing experimental groups<sup>67</sup>. However, even when fracture severity is quantified and factored into the analysis, the inherent variability in fracture severity must be considered a limitation of this model.

Another important advantage of the IAF model is that, as the first non-invasive mouse model of PTOA described, a relatively large body of literature has utilized this model for studies of PTOA development. For example, Ward *et al.*<sup>13</sup> investigated PTOA development following IAF in MRL/MpJ mice, which have shown unique regenerative abilities following injury. Injured knees of MRL/MpJ mice were protected against changes in bone density, subchondral bone thickness, and cartilage degeneration at 4 and 8 weeks post-injury. The differences in PTOA development between C57BL/6 mice and MRL/MpJ mice after IAF have been further explored<sup>68</sup>. Seifer *et al.* utilized this mouse model to investigate cartilage oligomeric matrix protein (COMP) in synovial fluid of mice following IAF<sup>69</sup>. Lewis *et al.* used this model to determine the effect of articular fracture severity on synovial inflammation, bone morphology, liberated fracture area, cartilage pathology, chondrocyte viability, and systemic cytokines and biomarkers levels<sup>67</sup>. Louer *et al.* utilized IAF in mice to determine whether diet-induced obesity influences the severity of PTOA development<sup>70</sup>. Diekmann *et al.* utilized this animal model to investigate whether delivery of mesenchymal stem cells (MSCs) could affect the development of PTOA by altering inflammation and regeneration after fracture<sup>71</sup>. In two other investigations, intra-articular administration of IL-1 receptor antagonist immediately after fracture limited the development of PTOA in C57BL/6 mice<sup>72,73</sup>. Altogether, the IAF mouse model is a useful method for studying joint degeneration following high trauma injuries to the knee. The model has been well characterized and accurately recapitulates joint degeneration observed in humans following this type of injury.

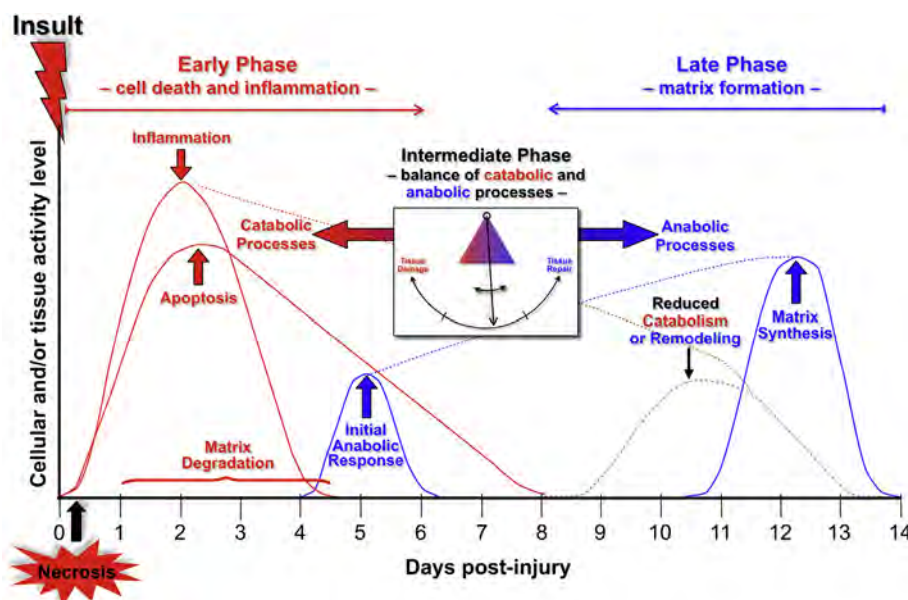


**Fig. 1.** Conceptual framework of the immediate cellular responses to acute joint trauma. Both catabolic and anabolic processes are involved in the response to the injury, and overlap with one another. Image courtesy of Susanna Chubinskaya. From Anderson *et al.*<sup>99</sup>. Used with permission.

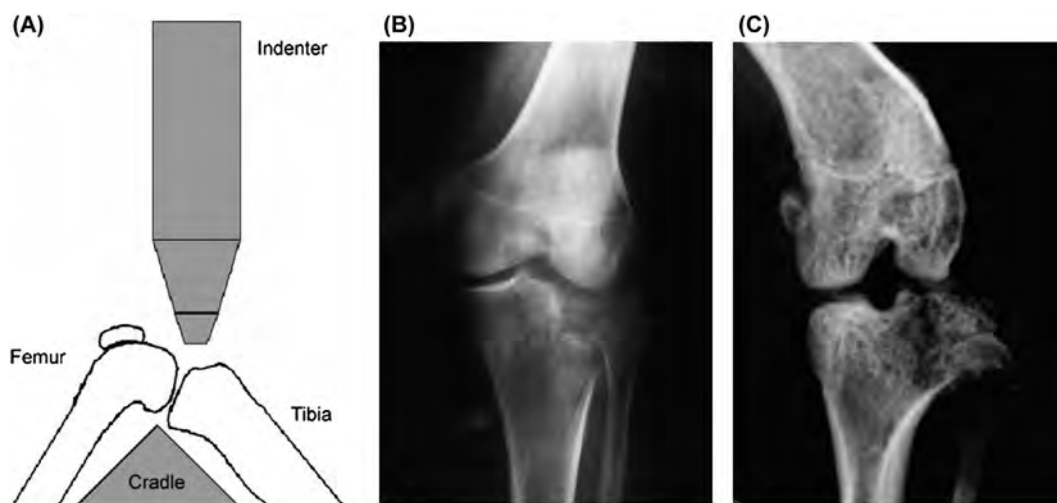


**Fig. 2.** (A) Alignment of the cradle and indenter for creating a closed articular fracture in the mouse knee. (B–C) Radiographs of clinically observed (B) human tibial plateau fracture and (C) experimentally created mouse tibial plateau fracture. From Furman *et al.*<sup>66</sup>. Used with permission.

#### Cyclic tibial compression of articular cartilage

Tibial compression is a commonly used technique for studies of bone adaptation in mice<sup>74–78</sup>. For this loading method, a mouse is subjected to cyclic axial compressive loads applied to the lower leg through the ankle and knee joints (Fig. 4), with loads transmitted through natural joint articulations. This technique has also proven useful for the study of articular cartilage degeneration following mechanical loading. Poulet *et al.* were the first to exploit this approach to investigate short- and long-term joint degeneration following single or multiple bouts of loading in male CBA mice<sup>79</sup>. In this study, a 9 N compressive load was applied every 10 s, with 40 cycles for each loading bout, and loading was performed 3 days per week. Loss of Safranin-O staining and articular cartilage lesions were observed on the lateral femur after 2 weeks of loading. When an additional 3 weeks of loading or non-loading was allowed after the initial 2 weeks of loading, the mean grade of lesion severity increased significantly in the loaded group, but the maximum lesion severity did not change. A single bout of tibial compression loading damaged the articular cartilage, but was not sufficient to create progressive lesions. Early signs of osteophytes were seen on the lateral femur in 57% of mice that were loaded for 2 weeks, while early signs of osteophytes on the medial and lateral femur were

observed in 83% of mice loaded for 5 weeks. This model has subsequently been used to explore interaction between mechanically-induced cartilage lesions and genetics using the STR/Ort mouse strain (a model of spontaneous OA) to show that increased susceptibility to OA in this mouse strain was unlikely due to greater vulnerability to mechanical trauma<sup>80</sup>. It has also been used to show that cyclic mechanical loading is sufficient to induce subchondral bone thickening, particularly in regions contiguous with articular cartilage lesions in young growing mice<sup>81</sup>.

A similar approach was used to examine the effect of compressive load magnitude on the structure and composition of articular cartilage and subchondral bone in the knees of young (10 week-old) and adult (26 week-old) male C57BL/6 mice<sup>82</sup>. *In vivo* tibial compression loading was performed at defined magnitudes of 4.5 N and 9.0 N in adult mice, and at a peak load of 9.0 N in young mice for 1, 2, and 6 weeks. Loading was applied for 1,200 cycles per day, 4 cycles per second, for 5 days per week. Tibial compression initiated cartilage damage in both young and adult mice, and the severity of cartilage damage was greater with longer duration of loading (Fig. 5). As reported by Poulet *et al.*<sup>79</sup>, cartilage degeneration occurred primarily at the lateral tibial plateau. Trabecular bone volume in the tibial metaphysis increased relative to contralateral controls with loading in young mice, but not in adult mice, whereas

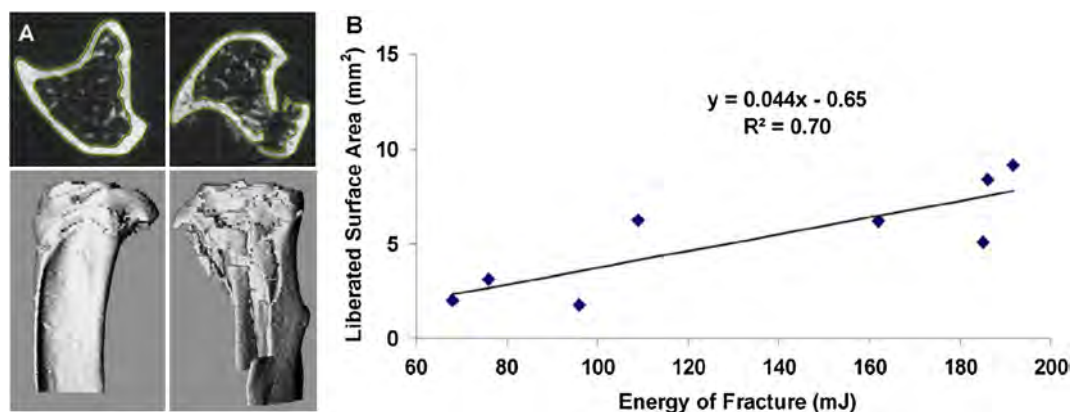


**Fig. 3.** Correlation between liberated surface area and measured energy of fracture for closed articular fracture in the mouse knee. Fracture severity, as measured from the liberated surface area, was well correlated to the energy of fracture, as calculated from the load–displacement data. From Lewis *et al.*<sup>67</sup>. Used with permission.

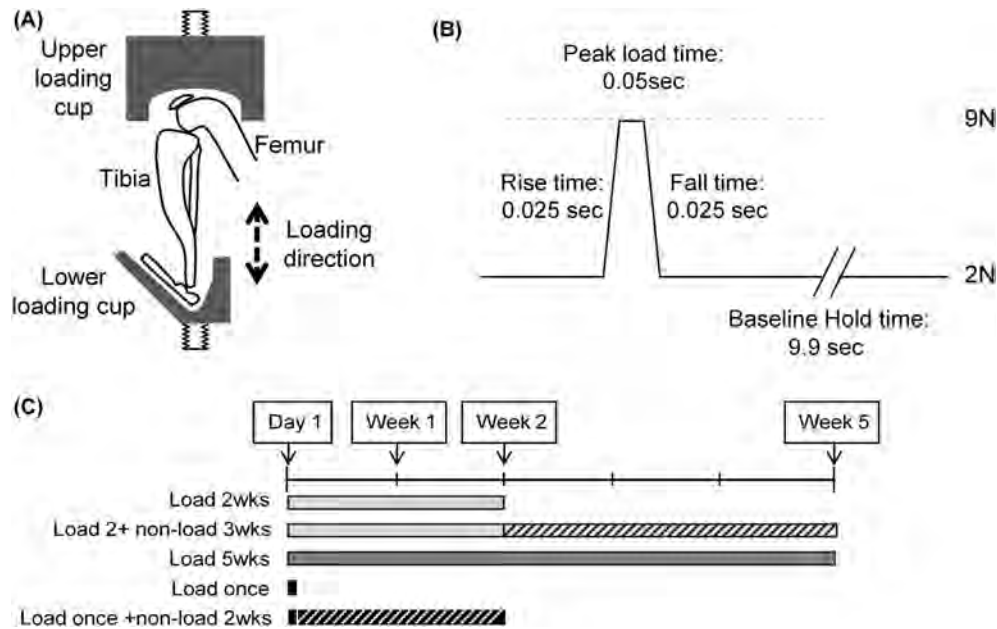


**Fig. 4.** Diagrammatic representation of the cyclic tibial compression loading model. (A) Estimated position of the hind limb and loading direction when placed in the loading apparatus. (B) Diagram of a single cycle of applied load, showing hold and peak load magnitudes, rate of load application, and intervening peak and baseline hold times. (C) Diagrammatic representation of the 5 different loading regimens. From Poulet *et al.*<sup>79</sup>. Used with permission.

trabecular bone volume in the tibial epiphysis decreased with 6 weeks of loading in both young and adult mice. In both age groups, articular cartilage thickness decreased, and subchondral cortical bone thickness increased in the posterior tibial plateau. Mice in both age groups developed periarticular osteophytes at the tibial plateau in response to the 9.0 N peak load, but no osteophytes were observed in mice subjected to 4.5 N loading.

Recently, tibial compression was used to investigate early molecular events following cartilage injury in mice<sup>83</sup>. The right lower leg of 8-week old male C57BL/6 mice was subjected to tibial compression loading at 3, 6, or 9 N peak force for 60 cycles (10 s rest between cycles) in a single loading period, and harvested 5, 9, and 14 days post-loading. The authors reported that loading to 9 N produced a sharp drop in recorded force during the 1<sup>st</sup> loading cycle, consistent with ACL rupture (Fig. 7). Histology, immunohistochemistry, and ELISA were performed to evaluate chondrocyte viability, cartilage matrix metabolism, synovitis, and serum COMP levels. All loading regimens induced chondrocyte apoptosis, cartilage matrix degradation, and disruption of cartilage collagen fibril arrangement. 6 N loading induced mild synovitis by day 5, while 9 N loading initiated severe synovitis and fibrosis, likely due to joint instability associated with ACL injury. Even with joint loading at low compressive forces, serum COMP was significantly increased in mice. The precise source of COMP is unknown, however evidence of COMP synthesis in the lower zone of mouse cartilage is observable, with more pericellular COMP at higher loading magnitudes over time. Wu *et al.* recently reported the same COMP response to compression in 3-dimensional cell culture<sup>84</sup>. Similarly, *ex vivo* studies showed that mechanical loading of cartilage explants increased COMP mRNA expression and synthesis of COMP, suggesting that cartilage tissue can remodel certain aspects of its extracellular matrix in response to an altered mechanical environment<sup>85</sup>.

The early molecular and cellular response to joint loading or injury is of particular interest for studies of OA, as these biological responses likely contribute to long-term joint degeneration. Surprisingly, the early response to a single loading session at 3 or 6 N

magnitudes demonstrated a molecular and cellular response similar to that associated with severe injury<sup>83</sup>. For example, a single loading episode at 3 or 6 N magnitude elicited apoptosis of chondrocytes at the site of cartilage compression. Concomitant with cartilage injury and chondrocyte apoptosis, safranin O staining was lost in the surrounding pericellular and interterritorial matrices, and the proteoglycan aggrecan appeared to be internalized into the chondrocyte. The internalization of aggrecan happens only in cells that are undergoing apoptosis (Fig. 6) and may reflect loss of membrane integrity. Longer-term studies suggest that these early events are not repaired, and no evidence of cell proliferation or migration of cells into the injured cartilage is observed (Xin, Rai and Sandell, unpublished data). At these low levels of cartilage injury, inhibition of cell death in cartilage or inhibition of synovial cell proliferation could potentially decrease cartilage damage<sup>86</sup>. Thus, joint loading at sub-injury magnitudes can cause focal damaged patches in the cartilage that have fewer cells and thus less ability to synthesize extracellular matrix and resist mechanical abrasion.

The cyclic tibial compression model provides several unique benefits for the study of OA development. The adjustability of this model is a major benefit. By loading at a higher compressive force or for longer duration, the severity of joint degeneration can be controlled. However, regardless of the loading protocol used, the subsequent joint degeneration is typically mild (in the absence of ligament failure), even when loading at high force for several weeks, therefore severe OA may not be easily achievable. This model is highly reproducible between individual mice (and theoretically between research groups; see “Additional Considerations” below), and produces predictable structural changes in articular cartilage and subchondral bone. Importantly, the joint degeneration observed with this model (for sub-injury forces) does not appear to be a secondary consequence of joint destabilization or altered joint biomechanics, but is ascribable to direct overload of articular cartilage. In fact, acute degeneration can be observed within a few days at the sites of contact between the femur and tibia (Fig. 6)<sup>83</sup>. A limitation of this approach is that multiple days of anesthesia and loading are required in order to initiate cartilage

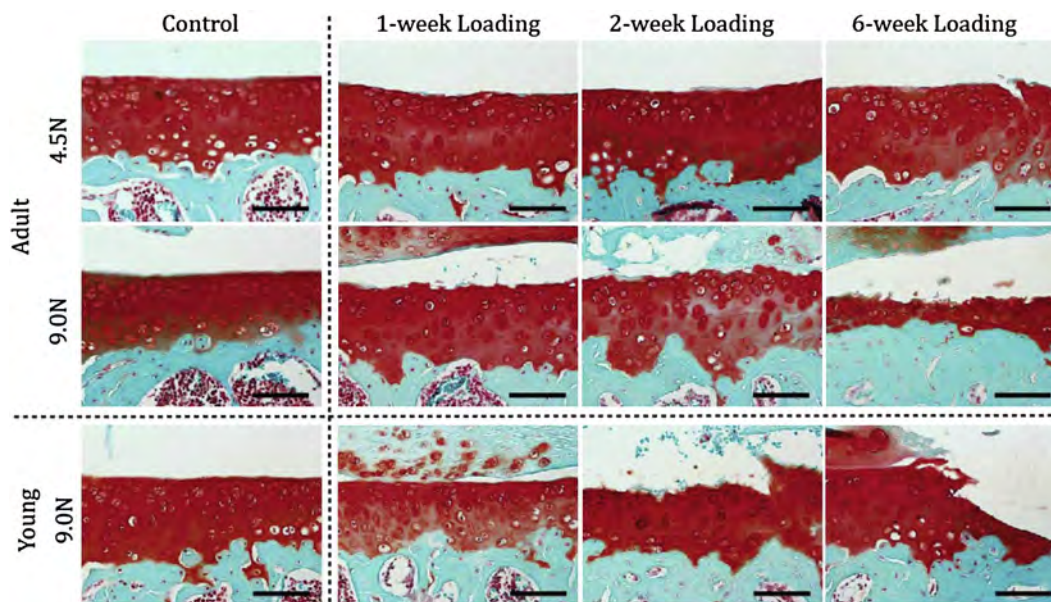


**Fig. 5.** Cartilage matrix changes in the tibia after cyclic tibial compression loading. The left tibiae of young and adult mice were loaded (peak loads of 4.5 N and 9.0 N in adult mice; 9.0 N in young mice) for 1, 2, and 6 weeks. The nonloaded contralateral limb at 6 weeks load duration served as control. Safranin O–fast green staining of the medial articular cartilage reveals that damage to the cartilage matrix occurred following mechanical loading in both young and adult mice, and was exacerbated with longer durations and a higher level of loading in adult mice. Bars = 100  $\mu$ m. From Ko *et al.*<sup>82</sup>. Used with permission.

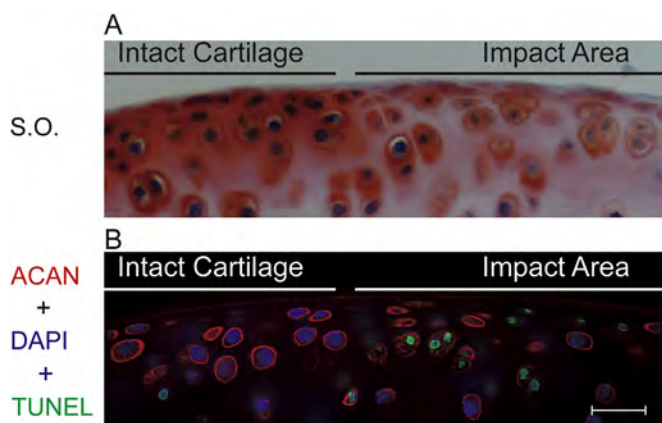


**Fig. 6.** Reduction in pericellular aggrecan (ACAN) thickness and in the intensity of extracellular distribution around the cells in the impact area in mouse knee joint cartilage injured by 3 N compressive loading. **(A)** Loss of Safranin O (S.O.) staining in the impact area. **(B)** Representative images from TUNEL assay combined with immunofluorescence staining for aggrecan. Note the inferior aggrecan encapsulation and thickness around apoptotic chondrocytes (nuclei stained green) in the injured area, compared to clear pericellular aggrecan in TUNEL-negative cells (nuclei stained blue). Bar = 20  $\mu$ m. From Wu *et al.*<sup>83</sup>. Used with permission.

degeneration. Despite the recent findings of Poulet *et al.*<sup>81</sup>, it is also unclear if bone changes induced with this model occur by a similar mechanism to PTOA, or if they are an anabolic response to cyclic mechanical loading. In fact, the same loading protocol that can be used to produce articular cartilage degeneration and epiphyseal bone changes<sup>79,82,83</sup> can also be used for studies of anabolic bone adaptation of metaphyseal trabecular bone in mice<sup>74–76</sup>. Altogether, the cyclic loading model is an extremely useful non-invasive model of OA in mice because it is adjustable (i.e., severity of initiated OA can be controlled), and can initiate OA features without disrupting joint function or altering the biomechanical stability of the joint in a measurable fashion (if the peak force is below the ACL-rupture

threshold). From this perspective, this model may be more representative of OA driven by chronic mechanical overuse rather than acute injury.

#### ACL rupture via tibial compression overload

A similar tibial compression loading method, first described by Christiansen *et al.*<sup>87</sup>, has been used for studies of PTOA by non-invasively creating an acute knee injury in mice by rupturing the ACL. This method is analogous to previous studies that have used external mechanical loading to non-invasively injure the ACL of rabbits<sup>88</sup>. A single compressive load was applied to the lower leg of C57BL/6 mice (10 weeks old at injury) using a tibial compression setup similar to those described above, to a target force of 12 N with a loading rate of 1 mm/s. Injury was noted by a release in compressive force and an audible “click” (Fig. 7). Mice were sacrificed at 1, 3, 7, 14, 28, or 56 days post-injury. MicroCT analysis revealed a dramatic loss of trabecular bone at the femoral and tibial epiphysis and tibial metaphysis by 7 days post-injury compared to contralateral knees. This bone volume deficit persisted for at least 56 days post-injury. Considerable mineralized osteophyte volume was also observed in the injured limb compared to the contralateral control by 28 and 56 days after injury. Histological results at 56 days post-injury indicated degenerative changes in the articular cartilage of injured knees, including loss of Safranin-O staining, fissuring in the cartilage surface, and chondrocyte cell death in the superficial zone.

A subsequent study using this model investigated biomechanical and structural changes in the joint following ACL rupture either with avulsion fracture or midsubstance tear<sup>89</sup>. This was achieved by increasing the loading rate during knee injury to decrease the likelihood of avulsion fracture<sup>90,91</sup>. Joint degeneration following low-speed injury (1 mm/s; ACL rupture with avulsion) or high-speed injury (500 mm/s; ACL rupture via mid-substance tear) was quantified at 10 days, 12 and 16 weeks to determine structural changes in subchondral bone and epiphyseal trabecular bone, osteophyte formation, articular cartilage degeneration, and

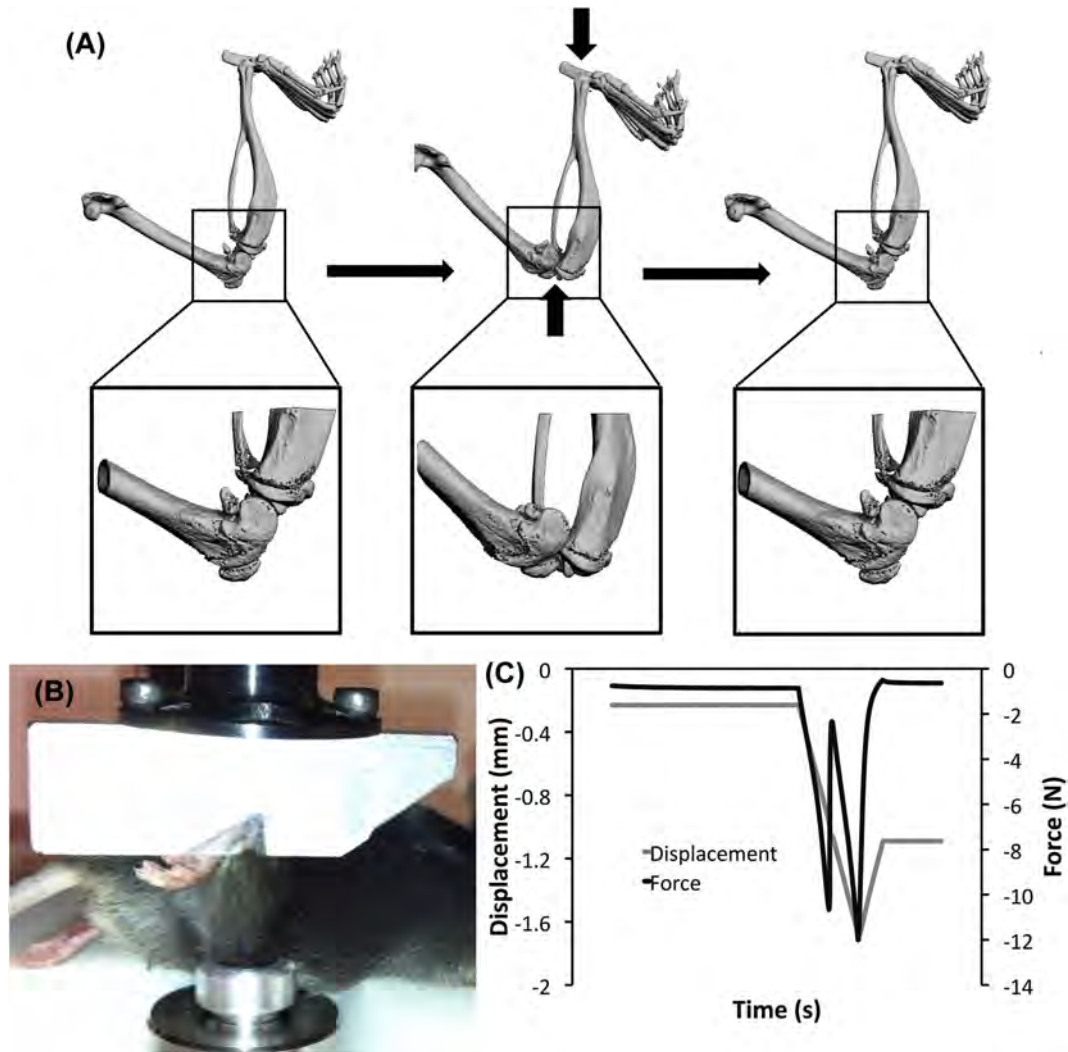


**Fig. 7.** Tibial compression overload ACL injury (A) Tibial compression loading caused a transient anterior subluxation of the tibia relative to the distal femur. (B) An anesthetized mouse with the right lower leg in the tibial compression loading system. (C) Knee injury during tibial compression loading was identified by a release of compressive force during the loading cycle, with a continued increase in actuator displacement. From Christiansen *et al.*<sup>37</sup>. Used with permission.

biomechanical stability of injured vs uninjured knees. Knee injury with both injury modes caused considerable trabecular bone loss by 10 days post-injury, with avulsion initiating a greater amount of bone loss than midsubstance tear. Immediately after injury, both injury modes resulted in greater than twofold increases in anterior-posterior (AP) joint laxity relative to control knees. However, by 12 and 16 weeks post-injury, AP laxity was restored to uninjured control values, possibly due to knee stabilization by osteophytes. By 12 and 16 weeks post-injury both high-speed and low-speed injury resulted in severe joint degeneration and osteophyte formation (Fig. 8). A primary site of degeneration was the posterior aspect of the medial tibia, similar to previously studies using surgical ACL transection in mice<sup>38</sup>.

A recent study by Onur *et al.*<sup>92</sup> subjected 3-month old FVB mice to cyclical axial loads of 12 N for 240 cycles or until the ACL ruptured. One and 8 weeks after this procedure, knees were evaluated histologically for OA. Consistent with Wu *et al.*<sup>83</sup>, the ACL-ruptured group exhibited significantly greater joint degeneration than either control (non-loaded) joints or joints that were cyclically loaded without ACL injury at both 1 and 8 weeks. Additionally, only ACL-ruptured knees consistently showed synovitis after 1 week and osteophyte formation after 8 weeks. The authors concluded

that ACL rupture consistently creates a severe OA phenotype, while a single bout of tibial compression loading alone did not consistently create an OA phenotype in this mouse strain.

The ACL rupture model applies loads with similar methods to those used for the cyclic tibial compression model, however the early biological response is likely very different. Once the tibial compression forces are high enough to cause rupture of the ACL, the cartilage is no longer loaded in the same way as it is in the cyclic compression model. In fact, once the ACL is ruptured, the position of the tibia and femur change in relationship to each other and thus the position of joint contact changes and is reflected in two or more zones of apoptosis<sup>83</sup>. This joint destabilization causes considerably more synovial cell proliferation than sub-injury cyclic compression, which sets the stage for the formation of cartilaginous nodules that will eventually mineralize and become visible on  $\mu$ CT. The rapid and considerable synovial response following ACL rupture may reflect several contributing factors, including soft tissue injury, destabilization of the joint, increased concentrations of inflammatory cytokines, and hemarthrosis.

The tibial compression overload/ACL rupture model has several unique advantages for studies of OA development. This model closely replicates ACL injury in humans, as ACL rupture is induced

with a single mechanical overload, with subsequent OA symptoms developing due to a known etiology. This method produces a highly reproducible injury, and a predictable pattern of joint degeneration. However, this model is not easily adjusted like the cyclic tibial compression model. Joint degeneration can likely be accelerated by applying additional compressive loads following ACL injury<sup>83,92</sup>, but producing joint degeneration of a lesser severity is difficult. Another consideration is that the observed joint degeneration is likely due in a large part to the joint instability initiated by this injury. The severe osteophyte formation observed at 8–16 weeks may also be part of the compensatory response to this joint instability<sup>93–95</sup>, although osteophyte formation is also present with sub-injury cyclic loading in which no instability is created<sup>79,82,83</sup>. Another limitation of this model is the severity of OA symptoms at long time points after ACL injury. The instability created by the failure of the ACL results in the distal femur translating posteriorly relative to the tibial plateau, creating a new articulating surface on the posterior aspect of the proximal tibia. Over time, this new articulation will erode articular cartilage from both the posterior tibial surface and the femoral condyles, particularly at the medial aspect of the joint, with degeneration often extending into the subchondral bone. This severe degeneration can be clearly observed by 12 and 16 weeks post-injury<sup>89</sup>, and often as early as 8 weeks post-injury<sup>96</sup>. For this reason, the tibial compression overload model may be more useful for studies of acute processes initiated by ACL rupture on a scale of hours or days following injury,

and may not be ideal for long-term studies investigating the onset of OA symptoms on a scale of weeks or months.

### Additional considerations

The selection of an appropriate mouse model involves not only the proposed research question, but also factors such as the logistics of performing the appropriate injury. For example, the non-invasive methods described in this review typically require specialized loading equipment with custom-made attachments. Much like surgical expertise and training, these specialized systems may not be readily available in all laboratories. If a suitable system is available, preliminary studies are still required to confirm the ability to reliably create the desired injury. Subtle differences in equipment and animal position may alter the site of maximal loading and the load-to-failure of the ACL, and thus possibly the pathology observed. These considerations are particularly important when attempting to create or avoid ACL rupture (as in the cyclic loading model) during tibial compression. Some tibial compression systems induce ACL rupture at relatively low forces (8–10 N), while others apply multiple loads of relatively high magnitude compression (11–12 N) without causing ACL injury. Contributing factors may include hip angle, which can create tension in the quadriceps during hip extension (pulling the tibia anteriorly, making ACL rupture more likely) or tension in the hamstrings during flexion (pulling the tibia posteriorly, making ACL

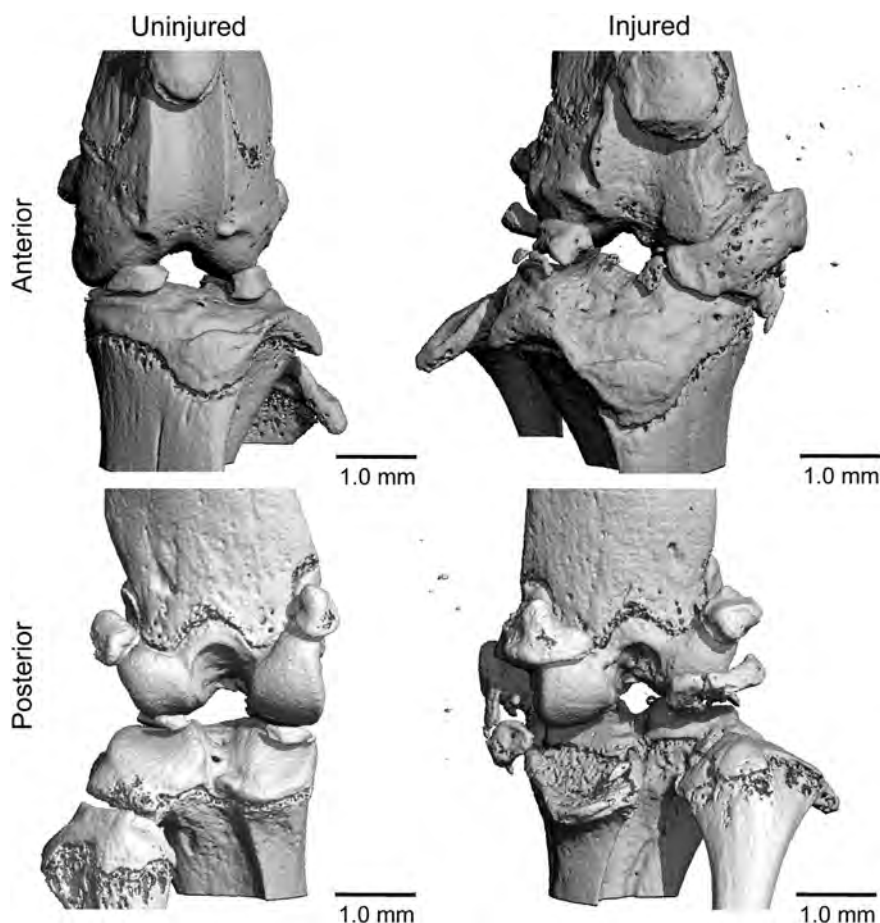


**Fig. 8.** MicroCT images of injured and uninjured mouse knees 12 weeks after non-invasive ACL injury. Substantial osteophyte formation and joint degeneration were observed in all injured knees. In particular, osteophytes were observed on the anteromedial aspect of the distal femur, the posteromedial aspect of the proximal tibia, and the medial meniscus. From Lockwood *et al.*<sup>89</sup>. Used with permission.

rupture less likely). The angle of extension of the ankle, along with any rotation of the lower limb also plays a role in the likelihood of inducing an ACL rupture during tibial compression. Even among groups that apply tibial compression without ACL rupture, subtle system-specific differences may exist in the loading of the joint that affect the tissue changes reported<sup>97</sup>. Because of these subtle differences, each team of investigators should carefully and rigorously characterize the methods used to initiate joint degeneration. The specific mechanical loading applied to the cartilage or the injury methods used may be subtly different than published results from other groups, and differences in OA development may reflect this.

The specific strain, sex, or age of mice used for studies of OA may also have a significant effect on outcomes. The majority of studies describing injury methods have used young, male, “wild-type” mice. Using mice of a different age, sex, or genetic strain will affect the ability to induce an injury, or the adaptation of the joint following the injury<sup>13,80</sup>. Indeed, studies examining such interplay have already revealed mechanisms contributing to susceptibility<sup>80</sup> or resistance<sup>13</sup> to OA following non-invasive injury. Further studies may reveal the roles of joint size and shape, the inherent mechanical properties of bone, ligaments, or other musculoskeletal tissues, or the biological response to injury in OA development. Each animal phenotype should be carefully characterized, and appropriate controls should be utilized to ensure the fidelity of results obtained with these models.

Careful consideration must also be given to appropriate controls for studies of OA that utilize non-invasive injury methods. Many studies compare the injured joint to the contralateral joint as an internal control. However, systemic effects of inflammation and bone turnover exist following an injury<sup>87,96,98</sup>, which may confound the results obtained when only the contralateral limb is used as a control. Therefore, each investigative team should independently perform a comparison of sham vs contralateral controls as part of the characterization of an animal model; when appropriate, uninjured (sham) controls should be utilized. This experimental design allows a true comparison of injured vs uninjured effects, and is necessary for investigators to determine contralateral or systemic effects of injury.

## Conclusion

Non-invasive mouse models of PTOA are a significant step forward for the study of OA mechanisms and therapies. Non-invasive models aseptically initiate joint degeneration, and are more representative of human injury conditions than surgical or invasive injury models because they use externally applied mechanical loading to directly damage bone, cartilage, or soft tissues of the joint. Non-invasive models are particularly useful for studying injury-induced biological processes at early time points following injury, which may be difficult with surgical models due to complications of the invasive injury methods. Non-invasive models are also typically faster and easier to perform than invasive or surgical injury methods, which often require special tools or training to consistently produce the desired injury. Currently, a small number of non-invasive mouse models have been described for studies of PTOA. These models vary in the methods and severity of injury, and are each translatable to specific human injuries and conditions that may lead to PTOA. These non-invasive models represent a unique and important spectrum of animal models for studying different aspects of PTOA, and may lead to novel insights into the underlying mechanisms of joint disease, although considerable work remains before results from these models will be truly translatable to human disease and treatment.

## Author contributions

All authors were fully involved in the preparation of this manuscript and approved the final version.

## Competing interest statement

The authors have no potential conflicts of interest to disclose.

## Acknowledgments

The authors would like to thank Christopher Little for providing helpful comments during drafting of this review. We would like to thank Susanna Chubinskaya and Donald Anderson for graciously allowing us to use Fig. 1 for this review. We would like to acknowledge the contributions of the various members of our laboratories who have contributed to these studies over the last few years. Research described in this review was supported in part by the Arthritis Foundation, the Department of Defense (PR110507), Arthritis Research UK (20581, 20413, 20258, 18768), Biotechnology and Biological Sciences Research Council (BB/I014608/1), and the National Institutes of Health (AR048182, AR050245, AR057235, AR062603, AR063757, AR064034, AG015768, AG046927).

## References

1. Arthritis Foundation, “Learn About Osteoarthritis”. Retrieved April 15, 2014, from Arthritis Foundation Web site: <https://www.arthritis.org/conditions-treatments/disease-center/osteoarthritis/>.
2. Felson DT. Epidemiology of hip and knee osteoarthritis. *Epidemiol Rev* 1988;10:1–28.
3. Lohmander LS, Englund PM, Dahl LL, Roos EM. The long-term consequence of anterior cruciate ligament and meniscus injuries: osteoarthritis. *Am J Sports Med* 2007;35(10):1756–69.
4. Oiestad BE, Engebretsen L, Storheim K, Risberg MA. Knee osteoarthritis after anterior cruciate ligament injury: a systematic review. *Am J Sports Med* 2009;37(7):1434–43.
5. Dirschl DR, Marsh JL, Buckwalter JA, Gelberman R, Olson SA, Brown TD, et al. Articular fractures. *J Am Acad Orthop Surg* 2004;12(6):416–23.
6. Marsh JL, Buckwalter J, Gelberman R, Dirschl D, Olson S, Brown T, et al. Articular fractures: does an anatomic reduction really change the result? *J Bone Joint Surg Am* 2002;84-A(7):1259–71.
7. Brown TD, Johnston RC, Saltzman CL, Marsh JL, Buckwalter JA. Posttraumatic osteoarthritis: a first estimate of incidence, prevalence, and burden of disease. *J Orthop Trauma* 2006;20(10):739–44.
8. Chateaubert J, Pritzker KP, Kessler MJ, Gryn timer MD. Spontaneous osteoarthritis in rhesus macaques. I. Chemical and biochemical studies. *J Rheumatol* 1989;16(8):1098–104.
9. Chateaubert JM, Gryn timer MD, Kessler MJ, Pritzker KP. Spontaneous osteoarthritis in rhesus macaques. II. Characterization of disease and morphometric studies. *J Rheumatol* 1990;17(1):73–83.
10. Das-Gupta EP, Lyons TJ, Hoyland JA, Lawton DM, Freemont AJ. New histological observations in spontaneously developing osteoarthritis in the STR/ORT mouse questioning its acceptability as a model of human osteoarthritis. *Int J Exp Pathol* 1993;74(6):627–34.
11. Jimenez PA, Glasson SS, Trubetskoy OV, Haimen HB. Spontaneous osteoarthritis in Dunkin Hartley guinea pigs: histologic, radiologic, and biochemical changes. *Lab Anim Sci* 1997;47(6):598–601.

12. Little CB, Smith MM. Animal models of osteoarthritis. *Curr Rheumatol Rev* 2008;4:175–82.
13. Ward BD, Furman BD, Huebner JL, Kraus VB, Guilak F, Olson SA. Absence of posttraumatic arthritis following intraarticular fracture in the MRL/MpJ mouse. *Arthritis Rheum* 2008;58(3):744–53.
14. Fitzgerald J, Rich C, Burkhardt D, Allen J, Herzka AS, Little CB. Evidence for articular cartilage regeneration in MRL/MpJ mice. *Osteoarthritis Cartilage* 2008;16(11):1319–26.
15. Zhou J, Chen Q, Lanske B, Fleming BC, Terek R, Wei X, et al. Disrupting the Indian hedgehog signaling pathway in vivo attenuates surgically induced osteoarthritis progression in Col2a1-CreERT2; Ihhf1/fl mice. *Arthritis Res Ther* 2014;16(1):R11.
16. Roudier M, Li X, Niu QT, Pacheco E, Pretorius JK, Graham K, et al. Sclerostin is expressed in articular cartilage but loss or inhibition does not affect cartilage remodeling during aging or following mechanical injury. *Arthritis Rheum* 2013;65(3):721–31.
17. Lodewyckx L, Luyten FP, Lories RJ. Genetic deletion of low-density lipoprotein receptor-related protein 5 increases cartilage degradation in instability-induced osteoarthritis. *Rheumatology (Oxford)* 2012;51(11):1973–8.
18. Hashimoto S, Rai MF, Janiszak KL, Cheverud JM, Sandell LJ. Cartilage and bone changes during development of post-traumatic osteoarthritis in selected LGXSM recombinant inbred mice. *Osteoarthritis Cartilage* 2012;20(6):562–71.
19. Malfait AM, Ritchie J, Gil AS, Austin JS, Hartke J, Qin W, et al. ADAMTS-5 deficient mice do not develop mechanical allodynia associated with osteoarthritis following medial meniscal destabilization. *Osteoarthritis Cartilage* 2010;18(4):572–80.
20. Chu CR, Szczodry M, Bruno S. Animal models for cartilage regeneration and repair. *Tissue Eng Part B Rev* 2010;16(1):105–15.
21. Pond MJ, Nuki G. Experimentally-induced osteoarthritis in the dog. *Ann Rheum Dis* 1973;32(4):387–8.
22. Brandt KD, Braunstein EM, Visco DM, O'Connor B, Heck D, Albrecht M. Anterior (cranial) cruciate ligament transection in the dog: a bona fide model of osteoarthritis, not merely of cartilage injury and repair. *J Rheumatol* 1991;18(3):436–46.
23. Marshall KW, Chan AD. Arthroscopic anterior cruciate ligament transection induces canine osteoarthritis. *J Rheumatol* 1996;23(2):338–43.
24. Guilak F, Ratcliffe A, Lane N, Rosenwasser MP, Mow VC. Mechanical and biochemical changes in the superficial zone of articular cartilage in canine experimental osteoarthritis. *J Orthop Res* 1994;12(4):474–84.
25. Palmoski MJ, Brandt KD. Immobilization of the knee prevents osteoarthritis after anterior cruciate ligament transection. *Arthritis Rheum* 1982;25(10):1201–8.
26. Palmoski MJ, Brandt KD. Proteoglycan aggregation in injured articular cartilage. A comparison of healing lacerated cartilage with osteoarthritic cartilage. *J Rheumatol* 1982;9(2):189–97.
27. Hayami T, Pickarski M, Wesolowski GA, McLane J, Bone A, Destefano J, et al. The role of subchondral bone remodeling in osteoarthritis: reduction of cartilage degeneration and prevention of osteophyte formation by alendronate in the rat anterior cruciate ligament transection model. *Arthritis Rheum* 2004;50(4):1193–206.
28. Chou MC, Tsai PH, Huang GS, Lee HS, Lee CH, Lin MH, et al. Correlation between the MR T2 value at 4.7 T and relative water content in articular cartilage in experimental osteoarthritis induced by ACL transection. *Osteoarthritis Cartilage* 2009;17(4):441–7.
29. Williams JM, Felten DL, Peterson RG, O'Connor BL. Effects of surgically induced instability on rat knee articular cartilage. *J Anat* 1982;134(Pt 1):103–9.
30. Batiste DL, Kirkley A, Laverty S, Thain LM, Spouge AR, Holdsworth DW. Ex vivo characterization of articular cartilage and bone lesions in a rabbit ACL transection model of osteoarthritis using MRI and micro-CT. *Osteoarthritis Cartilage* 2004;12(12):986–96.
31. Tiralloche G, Girard C, Chouinard L, Sampalis J, Moquin L, Ionescu M, et al. Effect of oral glucosamine on cartilage degradation in a rabbit model of osteoarthritis. *Arthritis Rheum* 2005;52(4):1118–28.
32. Messner K, Gillquist J, Bjornsson S, Lohmander LS. Proteoglycan fragments in rabbit joint fluid correlated to arthrosis stage. *Acta Orthop Scand* 1993;64(3):312–6.
33. Boyd SK, Muller R, Leonard T, Herzog W. Long-term peri-articular bone adaptation in a feline knee injury model for post-traumatic experimental osteoarthritis. *Osteoarthritis Cartilage* 2005;13(3):235–42.
34. Herzog W, Adams ME, Matyas JR, Brooks JG. Hindlimb loading, morphology and biochemistry of articular cartilage in the ACL-deficient cat knee. *Osteoarthritis Cartilage* 1993;1(4):243–51.
35. Teeple E, Elsaid KA, Fleming BC, Jay GD, Aslani K, Crisco JJ, et al. Coefficients of friction, lubricin, and cartilage damage in the anterior cruciate ligament-deficient guinea pig knee. *J Orthop Res* 2008;26(2):231–7.
36. Jimenez PA, Harlan PM, Chavarria AE, Haimes HB. Induction of osteoarthritis in guinea pigs by transection of the anterior cruciate ligament: radiographic and histopathological changes. *Inflamm Res* 1995;44(Suppl 2):S129–30.
37. Funakoshi Y, Hariu M, Tapper JE, Marchuk LL, Shrive NG, Kanaya F, et al. Periarticular ligament changes following ACL/MCL transection in an ovine stifle joint model of osteoarthritis. *J Orthop Res* 2007;25(8):997–1006.
38. Glasson SS, Blanchet TJ, Morris EA. The surgical destabilization of the medial meniscus (DMM) model of osteoarthritis in the 129/SvEv mouse. *Osteoarthritis Cartilage* 2007;15(9):1061–9.
39. Kamekura S, Hoshi K, Shimoaka T, Chung U, Chikuda H, Yamada T, et al. Osteoarthritis development in novel experimental mouse models induced by knee joint instability. *Osteoarthritis Cartilage* 2005;13(7):632–41.
40. Shapiro F, Glimcher MJ. Induction of osteoarthrosis in the rabbit knee joint. *Clin Orthop Relat Res* 1980;(147):287–95.
41. Meacock SC, Bodmer JL, Billingham ME. Experimental osteoarthritis in guinea-pigs. *J Exp Pathol (Oxford)* 1990;71(2):279–93.
42. Armstrong SJ, Read RA, Ghosh P, Wilson DM. Moderate exercise exacerbates the osteoarthritic lesions produced in cartilage by meniscectomy: a morphological study. *Osteoarthritis Cartilage* 1993;1(2):89–96.
43. Pastoureau P, Leduc S, Chomel A, De Ceuninck F. Quantitative assessment of articular cartilage and subchondral bone histology in the meniscectomized guinea pig model of osteoarthritis. *Osteoarthritis Cartilage* 2003;11(6):412–23.
44. Wancket LM, Baragi V, Bove S, Kilgore K, Korytko PJ, Guzman RE. Anatomical localization of cartilage degradation markers in a surgically induced rat osteoarthritis model. *Toxicol Pathol* 2005;33(4):484–9.
45. Karahan S, Kincaid SA, Kammermann JR, Wright JC. Evaluation of the rat stifle joint after transection of the cranial cruciate ligament and partial medial meniscectomy. *Comp Med* 2001;51(6):504–12.
46. Jones MD, Tran CW, Li G, Maksymowych WP, Zernicke RF, Doschak MR. In vivo microfocal computed tomography and micro-magnetic resonance imaging evaluation of

- antiresorptive and antiinflammatory drugs as preventive treatments of osteoarthritis in the rat. *Arthritis Rheum* 2010;62(9):2726–35.
47. Ma HL, Blanchet TJ, Peluso D, Hopkins B, Morris EA, Glasson SS. Osteoarthritis severity is sex dependent in a surgical mouse model. *Osteoarthritis Cartilage* 2007;15(6):695–700.
  48. Yang S, Kim J, Ryu JH, Oh H, Chun CH, Kim BJ, et al. Hypoxia-inducible factor-2alpha is a catabolic regulator of osteoarthritic cartilage destruction. *Nat Med* 2010;16(6):687–93.
  49. Moodie JP, Stok KS, Muller R, Vincent TL, Shefelbine SJ. Multimodal imaging demonstrates concomitant changes in bone and cartilage after destabilisation of the medial meniscus and increased joint laxity. *Osteoarthritis Cartilage* 2011;19(2):163–70.
  50. Li J, Anemaet W, Diaz MA, Buchanan S, Tortorella M, Malfait AM, et al. Knockout of ADAMTS5 does not eliminate cartilage aggrecanase activity but abrogates joint fibrosis and promotes cartilage aggrecan deposition in murine osteoarthritis models. *J Orthop Res* 2011;29(4):516–22.
  51. Marcelon G, Cros J, Guiraud R. Activity of anti-inflammatory drugs on an experimental model of osteoarthritis. *Agents Actions* 1976;6(1–3):191–4.
  52. Inoue S, Glimcher MJ. The reaction of cartilage and osteophyte formation after the intraarticular injection of papain. *Nihon Seikeigeka Gakkai Zasshi* 1982;56(5):415–30.
  53. van der Kraan PM, Vitters EL, van de Putte LB, van den Berg WB. Development of osteoarthritic lesions in mice by “metabolic” and “mechanical” alterations in the knee joints. *Am J Pathol* 1989;135(6):1001–14.
  54. van der Kraan PM, Vitters EL, van Beuningen HM, van de Putte LB, van den Berg WB. Degenerative knee joint lesions in mice after a single intra-articular collagenase injection. A new model of osteoarthritis. *J Exp Pathol (Oxford)* 1990;71(1):19–31.
  55. Borella L, Eng CP, DiJoseph J, Wells C, Ward J, Caccese R, et al. Rapid induction of early osteoarthritic-like lesions in the rabbit knee by continuous intra-articular infusion of mammalian collagenase or interleukin-1. *Agents Actions* 1991;34(1–2):220–2.
  56. van Osch GJ, van der Kraan PM, Vitters EL, Blankevoort L, van den Berg WB. Induction of osteoarthritis by intra-articular injection of collagenase in mice. Strain and sex related differences. *Osteoarthritis Cartilage* 1993;1(3):171–7.
  57. Hui W, Rowan AD, Richards CD, Cawston TE. Oncostatin M in combination with tumor necrosis factor alpha induces cartilage damage and matrix metalloproteinase expression in vitro and in vivo. *Arthritis Rheum* 2003;48(12):3404–18.
  58. Malfait AM, Tortorella M, Thompson J, Hills R, Meyer DM, Jaffee BD, et al. Intra-articular injection of tumor necrosis factor-alpha in the rat: an acute and reversible in vivo model of cartilage proteoglycan degradation. *Osteoarthritis Cartilage* 2009;17(5):627–35.
  59. van Beuningen HM, van der Kraan PM, Arntz OJ, van den Berg WB. Transforming growth factor-beta 1 stimulates articular chondrocyte proteoglycan synthesis and induces osteophyte formation in the murine knee joint. *Lab Invest* 1994;71(2):279–90.
  60. van Beuningen HM, Glansbeek HL, van der Kraan PM, van den Berg WB. Osteoarthritis-like changes in the murine knee joint resulting from intra-articular transforming growth factor-beta injections. *Osteoarthritis Cartilage* 2000;8(1):25–33.
  61. van Beuningen HM, Arntz OJ, van den Berg WB. In vivo effects of interleukin-1 on articular cartilage. Prolongation of proteoglycan metabolic disturbances in old mice. *Arthritis Rheum* 1991;34(5):606–15.
  62. Dunham J, Hoedt-Schmidt S, Kalbhen DA. Prolonged effect of iodoacetate on articular cartilage and its modification by an anti-rheumatic drug. *Int J Exp Pathol* 1993;74(3):283–9.
  63. van Osch GJ, van der Kraan PM, van den Berg WB. Site-specific cartilage changes in murine degenerative knee joint disease induced by iodoacetate and collagenase. *J Orthop Res* 1994;12(2):168–75.
  64. Guingamp C, Gegout-Pottier P, Philippe L, Terlain B, Netter P, Gillet P. Mono-iodoacetate-induced experimental osteoarthritis: a dose-response study of loss of mobility, morphology, and biochemistry. *Arthritis Rheum* 1997;40(9):1670–9.
  65. Frankl U, Pogrund H, Yosipovitch Z. The effect of intra-articular colchicine on the knee joint of the rat. *Clin Orthop Relat Res* 1983;(178):270–5.
  66. Furman BD, Strand J, Hembree WC, Ward BD, Guilak F, Olson SA. Joint degeneration following closed intraarticular fracture in the mouse knee: a model of posttraumatic arthritis. *J Orthop Res* 2007;25(5):578–92.
  67. Lewis JS, Hembree WC, Furman BD, Tippetts L, Cattel D, Huebner JL, et al. Acute joint pathology and synovial inflammation is associated with increased intra-articular fracture severity in the mouse knee. *Osteoarthritis Cartilage* 2011;19(7):864–73.
  68. Lewis Jr JS, Furman BD, Zeitler E, Huebner JL, Kraus VB, Guilak F, et al. Genetic and cellular evidence of decreased inflammation associated with reduced incidence of post-traumatic arthritis in MRL/MpJ mice. *Arthritis Rheum* 2013;65(3):660–70.
  69. Seifer DR, Furman BD, Guilak F, Olson SA, Brooks 3rd SC, Kraus VB. Novel synovial fluid recovery method allows for quantification of a marker of arthritis in mice. *Osteoarthritis Cartilage* 2008;16(12):1532–8.
  70. Louer CR, Furman BD, Huebner JL, Kraus VB, Olson SA, Guilak F. Diet-induced obesity significantly increases the severity of posttraumatic arthritis in mice. *Arthritis Rheum* 2012;64(10):3220–30.
  71. Diekman BO, Wu CL, Louer CR, Furman BD, Huebner JL, Kraus VB, et al. Intra-articular delivery of purified mesenchymal stem cells from C57BL/6 or MRL/MpJ superhealer mice prevents posttraumatic arthritis. *Cell Transplant* 2013;22(8):1395–408.
  72. Kimmerling KA, Furman BD, Mangiapani DS, Moverman MA, Sinclair SM, Huebner JL, et al. Sustained intra-articular delivery of IL-1Ra from a thermally-responsive elastin-like polypeptide as a therapy for post-traumatic arthritis. *Eur Cell Mater* 2015;29:124–39.
  73. Furman BD, Mangiapani DS, Zeitler E, Bailey KN, Horne PH, Huebner JL, et al. Targeting pro-inflammatory cytokines following joint injury: acute intra-articular inhibition of interleukin-1 following knee injury prevents post-traumatic arthritis. *Arthritis Res Ther* 2014;16(3):R134.
  74. De Souza RL, Matsuura M, Eckstein F, Rawlinson SC, Lanyon LE, Pitsillides AA. Non-invasive axial loading of mouse tibiae increases cortical bone formation and modifies trabecular organization: a new model to study cortical and cancellous compartments in a single loaded element. *Bone* 2005;37(6):810–8.
  75. Brodt MD, Silva MJ. Aged mice have enhanced endocortical response and normal periosteal response compared to young-adult mice following 1 week of axial tibial compression. *J Bone Miner Res* 2010;25(9):2006–15.
  76. Lynch ME, Main RP, Xu Q, Walsh DJ, Schaffler MB, Wright TM, et al. Cancellous bone adaptation to tibial compression is not sex dependent in growing mice. *J Appl Physiol* 2010;109(3):685–91.

77. Zaman G, Jessop HL, Muzylak M, De Souza RL, Pitsillides AA, Price JS, et al. Osteocytes use estrogen receptor alpha to respond to strain but their ERalpha content is regulated by estrogen. *J Bone Miner Res* 2006;21(8):1297–306.
78. De Souza RL, Pitsillides AA, Lanyon LE, Skerry TM, Chenu C. Sympathetic nervous system does not mediate the load-induced cortical new bone formation. *J Bone Miner Res* 2005;20(12):2159–68.
79. Poulet B, Hamilton RW, Shefelbine S, Pitsillides AA. Characterising a novel and adjustable non-invasive murine knee joint loading model. *Arthritis Rheum* 2011;63(1):137–47.
80. Poulet B, Westerhof TA, Hamilton RW, Shefelbine SJ, Pitsillides AA. Spontaneous osteoarthritis in Str/ort mice is unlikely due to greater vulnerability to mechanical trauma. *Osteoarthritis Cartilage* 2013;21(5):756–63.
81. Poulet B, de Souza R, Kent AV, Saxon L, Barker O, Wilson A, et al. Intermittent applied mechanical loading induces subchondral bone thickening that may be intensified locally by contiguous articular cartilage lesions. *Osteoarthritis Cartilage* 2015;23(6):940–8.
82. Ko FC, Dragomir C, Plumb DA, Goldring SR, Wright TM, Goldring MB, et al. In vivo cyclic compression causes cartilage degeneration and subchondral bone changes in mouse tibiae. *Arthritis Rheum* 2013;65(6):1569–78.
83. Wu P, Holguin N, Silva MJ, Fu M, Liao W, Sandell LJ. Early response of mouse joint tissues to noninvasive knee injury suggests treatment targets. *Arthritis Rheumatol* 2014;66(5):1256–65.
84. Wu P, DeLassus E, Patra D, Liao W, Sandell LJ. Effects of serum and compressive loading on the cartilage matrix synthesis and spatiotemporal deposition around chondrocytes in 3D culture. *Tissue Eng Part A* 2013;19(9–10):1199–208.
85. Wong M, Siegrist M, Cao X. Cyclic compression of articular cartilage explants is associated with progressive consolidation and altered expression pattern of extracellular matrix proteins. *Matrix Biol* 1999;18(4):391–9.
86. Carames B, Taniguchi N, Seino D, Blanco FJ, D'Lima D, Lotz M. Mechanical injury suppresses autophagy regulators and pharmacologic activation of autophagy results in chondroprotection. *Arthritis Rheum* 2012;64(4):1182–92.
87. Christiansen BA, Anderson MJ, Lee CA, Williams JC, Yik JH, Haudenschild DR. Musculoskeletal changes following non-invasive knee injury using a novel mouse model of post-traumatic osteoarthritis. *Osteoarthritis Cartilage* 2012;20(7):773–82.
88. Killian ML, Isaac DI, Haut RC, DeJardin LM, Leetun D, Donahue TL. Traumatic anterior cruciate ligament tear and its implications on meniscal degradation: a preliminary novel lapine osteoarthritis model. *J Surg Res* 2010;164(2):234–41.
89. Lockwood KA, Chu BT, Anderson MJ, Haudenschild DR, Christiansen BA. Comparison of loading rate-dependent injury modes in a murine model of post-traumatic osteoarthritis. *J Orthop Res* 2013;32(1):79–88.
90. Crowninshield RD, Pope MH. The strength and failure characteristics of rat medial collateral ligaments. *J Trauma* 1976;16(2):99–105.
91. Noyes FR, DeLucas JL, Torvik PJ. Biomechanics of anterior cruciate ligament failure: an analysis of strain-rate sensitivity and mechanisms of failure in primates. *J Bone Joint Surg Am* 1974;56(2):236–53.
92. Onur TS, Wu R, Chu S, Chang W, Kim HT, Dang AB. Joint instability and cartilage compression in a mouse model of posttraumatic osteoarthritis. *J Orthop Res* 2014;32(2):318–23.
93. van Osch GJ, Blankevoort L, van der Kraan PM, Janssen B, Hekman E, Huijskes R, et al. Laxity characteristics of normal and pathological murine knee joints in vitro. *J Orthop Res* 1995;13(5):783–91.
94. Pottenger LA, Phillips FM, Draganich LF. The effect of marginal osteophytes on reduction of varus-valgus instability in osteoarthritic knees. *Arthritis Rheum* 1990;33(6):853–8.
95. Suzuki T, Motojima S, Saito S, Ishii T, Ryu K, Ryu J, et al. Osteoarthritis of the patella, lateral femoral condyle and posterior medial femoral condyle correlate with range of motion. *Knee Surg Sports Traumatol Arthrosc* 2013;21(11):2584–9.
96. Satkunanthan PB, Anderson MJ, De Jesus NM, Haudenschild DR, Ripplinger CM, Christiansen BA. In vivo fluorescence reflectance imaging of protease activity in a mouse model of post-traumatic osteoarthritis. *Osteoarthritis Cartilage* 2014;22(10):1461–9.
97. Holguin N, Brodt MD, Sanchez ME, Kotiya AA, Silva MJ. Adaptation of tibial structure and strength to axial compression depends on loading history in both C57BL/6 and BALB/c mice. *Calcif Tissue Int* 2013;93(3):211–21.
98. Christiansen B, Emami A, Fyhrie D, Satkunanthan PB, Hardisty M. Trabecular bone loss at a distant skeletal site following non-invasive knee injury in mice. *J Biomech Eng* 2014;137(1).
99. Anderson DD, Chubinskaya S, Guilak F, Martin JA, Oegema TR, Olson SA, et al. Post-traumatic osteoarthritis: Improved understanding and opportunities for early intervention. *J Orthop Res* 2011;29(6):802–9.

Closed Joint ACL Disruption  
Murine Model of PTA

1  
2

7

Blaine A. Christiansen, Jasper H.N. Yik,  
and Dominik R. Haudenschild

3  
4

[AU1]

Introduction

Despite decades of effort and billions of dollars spent trying to cure established OA, the disease remains incurable. Because joint injuries and mechanical instability are widely thought to be the initiating events and underlying cause of many OA cases, current research has moved towards identifying intervention strategies after injury to prevent future OA. Given the powerful genetic information and relatively low expense of mice as experimental animals, there has been considerable effort to establish mouse models of OA that mimic aspects of the original joint injury and the subsequent degenerative changes observed in clinical OA progression. This chapter is focused on a recently developed OA model in

mice consisting of nonsurgical ACL rupture and briefly summarizes other mouse OA models to provide an appropriate context [1–7].

Historical Context

The earliest mouse models of induced OA used chemical forms of injury to the stifle (knee) joint, such as injection of iodoacetate or degradative enzymes such as collagenase. These approaches cause cell death and matrix degeneration through non-physiological means that clearly do not mimic the initiating events in clinical PTOA. However, once joint damage is established, there are aspects of the OA progression and further joint degeneration that correlate with what is seen clinically in PTOA. A review of ACL transection models of PTA is covered in Chap. 10.

The first noninvasive mouse model of induced posttraumatic osteoarthritis was described by Furman et al., in which they created an intra-articular fracture (IAF) of the proximal tibia in male mice [8]. The injury response included many aspects seen clinically with intra-articular fractures, including callus formation and subchondral bone thickening. Changes in the cartilage observed by histology indicated degeneration and progression toward terminal OA, including cartilage surface fibrillation, progressive proteoglycan loss, and finally exposure of subchondral bone at 50 weeks [8]. In this model, the extent of joint damage is somewhat adjustable by limiting

B.A. Christiansen, Ph.D. (✉)  
Department of Orthopaedic Surgery, University of California Davis, Research Building 1, Suite 2000, 4635 Second Avenue, Sacramento, CA, USA  
e-mail: [bchristiansen@ucdavis.edu](mailto:bchristiansen@ucdavis.edu)

J.H.N. Yik, Ph.D.  
University of California Davis, Research Building 1, Suite 2000, 4635 Second Avenue, Sacramento, CA, USA  
e-mail: [jyik@ucdavis.edu](mailto:jyik@ucdavis.edu)

D.R. Haudenschild, Ph.D.  
Department of Orthopaedic Surgery, University of California Davis, Research Building 1, Room 3004, 4635 Second Avenue, Sacramento, CA, USA  
e-mail: [drhaudenschild@ucdavis.edu](mailto:drhaudenschild@ucdavis.edu)

the maximum displacement of the indenter used to create the injury, and increasing joint damage at the time of injury creates more severe OA. The model has been extensively characterized and used to study aspects of PTOA pathogenesis from obesity to MSCs to inflammation to measurement of OA biomarkers like such as Cartilage Oligomeric Matrix Protein (COMP) [9–14]. The model is generally considered especially relevant for clinical studies of very high impact joint injuries with accompanying bone fracture.

A more recent noninvasive model of joint injury uses a method similar to that used by bone biologists to study the bone adaptation mechanical loading. These models replicate the loading seen by bone during walking or running, and typically many cycles of loading are applied to the mouse tibia through the ankle and knee joints. The first description of this setup to study mouse PTOA was by Blandine Poulet et al. in 2011 [15]. In this study, episodes of multiple axial compressions to 9 N were applied repeatedly three times weekly for up to 5 weeks. Non-progressing articular cartilage lesions were observed histologically with a single loading episode, and multiple loading episodes induced progressive changes consistent with PTOA. Osteophytes were observed in over half the mice receiving 2 weeks of loading episodes, and more consistently in mice loaded for 5 weeks. Ko et al. used a similar cyclical tibial loading setup to study PTOA in young and adult mice [16]. In this setup, loading consisted of 1,200 cycles/day at 4 Hz and either 4.5 N or 9 N, applied 5 days/week, for between 1 and 6 weeks. At the higher loads, mice developed osteophytes, and mice loaded for the longer times and/or at the higher loads showed signs of histological OA including cartilage thinning, loss of proteoglycan, and changes in subchondral bone quantified by microCT. A repetitive loading model was used by Onur et al. in 2014, to load joints up to 12 N for up to 240 cycles or until ACL rupture occurred [17]. A similar repetitive loading model was also used by Wu et al. in 2014 [18], who applied 60 cycles of loading to 3, 6, or 9 N. All loading regimens induced chondrocyte apoptosis, cartilage matrix degradation, and increased serum levels of OA biomarker COMP.

Higher loads initiated greater synovitis, and the highest load disrupted the ACL and initiated severe synovitis and ectopic cartilage formation. These models of joint injury are likely to be milder than the intra-articular fracture PTOA model described in the previous paragraph, although the relevance to the human clinical situation may not be as easy to interpret due to the multiple cycles of loading.

## Initiation of ACL Rupture Injury by a Single Mechanical Overload

The first noninvasive mouse model of ACL rupture was characterized by our group in 2012 [19]. In this model, knee injury is created using a single cycle of fibial compression, also with instrumentation adapted from studies of bone adaptation to tibial compression. The compression system consists of two loading platens machined out of aluminum and fixed to an electromagnetic materials testing instrument (Bose ElectroForce 3200) (Fig. 7.1a). The top platen is designed to hold the ankle flexed at approximately 30° (Fig. 7.1b). The bottom platen is designed to hold the flexed knee in a shallow cup with an indentation to accommodate the femur and upper leg (Fig. 7.1c). The top and bottom platen are aligned vertically to transmit force through the long axis of the tibia. The setup further includes a Teflon platform, on which the anesthetized mouse rests, an inhalation tube for continued administration of isoflurane anesthetic, and a load cell underneath the bottom platen.

Mice are anesthetized using isoflurane and then placed onto the loading device with continued administration of isoflurane anesthesia, as shown in Fig. 7.1a. The right ankle and knee are placed into the upper and lower platens, and a pre-load of 0.5–1.5 N is applied to hold the leg in place. To create the ACL rupture injury, the upper platen is lowered to a target axial compressive load of 12 N, or a target displacement of 1.7 mm, depending on the type of ACL disruption desired (discussed in detail below). The axial loading causes a transient anterior subluxation of the tibia relative to the distal femur, in effect moving the

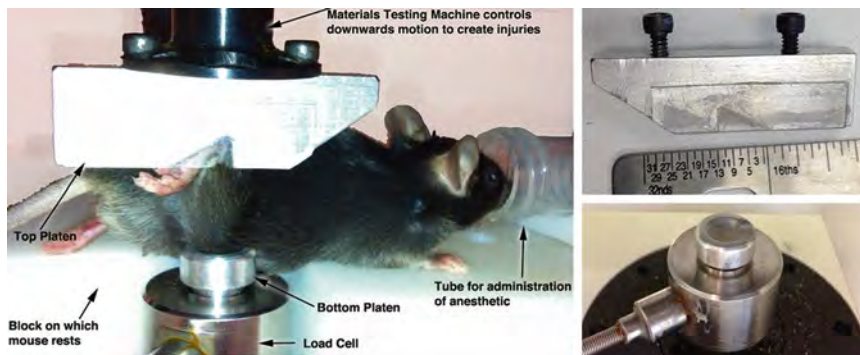


**Fig. 7.1** *Left:* Setup to initiate ACL rupture injuries, consisting of custom platens designed to hold the knee and ankle joints, a load cell, and a tube for administering anesthesia, assembled on an electromagnetic materials testing instrument (Bose ElectroForce 3200). *Top right:* Close-up

of the top platen showing a ruler calibrated in inches. *Bottom right:* Close-up of the bottom platen showing a shallow cup to hold the knee, with a groove on one side to accommodate the thigh

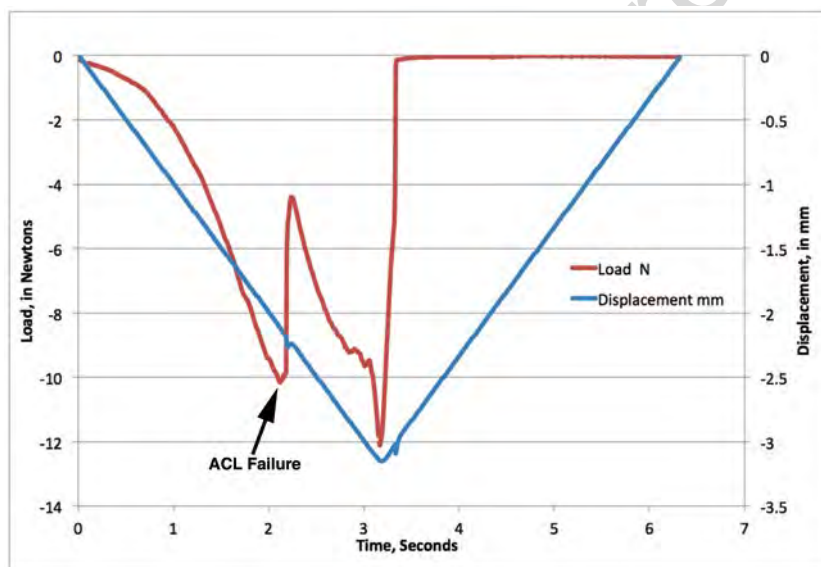


**Fig. 7.2** Typical loading profile to initiate ACL rupture by avulsion fracture. The *blue line* indicates displacement of the top platen that holds the ankle, and shows a slow constant movement from 0 mm down to -3 mm, and back to 0 mm. The *red line* is the readout from the load

cell under the knee. It shows that as the ankle is pushed downwards, there is a steady increase in load until just over 10 N, at which point the rapid release of compressive force (shown by the *arrow*) indicates disruption of the ACL

tibia in the direction that the anterior cruciate ligament stabilizes. A release of compressive force indicates failure of the ACL, which reproducibly occurs at 8–11 N compressive load for most mice (Fig. 7.2). After the target of 12 N or 1.7 mm is reached, the platen is returned to its initial position and the knee joint is restored to its

native orientation. The entire procedure takes less than 5 min including anesthetization, with tibial compression loading requiring only about 6 s, with injury typically occurring after about 2 s (Fig. 7.2). Mice are removed from the setup gently and given a dose of analgesic while still anesthetized. To date, all animals have survived the

injury with no fractures to the long bones, and they are typically mobile soon after recovering from anesthesia and show only very mild, if any, changes in appetite, behavior, or activity.

## Immediate Assessment of Injury

Experienced orthopedic surgeons that were blinded to the injury status assessed the immediate effect of injury semiquantitatively. All injured knees were correctly identified as injured, but one (of 5) uninjured was also identified as injured. The most commonly observed indicators of joint injury were increased anterior/posterior translation and external rotation of the knee, with some minor swelling and hemarthrosis [19]. Based on the extent and the type of laxity observed, the damage to the joint was considered consistent with ACL rupture, but not indicative of damage to either the medial or collateral ligaments. Analysis by either standard or contrast-enhanced microCT imaging confirmed that ACL rupture was present in all injured knees that were imaged [19, 20]. Damage to other joint structures such as the PCL, meniscus, patella, collateral ligaments, was not obvious by high-resolution contrast-enhanced microCT [20].

The mode of ACL rupture depends on the rate of axial compression [20]. A relatively slow compression rate of 1 mm/s causes ACL disruption with an avulsion fracture, in which the ACL is disrupted at the site of insertion into bone, and pulls a segment of bone usually from the posterior femur into the joint cavity. Clinically, ACL injuries with an avulsion fracture are more common in children than in adults. A much faster loading rate of 500 mm/s causes a midsubstance disruption of the ligament with no evidence by microCT of an avulsion fracture. Clinically, midsubstance ACL tears are more common in adults. On a technical note, due to limitations in the software and data acquisition rates of the materials testing setup used in these studies, we used a target load of 12 N as a trigger to stop the injury only with the slow injury rate of 1 mm/s. In the fast injury rate (500 mm/s) it became necessary to use a displacement of 1.7 mm as a trigger to

stop compression because of overshoot of the target force. In both cases, the loads required to induce injury were very similar, ranging from 8 N to 11 N in the majority of animals. Another technical limitation of our software and hardware setup is that the downward motion of the upper platen is not programmed to stop automatically when the ACL rupture injury occurs. Although we would ideally like to experimentally control this aspect of the ACL rupture injury in our mouse model, it is not necessary to do so in order to mimic clinically relevant human ACL injuries. In our system, the downward motion continues until a trigger point of either 12 N or 1.7 mm is reached. In general, for most of the assays with which we measured injury response, the fast injury midsubstance ACL tears induced very similar but somewhat milder injury responses than the slow injury avulsion fractures.

## Serum Markers of OA Progression

Biomarkers of OA progression and bone remodeling can be measured from synovial fluid, blood, or urine, and are used as confirmatory measures of PTOA progression. Cartilage Oligomeric Matrix Protein is one of the more promising OA biomarkers, and serves as a marker of the earlier stages of OA in which cartilage is still present and cartilage turnover is elevated. We found that ACL rupture caused statistically significant increases in the serum levels of COMP within 1 day after injury, and COMP levels remained elevated at all time points until at least 8 weeks after injury (except the 4-week time point, which trended higher but not significantly) [19]. A serum marker of bone resorption (CTX-I) was significantly increased at 7 and 14, but not 56 days after ACL Rupture injury. At the same time points, a marker of bone formation (PINP) remained unchanged [21]. Together these results suggest that in the earlier stages after joint injury, ACL rupture-induced changes in bone turnover are primarily caused by changes in bone resorption rather than formation, and that elevated cartilage turnover occurs throughout the first 8 weeks after injury.

**Histological Assessment of OA Progression**

Histological assessment of joints injured by ACL rupture revealed deterioration of cartilage and osteoarthritic changes consistent with PTOA progression [19]. At the early time points, grading by a veterinary pathologist revealed that injury caused synovial hyperplasia, inflammation, and fibrosis. Cartilage damage was only mild at early time points (Fig. 7.3), but by 8 weeks significant loss of proteoglycan was observed. There was fissuring of the articular cartilage, frequent loss of the surface lamina and the flattened chondrocytes of the superficial zone, and atrophy of articular chondrocytes. Blinded histological grading of the 8-week sections revealed that injury caused significant increases in the OARSI score [22] at the medial tibia, medial femur, and lateral femur. No differences in OARSI scores were measured at the femoro-patellar joint or the underlying surface of the femur.

**Radiographic Assessment of Injury Response**

ACL rupture through avulsion fracture caused a rapid and substantial loss of subchondral trabecular bone volume very early after injury as measured by microCT. This trabecular bone loss became significant within 3 days after injury, and reached a maximum of approximately 40 % loss after 7 days compared to the contralateral uninjured knee. This initial remodeling phase was followed by a partial recovery of bone volume. At the 4- and 8-week time points after injury, a new but lower steady-state bone volume was reached that was approximately 80 % of the day 1 volume [19]. This lower bone volume was maintained out to 12 and 16 weeks [20]. The loss of subchondral bone volume was somewhat less severe in the midsection ACL rupture injury than in the ACL avulsion fracture (–20 % loss versus –31 % at day 10). However, this difference in bone turnover between the modes of ACL disruption

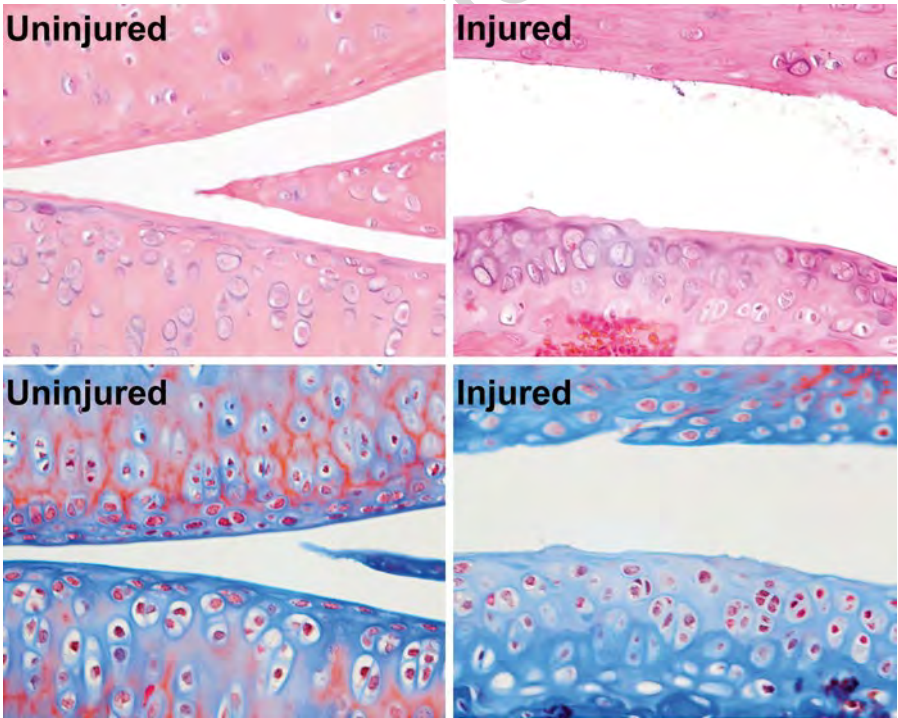


**Fig. 7.3** Histological assessment of cartilage damage at 8 weeks after injury, showing injury-induced loss of surface lamina and flattened superficial chondrocytes, fibrillations in the cartilage, and cluster formation in the middle or deep layers

was only seen at the early time points. The lower steady state bone volume reached at later time points was not statistically different between injuries created by midsection ACL rupture or ACL avulsion fracture.

We were somewhat surprised by the rate and extent of the early bone remodeling after the ACL rupture injury. Locally, a 40 % loss of subchondral trabecular bone after 7 days is a significant biological event, which alone may have consequences for the health of the joint over time. Bisphosphonates such as alendronate are specific inhibitors of osteoclast-mediated bone resorption. Given the substantial bone remodeling induced by the ACL rupture injuries, we tested whether treatment with alendronate would attenuate this response, with a secondary hypothesis that this may protect against cartilage degradation and osteoarthritis progression. We found that high doses of alendronate did prevent the short-term loss of subchondral trabecular bone volume, but did not inhibit the osteophyte formation at the later time points, or the cartilage degeneration induced by the ACL rupture injury [21].

Osteophyte formation is a hallmark of clinical OA. Osteophytes are newly formed fibrocartilage and bone growths that are prevalent at the peripheral margins of joints, and at the interface between cartilage and periosteum [23]. The ACL rupture injury models described here cause substantial nonnative new bone formation that is readily detectable within 10 days after injury, perhaps even earlier [20]. Much of this injury-induced new bone formation appears to be osteophyte formation, and thus the model reproduces aspects of clinical PTOA. In addition, a portion of the new bone formation may be enthesophytes, or new bone forming at the insertion sites of ligaments to the bone, specifically around the collateral ligaments (personal communication, Chris Little). To date we have not rigorously characterized the nonnative bone to differentiate whether it is primarily osteophytes or enthesophytes, but we suspect that both occur in response to the ACL rupture injuries. Interestingly, the milder midsection ACL tear injury tends to produce slightly greater nonnative bone volume at the later time points than ACL avulsion fractures, which is in

contrast to the generally milder response to the midsection tear. While the joint injuries caused an initial destabilization of the joint (as quantified [20] by anterior-posterior joint laxity), osteophyte formation appeared to correlate with a re-stabilization of the joint, albeit with a much reduced range of motion [20].

Sclerosis of the subchondral bone plate is also a hallmark of clinical OA. The sclerosis involves remodeling and hardening of the subchondral bone plate in early OA, often accompanied by an advancing tidemark of calcified cartilage, and decreased subchondral vascularity [23]. Analysis of the subchondral bone at the proximal tibia in our model of ACL rupture revealed that the injury induced a significant thickening of the subchondral bone plate [20], where we observed increases of 20–26 % in cortical thickness in both ACL midsection tear and avulsion fracture injuries at the 12- and 16-week time points. This is in contrast to the partial medial meniscectomy (PMM) surgical injury model, in which osteophyte formation and subchondral sclerosis was not seen by microCT scans until 20 weeks after surgery [24]. In our studies, all injured knees showed a similar extent of subchondral bone sclerosis, independent of whether the mode of ACL rupture was midsection tear or avulsion fracture.

In summary, the nonsurgical ACL rupture model includes many aspects of clinically relevant posttraumatic osteoarthritis. The immediate mechanical damage resulting from the ACL rupture injury is primarily limited to the ACL itself, which can occur through either midsection tear or avulsion fracture depending on the loading rate. The injury destabilizes the joint, and initiates a short-term biological response that includes mild inflammation, mild synovial hyperplasia, fibrosis, and a rapid remodeling of the subchondral trabecular bone. Longer-term outcomes include hallmarks of OA progression such as cartilage fibrillation, loss of superficial zone chondrocytes and cartilage proteoglycan content, subchondral bone sclerosis, and osteophyte formation. At the later time points joint stability is somewhat restored, perhaps because of the extensive osteophyte and ectopic bone formation, but the restored stability is at the expense of range of motion.

Additional Biological Response to ACL Rupture Injury

Having established that the ACL rupture injury model reproduces many aspects of clinical PTOA, we are pursuing additional characterization of the injury response. We placed specific emphasis on the very early time points, at which the native biological responses in other PTOA models may be masked by the injury method.

Gene Expression in Response to ACL Rupture Injury

Microarray gene expression analysis revealed that more than 500 genes are differentially regulated after 1 week in the injured knee compared to the uninjured contralateral knee of the same mouse. These genes included many with established roles in cartilage development, homeostasis or pathology, and a curated list is shown in Table 7.1. Analysis of molecular pathways induced by the ACL rupture injury was performed using Ingenuity Pathways Analysis. This revealed a significant involvement of pathways relevant to bone and cartilage turnover, as well as to osteoarthritis progression, shown in Table 7.2.

Table 7.1 Injury response genes at 7 days post-injury

Catabolic genes	Anabolic genes
ADAM12	Sox9
ADAMTS 1, 2, 3, 4, 12, 16	TGFβ 2, 3
MMP 2, 3, 7, 8, 14, 19, 23	Inhibin b-A, BMP-1
Calpain 6	Aggrecan, Cartilage link protein
	Collagens type 2, 3, 4, 5, 9, 10, 11, 13

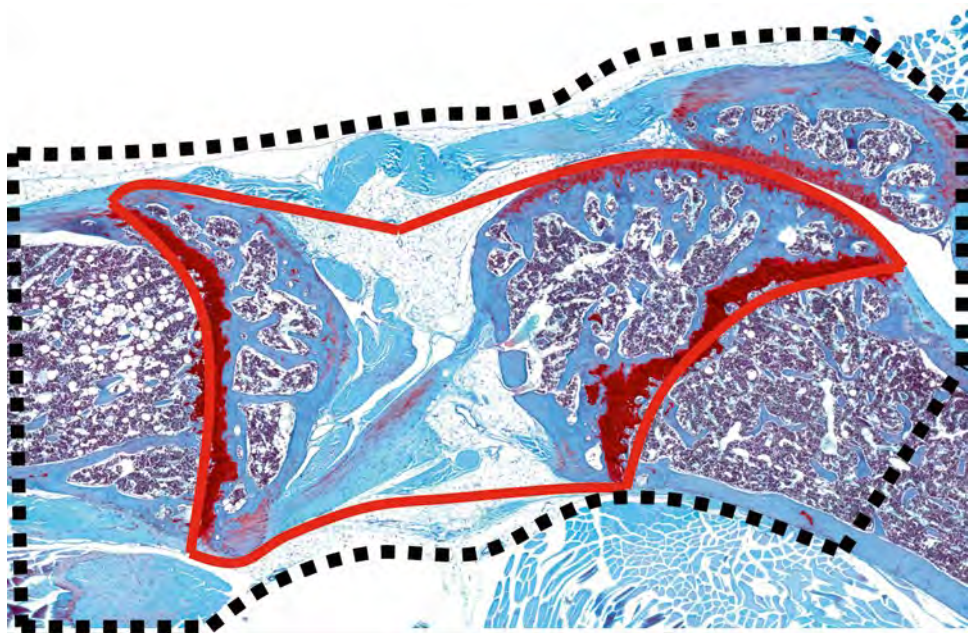
Curated list of the more than 500 genes with significantly different expression 1 week after ACL rupture injury. A total of 8 mice had the right legs injured, and the left legs served as uninjured contralateral controls. RNA was isolated after 1 week from all 16 joints, and cDNA from each joint was run on a separate Affymetrix microarray. Expression levels in the injured knee was normalized to the contralateral knee of the same mouse, and statistical comparisons were made to identify injury-induced genes that responded in all animals with a twofold cutoff and stringent filters for false-positives

The noninvasive initiation of the ACL rupture injury means that the acute biological response to the injury probably follows a relatively natural progression. We therefore examined the expression of several injury-response genes and inflammatory genes at the very early time points, minutes or hours after injury. Using careful microdissection of the joint, our first analysis was limited primarily to the tissues that were mechanically affected by the injury. This included the subchondral bone, cartilage, meniscus, ACL/PCL, but did not include synovium, patella, fat pads, or any other surrounding tissues (Fig. 7.4). In these samples we found a significant transient elevation of IL-6 mRNA expression within 2 h after injury. The magnitude of the response was quite large, on average over 40-fold greater mRNA expression in the injured knee than in the uninjured contralateral knee of the same mouse. The induction of IL-6 was transient, and levels returned to baseline after 6 h. When the patella, synovium, fat pad and the entire joint capsule were included in the analysis, IL-6 induction at 2 h was no longer significant, but a much larger peak of IL-6 mRNA induction (over 80-fold) was observed at 4 h. The response of the entire joint capsule was not only larger in magnitude, but also in the number of responding genes. For example, significant increases in IL-1b and MMP13 were also measured in the entire joint capsule at 4 h, but not in the tissues immediately affected by the injury. In all cases, the elevated gene expression returned to baseline by 6–8 h,

Table 7.2 Pathway analysis of injury response genes

Pathway	p-value
Focal adhesion	1.26E-08
Endochondral ossification	1.27E-08
Adipogenesis	3.32E-07
Matrix metalloproteinases	3.51E-05
Senescence and autophagy	6.16E-04
Wnt signaling pathway	0.0015
Inflammatory response pathway	0.0065
Osteoblast signaling	0.0140

Pathway analysis of injury response genes at 1 week after ACL rupture injury. Ingenuity pathways analysis revealed significant involvement of several pathways with known or suspected roles in osteoarthritis progression



IL-6

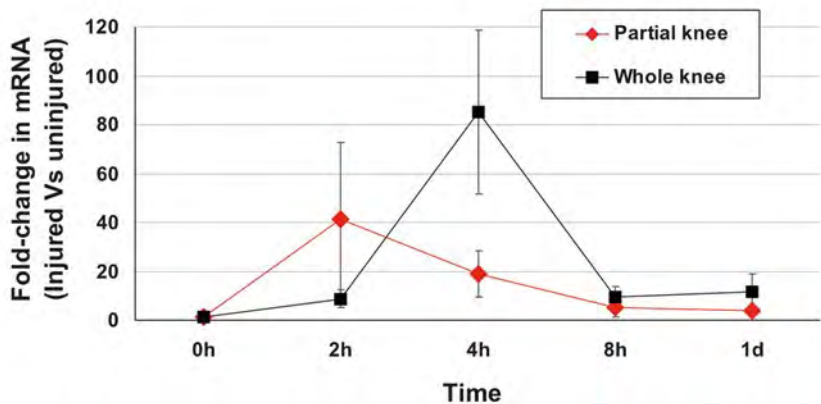


**Fig. 7.4** Acute response to ACL rupture injury: mRNA expression of injury response gene IL-6 was measured in the partial knee (*outlined in red*) and whole knee (*outlined in black*). The partial knee included primarily those tissues that were directly mechanically affected by the injury, including the cartilage, ligaments, meniscus, and subchondral trabecular bone. The whole knee included

the entire joint capsule, including the patella, patellar fat pad, and synovium. Gene expression analysis by real-time quantitative RT-PCR revealed that the partial knee responded within 2 h, and the whole knee responded with a delayed but much higher peak expression of IL-6 mRNA. The delayed response of the whole knee was larger in scope as well as magnitude (see text)

and remained at baseline at 24 h. From these observations, we are forming a model for understanding the biological response to joint injury, in which the tissues mechanically affected by the

injury exhibit an acute response very early (peaking within 2 h), which then elicits a slightly delayed response from the entire joint capsule that is larger in magnitude and in scope [25].

## Sex-Based Difference in Response to ACL Rupture Injury

Clinically, females account for almost two in three knee joint replacement surgeries. In the surgical DMM mouse model of joint injury, progression of OA is sex dependent, with differences in OA severity markedly greater in male mice as soon as 2 weeks after surgery [26]. In the DMM injury model, a protective role of female sex hormones was observed [26]. These observations in the DMM surgical model of PTOA are consistent with clinical findings of OA primarily in women, and of accelerated OA progression in postmenopausal women. To date we have not rigorously investigated the effect of sex on the injury response in our nonsurgical ACL rupture injury model. Using only a limited range of assays, we investigated sex-based differences in proteinase activity at early time points post-injury (using ProSense, MMPsense, and CatKsense in vivo imaging reagents), but while these assays demonstrated robust increases of in vivo proteinase activity upon injury in both sexes, and we found no differences between male and female mice. In the same study we examined terminal OA at 8 weeks by microCT and again found no significant differences in the injury-induced changes in bone between the sexes. Further investigation using histological analysis at intermediate time points needs to be performed to definitively establish whether there are sex-based differences in response to the nonsurgical ACL rupture injury model.

## Conclusion

Significant progress was made during the last decade in the development of mouse models for posttraumatic osteoarthritis. The surgical DMM model is the currently the most widely cited PTOA model. The DMM model and closed articular fracture models have contributed to many of the recent advances in our understanding of OA pathogenesis and progression. Newer noninvasive

models of PTOA represent another significant step forward, and are particularly useful for investigating the natural progression of biological processes at the very early time points after injury, which may be partially masked in more invasive models. Single impact noninvasive injury models such as the Intra-Articular Fracture model and our ACL rupture model may be more representative of clinically relevant human injuries, since the externally applied mechanical forces affect multiple joint tissues in a similar manner. The noninvasive single impact PTOA models have an additional advantage of being technically very simple to perform, and requiring much less time, than surgically induced PTOA. These new models approximate the human injuries more closely and may lead to novel insight into the biological and cellular responses to joint injury that are involved in OA initiation, which in turn holds promise for the development of more effective therapies and intervention strategies to reduce the tremendous burden of osteoarthritis.

## References

- Glasson SS, Askew R, Sheppard B, Carito B, Blanchet T, Ma HL, Flannery CR, Peluso D, Kanki K, Yang Z, Majumdar MK, Morris EA. Deletion of active ADAMTS5 prevents cartilage degradation in a murine model of osteoarthritis. *Nature*. 2005;434(7033):644–8.
- Glasson SS, Askew R, Sheppard B, Carito BA, Blanchet T, Ma HL, Flannery CR, Kanki K, Wang E, Peluso D, Yang Z, Majumdar MK, Morris EA. Characterization of and osteoarthritis susceptibility in ADAMTS-4-knockout mice. *Arthritis Rheum*. 2004;50(8):2547–58.
- Glasson SS, Blanchet TJ, Morris EA. The surgical destabilization of the medial meniscus (DMM) model of osteoarthritis in the 129/SvEv mouse. *Osteoarthritis Cartilage*. 2007;15(9):1061–9.
- Moilanen T, Sirkkola H, Vuolteenaho K, Moilanen E. A new model of experimental osteoarthritis by cruciate ligament transection in mouse knee. *Osteoarthritis Cartilage*. 2002;10(S55):S31.
- Kamekura S, Hoshi K, Shimoaka T, Chung U, Chikuda H, Yamada T, Uchida M, Ogata N, Seichi A, Nakamura K, Kawaguchi H. Osteoarthritis development in novel experimental mouse models induced by knee joint instability. *Osteoarthritis Cartilage*. 2005;13(7):632–41.

6. Clements KM, Price JS, Chambers MG, Visco DM, Poole AR, Mason RM. Gene deletion of either interleukin-1 $\beta$ , interleukin-1 $\beta$ -converting enzyme, inducible nitric oxide synthase, or stromelysin 1 accelerates the development of knee osteoarthritis in mice after surgical transection of the medial collateral ligament and partial medial meniscectomy. *Arthritis Rheum.* 2003;48(12):3452–63.
7. Eltawil NM, De Bari C, Achan P, Pitzalis C, Dell'Accio F. A novel in vivo murine model of cartilage regeneration. Age and strain-dependent outcome after joint surface injury. *Osteoarthritis Cartilage.* 2009;17(6):695–704. PMID: 2706394.
8. Furman BD, Strand J, Hembree WC, Ward BD, Guilak F, Olson SA. Joint degeneration following closed intraarticular fracture in the mouse knee: a model of posttraumatic arthritis. *J Orthop Res.* 2007;25(5):578–92.
9. Seifer DR, Furman BD, Guilak F, Olson SA, Brooks 3rd SC, Kraus VB. Novel synovial fluid recovery method allows for quantification of a marker of arthritis in mice. *Osteoarthritis Cartilage.* 2008;16(12):1532–8. PMID: 2602808.
10. Lewis JS, Hembree WC, Furman BD, Tippets L, Cattel D, Huebner JL, Little D, Defratre LE, Kraus VB, Guilak F, Olson SA. Acute joint pathology and synovial inflammation is associated with increased intra-articular fracture severity in the mouse knee. *Osteoarthritis Cartilage.* 2011;19(7):864–73.
11. Loefer CR, Furman BD, Huebner JL, Kraus VB, Olson SA, Guilak F. Diet-induced obesity significantly increases the severity of posttraumatic arthritis in mice. *Arthritis Rheum.* 2012;64(10):3220–30. PMID: 3426642.
12. Diekmann BO, Wu CL, Loefer CR, Furman BD, Huebner JL, Kraus VB, Olson SA, Guilak F. Intra-articular delivery of purified mesenchymal stem cells from C57BL/6 or MRL/MpJ superhealer mice prevents posttraumatic arthritis. *Cell Transplant.* 2013;22(8):1395–408. PMID: 3891895.
13. Ward BD, Furman BD, Huebner JL, Kraus VB, Guilak F, Olson SA. Absence of posttraumatic arthritis following intraarticular fracture in the MRL/MpJ mouse. *Arthritis Rheum.* 2008;58(3):744–53.
14. Lewis Jr JS, Furman BD, Zeitler E, Huebner JL, Kraus VB, Guilak F, Olson SA. Genetic and cellular evidence of decreased inflammation associated with reduced incidence of posttraumatic arthritis in MRL/MpJ mice. *Arthritis Rheum.* 2013;65(3):660–70. PMID: 3721663.
15. Poulet B, Hamilton RW, Shefelbine S, Pitsillides AA. Characterizing a novel and adjustable noninvasive murine joint loading model. *Arthritis Rheum.* 2011;63(1):137–47.
16. Ko FC, Dragomir C, Plumb DA, Goldring SR, Wright TM, Goldring MB, van der Meulen MC. In vivo cyclic compression causes cartilage degeneration and subchondral bone changes in mouse tibiae. *Arthritis Rheum.* 2013;65(6):1569–78. PMID: 3672344.
17. Onur TS, Wu R, Chu S, Chang W, Kim HT, Dang AB. Joint instability and cartilage compression in a mouse model of posttraumatic osteoarthritis. *J Orthop Res.* 2014;32(2):318–23.
18. Wu P, Holguin N, Silva MJ, Fu M, Liao W, Sandell LJ. Early response of mouse joint tissue to noninvasive knee injury suggests treatment targets. *Arthritis Rheum.* 2014;66(5):1256–65.
19. Christiansen BA, Anderson MJ, Lee CA, Williams JC, Yik JH, Haudenschild DR. Musculoskeletal changes following non-invasive knee injury using a novel mouse model of post-traumatic osteoarthritis. *Osteoarthritis Cartilage.* 2012;20(7):773–82.
20. Lockwood KA, Chu BT, Anderson MJ, Haudenschild DR, Christiansen BA. Comparison of loading rate-dependent injury modes in a murine model of post-traumatic osteoarthritis. *J Orthop Res.* 2014;32(1):79–88.
21. Khorasani M, Diko S, Anderson MA, Genetos DC, Haudenschild DR, Christiansen BA. Effect of alendronate on post-traumatic osteoarthritis induced by ACL rupture in mice. Submitted 2014.
22. Glasson SS, Chambers MG, Van Den Berg WB, Little CB. The OARSI histopathology initiative—recommendations for histological assessments of osteoarthritis in the mouse. *Osteoarthritis Cartilage.* 2010;18 Suppl 3:S17–23.
23. Di Cesare PE, Haudenschild DR, Samuels J, Abramson SB. Pathogenesis of Osteoarthritis. In: Firestein GS, Kelley WN, editors. *Kelley's textbook of rheumatology.* 9th ed. Philadelphia, PA: Elsevier Science Publisher; 2013. p. 1617–35.
24. Sampson ER, Beck CA, Ketz J, Canary KL, Hilton MJ, Awad H, Schwarz EM, Chen D, O'Keefe RJ, Rosier RN, Zuscik MJ. Establishment of an index with increased sensitivity for assessing murine arthritis. *J Orthop Res.* 2011;29(8):1145–51.
25. Yik JH, Christiansen BA, Haudenschild DR. Early transient induction of IL-6 in a mouse joint injury model. *Osteoarthritis Cartilage.* 2013;21(Supplement):S235–6.
26. Ma HL, Blanchet TJ, Peluso D, Hopkins B, Morris EA, Glasson SS. Osteoarthritis severity is sex dependent in a surgical mouse model. *Osteoarthritis Cartilage.* 2007;15(6):695–700.

# Articular Cartilage Injury and Potential Remedies

Susanna Chubinskaya, PhD,\* Dominik Haudenschild, PhD,† Seth Gasser, MD,‡ James Stannard, MD,§  
Christian Krettek, MD,|| and Joseph Borrelli, Jr, MD¶

**Summary:** Osteoarthritis affects millions of people worldwide, is associated with joint stiffness and pain, and often causes significant disability and loss of productivity. Osteoarthritis is believed to occur as a result of ordinary “wear and tear” on joints during the course of normal activities of daily living. Posttraumatic osteoarthritis is a particular subset of osteoarthritis that occurs after a joint injury. Developing clinically relevant animal models will allow investigators to delineate the causes of posttraumatic osteoarthritis and develop means to slow or prevent its development after joint injury. Chondroprotectant compounds, which attack the degenerative pathways at a variety of steps, are being developed in an effort to prevent posttraumatic osteoarthritis and offer great promise. Often times, cartilage degradation after joint injury occurs despite our best efforts. When this happens, there are several evolving techniques that offer at least short-term relief from the effects of posttraumatic osteoarthritis. Occasionally, these traumatic lesions are so large that dramatic steps must be taken in an attempt to restore articular congruity and joint stability. Fresh osteochondral allografts have been used in these settings and offer the possibility of joint preservation. For patients presenting with neglected displaced intra-articular fractures that have healed, intra-articular osteotomy techniques are being developed in an effort to restore joint congruity and function. This article reviews the results of a newly developed animal model of posttraumatic osteoarthritis, several promising chondroprotectant compounds, and also cartilage techniques that are used when degenerative cartilage lesions develop after joint injury.

**Key Words:** articular cartilage, posttraumatic osteoarthritis, model, chondroprotectant, microfracture, fresh osteo-articular allograft, intra-articular osteotomy

(*J Orthop Trauma* 2015;29:S47–S52)

## INTRODUCTION

Despite billions of dollars spent over several decades worldwide by academic laboratories, biotech companies, and large pharmaceutical companies, we currently do not have a cure for osteoarthritis (OA). Perhaps, even more

disappointing is that there are no cures in the developmental pipelines and that the commercial focus has shifted toward providing palliative care products until joint replacement becomes necessary. This review will outline our current understanding of OA and posttraumatic osteoarthritis (PTOA), current treatment capabilities, preventive measures being developed, and techniques to treat localized cartilage defects when all else has failed.

## WHEN DOES OA BEGIN?

Because most OA is idiopathic (arising by itself without known cause), its inception is very difficult to determine. The current understanding of OA is that it is an organ-level or tissue-level pathologic process that ultimately ends with joint pain, stiffness, and loss of function. However, as imaging and arthroscopy capabilities improve, tissue degradation can be identified earlier. Yet, it seems likely that cellular and molecular changes begin to occur within the joint tissues even before any tissue-level changes can be visualized.

## POSTTRAUMATIC OA

PTOA is a form of OA that is initiated by joint injury. Because the OA-initiating injury event is usually clearly defined, animal models of PTOA are a convenient way to study the early cellular and molecular changes caused by injury and how these affect the progression of PTOA. Approximately 12% of all OA is a result of an injury, and studies by Lohmander et al and others indicate that approximately 50% of patients who sustain a significant knee injury develop PTOA in 5–20 years. This percentage increases to 75% with more traumatic injuries that include intra-articular fracture.<sup>1</sup> As such, it is apparent that mitigating the effects of joint injury on articular cartilage would potentially decrease the development of PTOA.

## EXAGGERATED RESPONSE TO INJURY

It is hypothesized that attenuating excessive cellular and molecular responses to injury might benefit the long-term health of the joint. This is based on the rationale that after joint injury, the body responds as though the wound was open and contaminated, initiating a significant inflammatory response to fight foreign pathogens. Other than increasing the odds of survival for the entire organism, this response probably does not directly benefit the long-term function of the injured joint. Because cartilage is an avascular, aneural, and alymphatic tissue, injury responses originating from the chondrocytes themselves are initially predominant. It is believed that

Accepted for publication September 17, 2015.

From the \*Rush University, Chicago, IL; †University of California at Davis, Sacramento, CA; ‡Florida Orthopedic Institute, Tampa, FL; §University of Missouri, Columbia, MO; ||Hannover Medical School, Hannover, Germany; and ¶Texas Health Arlington Memorial Hospital, Arlington, TX. Dr. J. Stannard reports an institutional grant from the Department of Defense. The remaining authors report no conflicts of interest.

Reprints: Joseph Borrelli, Jr, MD, Texas Health Physicians Group, Orthopedic Medicine Specialists, 902 West Randol Mill Rd, Suite 120, Arlington, TX 76012 (e-mail: josephborrelli@texashealth.org).

Copyright © 2015 Wolters Kluwer Health, Inc. All rights reserved.

attenuating these early cellular responses will benefit the joint long term by reducing the irreversible molecular degradation of the chondrocytes and the surrounding joint tissues, which occurs during this inflammatory response.

### MOUSE MODELS OF PTOA

To study the means of mitigating the effects of joint injury, a noninvasive model of PTOA in mice has been developed.<sup>2</sup> Using one of these models, PTOA consistently develops within 8 weeks of the injury and includes the hallmarks of OA at the tissue and cellular level. Although the time scale for progression to advanced PTOA is greatly accelerated in mice as compared to humans, the actual mechanisms are likely the same. With this noninvasive model of PTOA, one of the earliest *in vivo* injury responses identified was an increase in proteolytic activity as measured through proteolytic cleavage. After the injection of MMPsense probes (Perkin Elmer, Waltham, MA) into mice after injury, an increased matrix metalloproteinase (MMP) activity at the injured joint within 1–2 hours after injury was detected, and this MMP activity remained elevated for at least 8 weeks. Additional responses to injury were also observed in the days after joint injury, including temporary loss of subchondral trabecular bone. At this point, it is unclear as to which response is responsible for the loss of joint function. It is likely, however, that all observed and some still unidentified changes play a role in articular cartilage degeneration after joint injury. Microarray analysis was used to assess the injury response of healthy young (12 week) and old (54 week) mice. Baseline gene expression was found to be quite different between young and old mice. This suggests that baseline gene expression in addition to injury response genes may jointly affect the repair capacity after injury and the trajectory of PTOA progression.

In summary, based on the mice model for PTOA, there is a rapid biological response to joint injury that occurs before clinical PTOA symptoms occur.<sup>3</sup> Therefore, it seems practical that attenuating these early injury responses will protect the long-term health of the joint by preventing irreversible molecular damage to each of the joint tissues.

### BIOLOGIC OPTIONS FOR THE TREATMENT OF ARTICULAR CARTILAGE INJURY

Biologic compounds are currently being investigated to mitigate the effects of cartilage and joint injuries. These compounds include chondroprotective agents, inhibitors of proinflammatory mediators, matrix protectants, and growth factors. Two chondroprotectant agents under investigation include p188 and rotenone.<sup>4,5</sup> P188 is best known as a cellular membrane stabilizer, but it has also been shown to inhibit or block stress-related p38 mitogen-activated protein kinase signaling, apoptosis-related glycogen synthase kinase-3 activation, and inflammation related to interleukin-6 (IL-6). The use of these types of compounds seems to be most effective when administered as close to the time of injury as possible.

Inhibitors of proinflammatory mediators have also been investigated in an effort to limit the long-term effects of

inflammatory cytokines. Compounds such as IL-1 receptor antagonist (IL-1RA) and tumor necrosis factor- $\alpha$  (TNF- $\alpha$ ) antagonist have been studied. IL-1RA has been studied as an injectable protein and as a gene in both *in vitro* and *in vivo* models. When injected as an adenoviral gene intra-articularly, it has been shown to decrease subchondral edema, joint fibrillation, and chondrocyte necrosis. IL-1RA has also been shown to increase prostaglandin synthesis by the viable cells, but this effect is lost after the agent is removed.

TNF- $\alpha$ , a cytokine, has been associated with cartilage loss in OA and PTOA after joint injury. TNF- $\alpha$  receptor 1 is an antagonist of TNF- $\alpha$  and has been shown to downregulate MMP1, MMP3, and MMP13 expression and preserve cartilage by reducing the release of prostaglandins and increasing the release of lubricin in a rat model of PTOA.<sup>6</sup>

Although both IL-1RA and TNF- $\alpha$  receptor 1 hold promise as anti-inflammatory agents in the protection of cartilage after injury, they probably play a secondary role to the true chondroprotective agents.

### AGENTS FOR MATRIX PROTECTION

MMPs, A disintegrin and metalloproteinases (ADAMs), A disintegrin and metalloproteinases with thrombospondin motif, and cathepsins are families of proteolytic enzymes, which cause degradation of cartilage matrix components after joint injury. Two potential pathways can be used to disrupt these mechanisms: direct inhibition of matrix-degrading proteinases and inhibition of factors responsible for their activation. Potential players in this arena are radical oxygen species scavengers, inhibitors of nitric oxide, inflammatory cytokines, and specific MMP inhibitors. L-N6-(1-iminoethyl) lysine has been shown to slow the progression of PTOA in canine experiments, suggesting that nitric oxide synthase could be a good target for matrix protection.<sup>7</sup> Unfortunately, MMP inhibitors are not widely available, and investigators have had to resort to transgenic modifications with only limited success.

A very promising approach to the prevention of PTOA after joint injury is the use of growth factors to stimulate the production of cartilage matrix and induce an anabolic response.<sup>8</sup> Transforming growth factor- $\beta$  superfamily members, including bone morphogenetic proteins (BMPs), fibroblast growth factors 2 and 18, and insulin-like growth factor-1, have been widely studied.<sup>8</sup> Results thus far suggest that BMP-7 may be the best of these compounds in modifying the progression of OA and PTOA because of its proanabolic and anticatabolic properties.<sup>9</sup> In several different models of cartilage injury, BMP-7 was shown to stimulate regeneration of articular cartilage, increase repair tissue, and improve integrative repair between new cartilage and surrounding articular cartilage.<sup>10</sup> In PTOA-related studies, fibroblast growth factor 18 has been shown to induce anabolic effects on chondrocytes and chondroprogenitor cells and to stimulate cell proliferation and type II collagen production.<sup>11</sup> Although many biologically active compounds show promise, much work is still needed to ensure safety and to determine the most effective route of administration, dosage, and dosing regimens, and also the best timing relative to joint injury. Unfortunately,

there are few biologic products commercially available that can positively influence injured cartilage.

### **SURGICAL TREATMENT OF CHONDRAL LESIONS: CHONDROPLASTY, MICROFRACTURE, AND CELLULAR OPTIONS**

Articular cartilage is a highly organized complex tissue. Its viscoelastic properties allow it to withstand high levels of stress and repetitive loading over time. Unfortunately, articular cartilage injury is common, particularly involving the knee.<sup>12</sup> Partial thickness lesions have limited capacity to heal, whereas full-thickness lesions that penetrate the subchondral bone often “heal” with fibrocartilage. Numerous treatments for focal full-thickness chondral defects of the knee are available, but none have been proven to consistently restore normal hyaline cartilage and knee function.

Initial surgical intervention for the treatment of these lesions has included simple arthroscopic debridement (chondroplasty) with or without marrow stimulation (microfracture). More advanced treatment options, such as osteochondral autograft transfer (OATS/mosaicplasty), fresh osteochondral allograft transplantation, and chondrocyte transplantation (autologous chondrocyte implantation/ACI), are reserved for larger lesions or those that have failed previous treatment.

The goals of arthroscopic debridement/chondroplasty are to define the pathology, remove particulate debris, inflammatory mediators, and degradative enzymes, and create a smooth articular surface with stable borders. It is a single-stage procedure that requires no special instrumentation, allows easy access to the entire joint, is relatively inexpensive, and has a quick recovery time. Disadvantages include the possible removal of normal articular cartilage, difficulty in creating smooth surfaces with stable margins, and the lack of stimulating any significant healing response. In general, results are better for smaller, low-grade lesions, but these results tend to deteriorate over time.<sup>13,14</sup>

Microfracture is a popular treatment for full-thickness chondral defects of the knee. The technique involves using an arthroscopic awl to create multiple 3–4 mm deep holes, 3–4 mm apart, throughout the base of the lesion.<sup>15</sup> Penetration of the subchondral bone is essential and is believed to allow release of stem cells and growth factors from the bone marrow. It is best indicated for patients <55 years with full-thickness defects that are well contained and <2.5 cm<sup>2</sup>. Unfortunately, fibrocartilage lacks the structure, composition, mechanical properties, and durability of normal articular cartilage. Consequently, clinical results tend to diminish over time.<sup>16</sup> Additional disadvantages of microfracture include postoperative restrictions, possible formation of subchondral cysts and osteophytes, and poor results in athletes.<sup>15,17,18</sup> Evidence-based analysis has shown microfracture to provide effective short-term functional improvement; however, there are insufficient data documenting long-term success.<sup>16,19</sup>

OATS/mosaicplasty involves the transfer of autogenous cylindrical osteochondral plugs from nonvital articular areas to the weight-bearing surfaces of the knee. This is a single-stage procedure that can be performed either arthroscopically or open,

is cost effective, preserves hyaline cartilage viability, and allows for a relatively quick recovery. The main disadvantages include the limited number and size of the donor sites, potential donor site morbidity, and the technical demands of the procedure required for precise fit and contouring of the plugs.<sup>20–22</sup>

ACI is a 2-stage procedure requiring an initial arthroscopy to harvest normal articular cartilage and a second open surgery to insert the culture expanded chondrocytes back into the defect.<sup>23</sup> Problems include difficulty with harvesting and suturing the periosteal patch, cell leakage, uneven distribution of cells, chondrocyte dedifferentiation in vivo, formation of “hyaline-like” cartilage or fibrocartilage, higher failure rates after microfracture, and high costs.<sup>18</sup> Reported complications include arthrofibrosis, and graft hypertrophy, delamination, or failure. In addition, prolonged rehabilitation is required to allow cartilage growth and maturation.<sup>24</sup> The literature is divided as to the optimal method when ACI is compared to microfracture and OATS.<sup>25–28</sup> Second-generation ACI was developed in an attempt to improve these results. In this procedure, an expanded population of chondrocytes that express a marker predictive of the capacity to form hyaline-like cartilage is selected for implantation (characterized chondrocyte implantation).<sup>26</sup> A third-generation procedure, known as matrix-assisted ACI, has now been developed. This technique involves seeding the culture-expanded cartilage cells onto a 3-dimensional scaffold, which is then inserted into the prepared defect. There are significant advantages to this procedure; however, at this time, matrix-assisted ACI is not Food and Drug Administration approved for use in the United States.

Evolving tissue engineering-based strategies have recently been developed, the goals of which are to create cartilage constructs that can be reimplanted in a single-stage procedure, and that result in the production of durable repair tissue. Necessary components include cells, scaffolds, and growth factors. Numerous scaffolds are under investigation, including protein-based platelet-rich plasma, carbohydrate-based, synthetics, and combination scaffolds. Additionally, several other means of using bone marrow aspirate and manipulated chondrocytes, including those from juveniles, are under developed to treat osteochondral defects.<sup>29–34</sup>

Overall, cartilage tissue engineering has advanced rapidly in the past decade. New products continue to be developed; however, engineered cartilage with properties that mimic native articular cartilage is currently unavailable, and multiple obstacles must still be overcome. Future scientific advances may ultimately be able to deliver the ideal construct with the optimal cell, ideal scaffold, and appropriate growth factors to provide a better solution for the treatment of focal chondral lesions.

### **OSTEOCHONDRAL ALLOGRAFTS IN THE TREATMENT OF LARGE FULL-THICKNESS OSTEOCHONDRAL DEFECTS**

Large osteochondral defects can be quite a challenge to treat, as an appropriately sized and shaped osteochondral fragment(s) to fill the defect must be found, and cartilage and bone integration must be achieved. A potential solution is to use fresh osteochondral allografts.<sup>35,36</sup> These allografts

contain viable chondrocytes but must be obtained and inserted in a timely fashion using techniques that preserve the viability of the chondrocytes and maximize the chance of bony integration. Allograft cell survival, cost, and availability make this option only feasible in certain centers. In general, chondrocyte viability is believed to be 28 days on average with current storage techniques. New allograft preservation systems can now extend the survival of these allografts to 60 days with more viable chondrocytes (New Missouri Allograft Preservation System), increased glycosaminoglycan content, and maintenance of the biomechanical properties of the articular cartilage and collagen content.<sup>37,38</sup>

In general, one should maximize chondrocyte viability (ideally greater than 70%) and ensure bone and cartilage healing and incorporation of the grafts.

## TREATMENT OF INTRA-ARTICULAR MALUNIONS

Although many treatment concepts exist for extra-articular deformities, there is limited information regarding the treatment of intra-articular deformities.<sup>39</sup> In this section,

the current understanding of the surgical treatment of intra-articular malunions is described. The technique includes identification of the original articular fracture lines, thorough analysis of the overall deformity, and development of a comprehensive preoperative plan to ensure each mechanical and biologic issue is addressed, all of which has been developed over several years during the treatment of numerous patients with clinically significant intra-articular deformity.<sup>40</sup>

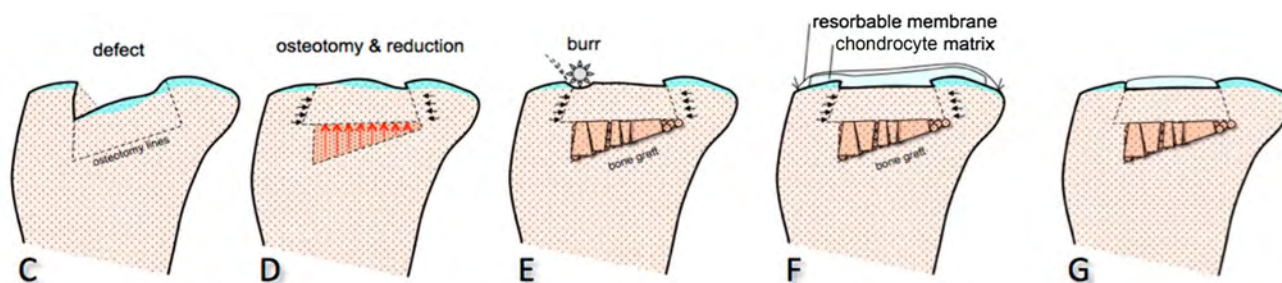
## ASSESSMENT

### Physical Examination

The limb and joint articulation of concern must be thoroughly examined to detect additional deformities, including shortening, malrotation, and angulation, and to determine the joint range of motion (ROM) and stability.

### Imaging

Computed tomography (CT) with 2-dimensional and 3-dimensional reconstructions is an essential part of the



Krettek et al (2013) Intraarticular Segmental Osteotomy Unfallchirurg 116(5) 413-426

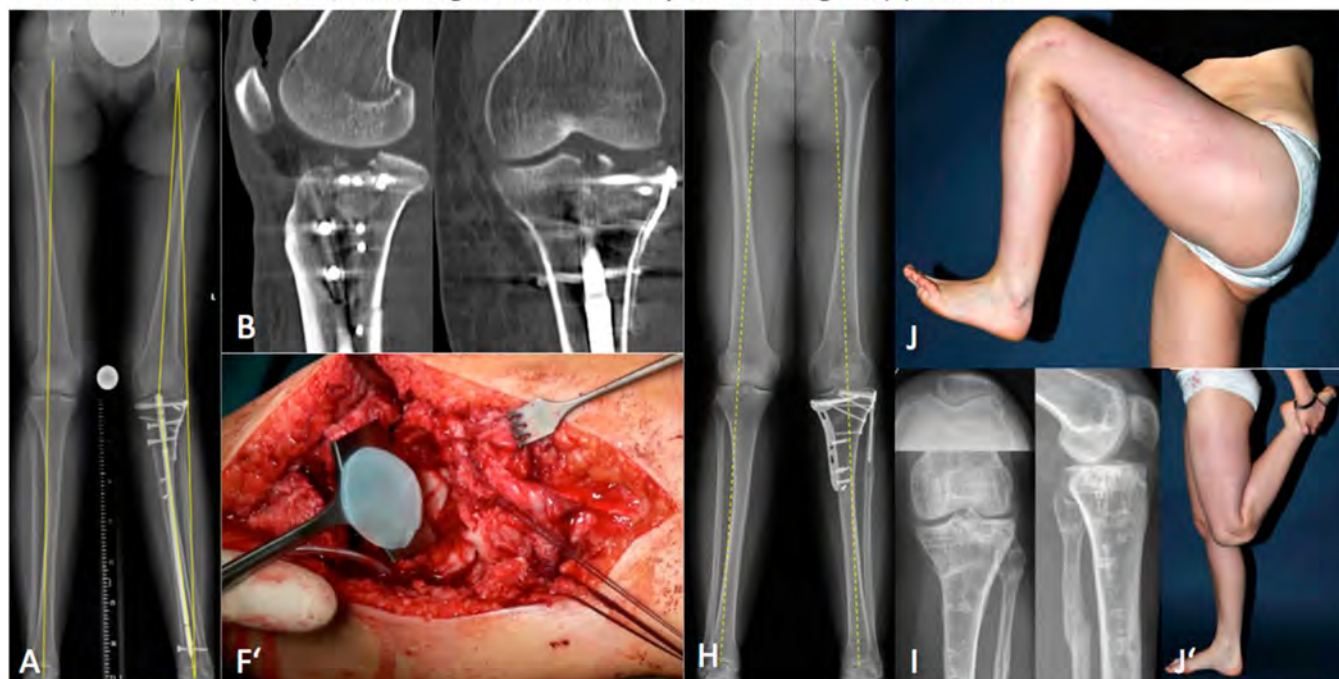


**FIGURE 1.** Pre-operative images of intra-articular defect of the left lateral tibial plateau (A, B), pre-operative plan for correction of defect (C–G), intra-operative photograph of articular correction (F') and post-operative radiographic outcome (H, I) and knee range of motion (J, J'). Reprinted from Krettek et al<sup>40</sup> with permission of the publisher. Copyright © 2013, Springer.

assessment process. Articular steps and gaps must be fully appreciated and thoroughly analyzed, including their size and location. Additional analysis of length and torsional differences is crucial, and therefore the CT should generally include the contralateral uninjured limb. Long-standing radiographs are also needed for frontal plane alignment analysis under loading conditions. Magnetic resonance imaging is necessary for determining articular cartilage thickness and detailed surface structure, and also meniscal and ligamentous integrity.

## Preoperative Planning

Essential for preoperative planning is radiographic analysis of the contralateral uninjured side. Virtual subtraction computerized techniques using the uninjured and injured sides enable the investigator to definitively assess the geometric deviations between the 2 and allow manipulation of the defective side to elucidate a means of correction.

## Decision Making

Planning and decision making must take into account local factors such as intra-articular deformities, quality of the articular surfaces, extra-articular deformities, condition of the menisci and ligaments, joint stability, frontal plane alignment, ROM, and muscle strength. Additional factors include pain, presence of comorbidities, patient's age and activity level, and, perhaps most importantly, the patient's expectations.

## Descriptive Case/Surgical Technique

A 24-year-old woman sustained a split-depression lateral tibia plateau fracture that was not reduced during her original surgery. Ten months postoperatively, she presented with severe knee pain, valgus deformity, and knee instability. Physical findings include 5° extension, 130° flexion, and lateral instability. Preoperative assessment included standing long radiographs (Fig. 1A), a CT (Fig. 1B), and magnetic resonance imaging. A preoperative plan was developed (Fig. 1C–G), and a meticulous operative correction and stabilization were performed (Fig. 1F').

The operative procedure included an intra-articular segment osteotomy, fragment elevation, reduction, and fixation (Fig. 1D). Because the cartilage was partially degenerative, a chondrocyte matrix with cultured chondrocytes was applied after the preparation of the articular surface (Fig. 1E–G). A high tibial osteotomy was performed to correct the frontal plane alignment (Fig. 1H). At 3 years, the patient had a good lateral joint space (Fig. 1I) and full knee ROM (Fig. 1J, J'), and her knee function and comfort had improved significantly.

## CONCLUSIONS

PTOA is a worldwide problem for which there is no prevention or cure. Development of a clinically relevant animal model would support the identification and testing of chondroprotectant agents that could mitigate the effects of articular injury. However, at this time, depending on the size of the cartilage lesions, only techniques that either stimulate cartilage repair (fibrocartilage) or attempt to replace lost cartilage with chondrocytes or cartilage and bone fragments

are available, with varying degrees of long-term success. Intra-articular osteotomies and mechanical realignment techniques are being explored for those patients with potentially repairable joints. Until a more complete understanding of the pathophysiological processes of PTOA is determined, it will be difficult to develop agents that prevent degeneration after joint injury. As such, chondrocyte and osteochondral transplantation, and occasionally intra-articular osteotomies, will be relied on to relieve pain and improve joint function in these degenerative joints.

## REFERENCES

1. Lohmander LS, Englund PM, Dahl LL, et al. The long-term consequence of anterior cruciate ligament and meniscus injuries: osteoarthritis. *Am J Sports Med.* 2007;35:1756–1769.
2. Christiansen BA, Guilak F, Lockwood KA, et al. Non-invasive mouse models of post-traumatic osteoarthritis. *Osteoarthritis Cartilage.* 2015; 23:1627–1638.
3. Christiansen BA1, Anderson MJ, Lee CA, et al. Musculoskeletal changes following non-invasive knee injury using a novel mouse model of post-traumatic osteoarthritis. *Osteoarthritis Cartilage.* 2012; 20:773–782.
4. Bajaj S, Shoemaker T, Hakimiyan AA, et al. Protective effect of P188 in the model of acute trauma to human ankle cartilage: the mechanism of action. *J Orthop Trauma.* 2010;24:571–576.
5. Goodwin W, McCabe D, Sauter E, et al. Rotenone prevents impact-induced chondrocyte death. *J Orthop Res.* 2010;28:1057–1063.
6. Elsaid KA1, Machan JT, Waller K, et al. The impact of anterior cruciate ligament injury on lubricin metabolism and the effect of inhibiting tumor necrosis factor alpha on chondroprotection in an animal model. *Arthritis Rheum.* 2009;60:2997–3006.
7. More AS1, Kumari RR, Gupta G, et al. Tandan SK Effect of iNOS inhibitor S-methylisothiourea in monosodium iodoacetate-induced osteoarthritis pain: implication for osteoarthritis therapy. *Pharmacol Biochem Behav.* 2013;103:764–772.
8. Fortier LA, Barker JU, Strauss EJ, et al. The role of growth factors in cartilage repair. *Clin Ortho Rel Res.* 2011;469:2706–2715.
9. Badlani N, Inoue A, Healey R, et al. The protective effect of OP-1 on articular cartilage in the development of osteoarthritis. *Osteoarthritis Cartilage.* 2008;16:600–606.
10. Chubinskaya S1, Hurtig M, Rueger DC. OP-1/BMP-7 in cartilage repair. *Int Orthop.* 2007;31:773–781.
11. Ellsworth JL1, Berry J, Bukowski T, et al. Fibroblast growth factor-18 is a trophic factor for mature chondrocytes and their progenitors. *Osteoarthritis Cartilage.* 2002;10:308–320.
12. Curl WW, Krome J, Gordon ES, et al. Cartilage Injury: a review of 31,516 knee arthroscopies. *Arthroscopy.* 1997;13:456–460.
13. Hunt SA, Jazrawi LM, Sherman OH. Arthroscopic management of osteoarthritis of the knee. *JAAOS.* 2002;10:356–363.
14. Jackson RW. Arthroscopic surgery and a new classification system. *Am J Knee Surg.* 1998;11:51–54.
15. Steadman JR, Briggs KK, Rodrigo JJ, et al. Outcomes of microfracture for traumatic chondral defects of the knee: average 11-year follow-up. *Arthroscopy.* 2003;19:477–484.
16. Mithoefer K, McAdams T, Williams RJ, et al. Clinical efficacy of the microfracture technique for articular cartilage repair in the knee. *Am J Sports Med.* 2009;37:2053–2063.
17. Mithoefer K, Williams RJ, Warren RF, et al. High-impact athletes after knee articular cartilage repair: a prospective evaluation of the microfracture technique. *Am J Sports Med.* 2006;34:1413–1418.
18. Minas T, Andreas GH, Rosenberger R, et al. Increased failure rate of autologous chondrocyte implantation after Previous treatment with marrow stimulation techniques. *Am J Sports Med.* 2009;37:902–908.
19. Kreuz PC, Steinwachs MR, Erggelet C, et al. Results after microfracture of full-thickness chondral defects in different Compartments in the knee. *Osteoarthritis and Cartilage.* 2006;14:1119–1125.
20. Ma HL, Hung SC, Wang ST, et al. Osteochondral autografts transfer for Post-Traumatic osteochondral defect of the knee – 2 to 5 Years Follow-up. *Injury.* 2004;35:1286–1292.

21. Hangody L, Kish G, Karpati Z, et al. Mosaicplasty for the treatment of articular cartilage defects: Application in clinical Practice. *Orthopedics*. 1998;21:751–756.
22. Hangody L, Vasarhelyi G, Hangody LR, et al. Autologous osteochondral Grafting-technique and long term results. *Injury*. 2008;39 Suppl:32–39.
23. Brittberg M, Lindahl A, Nillson A, et al. Treatment of deep cartilage defects in the knee with autologous chondrocyte transplantation. *N Engl J Med*. 1994;331:889–895.
24. Niemeyer P, Pestka JM, Kreuz PC, et al. Characteristic complications after autologous chondrocyte implantation for cartilage defects of the knee joint. *Am J Sports Med*. 2008;36:2091–2099.
25. Knutsen G, Drogset JO, Engebretsen, et al. Randomized Trial comparing autologous chondrocyte implantation with microfracture: findings at Five Years. *J Bone Joint Surg Am*. 2007;89:2105–2112.
26. Saris DB, Vanlauwe J, Victor J, et al. Characterized chondrocyte implantation results in better Structural repair when treating Symptomatic cartilage defects of the knee in a Randomized Controlled Trial versus microfracture. *Am J Sports Med*. 2008;36:235–246.
27. Dozin B, Malpeli M, Cancedda R, et al. Comparative evaluation of autologous chondrocyte implantation and mosaicplasty: a Multicentered Randomized clinical Trial. *Clin J Sport Med*. 2005;15:220–226.
28. Bekkers JE, Inklaar M, Saris DB. Treatment Selection in articular cartilage lesions of the knee: a systematic review. *Am J Sports Med*. 2008;37 (suppl 1):148–155.
29. Haleem AM, Chu CR. Advances in tissue engineering techniques for articular cartilage repair. *Oper Tech Orthop*. 2010;20:76–89.
30. de Girolamo L, Bertolini G, Cervellin M, et al. Treatment of chondral defects of the knee with one step matrix-assisted technique Enhanced by autologous Concentrated bone Marrow: In vitro Characterization of Mesenchymal stem cells from Iliac Crest and subchondral bone. *Injury*. 2010;41:1172–1177.
31. Abrams GD, Mall NA, Fortier LA, et al. Biocartilage: Background and operative technique. *Op Tech Sports Med*. 2013;21:116–124.
32. Gille J, Schuseil E, Wimmer J, et al. Mid-term results of autologous matrix-induced Chondrogenesis for treatment of focal cartilage defects in the knee. *Knee Surg Sports Traumatol Arthrosc*. 2010;18:1456–1464.
33. Farr J, Tabet SK, Margerrison E, et al. Radiographic, and Histological Outcomes after cartilage repair with Particulated juvenile articular cartilage: a 2-Year prospective study. *Am J Sports Med*. 2014;42:1417–1425.
34. Adkisson HD, Martin JA, Emendola RL. The potential of human Allogeneic juvenile chondrocytes for Restoration of articular cartilage. *Am J Sports Med*. 2010;38:1324–1333.
35. De Caro F, Bisicchia S, Amendola A, et al. Large fresh osteochondral allografts of the knee: a systematic clinical and basic science review of the literature. *Arthroscopy*. 2015;31:757–765.
36. Sherman SL, Garrity J, Bauer K, et al. Fresh osteochondral allograft transplantation for the knee: current concepts. *J Am Acad Ortho Surg*. 2014;22:121–133.
37. Cook JL, Stoker AM, Stannard JP, et al. A novel system improves preservation of osteochondral allografts. *Clin Ortho Rel Res*. 2014;472: 3404–3414.
38. Stoker A, Garrity JT, Hung CT, et al. Improved preservation of fresh osteochondral allografts for clinical use. *J Knee Surg*. 2012;25:117–125.
39. Marti R, Kerkhoffs GMMJ. *Malunions and Nonunions about the Knee. Skeletal Trauma*. 4th ed.. Chapter 57. Elsevier; 2009.
40. Krettek C, Hawi N, Jagodzinski M. Intracondylar segment osteotomy: correction of intra-articular malalignment after fracture of the tibial plateau. *Der Unfallchirurg*. 2013;116:413–426.

# CDK9 Inhibition Attenuates Acute Inflammatory Response, Reduces Bone Loss in a Post-Traumatic Osteoarthritis Mouse Model

UCDAVIS  
UNIVERSITY OF CALIFORNIA

Hu, Z; Yik, JHN; Fong, JY; Michelier, P; Shidara, K; Liu, N; Huang, B;  
Cissell, D; Christiansen, BA; and Haudenschild, DR  
Department of Orthopaedic Surgery, Lawrence J. Ellison Musculoskeletal Research Center, Sacramento CA 95817

## Objective

Although joint injuries often lead to post-traumatic osteoarthritis (PTOA), few studies have focused on the immediate effects of an acute injury response on the progression and development of PTOA. Acute injury responses are characterized by the transcriptional activation of primary inflammatory genes such as IL-1 $\beta$ , IL-6, and TNF $\alpha$ , and other inflammatory mediators. These events lead to increased production of matrix degrading enzymes that contribute to the catabolic destruction of cartilage and subchondral bone. We **hypothesize** that excessive inflammatory response to joint injuries is a major contributor to the observed cartilage and bone loss preceding the onset of PTOA. Despite being triggered by various inflammatory stimuli, diverse signaling pathways converge onto a single mechanism that activates the transcription of primary inflammatory response genes. **This rate-limiting step of inflammatory gene activation is controlled by the transcription factor cyclin-dependent kinase 9 (CDK9).** CDK9 functions to phosphorylate RNA Polymerase II to overcome its promoter proximal pausing and to stimulate transcriptional elongation of mRNAs. Thus, CDK9 is an attractive and novel target for anti-inflammatory therapy, and we showed that CDK9 inhibition protects cartilage from catabolic cytokines in vitro<sup>(1)</sup>. Here we investigated the effects of CDK9 inhibition, by the pharmacological small molecule inhibitor Flavopiridol, on:

- 1) suppressing the acute injury response, and
- 2) the subsequent cartilage/ bone loss in an in vitro cartilage explant injury model, and in a non-invasive PTOA mouse model.

## Methods

**Cartilage explant injury:** Cartilage explants were harvested by 6mm biopsy punches from bovine stifled joints obtained from a local slaughter house. The explants were trimmed to a height of 3mm and cultured in DMEM+10% FBS for 24 hrs. The explants were then subjected to a single load of compression with 30% strain, and then placed into culturing media with or without 300 nM Flavopiridol (Santa Cruz Biotech). The expression of inflammatory and catabolic/anabolic genes was determined by qPCR described below.

**Mechanical properties:** After 4 weeks of culture, mechanical properties were measured in a sample of the cartilage (2mm height by 3mm diameter). A Bose Enduratec instrument was used to apply 10% and 20% compressive strain and custom MatLab software to estimate the instantaneous and relaxation moduli.

**PTOA mouse model:** The right knees of skeletally matured C57BL6 mice were injured with a single mechanical compression as described (2), with the contralateral knees as uninjured control. These knee injuries consistently lead to a rapid bone loss at 1 week and apparent PTOA at 8 weeks. Half of these mice received intra-peritoneal injections of Flavopiridol at a dosage of 7.5mg/kg at 0- and 4-hours post-injury, and the other half received placebo injections. The knee joints and capsules were harvested and dissected at various time points (n=6/time point) and processed for gene expression, histology (H&E staining), and microCT analysis for femoral epiphysis bone volume. All animal procedures were performed according to an IACUC approved protocol.

**qPCR:** Total RNA from cartilage explants or dissected mouse knees were isolated by the miRNeasy Kit (Qiagen) and reverse transcribed by the QuantiTect Reverse Transcription Kit (Qiagen). Expression of pro-inflammatory cytokines, catabolic and anabolic genes were determined by qPCR in a 7900HT PCR system with gene-specific probes (ABI) and normalized to 18s rRNA.

**In vivo Functional Imaging of MMP activity:** MMP activities at the knee joints were determined by in vivo fluorescence imaging at 1-hour to 7-days post injury. MMP-Sense 680 probe was systemically administered, the animals were imaged in an IVIS imaging system under isoflurane anesthesia while held in place by a custom built adaptor. For each mouse, fluorescence (MMP activity) was expressed as a ratio of the injured to uninjured knee.

**Statistical analysis:** One-way ANOVA with Tukey's correction for multiple comparisons was used to determine significance.

## Results

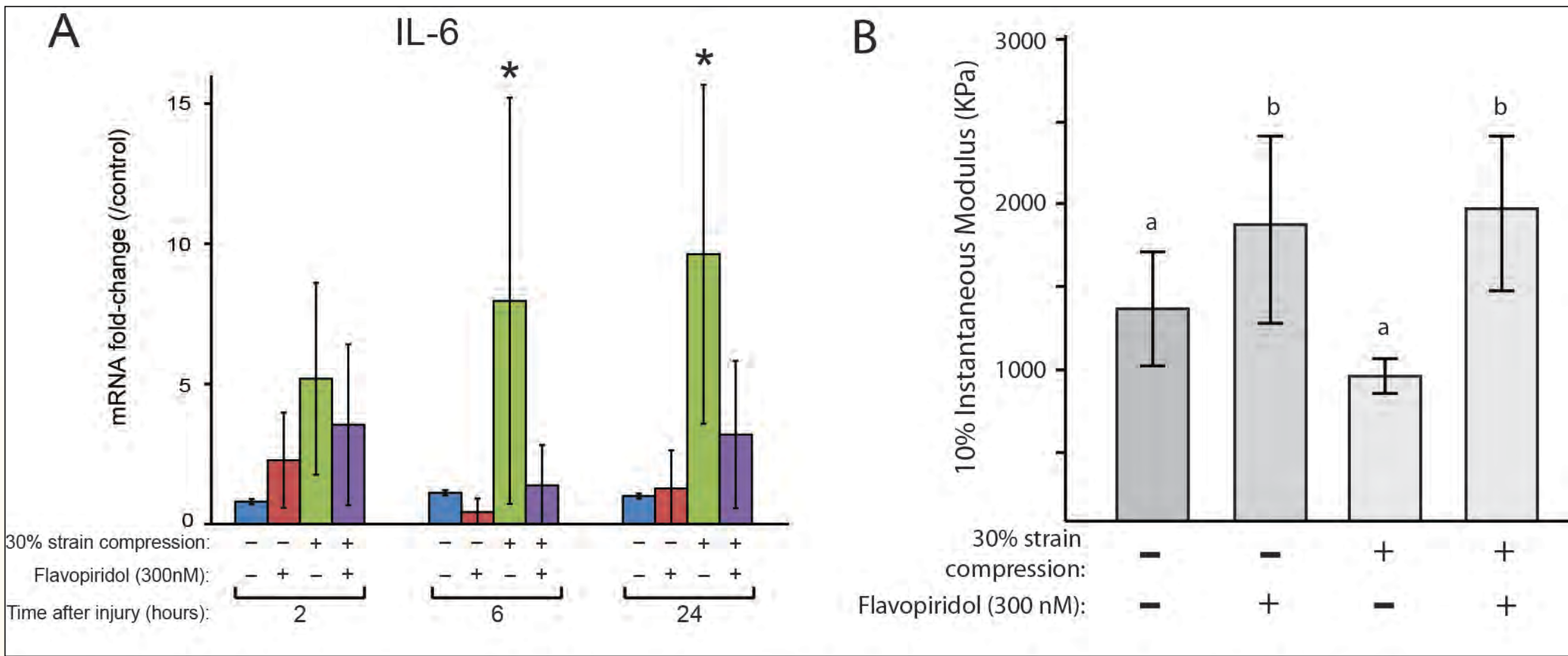


**Fig. 1. Mechanically injured cartilage explants express pro-inflammatory cytokines.**

**A) CDK9 inhibition suppressed IL-6 induction.** Bovine cartilage explants were compressed by a single load of 30% strain rate and analyzed for the mRNA expression of the injury marker IL-6. The results showed that IL-6 expression was markedly increased at 6 and 24 hours post-injury, but the increase was suppressed by Flavopiridol ( $P<0.05$ ). Importantly, Flavopiridol did not affect anabolic genes expression nor chondrocyte viabilities (not shown).

**B) CDK9 inhibition preserved cartilage mechanical properties.** The mechanical properties of the explants were determined 4 weeks post-injury. The results showed that injury caused a reduction in the instantaneous modulus but the effects were reversed by Flavopiridol.

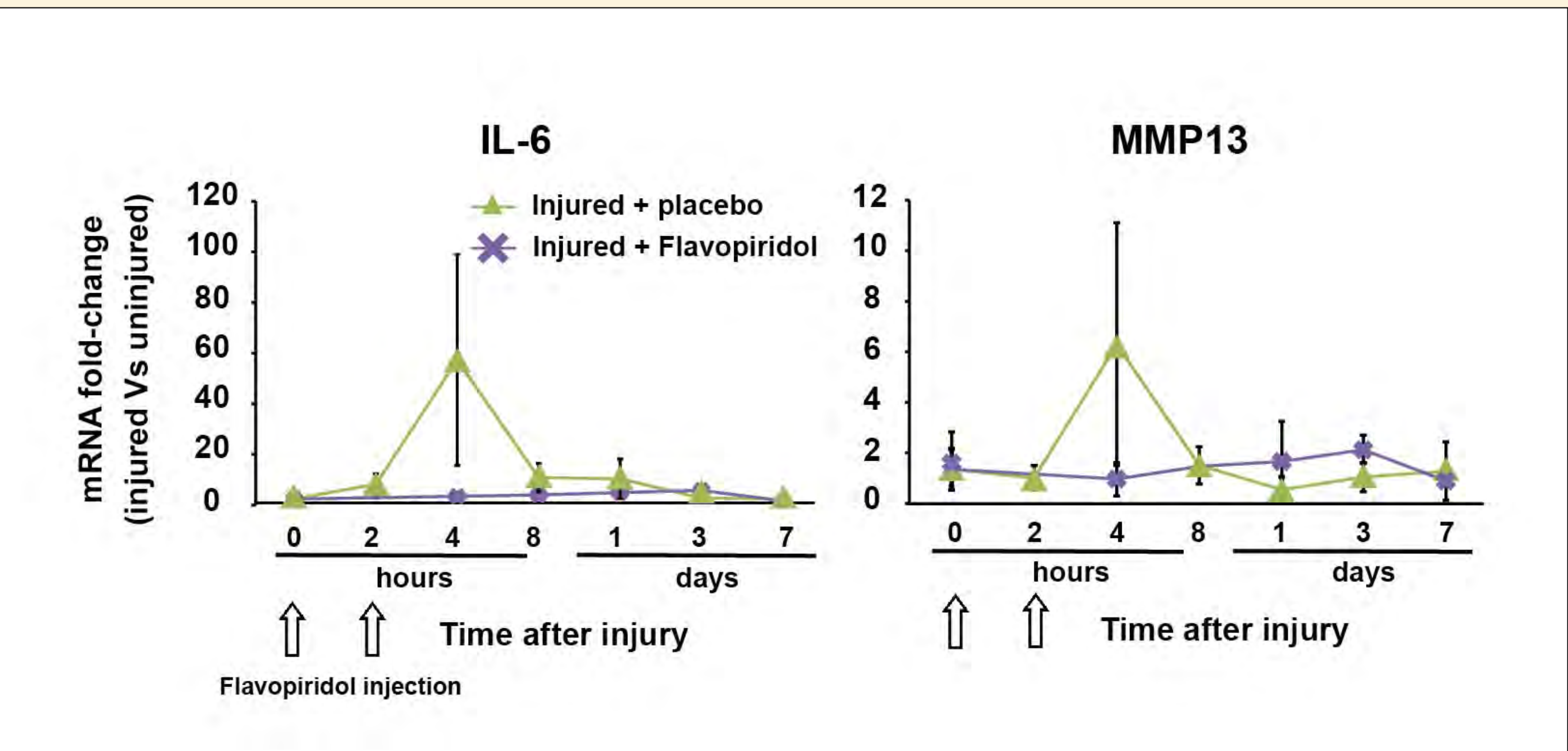


**Fig. 2. In vivo CDK9 inhibition suppresses pro-inflammatory cytokine and catabolic gene mRNA induction after traumatic knee injury.** In the PTOA mouse model, the expression of IL-6 and MMP13 mRNA increased rapidly 2 hrs after knee injury and peaked at 4 hrs, then returned gradually to baseline after 3-7 days. However, their induction was greatly reduced by Flavopiridol ( $*P<0.05$ ). Similar results were seen in other catabolic genes such as IL-1 $\beta$  and ADAMTS4 (not shown). In contrast, at these time points the expression of anabolic genes Col2a1 and aggrecan were not affected by knee injury or Flavopiridol.

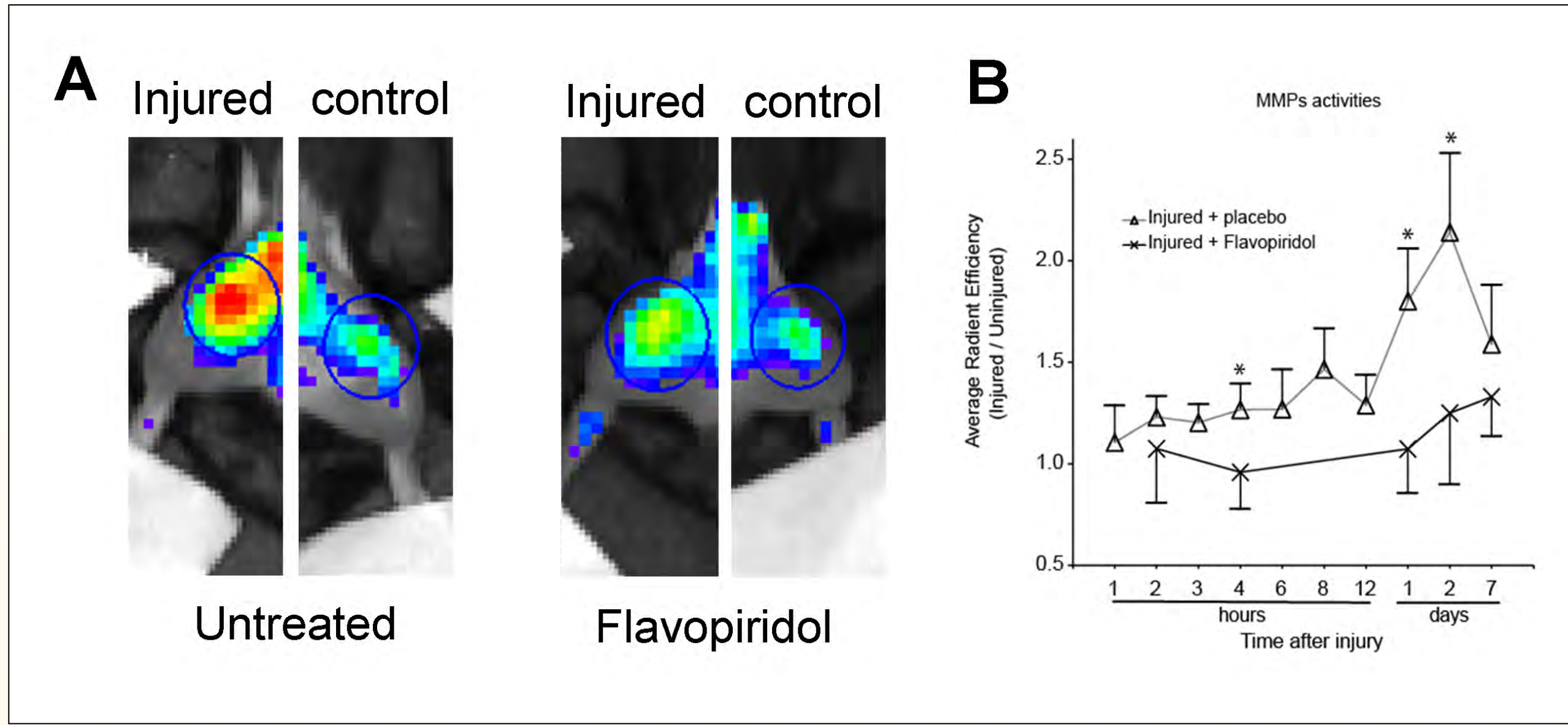


**Fig 3. Functional imaging of MMP activity in vivo.** C57BL/6 mice (n=8/time point) were pre-injected with the MMP-Sense 680 substrates (Perkin-Elmer) 24-hr prior. Their right knees were then injured, with the left knees as uninjured control. The mice were then immediately injected with 7.5 mg/Kg Flavopiridol or vehicle. At the indicated times while under anesthesia, MMP activities at the mouse knees were determined by in vivo fluorescence IVIS imaging system. **(A)** Representative fluorescence images of injured and uninjured knees. **(B)** For each mouse, fluorescence (MMP activity) was expressed as a ratio of the injured to uninjured knee.

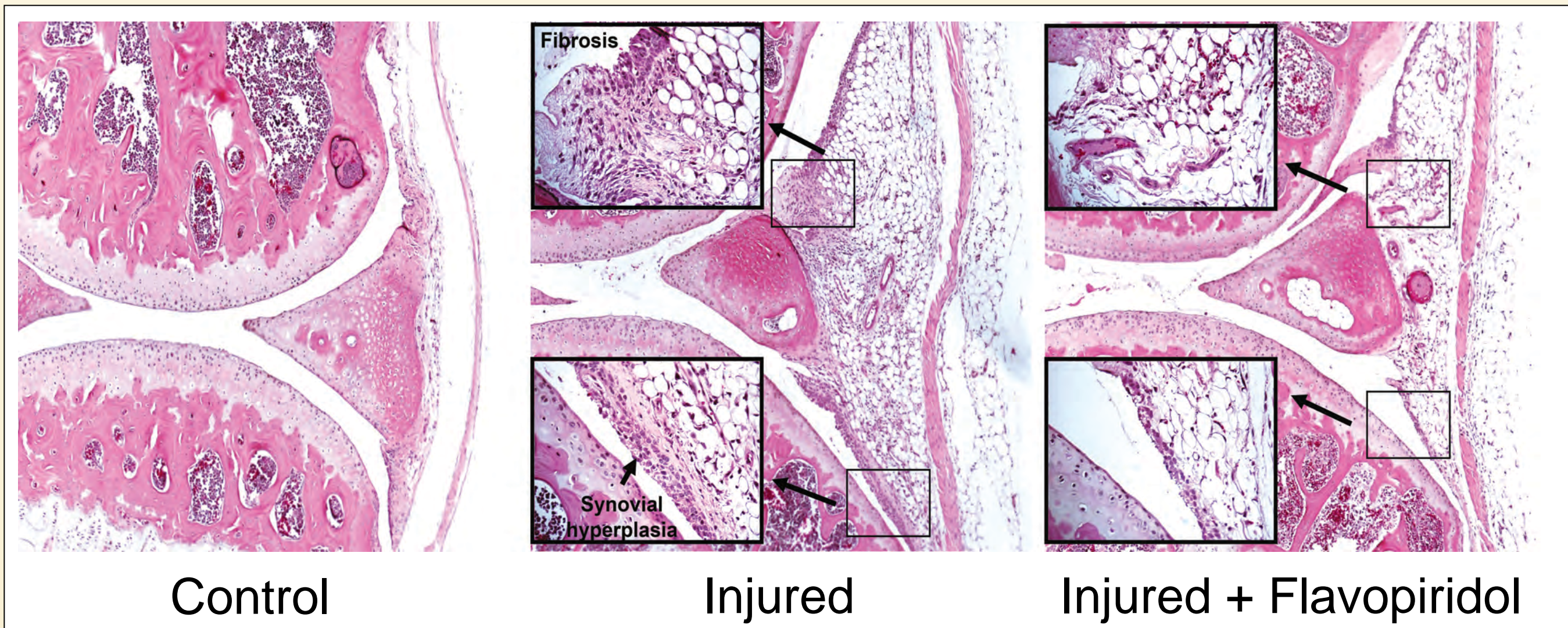


**Fig. 4. Cdk9 inhibition reduced inflammation at the injured joints.** Histological analysis of knees 3-days post-injury showed heavy signs of inflammation, fibrosis, synovial hyperplasia, pannus formation, and leukocyte infiltration. However, these clinical presentations were reduced by Flavopiridol treatment.

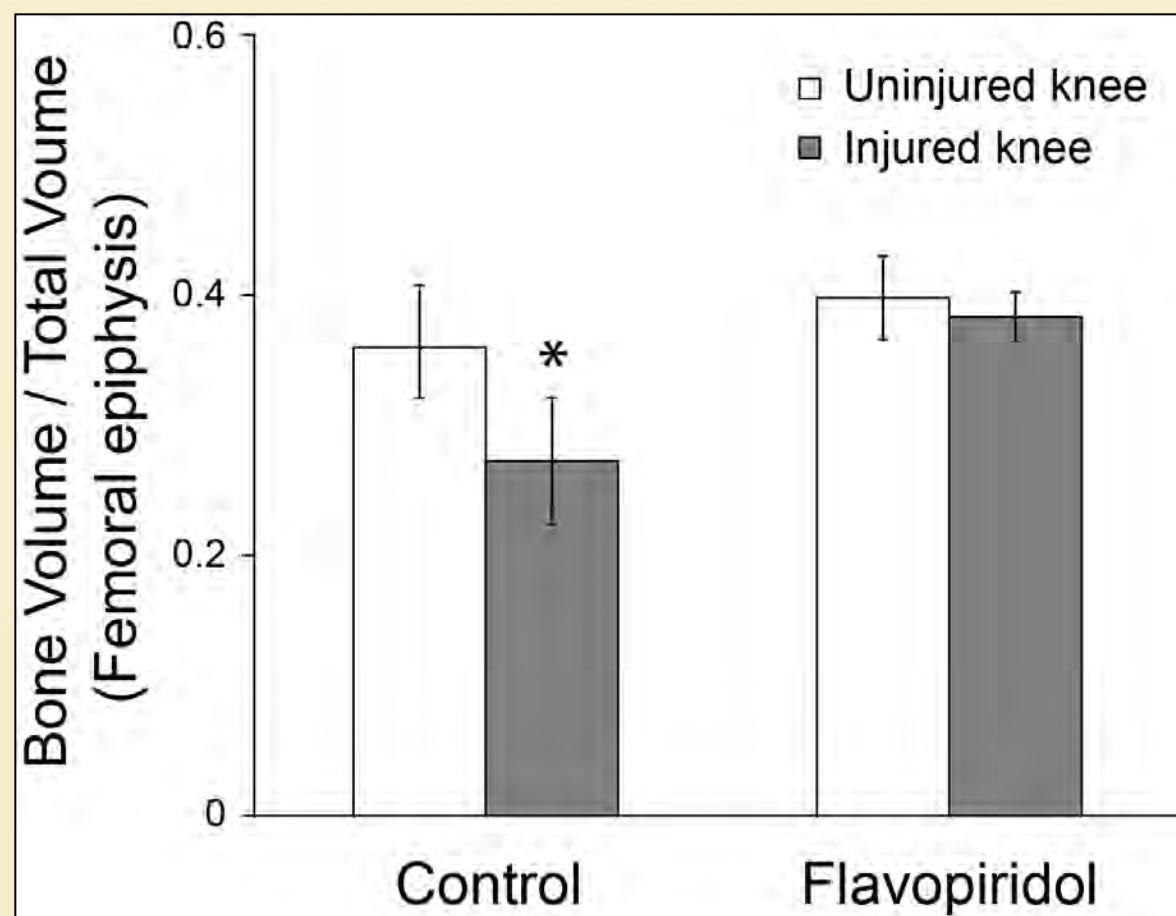


**Fig. 5. CDK9 inhibition prevents bone loss after joint injury.** The femoral epiphysis bone volumes were determined by  $\mu$ CT. Injury caused a significant bone loss in 3 days but this was prevented by Flavopiridol treatment.

## Discussion

**The acute inflammatory reaction to joint injury is largely dependent on CDK9 kinase activity. Inhibition of CDK9 activity after injury will:**

- Reduce pro-inflammatory gene expression in explants and in-vivo
- Preserve the mechanical integrity of cartilage explants
- Reduce post-injury MMP activity in-vivo
- Reduce inflammation, fibrosis, synovial hyperplasia, and leukocyte infiltration
- Prevent post-traumatic loss of sub-chondral bone

**Significance:** PTOA is commonly associated with joint injuries in young active patients. Currently there is no clinical treatment available to prevent the development of PTOA. Our studies suggest that CDK9 inhibition shortly after injuries can prevent cartilage and bone loss, and may prevent or delay the onset of PTOA.

## References

- (1) Yik JHN, Hu Z, Kumari R, Christiansen BA, and Haudenschild DR. *Arthritis Rheumatology* 2014, ePublished
- (2) Christiansen BA, Anderson MJ, Lee CA, Williams JC, Yik JNH, and Haudenschild DR. *Osteoarthritis Cartilage* 2012, **20**(7): 733-82.

**Acknowledgement:** This study was supported by the Arthritis Foundation, the Dept. of Defense (PR110507) and NIH (R21-AR063348)

# ACUTE CHANGES IN NADPH OXIDASE 4 IN EARLY POST-TRAUMATIC OSTEOARTHRITIS

Wegner, Adam M.<sup>1</sup>, Campos, Nestor, R.<sup>1</sup>, Robbins, Michael A., Haddad, Andrew F.<sup>1</sup>, Yik, Jasper H.N.<sup>1</sup>, Christiansen, Blaine, A. <sup>1</sup>, Carlson, Cathy, S.<sup>2</sup>, Haudenschield, Dominik R.<sup>1</sup>

<sup>1</sup> Lawrence J. Ellison Musculoskeletal Research Center, Department of Orthopaedic Surgery, UC Davis, Sacramento, CA

<sup>2</sup> College of Veterinary Medicine, University of Minnesota, St. Paul, MN

## OBJECTIVE

Reactive oxygen species (ROS) are one component of the multifactorial inflammatory cascade activated after joint injury. Although some components of this cascade may be beneficial to healing, others may be damaging to the structure of the joint, initiating early changes in post-traumatic osteoarthritis (PTOA). The role of reactive oxygen species (ROS), one component of the inflammatory cascade, in the pathogenesis of PTOA is poorly understood, and there is currently no disease modifying treatment for the disease. This study used cultured primary human chondrocytes and a non-invasive mouse model of PTOA to elucidate the role of ROS in its pathogenesis in the acute phase after joint injury. After simulated joint injury in chondrocytes with cytokines or joint injury in a non-invasive mouse model of PTOA, NADPH Oxidase 4 (Nox4), a component of the initial inflammatory response, was inhibited by the small molecule inhibitor GKT137831. Our results show that there is a decrease in Nox4 activity in the acute phase after injury, and then a subsequent sustained low level increase after 24 hours both in vivo and in vitro, a novel finding not seen in any other system. Inhibition of Nox4 activity by GKT137831 was protective against early structural changes from occurring after non-invasive knee injury in a mouse model of PTOA. We conclude that Nox4 plays a significant role in the acute phase after joint injury and that targeted inhibition of inflammation caused by Nox4 may be protective against the early joint changes in the pathogenesis of PTOA.

## METHODS

### Human Articular Chondrocyte culture

Primary human articular chondrocytes were obtained from young healthy patients undergoing ACL reconstruction, cultured in monolayer, and used before P4. Hydrogen Peroxide (H<sub>2</sub>O<sub>2</sub>) was measured by Amplex Red Assay (Life Technologies, Waltham, MA), mRNA was measured by real time quantitative PCR, and protein was measured by western blot.

### Mouse Model of Post-traumatic Osteoarthritis

Wild-type or Nox4 knockout C57Bl/6 mice (Jackson Labs, Bar Harbor, ME) were subjected to ACL rupture through non-invasive tibial compression (Fig. 1). Mouse knees were homogenized and mRNA quantified by real time quantitative PCR and protein quantified by western blot, or whole knees were fixed in paraformaldehyde and scanned by  $\mu$ CT. Bone analysis was carried out per manufacturer instructions.

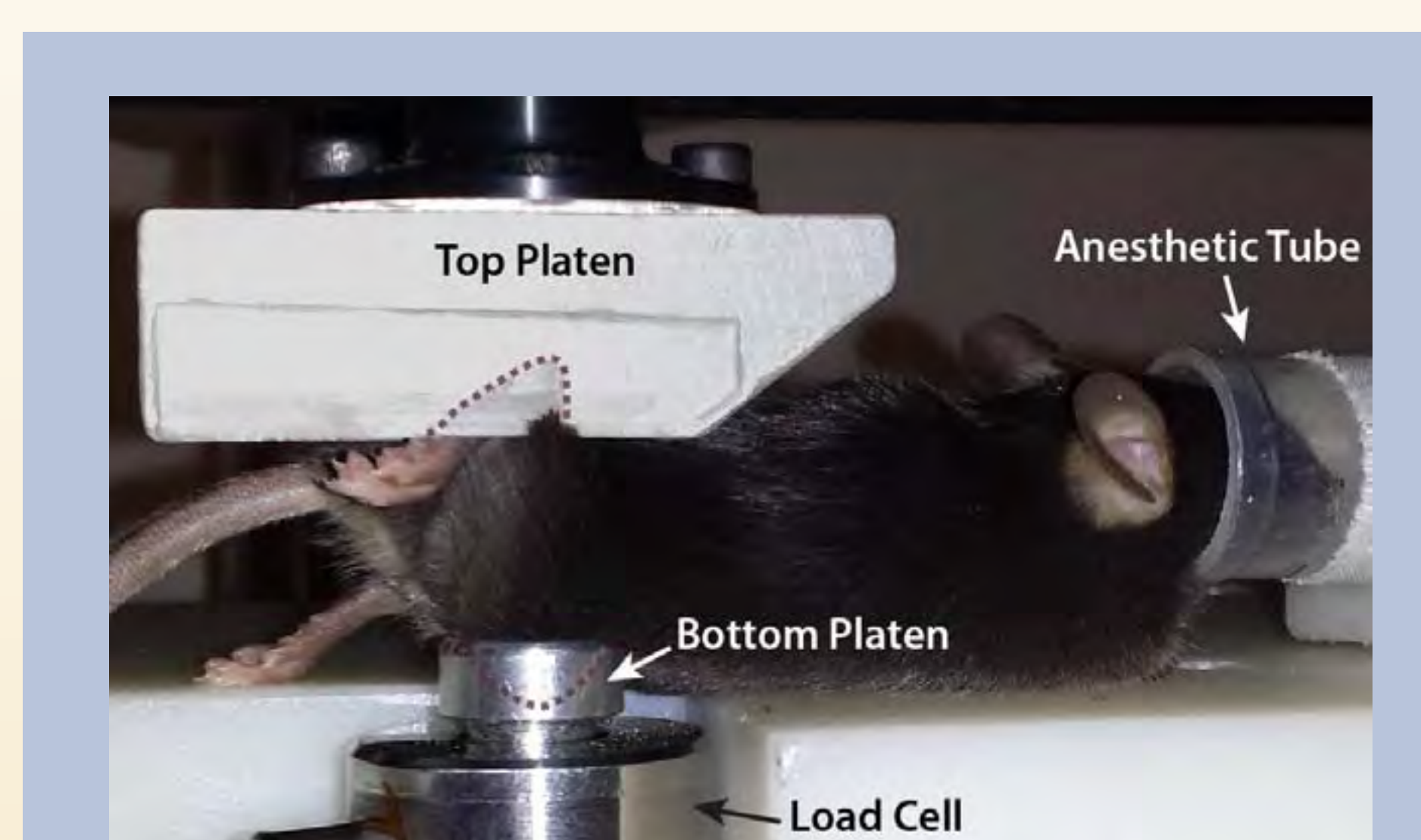


Figure 1. Non-invasive mouse model of post-traumatic osteoarthritis

## RESULTS

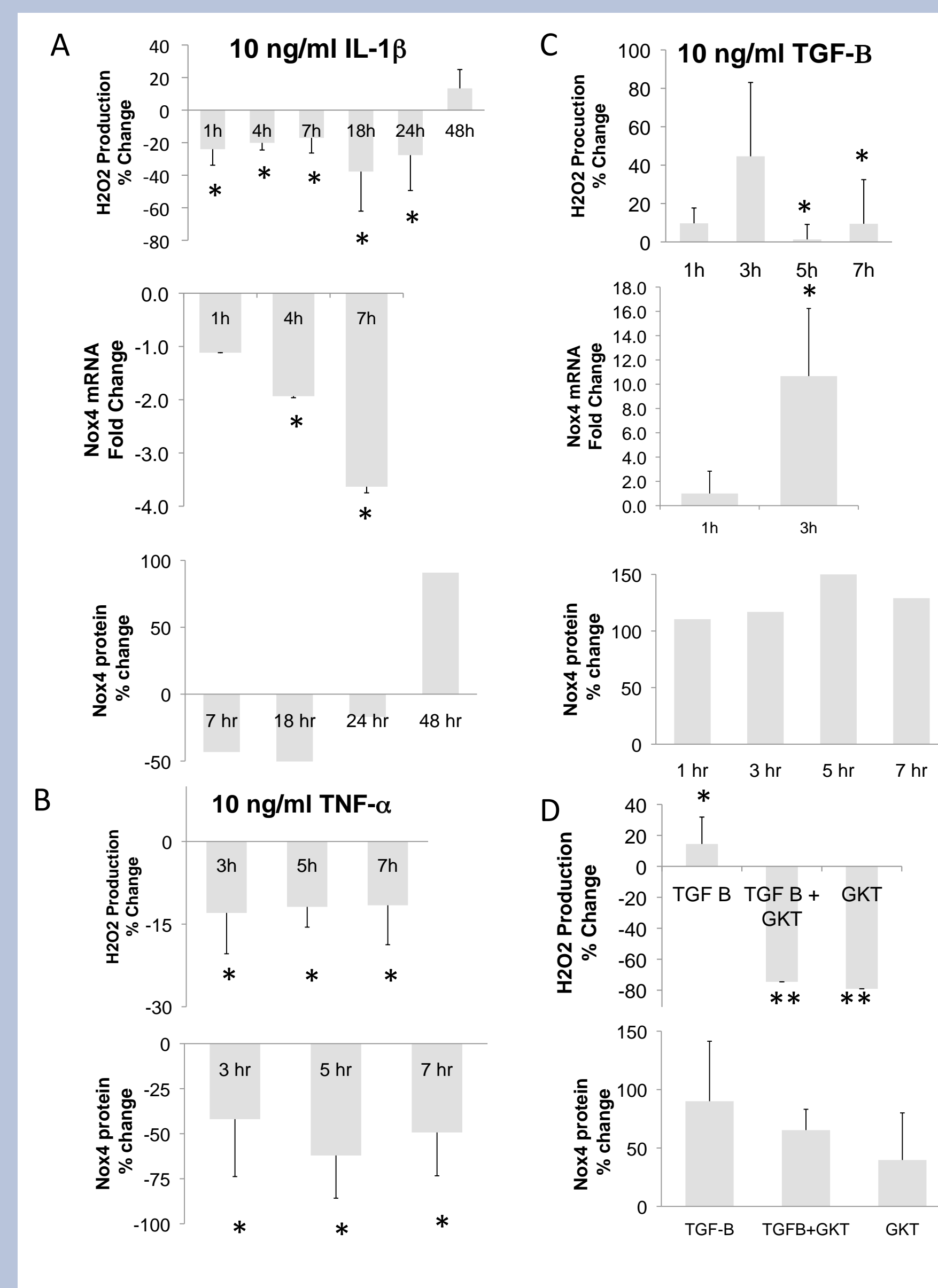


Figure 3. Nox4 acutely decreases after simulated joint injury in primary human chondrocytes.

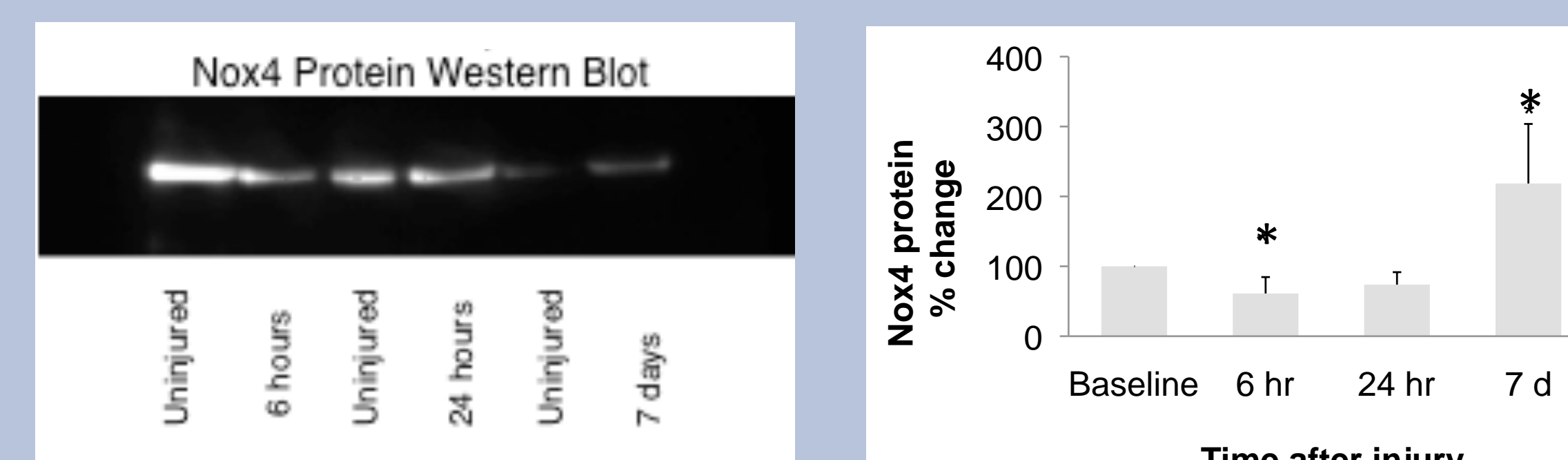
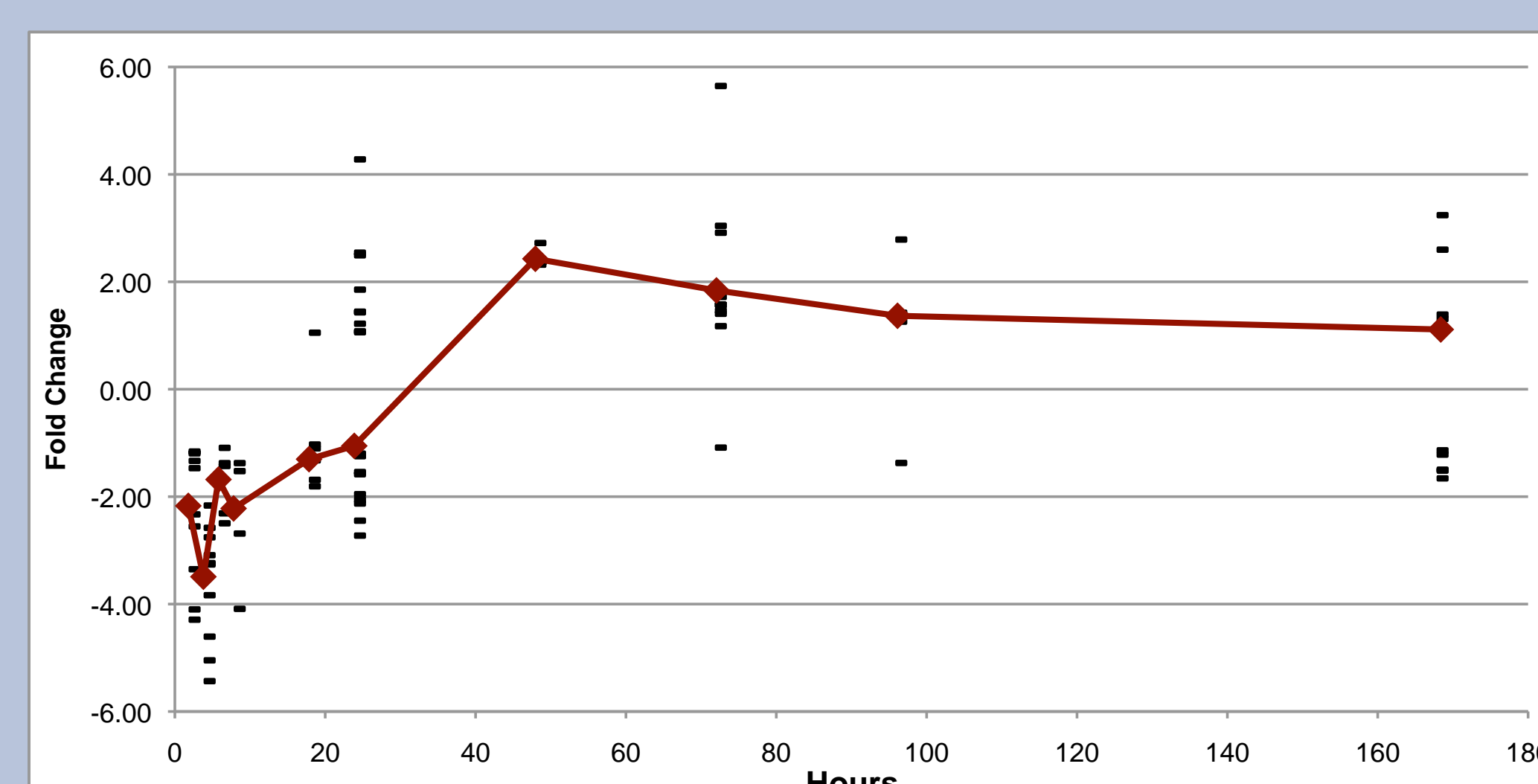


Figure 3. Nox4 acutely decreases after knee injury in mice.

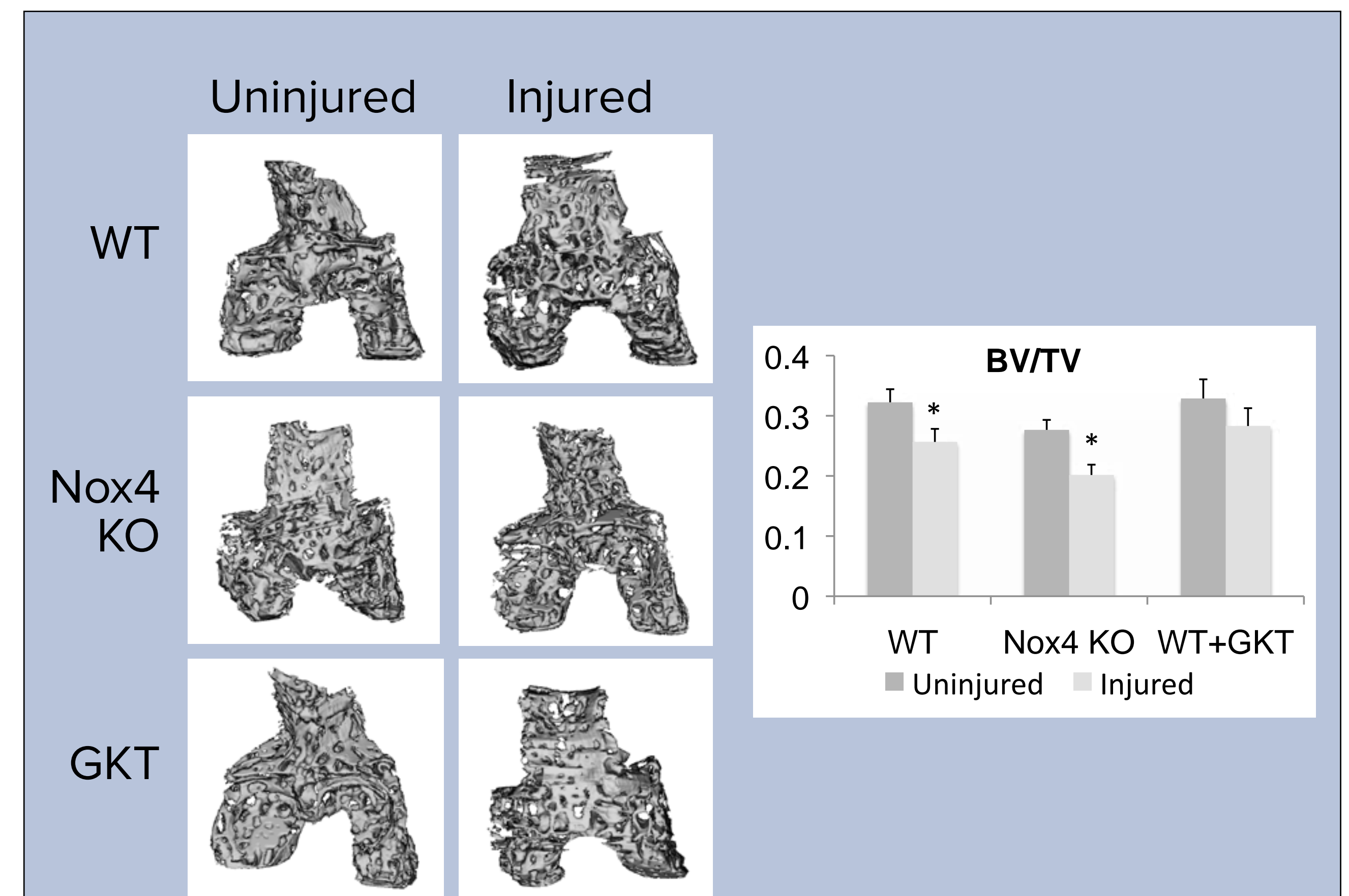


Figure 4. GKT137831 protects the joint after knee injury.

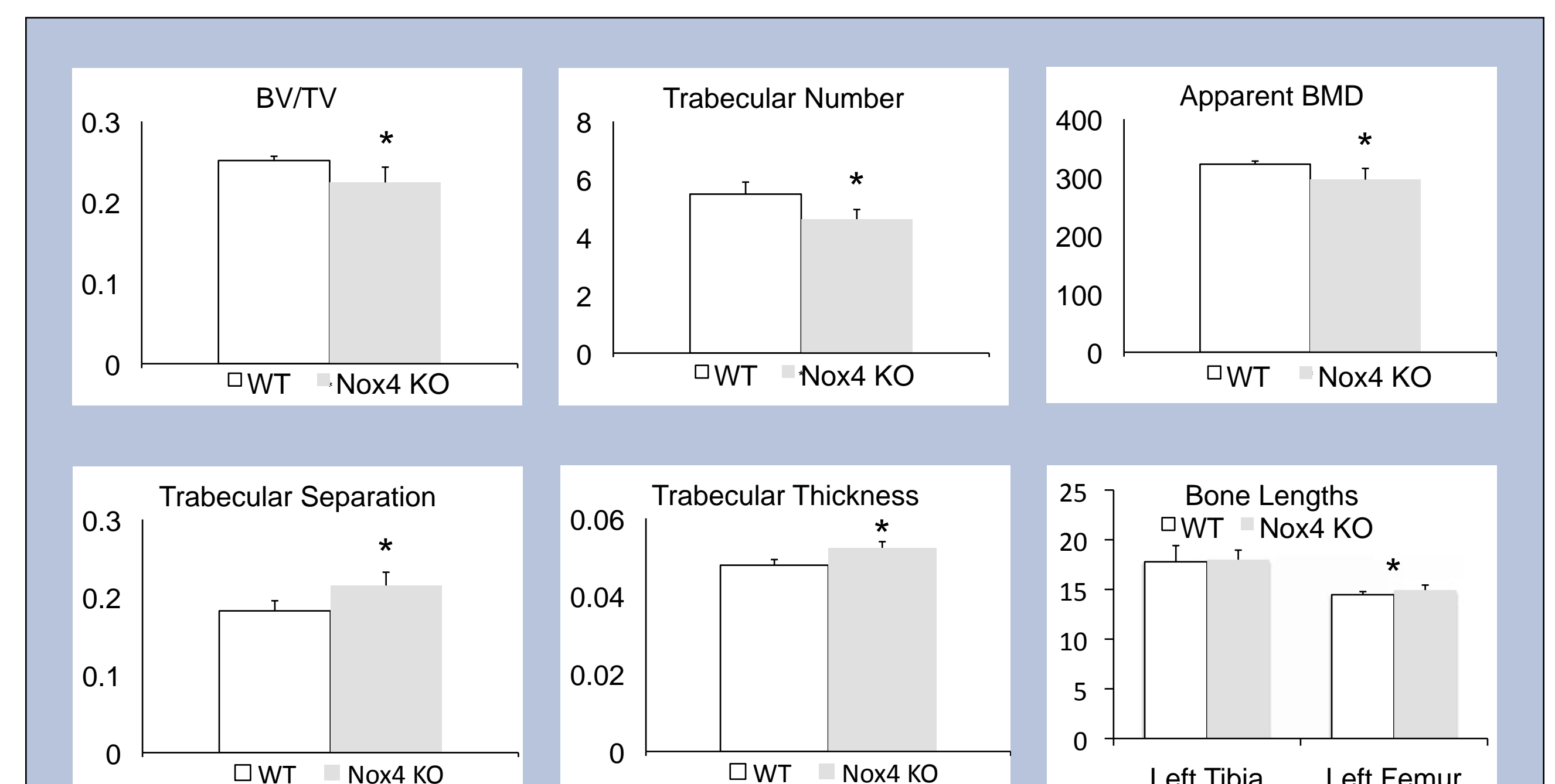


Figure 5. Nox4 Knockout mice have decreased trabecular bone.

## CONCLUSIONS

1. Nox4 activity and protein levels acutely decrease for the first 24 hours after joint injury, a novel finding not seen in any other system.
2. Nox 4 knockout mice have decreased trabecular bone density, similar to the phenotype of aged or osteoarthritic mice.
3. The Nox4 inhibitor GKT137831 protects the knee joint from early changes of post-traumatic osteoarthritis after injury, and could lead to future treatment strategies to prevent PTOA.
4. Further investigation of the acute changes in Nox4 activity after joint injury will further elucidate the early pathogenesis of PTOA.

## REFERENCES

Obortis acilisisi. Olenit iriustis nonsequat la con ut wisim eriliquam dolore do od ex eum eum ilisl utat, quis augue faccum alit, sequat veros euipit vent vel dolorper at alis augait, quatum zzril ullan utpat nis

## ACKNOWLEDGEMENTS

Salary (A.M.W) and research funding to support this project was generously provided by a gift of Denny and Jeanene Dickenson. This project was also supported by an Resident Clinician Scientist Training Grant (14-025) from the Orthopaedic Research and Education Foundation (OREF), with funding provided by the Ira A. Rochelle Family foundation, to A.M.W and an Orthopaedic Trauma Association (OTA) Grant to A.M.W. Portions of the project described was supported by the National Center for Advancing Translational Sciences (NCATS), National Institutes of Health (NIH), through grant #UL1 TR000002.\* GKT137831 was generously provided by Genkyotex.

# Early Cellular Responses Degrade Cartilage Mechanical Properties after Joint Injury

Jasper Yik<sup>1</sup>, Basak Doyran<sup>2</sup>, Dominik Haudenschild<sup>1</sup>, and Lin Han<sup>2</sup>

<sup>1</sup> Lawrence J. Ellison Musculoskeletal Research Center, Department of Orthopaedic Surgery, UC Davis, Sacramento, CA

<sup>2</sup> NanoBiomechanics Laboratory, School of Biomedical Engineering, Drexel University, Philadelphia, PA

2016.OARSI Abstract #674

## PURPOSE

Knee injuries can initiate changes that lead to post-traumatic osteoarthritis (PTOA). There are the immediate structural damage to the joint structures resulting from the injury itself. Perhaps more importantly, knee injury initiates cellular responses that may also contribute to joint degradation and loss of cartilage integrity.

Here we determine the contribution of cellular responses to the loss of cartilage mechanical properties after ACL-rupture. Specifically, we examine the contribution of primary response gene transcription using small molecule inhibitors against Cdk9 and Brd4. We use an *in-vivo* murine ACL-rupture model, and atomic force microscopy (AFM) based nanoindentation.

We found that injury substantially reduced the effective indentation modulus of cartilage on the femoral condyle measured 1-week post-injury, especially on the medial side. However, inhibition of Cdk9/Brd4 partially prevented this loss of cartilage modulus. Additional assays suggest mechanisms involving MMP activity.

We conclude that acute cellular responses contribute substantially to the loss of cartilage mechanical properties after joint injury.

## METHODS

### Mouse ACL-Rupture

Mouse joint injury was by non-surgical ACL rupture using a single mechanical overload, applied to the knee joint such that there is anterior-posterior translation of the tibia to the point of ACL failure. (Fig 1)

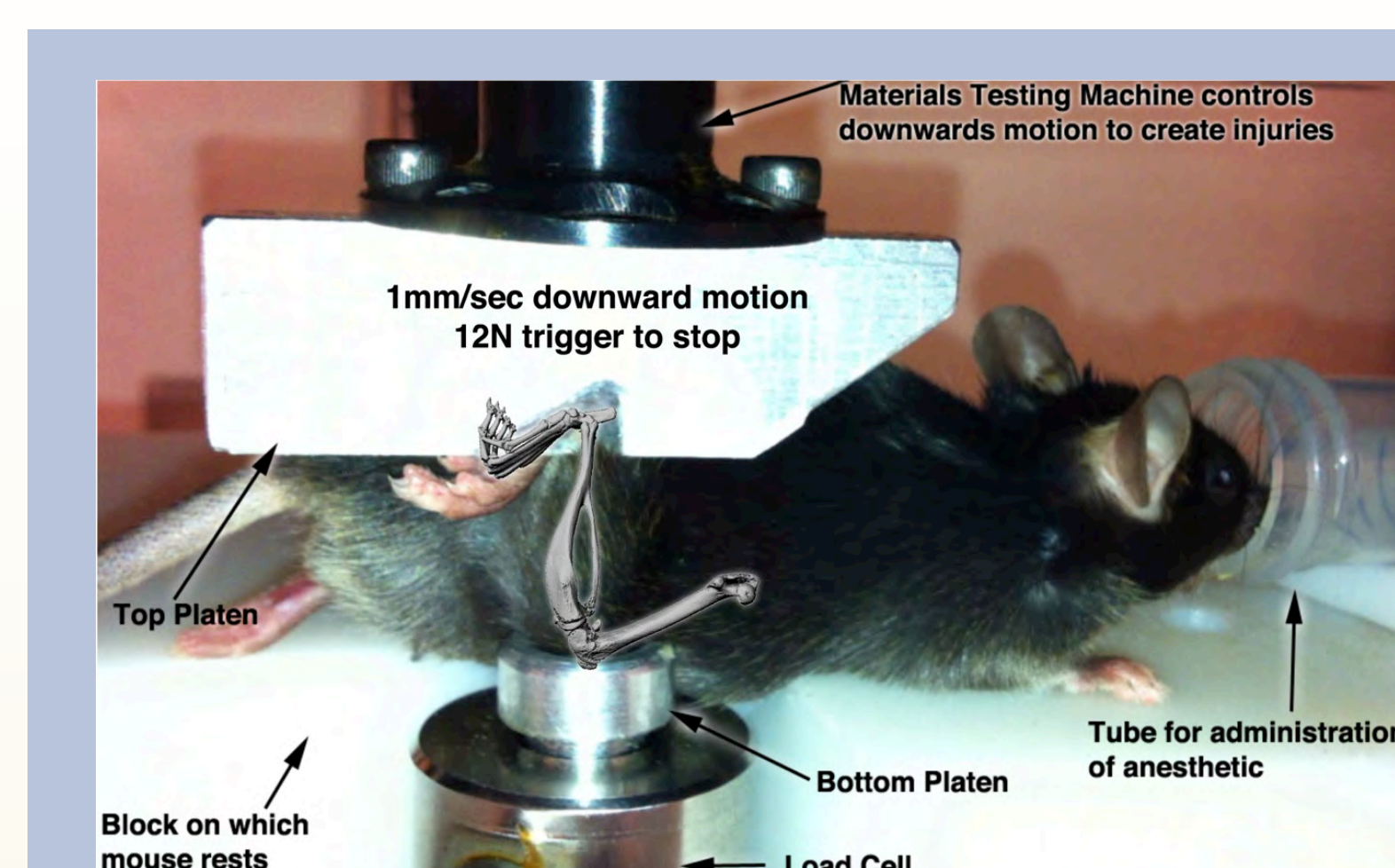


Figure 1. Non-invasive mouse model of post-traumatic osteoarthritis

### Inhibition of Acute Primary Response Gene Activation

Cellular responses to injury were attenuated by preventing the transcriptional elongation of primary response genes, accomplished by intraperitoneal injection of cyclin dependent kinase 9 (Cdk9) inhibitor flavopiridol (2.5mg/kg) and Bromodomain containing protein 4 (Brd4) inhibitor JQ1 (17mg/kg) daily for 3 days after injury. Cdk9/Brd4 inhibition prevents phosphorylation of RNA Polymerase II by Cdk9, which is the rate-limiting step for the transcriptional elongation of primary response genes. Control groups included uninjured naïve mice, injured mice without drug treatment, and drug-treated mice without injury.

## REFERENCES

1. Hu, Yik, Cissel, Michelier, Athanasiou, and Haudenschild. Inhibition of CDK9 prevents mechanical injury-induced inflammation, apoptosis and matrix degradation in cartilage explants. *Eur Cell Mater.* 2016;30:200-9.
2. Christiansen, Guilak, Lockwood, Olson, Pitsillides, Sandell, Silva, van der Meulen, Haudenschild. Non-invasive mouse models of post-traumatic osteoarthritis. *OA&C* 2015. 23(10): p. 1627-38.
3. Christiansen, Anderson, Lee, Williams, Yik, Haudenschild. 2012. Musculoskeletal changes following non-invasive knee injury using a novel mouse model of post-traumatic osteoarthritis. *OA&C* 20, 2012. 20(7): 773-782.

## RESULTS

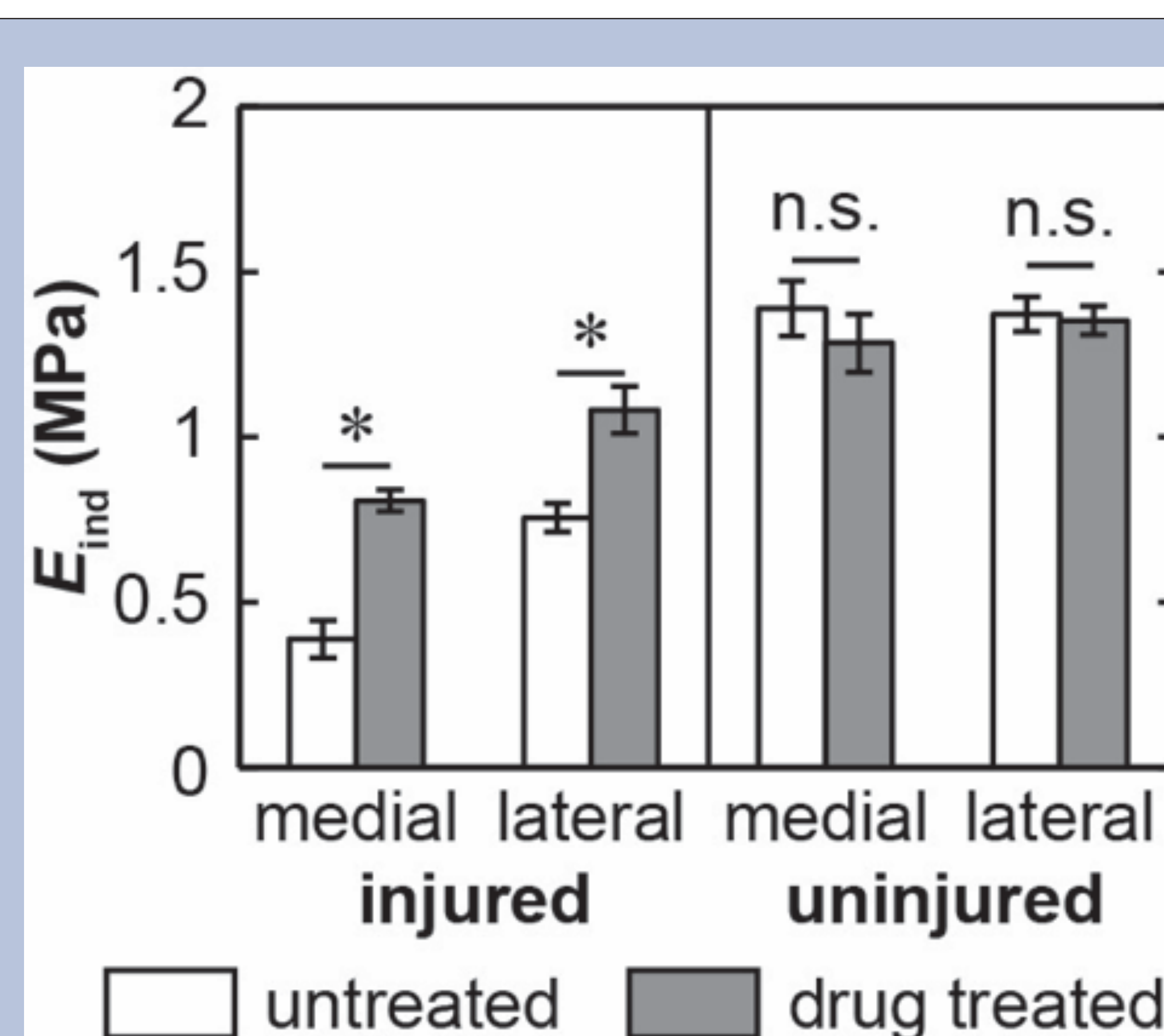


Figure 2: Indentation Modulus,  $E_{ind}$ , of condyle cartilage, measured 1 week after ACL-rupture injury, with or without flavopiridol/JQ1 treatment. Flavopiridol/JQ1 treatment blocks the acute transcriptional activation of primary response genes by inhibiting Cdk9 and Brd4. (\*:  $p < 0.05$ ,  $n = 6$ )

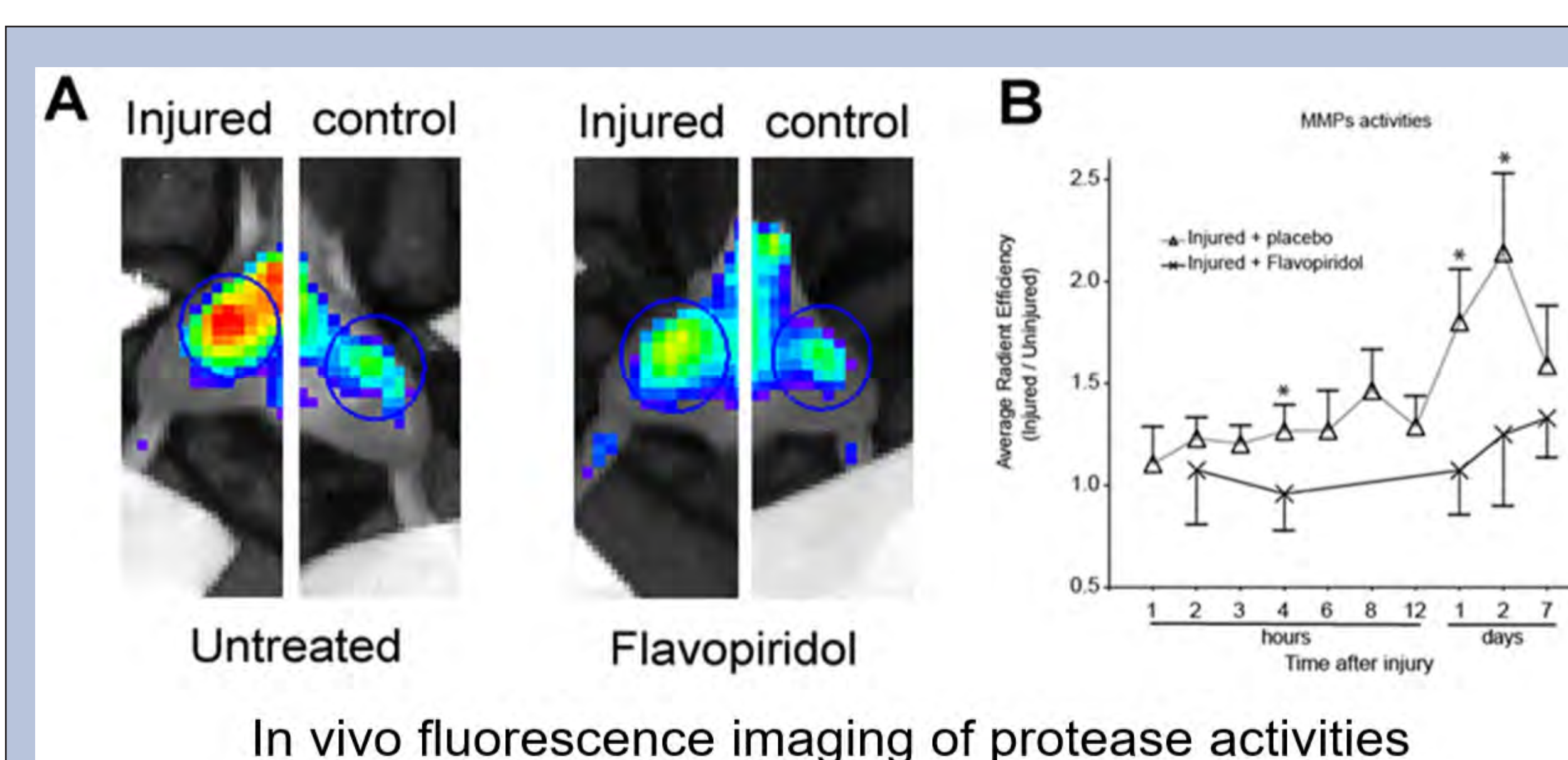


Figure 3. Supporting Evidence: shows that in-vivo MMP activity is induced within 2 hours by ACL-Rupture Injury, and that this proteolytic activity is greatly reduced by the presence of Cdk9 inhibitor Flavopiridol.  $n = 6$  mice per time point. \* indicates significant difference ( $p < 0.05$ ) between normalized MMP-Sense activity in Flavopiridol treated injured mouse knees versus and untreated injured knees.

## ACKNOWLEDGEMENTS

We gratefully acknowledge NIH/NIAMS funding to DRH, Zi'iang (Ethan) Hu and Jaime Fong for the in-vivo imaging, and a recently published manuscript (eCM) in which we've described the explant study. "Research reported in this publication was supported by the National Institute of Arthritis and Musculoskeletal and Skin Diseases of the National Institutes of Health under Award Number . The content is solely the responsibility of the authors and does not necessarily represent the official views of the National Institutes of Health."

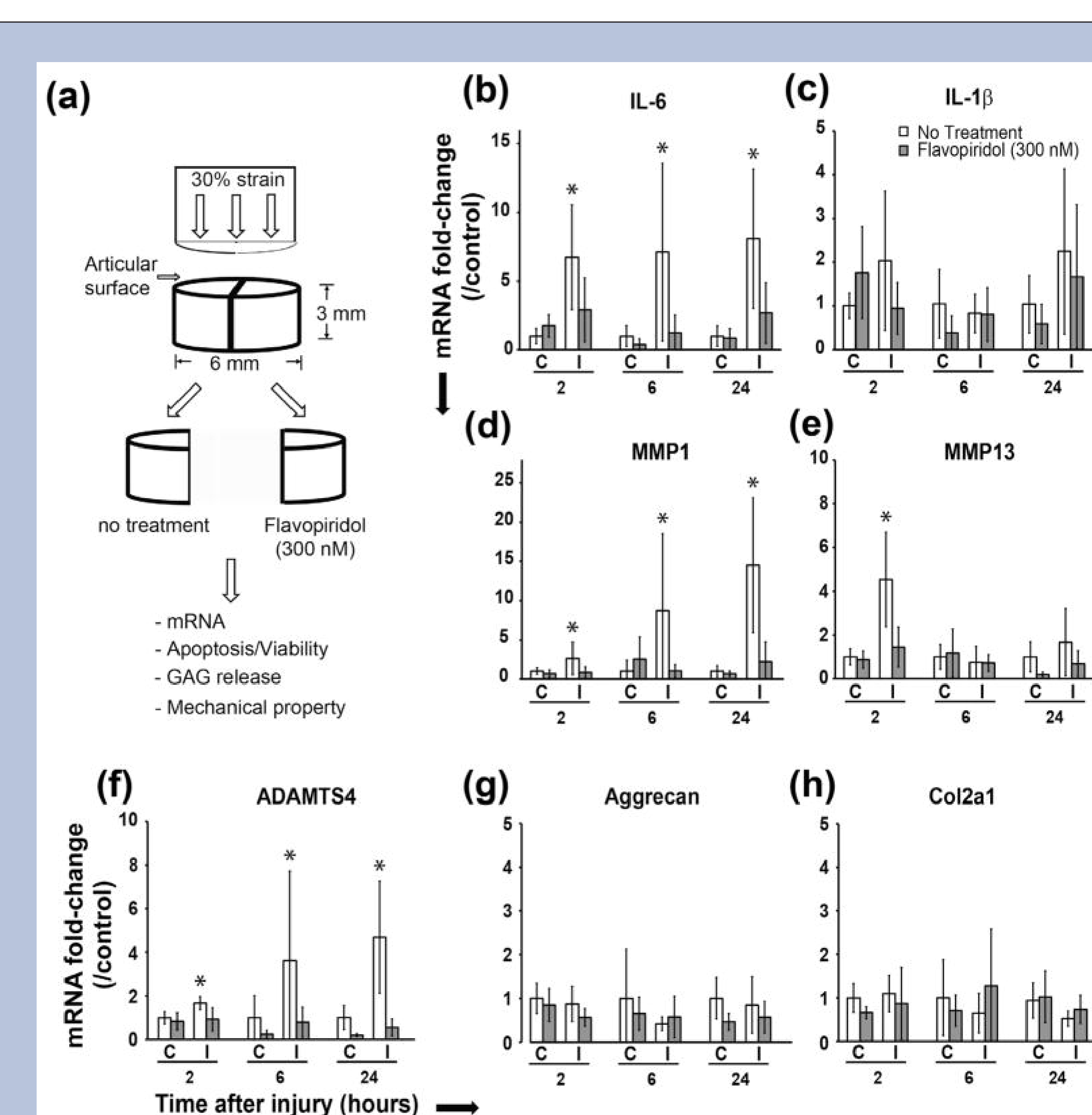


Figure 4. Supporting Evidence: In bovine cartilage explants, mRNA expression of degradative enzymes MMPs and ADAMTSs are rapidly induced by mechanical impact, while anabolic genes for collagen and aggrecan remain relatively constant.

## CONCLUSIONS

1. ACL-Rupture causes very rapid degradation of cartilage mechanical properties as measured by nanoindentation AFM in-vivo.
2. Degradation of cartilage mechanical properties is not just a result of the impact, but also a direct result of acute post-injury transcriptional activation of primary response genes.
3. These in-vivo results support earlier observations in bovine cartilage explants subjected to compressive loading. Possible mechanisms include acutely increased MMP transcription and activity in the joint post-injury.
4. An intervention strategy to attenuate cellular responses during the acute post-injury stage may benefit OA progression by preserving cartilage mechanical properties.